A one-year, postfire record of element deposition and cycling in the Kogelberg sandstone fynbos mountain ecosystem of the Western Cape, South Africa

by

Eugene W. Bergh

A thesis presented for the degree of Master of Science in Geology

Department of Geological Sciences

University of Cape Town

Supervisor: Associate Professor John S. Compton

May 2012

PLAGIARISM DECLARATION

I know that plagiarism is wrong. Plagiarism is to use another's work and pretend that it is one's own. Each significant contribution to, and quotation in this thesis from the work of other people has been attributed and has been cited and referenced. I have not allowed, and will not allow anyone to copy my work with the intention of passing it off as his or her own work.

Signature: _____

Date: _____

Acknowledgements

The completion of this thesis would not have been possible without the assistance of the following people:

My supervisor, associate professor John Compton is thanked for his commitment, knowledge and helpful nature throughout the course of the project.

Dr. Jason Neff from the University of Colorado, Boulder is thanked for his advice and thoughts on some of the aspects of this thesis.

Dr. Richard Reynolds from the USGS in Denver, Colorado for his assistance in analyzing the soil samples.

Mr. Patrick Sieas is thanked for his advice in the laboratory.

Dr. Nicole Barger (Colorado University, Boulder), Associate Professor Michael Cramer (Botany Department at UCT), Dr. Sampson Chimphango (Botany Department at UCT), Ms. Taryn Morris (Ph.D. student at Colorado University, Boulder) and Mr. Justine Nyaga (Ph.D. student in the Botany Department at UCT) for their advice, input and assistance during the initial planning stages of the project.

Mr. Mark Johns, conservation manager at the Kogelberg Biosphere Reserve for permission to conduct field research in the reserve.

Mr. Werner Voigt is thanked for permission to conduct fieldwork in the Harold Porter National Gardens. A special thanks to Ms. Jane Forrester at HPNBG for assisting in all my queries and requests. I would also like to thank the staff of HPNBG for their assistance and providing me with needed information.

Mr. Roger Diamond (Ph.D. student in the Geological Sciences Department at UCT) and Dr. Julia Angstmann (Arizona State University) are thanked for their advice and input during progress meetings.

Mr. John Harrison and Mr. Bruce Cairns for assisting in the construction of the field samplers.

Prof. Dave Reid and Ernest Stout for advice on sample preparation and XRF analysis.

Ms. Christel Tinguely (Geological Sciences department) for assisting me in ICP-MS analysis.

Mr. Matt Gordon (Soil Sciences Department, Stellenbosch University) for assistance in Ion Chromatography in his laboratory.

Dr. Howard Waldron (Oceanography Department at UCT) for allowing me to conduct nutrient analysis in his laboratory and Ms. Raïssa Philibert is also thanked for assistance with the last batch of samples.

Mr. Ian Newton from the Archaeology department at UCT for running my samples in the isotope lab is thanked.

Mr. David Wilson (Geological Sciences department) is thanked for the preparation of thin sections from the bedrock samples.

Two of my fellow M.Sc. students, Kaylan Hamel and Jarryd Finkelstein, are thanked for their help in the field.

Ms. Hayley Cawthra (Council for Geosciences) for help with GIS.

The director of the Natural History Department at the Iziko South African Museum (ISAM), Dr. Hamish Robertson, as well as the staff of ISAM for their support and motivation.

The South African Weather Service supplied weather data.

This project was funded by the National Research Foundation (NRF) and the Mellon Foundation.

Abstract

The Kogelberg Sandstone Fynbos biome of the Harold Porter National Botanical Gardens (HPNBG) and Kogelberg Biosphere Reserve (KBR) in the southwestern Cape of South Africa thrives on thin soils derived from sandstone bedrock and constitutes a biodiversity 'hotspot' with approximately 1650 plant species of which 77 species are endemic to the Kogelberg region. The sandstone bedrock substrate with >97 wt% SiO_2 (quartz) provides few nutrients to the overlying thin (2 to 20 cm), acidic soils. Additional nutrients enter the ecosystem through marine and mineral (dust) aerosols. Rainwater, stream and mountain seep water, soil and bedrock samples were collected over a one-year period in an attempt to understand the dynamics of nutrient sources to the fynbos ecosystem. Fire is a critical component of the fynbos ecosystem and this study documents the macronutrient (Cl, Na, SO_4, Mg, Ca and K) dynamics of the fynbos for one year following a major fire event on 3 June 2010. Chloride and sodium in rainwater and stream water were found to be primarily derived from a marine aerosol source. The outflux of the ions Cl, Na and K was found to be greater than the influx for these ions. Sulphate, magnesium, calcium and potassium reflected a mixed source of marine and mineral dust aerosols. The influx of SO_4 increased at sites where all the other ions recorded a decreasing influx. The influx of SO_4 was greater at sites to the north relative to sites closer to a marine source suggesting a strong influence from a terrestrial source for SO_4. Rainout of chloride and sodium ions decreases away from the coast and net evaporative loss from rainfall to streams is around 38% over the year assuming Cl ion behaves conservatively. Stream concentrations were lowest during warm and dry summer months when salts accumulate in soils. Summer accumulated salts are then flushed out into streams during the cool, wet winter months. Sulphate, magnesium, calcium and potassium concentrations in rainwater and stream water increased after the June 2010 fire event and then slowly decreased with time. For example, elevated rainwater and stream water SO_4/Cl molar ratios returned to near marine values 8 months after the June 2010 fire event. Magnesium and calcium appear to have a strong mineral/ash source and may have been influenced by a fire that burnt a region bordering the study area in March 2011. Minor amounts of mica minerals occur in the sandstone bedrock and clay minerals within the soils include minor amounts of illite/mica and trace amounts of smectite and kaolinite. The clay minerals in the soil reflect a mixed source of bedrock derived and windblown mica and feldspar minerals. Mica in the bedrock and

clay mineral deposition in the soil may provide additional ions, particularly K and Ca, by chemical weathering. Potassium showed the largest bedrock reservoir and has the greatest weathering flux to the overlying soil. Windblown inputs may include mineral and organic matter dust from the continental interior and ash particles from fires in the region. Afromontane vegetation along the sheltered ravines and stream banks was largely unaffected by the fire, but nearly all above ground fynbos vegetation was destroyed on the surrounding slopes. Vegetation slowly increased within the first year after the fire event, but did not recover sufficiently to take up all of the nutrients available which were lost through stream flow from the ecosystem. Plant regrowth was slower on steep slopes than valley floors reflecting the importance of hydrology and soil thickness. Partially burnt plant debris was washed down slope to accumulate on lower slopes which fed additional nutrients into streams where plant regrowth and total biomass are higher. The regrowth of vegetation is dependant on both macro- and micro-nutrient (N and P) supply. Nitrogen may limit regrowth as there was in general an over supply of macronutrients to the ecosystem. Excess nutrient loss was reduced to pre-fire levels as the vegetation mass increased with future vegetation growth limited by the nutrient influx from a mixture of marine and mineral aerosol sources.

Table of Contents

List of Figures

List of Tables

Chapter 1 : Introduction

1.1 The Cape Floristic Region

The Cape Floristic Region (CFR), also known as the Cape Floral Kingdom (CFK) (Moll *et al*., 1984) is one of six in the World. The CFR, with a total land surface area of approximately 90 000 km^2 (0.04% of Earth's total surface) is the smallest of all floristic regions, but the most diverse worldwide. The other floral kingdoms are spread across the Northern Hemisphere and Australia (Taylor *et al*., 2001). The CFR comprises roughly 20% of Africa's floral species (Burgoyne *et al.*, 2005). The evolution of the Cape flora is thought to be a response of a combination of factors. Goldblatt (1997) outlines soil, landscape and rainfall patterns as important in determining vegetation patterns in the CFR. Linder (1991) suggests rainfall and altitude to be more important variables in sandstone mountain fynbos ecosystems. Areas with lower rainfall and elevation may show a decreased species richness. Cowling *et al.* (1998), Linder and Hardy (2004) and Burgoyne *et al.* (2005) all mention geographic and climatic changes throughout the geologic record as crucial in the development of the CFR. Speciation and species coexistence further contributes to enriching a diverse floral region such as the CFR. Climatic and environmental conditions are not entirely homogeneous across the CFR and microenvironments play an important role in determining speciation under different conditions.

The CFR also forms part of one of the five Mediterranean-type ecosystems in the world (Deacon, 1983; Crosti *et al*., 2006; Cox and Underwood, 2011). Mediterranean-type ecosystems are located on five continents (Klausmeyer and Shaw, 2009) between the latitudes 30º to 40º north and south of the Equator (Deacon, 1983; Rambal, 2001). Regions where Mediterranean-type ecosystems occur include parts of the Mediterranean Basin, southwestern and southeastern Australia, California and northwest Baja (Mexico), central Chile and the southwest of South Africa (Figure 1.1 and Table 1.1). Rambal (2001) describes Mediterranean-type ecosystems as having highly diverse species distribution in a relatively small area. These ecosystems are characterized by seasonal rainfall (Lamont, 1983) with dry, windy summers and cool, wet winters (Miller, 1983;

Orshan, 1983; Crosti *et al*., 2006) with more than 50% of the annual precipitation falling during the winter months (Klausmeyer and Shaw, 2009)

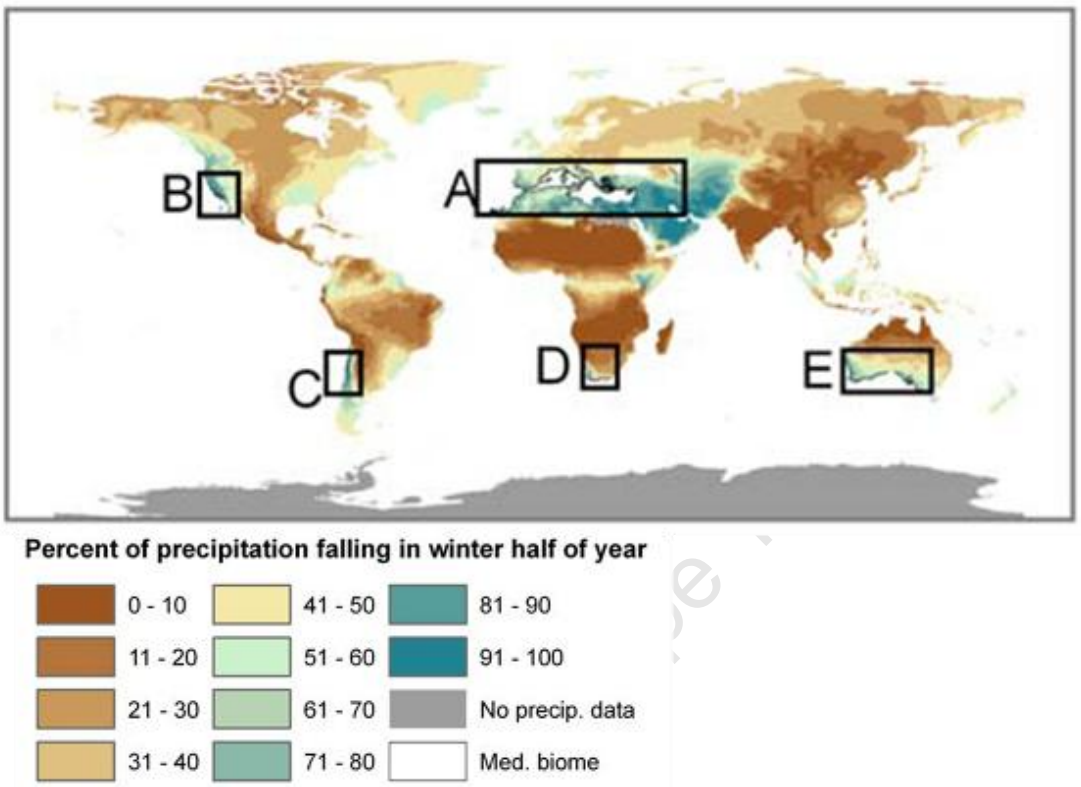

Figure 1.1. The five Mediterranean-type ecosystems of the world with percentage of total annual precipitation falling in the winter months of the year. The Mediterranean regions are indicated by the black boxes. A = Mediterranean Basin. B = California (USA) and NW Baja (Mexico). C= Central Chile. D = Southwestern South Africa. E = Australia. Figure from Klausmeyer and Shaw (2009)

Table 1.1. The five Mediterrean-type ecosystems of the world with the total surface area (km^2) that each cover, and the number of native species within the regions. Estimates on the number of species are from Cowling *et al.* (1996)

Region	Area (km^2)	Number of native species
Mediterranean Basin	2 077 131	25 000
Australia	802 523	8 000
California and northwest Baja	176 425	4 300
Central Chile	148 408	2 400
South Africa	96 953	8 550

The main vegetation type of the CFR is fynbos (Brown, 1993; Mucina and Rutherford, 2006; Abanda *et al*., 2011) and is focused in southwestern South Africa (Figure 1.2). The

fynbos biome comprises 4/5 of the CFR and according to Cowling (1995) hosts approximately 8 600 plant species of which 5 800 are endemic. More recent reports from Goldblatt and Manning (2002) and Paterson-Jones and Manning (2007) raise the number of plant species to more than 9 000, of which 70% are endemic. The fynbos biome is dominated by protea shrubs, heath-like shrubs (ericoids) and reed-like restioids (Kruger, 1979b; Siegfried and Crowe, 1983; Campbell, 1986; Witkowski and Mitchell, 1987; Cowling, 1995; DeBano, 2000; Born *et al*., 2007). Linder and Hardy (2004) document the increase of fynbos species through geologic time. The number of species almost doubled over the last 8 million years. Goldblatt (1997) emphasizes the development of the cold Benguela Upwelling System off the southwestern coast of Africa during the late Miocene as probably the most important factor in initiating the radiation of fynbos vegetation in the southwestern Cape. Fynbos vegetation was the dominant feature on the landscape 3 million years ago and by the beginning of the Pleistocene (1.8 Ma) the number of fynbos species had increased to over 1 200 (Cowling, 1995). Species diversity may have accelerated in the last 1 to 2 million years (Goldblatt, 1978; 1997). Modern fynbos did not only invade vacant areas during their evolutionary history, but also competitively displaced other vegetation present at the time. The adaptation of fynbos to drought and fire may also have given this species-rich vegetation an advantage over other vegetation types, especially during the Miocene (Linder, 1991).

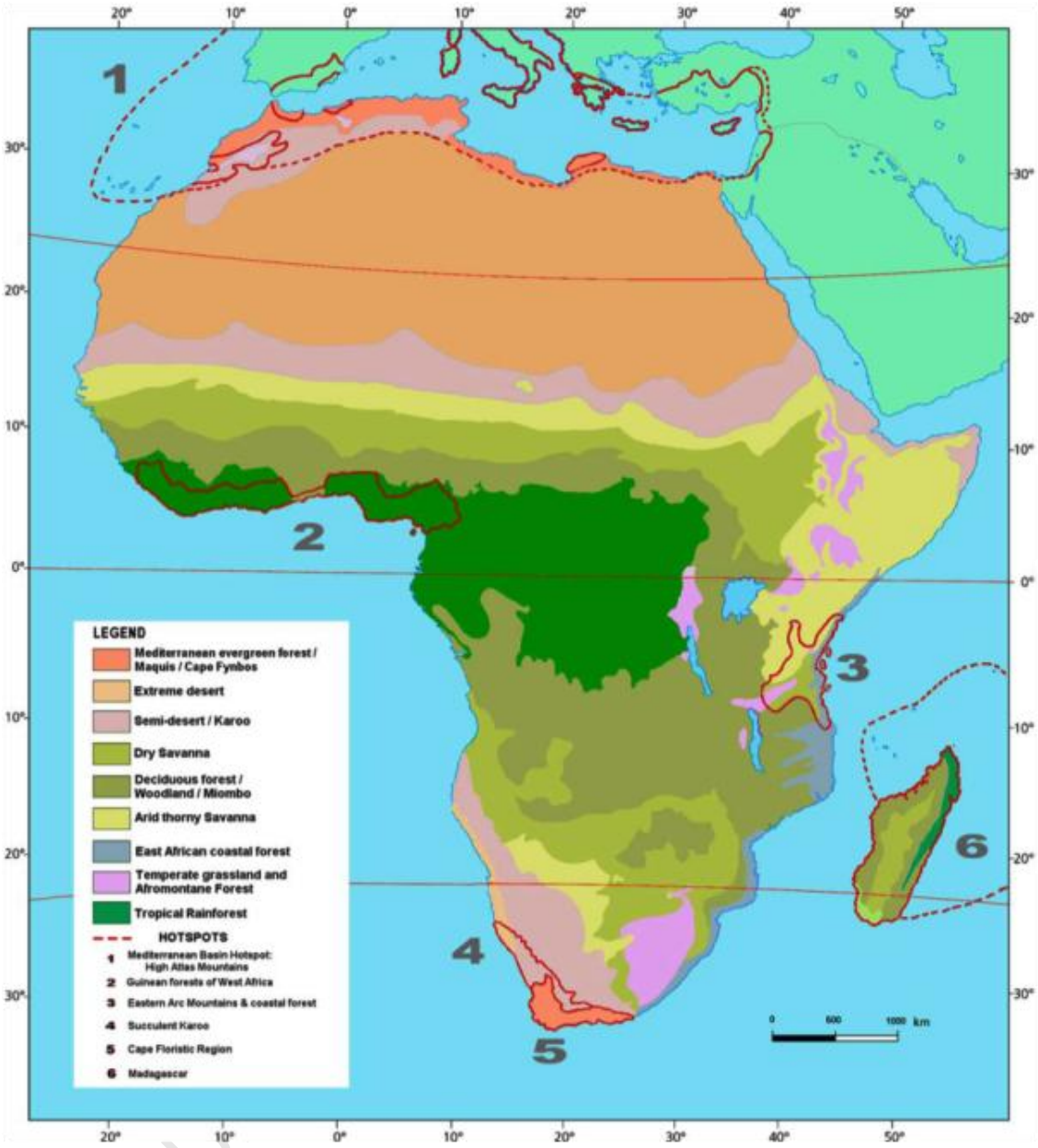

Figure 1.2. Vegetation types of Africa. Biodiversity hotspots are highlighted in red. The location of the Cape Floristic Region is indicated by the number 5. Figure from Burgoyne *et al*. (2005).

The fynbos biome is influenced by a Mediterranean-type climate with dry windy summers and cool wet winters (Cowling, 1995; Goldblatt, 1997). Winter rainfall decreases eastward and northward (Fuggle and Ashton, 1979; King and Day, 1979; Cowling, 1995). South Africa can be divided into three main rainfall regions (Figure 1.3). The western-most part of the country receives rainfall mainly in winter, the southern coastal region receives rain all year round and the rest of South Africa receives rain mainly during summer. The study area discussed in this thesis is located in the southwestern part of South Africa and falls within the winter rainfall region.

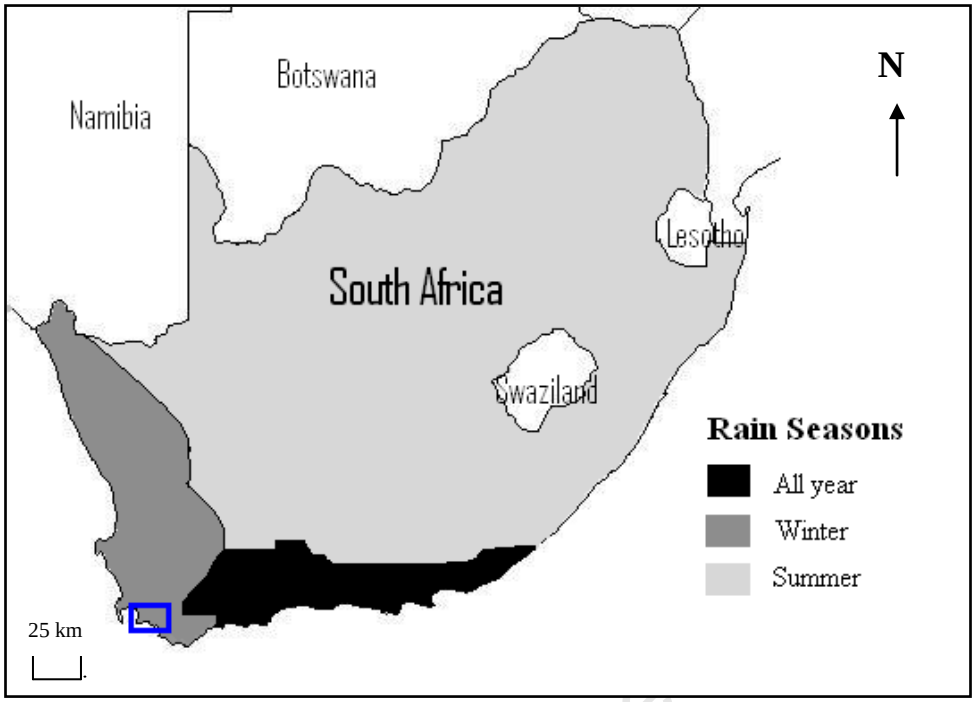

Figure 1.3. The three seasonal rainfall regions of South Africa as outlined by Wessels *et al.* (2007). The study area discussed in this thesis is shown by the blue square.

Fuggle and Ashton (1979) mention topography and exposure of mountain slopes to northwesterly and southeasterly winds as being closely related to the general rainfall pattern in the southwestern Cape. A succession of cold fronts associated with rain-bearing northwester winds dominate during winter. Scattered rainfall showers are accompanied by the front moving inland and the wind direction changes to westerly and southwesterly. High pressure cells and southeasterly winds are dominant throughout summer (Cowling, 1995). A sea-breeze influence on prevailing winds is common throughout the year from Cape Hangklip eastwards (Fuggle and Ashton, 1979). South-facing mountain slopes may benefit from summer moisture delivered by the southeast trade winds and may also receive more precipitation than lee-slopes (Goldblatt and Manning, 2002).

Paterson-Jones and Manning (2007) suggest that high adaptability and plant physiology are the main factors which contribute to the biome's survival. The fynbos ecosystem is complex (Cowling, 1992) and various factors ensure the survival of this biome. Geomorphic and geologic evolution (Cowling, 1992; Cowling *et al.* 2009), micro-climate conditions (Miller, 1983; Cowling, 1992), physiology (Cowling, 1992; Paterson-

Jones and Manning, 2007), bedrock substrate (Paterson-Jones and Manning, 2007), atmospheric deposition (Brown *et al.*, 1984; Smit, 2003; Soderberg, 2003; Soderberg and Compton, 2007), hydrology (Smit, 2003) and regular, but not too frequent fire events (Kruger, 1979a; van Wyk *et* al., 1992; Higgins, *et al.* 1997) are thought to be the main factors in controlling the survival of this floral rich ecosystem.

Mountain fynbos grows predominantly on soils derived from the underlying Table Mountain Group (TMG) bedrock. The TMG is highly arenaceous with the Peninsula Formation being the most quartzitic (>95 wt% quartz) (Smit, 2003; Soderberg, 2003; Soderberg and Compton, 2007). The Peninsula Formation contains few feldspar and mica minerals to release K, Na and Ca to the soil through chemical weathering of the bedrock (Smit, 2003). Bedrock from the TMG weathers slowly at rates of 1–10 m/Myr (Kounov *et al.*, 2007). The slow weathering TMG quartzites give rise to nutrient-poor, acidic soils (Campbell, 1986). This poses the question of how such a diverse floral ecosystem can be supported by such nutrient-poor soils.

1.2 Possible Sources and Delivery of Nutrients to an Ecosystem

Plants derive their nutrients primarily through interception from atmospheric deposition and through nutrient uptake from soil. Atmospheric deposition through dryfall onto soil surfaces and rain provide major nutrient inputs into the soil profile. Minerals and nutrients may further be broken down through microbial activity. Nutrient uptake by plants may be enhanced by specialized roots especially in nutrient-poor soils and bedrock. The roots of the vegetation may penetrate through rock fractures, but a tough, extensive root network attempts to maximize nutrient uptake. Read and Mitchell (1983) describe plant mineral nutrients in soil as being complex molecular aggregates from which they must be released for utilization by the plants. The rate of nutrient input and release limits the primary productivity of an ecosystem (Read and Mitchell, 1983). Nutrient input rates are in turn dependent on the nature and source of ions that are made available to the ecosystem.

Smit (2003) emphasized the importance of hydrology on nutrient cycling within the fynbos ecosystem of the Kogelberg Sandstone Fynbos biome in the southwestern Cape

of South Africa. Rivers, seepages and streams provide a means of transport for ions and nutrients through erosional products and transport of depositional aerosols which have entered the system. Stream chemistry and nutrient cycling contain a variety of interacting factors such as the inputs of atmospheric deposition, groundwater recharge, vegetation, rock weathering and soil nutrients (Smit, 2003).

Soderberg (2003) identifies wet (rain) and dry (terrestrial dust) deposition as essential elements of atmospheric inputs into the fynbos ecosystem of the Citrusdal area in the southwestern Cape of South Africa. Rainfall forms an integral part of atmospheric deposition. Atmospheric deposition can be divided into wet and dry deposition. Wet deposition involves the removal of gases, liquids and aerosols from the atmosphere by precipitation (Galloway, 1978; Lovett, 1994; Drever, 1997). Soluble gas phases may diffuse into water droplets, become incorporated and eventually fall to Earth's surface. Marine and mineral aerosols may form raindrop nuclei and be removed during rainfall events from the atmosphere to the surface as rainout. Dry deposition is the movement of gas or solid phase substances through an ecosystem without the incorporation of water droplets (Lovett, 1994; Drever, 1997). Galloway (1978) divides dry deposition into three subcomponents, namely dry fallout, impacted aerosols and adsorbed gases. Dry fallout is defined as gravity driven particles, mainly >2 μm in diameter, falling to Earth's surface. These particles are usually derived from soils, plant debris or condensed aerosols. Impacted aerosols are particles usually <2 μm that are impacted onto Earth's surface. Adsorbed gases are defined as gases that are adsorbed at Earth's surface. The process of dry deposition may be influenced by a range of atmospheric and meteorological conditions in addition to the physical and chemical properties of the particle concerned (Pryor and Barthelmie, 2000). Dry deposition can be difficult to quantify and for the purposes of this study, a combination of wet and dry deposition or total deposition in the form of precipitation is considered. Particles not associated with water droplets may be incorporated into rainfall through rainout events. Rainout may be defined as the loss of airborne particles in the atmosphere through droplet formation and wet particle impaction in the form of rainfall.

Rainout can be collected through a simplified rain collector (Section 2.1.1). The rain collector enables for the determination of rain amount as well as the capturing of rainout

ions. There are however a few drawbacks to this method of measuring rainout content. Leaving the collectors out in the field makes it vulnerable to contamination from birds that may perch on the collectors or insects entering the samplers. Laboratory contamination can also not be ruled out. The surfaces of the funnels are not the same as the vegetation surfaces and may cause oversampling. Rain collectors do not account for gas exchange. Plants are adapted not only to take up water molecules, but also gain a proportion of their nutrients through gas exchange.

Soderberg (2003) found wet deposition to be enriched in ions with a seawater signature (Na, Cl, Mg and SO_4) in the Olifants River, 170 km NNE of Cape Town. Soils were found to be richer in elements such as Fe, Al and K compared to relative abundances in bedrock composition (Soderberg and Compton, 2007) suggesting an additional source of nutrients to the fynbos vegetation. Clay minerals are another source of nutrients to the plants. The weathering and breakdown of minerals in the soil releases ions and add to the nutrient pool made available to plants. Clay minerals typically contain a variety of essential elements to plant growth such as Ca and K and may form part of windblown dust. Soderberg (2003) identifies the source of windblown dust and clay minerals as coming from the semi-arid Karoo.

Neff *et al.* (2006) suggest that there is a limited understanding of biogeochemical and hydrological aspects for the relationship between plant species and their geological environments. Reynolds *et al.* (2006a; 2006b; 2006c) attempted to address this by studying the nutrient input into a Colorado Plateau ecosystem in the United States. They outlined two major sources of rock-derived nutrients in soil. These nutrients may come from weathering of local bedrock or dust from distant sources. The distinction between minerals derived from bedrock weathering and those of mineral dust may be determined by an integration of isotopic, mineralogic, textural and geochemical analyses (Reheis *et al.*, 2002). The detection of mineral dust may be accounted for by the presence of titanium-bearing magnetite grains. These grains are generally absent in sedimentary rocks. Their magnetic properties can be determined by isothermal remanent magnetization (IRM) (Reynolds *et al.*, 2006a). Although these studies were not carried out in a fynbos ecosystem context, it can be held true for most ecosystems and environments.

Mineral dust input into a system may alter the texture and composition of surficial sediments and soils. This in turn may influence landscape characteristics, soil fertility and soil infiltration. Dust input may account for a relatively small proportion of the surficial material (Chadwick *et al.* 1999; Reynolds *et al.* 2006a; Reynolds *et al.* 2006b). Goldstein *et al.* (2008) used natural rock cavities generally referred to as potholes to study dust captured by these traps. The mineral dust trapped in the potholes may be regarded as dust entering the system. Dust samples from the sandstone potholes showed a higher presence of magnetic minerals in the depressions than the surrounding bedrock. Their study suggested that dust from outside the Colorado Plateau may aid in the fertilization of the Plateau.

1.3 Fynbos and Fire

Fire can cause extensive damage to property and life, but proves to be beneficial to fynbos (Brown, 1993; Crosti *et al*., 2006; Rutherford *et al*., 2011). Kruger (1979a; 1983) mentions that fire is foremost a natural occurrence in the ecosystem and de Klerk *et al*. (2011) outline fire as a critical process in regulating species-richness in the fynbos biome. Ash deposition provides an efficient mechanism to redistribute plant nutrients broadly over the landscape. Erosion increases due to the removal of biomass and roots in the soil and can be further amplified by increased precipitation (Pérez-Cabello *et al*., 2009). Nutrient turnover and decomposer populations are affected which will in turn lead to a change in stream water chemistry and biological activity (Neary *et* al., 1999; Certini, 2005; Pérez-Cabello *et al*., 2009). Fire can have a great effect on aboveground biomass as well as belowground physical and chemical processes (Neary *et al*., 1999). A wildfire can destroy nearly all of the aboveground biomass. Nearly half of the original pre-fire canopy cover in a sandstone mountain fynbos ecosystem returns by the end of the second year followed by a rapid increase in the third year (Rutherford *et al*., 2011). Manry and Knight (1986) suggest that the accumulation time for sufficient fuel to buildup for another fire ranges between four and six years.

Fynbos vegetation can generally be divided into seeders and sprouters (Kruger, 1983; le Maitre, 1992; Smith *et al*., 1992; van Wilgen and Forsyth, 1992). Seeders release their

seeds during a fire event or store their seeds in the soil until it germinates as a survival mechanism (le Maitre, 1992; Brown, 1993). Fire can also stimulate flowering in certain geophytes (le Maitre and Brown, 1992). Proteas are an example of seeder vegetation. Seeders have higher stomatal conductivities than sprouters, have a higher tolerance against drought, lower shade tolerance, function at higher photosynthetic rates and grow more rapidly. Brown (1993) suggests that fire may be the most important factor in the germination of seeds in a mountain fynbos ecosystem. Sprouters, like restios and the palmiet, have a more competitive advantage over seeders as they take less time to regenerate (Kruger, 1983; Pérez-Cabello *et al*., 2009). The entire plant is not destroyed by the fire and will effectively start to regrow almost immediately after the fire. Sprouters also reach reproductive maturity at a faster rate than seeders (Smith *et al*., 1992). Most fynbos fires do not penetrate into afromontane forest areas. Van Wilgen and van Hensbergen (1992) attribute the inability of fynbos fires to penetrate forested areas to increased moisture content and decreased crude fats relative to low canopy shrub fynbos vegetation.

Belowground factors that are influenced by a wildfire include soil mineralogy, belowground biomass, soil microbial activity, organic matter content and soil porosity (Pérez-Cabello *et al*., 2009). The temperature of wildfires depends on moisture content of the fuel and atmosphere, the fuel load, biomass and soil type. Temperatures may reach 700°C in the most intense of circumstances. Approximately 85% of the plant litter layer combusts at 180°C. Organic compounds and nutrients within the upper soil layer starts to volatize at 200°C. Nearly all organic matter is consumed at 450°C. A temperature of 100°C affects the soil to a depth of 5 cm. Temperatures exceeding 250°C can lead to physical and mineralogical changes in the soil up to a depth of 10 cm. Clay minerals are usually not affected during low intensity fires (Neary *et al*., 1999).

Fire through arson and other human activities increase the frequency of fires placing some species at risk (Pérez-Cabello *et al*., 2009). Fire frequency may be described as the number of fires per annum in a given area or the average time between burns in a certain area (Kruger, 1979a). Productivity in fynbos may allow accumulation of fuel for the spread of fires after four years of a preceding fire. Kruger (1979a) mentions human activities as the leading cause of fires in or close to major population centres. Lightning

strikes are seen to be the major cause of natural fires in the fynbos biome. Wildfires may increase during summer, but they may occur throughout the year irrespective of the season (Kruger, 1983). It is thus weather conditions, rather than season that dictate the occurrence of wildfires.

1.4 Study Area

The Harold Porter National Botanical Gardens (HPNBG) and Kogelberg Biosphere Reserve (KBR) near the coastal town of Betty's Bay (Figure 1.4) in the Western Cape were chosen as the study area in an attempt to focus on the geochemistry and nutrient source dynamics of a highly diverse fynbos ecosystem. The Kogelberg Biosphere Reserve, a conservation area of 100 000 ha, is situated 40 km east of Cape Town. The area lies adjacent to the Atlantic Ocean to the south and the Hottentots Holland Mountain range to the north. The Kogelberg Biosphere Reserve can be regarded as the heart of the Cape Floristic Region comprising the Kogelberg Sandstone Fynbos biome (Mucina and Rutherford, 2006) and is home to ~1650 plant species, of which 77 occur only within the boundaries of the KBR (Johns and Johns, 2001).

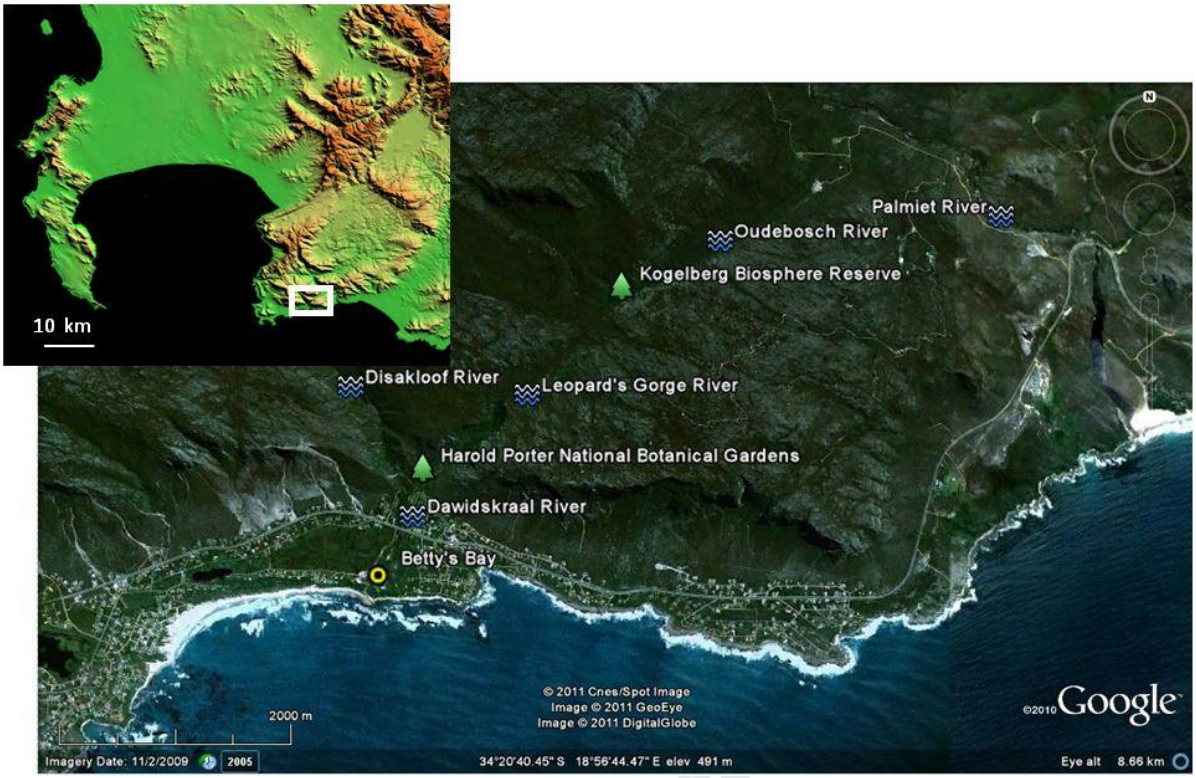

Figure 1.4. The location of the Harold Porter National Botanical Gardens (HPNBG) and the Kogelberg Biosphere Reserve (KBR) with the major rivers flowing through the nature conservation areas. The elevation map of the southwestern Cape (upper left corner) is courtesy of Computamaps.

The geology of the southwestern corner of Africa is dominated by the Cape Granite Suite (~540 Ma) and Cape Supergroup (~510 Ma). The mountains of the HPNBG and KBR are entirely composed of the Cape Supergroup, which consist of the Table Mountain, Bokkeveld and Witteberg groups. The Cape Supergroup forms part of the Cape Fold Belt Mountains, which folded and faulted during the collision of Africa, South America and Antarctica (Compton, 2004). The Cape Fold Belt is characterized by pronounced anticlinal mountain ranges with two main zones of folding. These two zones include a north-south trending western zone and an east-west trending eastern zone (Lambrechts, 1979). A syntaxis forms where the two zones meet in the southwest. The mountain ranges of the HPNBG and KBR form part of the weathered remains of the Cape Fold Belt orogeny that occurred approximately 300 million years ago (Johns and Johns, 2001). The Cedarberg Formation is composed of shale and the Pakhuis Formation formed from glacial till. Trace fossils from the TMG rocks suggest an age of 500 million years. Dating of zircon grains constrain the age of the lower TMG rocks to between 510 and 500 million years old. The topography of the mountains of the HPNBG and KBR reflect the underlying bedrock geology (Figure 1.5). The Peninsula Formation sandstone

forms higher more weather-resistant peaks whereas the Cedarberg, Goudini and Pakhuis Formations form the lower slopes of the mountains. River drainage and valleys are largely related to bedrock faults. The Peninsula Formation dominates in the south of the HPNBG and KBR. All sampling sites and material sampled in this study were located on or collected from Peninsula Formation sandstone. The mountains of the HPNBG show large-scale folding and faulting. Quartz veins on rocky outcrops were also observed. These observations bear testament to the deformational past of the area.

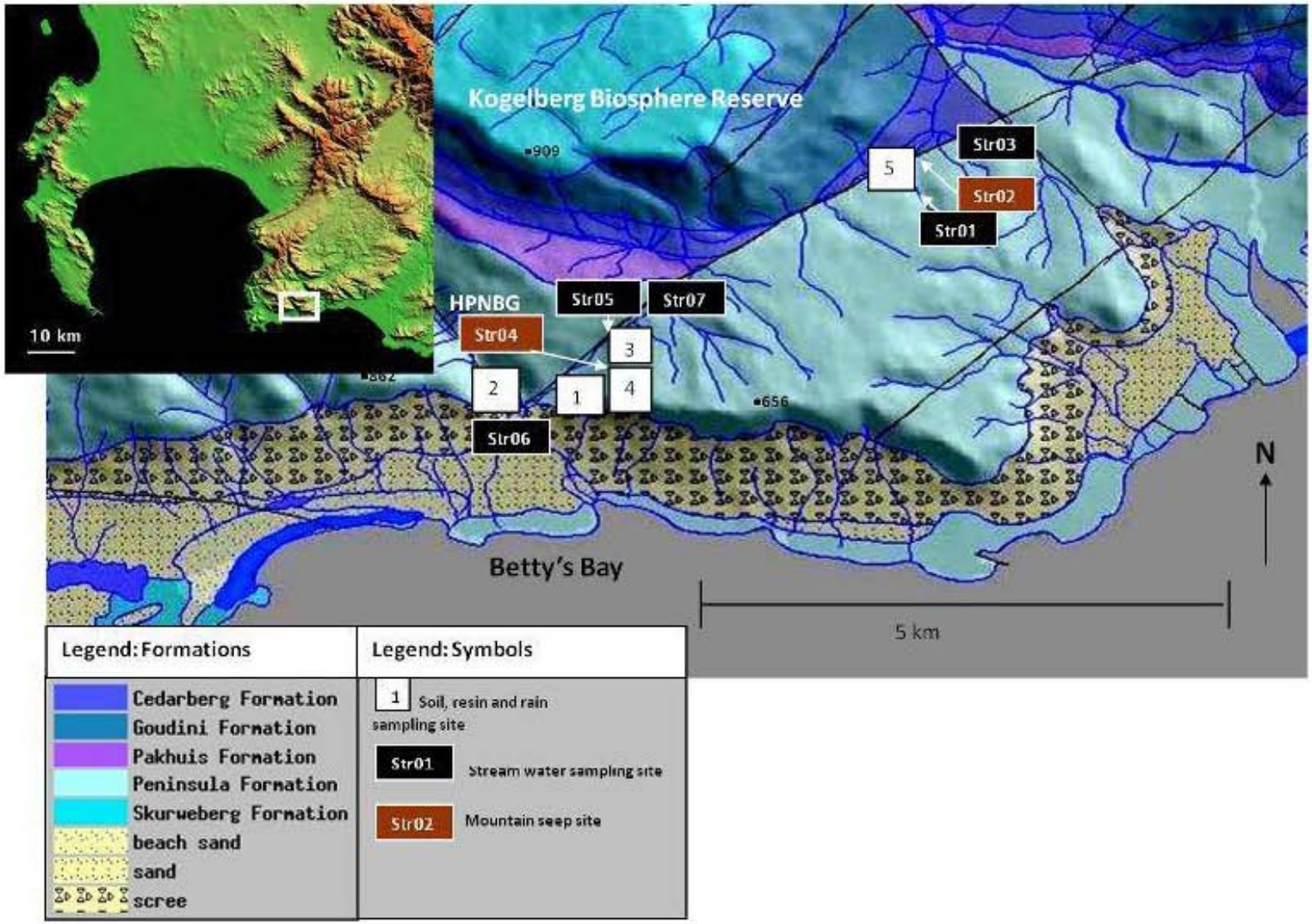

Figure 1.5. The location of the study area with its underlying bedrock geology illustrating the sampling sites in the Harold Porter National Botanical Gardens (HPNBG) and Kogelberg Biosphere Reserve (KBR). Black lines represent faults. Note that the formations outlined in the legend are not in stratigraphic order. Map modified from Smit (2003). The elevation map of the southwestern Cape is courtesy of Computamaps.

The soil of the study area is thin and quartz-rich. The roots of the vegetation may penetrate through rock fractures, but a tough, extensive root network attempts to maximize nutrient uptake. The chemistry of the soils will primarily reflect the underlying bedrock as no formations overlie the Peninsula sandstone.

The interplay of hydrology, surface and atmospheric processes can be assessed more thoroughly on the slopes of the HPNBG and the KBR than in other parts of the CFR. The sites form part of a protected area where anthropogenic influences are limited. Cultivation of fynbos vegetation takes place to the southeast of the KBR on Mountain Rose Farm. The full extent of the farming activities that takes place there is however not known. The Oudebosch and Leopard's Gorge Rivers together with its major tributaries provide a suitable source for the collection of surface water samples. The geology of the area allows for the sampling of homogeneous sandstone bedrock on both the seaward and leeward side of the mountainous terrain. The proximity of the HPNBG and the KBR to the Atlantic Ocean also provides an excellent opportunity to study the contribution of marine aerosol inputs to the fynbos ecosystem.

1.5 Study Objectives

The Peninsula Formation sandstone is nutrient poor (Soderberg and Compton, 2007). Silicate minerals within the sandstone (mica, feldspar, etc.) may weather and leach out of the bedrock, providing certain nutrients to the soil. Soderberg (2003) and Soderberg and Compton (2007) found that trace elements in soil such as Ni, Rb. Sc, Th, U, V, Y and Zr are supplied by bedrock weathering and are generally absent in rainwater. The weathering and breakdown of small amounts of interstitial mica and feldspar minerals may provide elements such as Ca, Mg and K to the soil. Bedrock weathering may not be the major source of nutrients to the ecosystem, but contributes nonetheless. It is for these reasons that bedrock analyses are included in this study. Peninsula Formation sandstone weathers slowly at a rate of 1 to 10 m/Myr (Kounov *et al*., 2007) and contains few minerals other than quartz, the supply of nutrients from the bedrock is unlikely to meet the demand of the plants. Additional inputs into the system are thus required. The source of these additional

nutrients to the sandstone fynbos biome is generally poorly understood and will form the focus of this study.

The main aim of this study is to quantify the input and output of different elements, some of which are important nutrients to the ecosystem, following a major fire event in an attempt to understand the interrelationships between various components of the Kogelberg Sandstone Fynbos Biome (Mucina and Rutherford, 2006). This will be done through the investigation of geochemical aspects of the Kogelberg Sandstone Fynbos within the Harold Porter National Botanical Gardens (HPNBG) and the southeastern sector of the Kogelberg Biosphere Reserve (KBR). Peninsula Formation bedrock was selected because of its homogeneous and simple chemistry. Bedrock geology influences the soil types (thickness and composition) as well as hydrology. Marine aerosols are predicted to be abundant from the adjacent coastline and dust may arrive from the continental interior. The study aims to determine the relative importance of marine and mineral (dust) aerosol deposition of elements important to the vegetation after a fire swept through the HPNBG and the KBR on 3 June 2010. This study addresses the following four objectives:

1. To determine and compare the chemical composition of rain water (wet and dry deposition), mountain seep and stream waters, Peninsula Formation bedrock and soils.

2. To determine the extent of a marine influence on ions in rain and stream water.

3. To determine the presence of clay minerals in the soil derived from weathering of the bedrock and from deposition of mineral dust (including fire ash).

4. To determine any changes in nutrient input over a one year period after the fire event of 3 June 2010.

It is hoped that the four objectives of this study will provide a better understanding into the geochemical aspects of nutrient dynamics of the sandstone fynbos ecosystem.

Chapter 2 : Materials and Methodology

Five sites were identified in the Harold Porter National Botanical Gardens (HPNBG) and the Kogelberg Biosphere Reserve (KBR) for the sampling of rain water, soil and bedrock (Table 2.1). Four sites along different topographic elevations were selected in the HPNBG (site 1 at an elevation of 43 m; site 2 at 205 m; site 3 at 370 m; site 4 at 543 m) and one site in the KBR (at 123 m elevation). The sites are spread along seaward and landward facing slopes.

Table 2.1. The sites within the study area where resin and rain collectors were deployed, their location, GPS coordinates and elevation.

Site	Gardens / Reserve	Coordinates	GPS Elevation
1	Harold Porter	34º20'57.9"S18º55'43.3"E	43m
2	Harold Porter	34º20'42.3"S18º55'44.9"E	201m
3	Harold Porter	34º20'37.9"S18º56'21.0"E	362m
4	Harold Porter	34º20'53.5"S18º56'21.7"E	537m
5	Kogelberg	34º19'47.0"S18º57'22.3"E	123m

A lightning storm broke out in the early morning hours of Thursday, 3 June 2010 causing a widespread fire in the Kogelberg Biosphere Reserve (KBR). A northwester wind blew through the area in a southeasterly direction towards and across the slopes of the Harold Porter National Botanical Gardens (HNBG) stripping the landscape of aboveground plant biomass (Figure 2.1). The last fire in the KBR and HPNBG was in 1991. The fire event of 2010 wiped out 90% of nearly 20 years of vegetation growth (Ms. J. Forrester, personal communication, 2010). This study was initiated immediately prior to the fire event and the study objectives were modified to include the monitoring of geochemical changes of the ecosystem after the fire as vegetation was re-established.

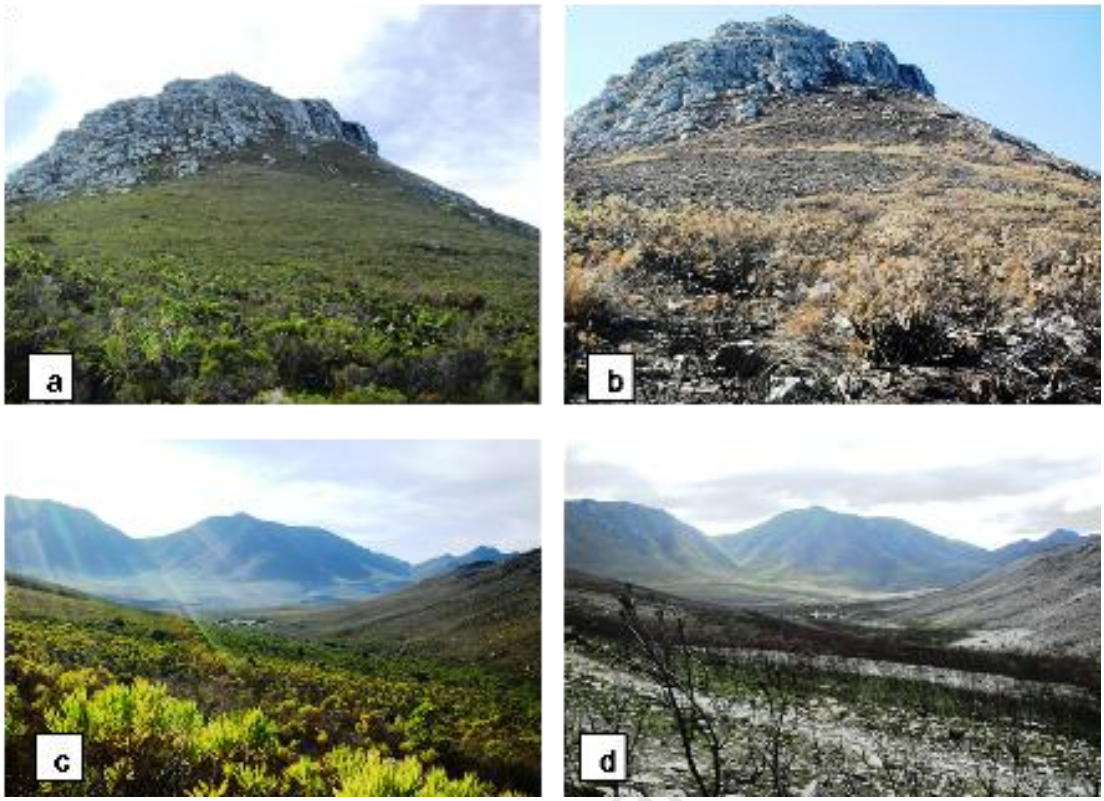

Figure 2.1. Before and after the fire at sites 1 and 5. a) Picture taken at site 1 on 30 May 2010 before the fire of 3 June 2010 b) Picture taken at site 1 on 17 June 2010 two weeks after the fire. c) Picture taken before the fire of 3 June 2010 at site 5 in the KBR. d) Picture taken at site 5 on 22 September 2010.

Vegetation before the fire on the slopes where site 2 was situated included mainly brunias and proteas. The slope of sites 1, 3 and 4 contained a very different plant species assemblage. Protea abundance decreased and ericas, restios and the bergpalmiet were more abundant on the slope to the east of the Leopard's Gorge. Afromontane vegetation can be found along the river banks of str01, str05, str06 and str07 (refer to Figure 1.5 for their locations) and was largely unaffected by the fire. Certain plant types such as ericas were ashed during the fire event. Taller and woodier vegetation such as proteas and brunias were left as partially burnt charcoalized wood. Proteas regenerated through the release of their seeds. The bergpalmiet proved more resilient and was largely unaffected. Vegetation grew back and started to repopulate the landscape within a period of less than four months. Regrowth of the vegetation was however very slow and large patches of land were still bare after one year following the fire event (Figure 2.1 and Appendix D).

2.1 Field Sampling and laboratory preparation

Field samplers (Figure 2.2) were placed at the 5 sites throughout a period of one year. The samplers were constructed to capture rainwater using an ion exchange resin column and a simplified rain collector. All collectors were placed at an E-W orientation, perpendicular to the dominant wind directions to ensure consistency. Soil and bedrock samples were collected within a 5 m radius of the 5 field sites. Stream waters were sampled along rivers, tributaries and mountain seeps.

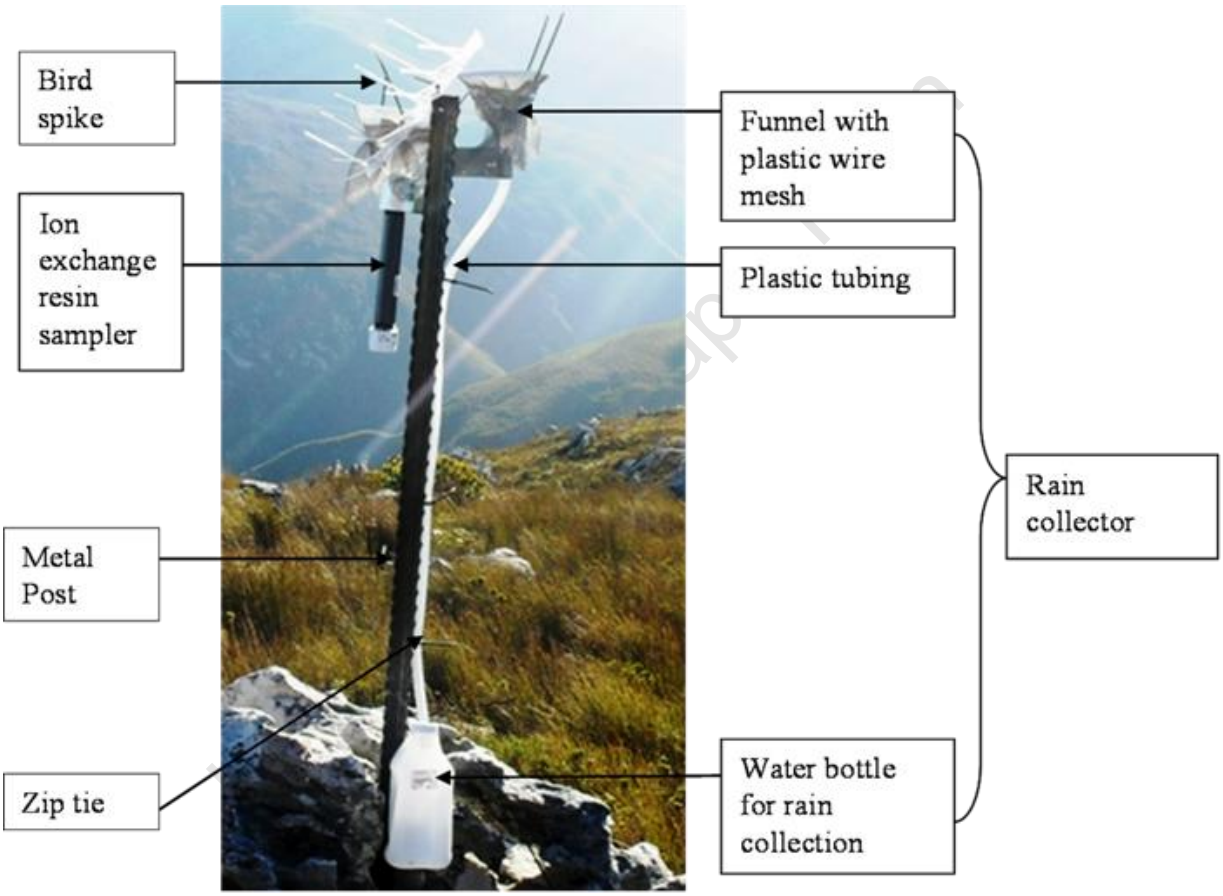

Figure 2.2. Ion exchange resin collector for sampling atmospheric aerosols and a rainwater collector attached to a metal post at site 4 in the Harold Porter National Botanical Gardens.

Resin extracts, rainwater and stream water samples were collected roughly every month (Table 2.2). Ion exchange resin columns were deployed in the field. The resin extraction method was later found to be problematic and for this reason, the protocol was not recorded in this thesis.

Table 2.2. The sampling periods for this study. SPEs = (soil) saturated paste extracts.

Sampling period	Total number of days	Abbreviation used for resin and rain data	Abbreviation used for streams and soil SPEs data
17 June 2010 to 15 July 2010	28	**Jun/Jul**	**17 Jun**
15 July 2010 to 17 August 2010	33	**Jul/Aug**	**15 Jul**
17 August 2010 to 22 September 2010	36	**Aug/Sep**	**17 Aug**
22 September 2010 to 22 October 2010	30	**Sep/Oct**	**22 Sep**
22 October 2010 to 23 November 2010	32	**Oct/Nov**	**22 Oct**
23 November 2010 to 11 January 2011	49	**Nov/Jan**	**23 Nov**
11 January to 10 February 2011	29	**Jan/Feb**	**11 Jan**
10 February to 25 March 2011	43	**Feb/Mar**	**10 Feb**
25 March to 29 April 2011	35	**Mar/Apr**	**25 Mar**
29 April to 1 June 2011	33	**Apr/Jun**	**29 Apr**

Soil samples were collected quarterly and bedrock samples only once throughout the one year period of this study (Table 2.3).

Table 2.3. Dates of sampling atmospheric aerosols, rainwater, stream water, soils and bedrock. Shaded regions indicate date of sampling.

	17 Jun	**15 July**	**17 Aug**	**22 Sep**	**22 Oct**	**23 Nov**	**11 Jan**	**10 Feb**	**25 Mar**	**29 Apr**	**1 Jun**
Rainwater											
Streamwater											
Soils											
Bedrock											

2.1.1 Rainwater Sampling

The collectors were designed to be inexpensive and in any event of damage, could be easily replaced and in the least amount of time possible. The funnels of the rainwater collectors were fastened with an aluminum plate to the metal post in an easterly direction at all sites. A 12 cm diameter funnel lined with plastic mesh (as with the resin collectors) was connected to a 10 mm diameter thick walled plastic tube, approximately 1 m in length. The tube entered a 2 litre plastic bottle. The tube and bottle were fastened to the metal post by means of zip-ties. Plastic spikes were tied on top of the posts and zip-ties lined along the funnels in an attempt to prevent birds from perching on the collectors. Ant repellant was applied at the bottom of the metal post below the rain collectors in an attempt to prevent insects from crawling on and into the collectors. The collectors were approximately at a height of 1.5 m to mimic the height of the vegetation.

Upon returning to UCT, the rain water samples were filtered with a 0.45 μm, size 47 mm filter membrane in a Millipore filter vacuum system. The 0.45 μm filter membrane is standard and prevents any larger particles (ash, dust, sand and organic debris) from being incorporated in the analyses. All filtration materials and self-standing centrifuge tubes were triple rinsed in milli-Q water and the inside of the centrifuge tubes shaken with 5 to 10 ml of the sample. Rainwater samples were then divided into 50 ml self-standing centrifuge tubes and refrigerated before ICP-MS and IC analyses were carried out on the samples.

2.1.2 Stream water sampling

Stream water (main streams and mountain seeps) samples were sampled monthly. Five main streams (str01, str03, str05, str06 and str07) and two mountain seeps (str02, str04) were sampled (Table 2.4). The first batch of samples was collected on 17 June 2010, two weeks after a fire broke out in the HPNBG and KBR. Stream water was collected in pre-cleaned 250 ml sampling bottles. The samples were then taken to UCT for ICP-MS and IC analyses. The samples were filtered through a 0.45 μm, size 47 mm filter membrane in a Millipore filtration vacuum system and placed into 50 ml milli-Q triple rinsed self-standing centrifuge tubes before analysis.

Table 2.4. Location, GPS coordinates and elevation of stream and mountain seep water sampled during the course of this study.

Sample name	Location	GPS coordinates	Elevation (m above sea level)
str01	Kogelberg Reserve. Main stream crossing the hiking trail along the Oudebosch River near site 5.	34º19'48.8"S18º57'24.1"E	105
str02	Kogelberg Reserve. Seepage flowing into the Oudebosch River. Drains only Peninsula sandstone	34º19'47.2"S18º57'28.1"E	105
str03	Kogelberg Reserve. Stream flowing into weir next to the Oudebosch River. Drains only Peninsula sandstone	34º19'43.3"S18º57'41.5"E	96
str04	A mountain seep on the slope of the HPNBG near sites 3 and 4. Flowed only during periods of high rainfall. Drains only Peninsula sandstone	34º20'48.7"S18º56'25.1"E	500
str05	Harold Porter National Botanical Gardens (HPNBG) near the Leopard's Gorge waterfall.	34º20'33.6"S18º56'08.5"E	260
str06	Forms part of the Dawidskraal River in the HPNBG. The stream drained catchments that may have been unaffected by the fire, but the extent is unclear.	34º21'02.1"S18º55'35.0"E	31
str07	Forms part of a major tributary of the Leopards Gorge River in the HPNBG.	34º20'25.6"S18º56'23.5"E	301

Samples from the Oudebosch River were labeled stream 1 (str01). The Oudebosch River forms a major eastward flowing tributary of the Palmiet River. Samples labeled stream 3 (str03) were collected immediately to the north of the border between the KBR and the Mountain Rose Farm. These samples were collected just before the stream reached a weir. Samples labeled stream 5 (str05) were collected along the course of the Leopard's Gorge River before the river reaches a waterfall and joins the Dawidskraal River to the south. Samples labeled stream 6 (str06) were collected along the Dawidskraal River to the west of the HPNBG. Samples labeled str07 were collected up course of the Leopard's Gorge River.

In addition to the stream water samples, samples were also collected from mountain seeps. Mountain seeps did however not flow throughout the year and were present during months of high precipitation. Samples labeled str02 were collected from a mountain seep located along a footpath in the KBR approximately midway between str01 and str03. Mountain seep str02 joined up with the Oudebosch River during high rainfall months. Samples labeled str04 were collected from a mountain seep close to the rainwater sampling site 4 in the HPNBG. Mountain seep str04 was located at a higher elevation and was also dried up for most of the year.

Measurement of rain and stream water pH was taken with a portable PHM201 pH meter which has a glass combination electrode. The pH values on the pH meter are displayed on an electronic readout. Stream water pH readings were taken in the stream as the water was flowing and in standing water within the sampling bottle.

2.1.3 Soil sampling and saturated paste extracts

Soil samples were collected by taking and mixing four subsamples in four different directions at a distance of 5 m from the field samplers at sites 1 to 5. Top soil (uppermost 2-4 cm) and subsoil (2-8 cm below the surface) samples were taken where the soil was sufficiently thick. Where the soil profile was too thin (<4 cm), only a total soil sample was collected.

The soil samples that were collected in the field were first air-dried and sieved into larger than and less than 2 mm fractions upon return to UCT. Soil can be defined as having grain

sizes less than 2 mm. An amount of between 150 and 250 g of the air-dried sieved samples were placed into a plastic container. A saturated paste extract of the soil was obtained by gradually adding Milli-Q water whilst mixing with a wooden spatula. The paste surface should glisten and have a slight flow (Zhang *et al*., 2005; Gartley, 2009). Water should not collect freely at the top of the surface. Each sample was then slightly oversaturated with a few more millimeters of Milli-Q water to counteract the effect of evaporation. The saturated pastes were then extracted within a maximum period of 24 hours under vacuum and filtered with number 42 Whatman filter paper. The extractant was then divided into pre-cleaned 50 ml freestanding centrifuge tubes. The soil SPE samples were then analysed by ICP-MS and IC.

A homogeneous subsample of 80 g of the air-dried soil samples were crushed into fine powders in a sieb mill and submitted for X-ray diffraction (XRD), X-ray fluorescence (XRF), and organic carbon analysis.

2.1.4 Bedrock sampling

Bedrock samples were collected by hammering off pieces of exposed bedrock or large in place boulders in four directions at a distance of 5 m from the field samplers at sites 1 to 5. The rock type was exclusively Peninsula Formation sandstone and the least altered bedrock was sampled (hardest and not showing signs of chemical leaching). Bedrock samples were crushed by a jaw crusher and powdered by a sieb mill in the geological sciences building at UCT. Powdered samples were submitted for XRF analysis.

2.2 Laboratory Analyses

Rainwater, stream and mountain seep water samples were analysed for major ions (Cl, Mg, SO_4, Mg, Ca and K) through ICP-MS and IC. Soils were saturated in Milli-Q water to get a saturated paste extract (SPE). The soil SPE samples were analysed through ICP-MS and IC. Powdered sand size fractions (<2 mm) of the soil samples were analysed for element composition by XRF, mineralogy by XRD and organic carbon content by an elemental analyzer. The mineralogy of the powdered bedrock samples was determined through XRD analysis.

Table 2.5. Laboratory analyses undertaken for the different types of samples collected in this study. The shaded regions indicate the analytical method used for each sample type.

Analytical Method	Rain water	Stream water	Soils	Bedrock
Inductively coupled plasma mass spectrometry (ICPMS)				
Ion chromatography (IC)				
X-Ray fluorescence (XRF)				
X-Ray diffraction (XRD)				
Organic carbon (δ13C)				

2.2.1 ICP-MS Analysis

The major cations, Mg and Ca and trace elements, Mn and Sr in rainwater, stream water and soil paste extract samples were measured with the inductively-coupled plasma mass spectrometer facility in the geological sciences department at UCT. The samples were diluted by a factor of 1:100 and an internal standard of 10 ppb In, Re, Rh and Bi and 5% nitric acid were added. The samples were run against a blank and three standards made from artificial solutions.

2.2.2 IC Analysis

Anions (Cl and SO_4) and cations (Na, K, Mg and Ca) in rainwater, stream water and soil paste extract samples were measured at the ion-chromatography facility in the soil sciences department at Stellenbosch University using a Dionex DX-120 Ionchromotograph.

2.2.3 Petrography and Photomicrography

Thin sections from all 5 bedrock samples were examined under an Olympus SZX12 microscope mounted with an Olympus SC-5060 camera, as well as a computer-linked Nikon Optiphoto microscope fitted with an Olympus SC20 digital camera. This allowed for the visual identification of minerals and description of texture.

2.2.4 Grain Size Analysis

Soil samples were sieved into greater than and less than 2 mm fractions after air-drying. Approximately 80 g of <2 mm fractions were suspended in water and wet-sieved through a 63 μm and 38 μm sieve to separate the sand and coarse silt fractions, respectively. The fine silt fraction (2-38 μm) was allowed to settle. The sand and silt fractions were dried and weighed. The mass of the clay fraction was determined by the difference. The settled clay size fractions were further analysed by XRD analysis.

2.2.5 X-Ray Diffraction (XRD) Analysis

Mineralogy of soil and bedrock samples were analysed by X-ray diffraction. Settled clay fractions of each soil sample were pipetted onto a glass slide and allowed to dry (usually after a period of 24 hours). The dried clay fraction slide was then placed into an x-ray diffractometer where a continuous scan of 2 theta was measured. The oven-dried (at a temperature of 60°C) clay fraction of the subsoil of site 1 was powdered by hand with mortar and pestle. The powdered fraction was then evenly smeared onto a slide and placed into the x-ray diffractometer.

2.2.6 X-Ray Fluorescence (XRF) Analysis

The element composition (major and trace oxides) of soil and bedrock samples were analysed by X-Ray Fluorescence. Rock samples were split, crushed and finally ground in a sieb mill. Soil samples were also ground to a fine powder in a sieb mill. All samples (approximately 2 g) were dried at 110°C for at least four hours and weighed, after which they were roasted at 850°C overnight and reweighed. Six grams of flux (lithium tetraborate; dried overnight at 450°C) was used to dilute 0.7 g of sample (both accurate to four decimal

places). The resulting mixture was stored briefly in a desiccator, before fusion discs were prepared and XRF analysis run on the samples.

2.2.7 Organic Carbon and Carbon Isotope Analysis

Soil samples were analyzed for organic carbon in the Archaeology department of UCT. Samples were weighed on a Sartorius micro-balance to 1 mg into tin cups. The samples were then combusted in a Flash EA 112 series elemental analyzer. The gases were passed into a Delta Plus XP IRMS (Isotope Ratio Mass Spectrometer) through a Conflo III gas control unit. Standards used in the analysis included a Merck proteinaceous gel and dried lentils. All in-house standards were calibrated against IAEA (International Atomic Energy Agency) standards. Carbon isotopes are expressed relative to PDB (Pee-Dee Belemnite).

Chapter 3 : Results

3.1 Rainfall

Rainfall was measured at all 5 sites and compared to rainfall data from the HPNBG office (Table 3.1 and Table 3.2). Temperature and wind direction were also supplied by the office.

Table 3.1. Temperature, wind and days with rain in the HPNBG.

	Jun/ Jul	**Jul/ Aug**	**Aug/ Sep**	**Sep/ Oct**	**Oct/ Nov**	**Nov/ Jan**	**Jan/ Feb**	**Feb/ Mar**	**Mar/ Apr**	**Apr/ Jun**
Average Maximum T (°C)	18.0	18.5	19.0	19.5	21.0	22.0	25.0	25.0	24.0	20.0
Average Minimum T (°C)	11.0	11.0	12.0	13.0	14.5	16.0	13.0	18.0	14.0	13.0
Number of rain days	7	7	9	7	14	13	6	4	6	11
Days with NW winds	23	20	16	17	18	6	13	2	13	29
Days with NE winds	-	3	3	-	1	1	4	9	2	3
Days with SW winds	-	-	-	-	-	2	-	-	-	-
Days with SE winds	3	8	14	11	11	43	11	26	14	1

Table 3.2. Average daily rainfall in mm for the 5 sites in this study and for the site at the HPNBG monitored by their offices. NM = not measured due to rain collector malfunction.

	Jun/Jul	Jul/Aug	Aug/Sep	Sep/Oct	Oct/Nov	Nov/Jan	Jan/Feb	Feb/Mar	Mar/Apr	Apr/Jun
Site 1	5.9	2.1	3.4	2.8	5.7	2.4	0.5	1.1	2.6	4.8
Site 2	3.9	1.2	1.6	1.8	5.8	1.7	0.5	0.7	2.1	3.9
Site 3	7	1.3	4.6	NM	6.5	3.2	0.4	1	3	4.5
Site 4	4.4	1.5	1.7	1.6	6.3	3	1	1.7	1.4	2.2
Site 5	7	1.9	4.8	3.5	5.7	3.3	1	1.5	3.7	5.7
HPNBG	4.3	1.2	3.1	1.7	6.3	1.9	1.8	0.5	1.7	3.4

3.2 Major and Trace Element Composition in Rainwater

This section presents rainwater chemistry results as determined by ICP-MS and IC analyses (Table 3.3 to Table 3.12). Concentrations of major ions (Cl, Na, SO_4, Mg, Ca and K) in rain, surface waters (rivers and mountain seeps) and soil saturated paste extracts (SPEs) are presented in mmol/l. Concentrations of trace elements (Mn and Sr) in rainwater samples are presented in nmol/l. Duplicate analyses were run for randomly selected samples based on the availability of samples. ICP-MS duplicates were carried out at UCT and at the University of Colorado, Boulder. Duplicate samples were analysed through the IC facility at Stellenbosch University. Anion (Cl, and SO_4) concentrations could not be determined for resin extract samples as acid treated samples present an artificially high Cl peak which may render the sample unsuitable for anion analysis.

Standard solutions were not run on ICP-MS and IC as it is difficult to mimic the natural composition of rainwater and stream water. Rainwater may contain fine ash particles and land-derived dust. Stream water will additionally also contain soil derived particles, decomposing plant litter and dissolved organic carbon.

Table 3.3. Chloride concentrations in rainwater samples expressed in mmol/l as determined by IC analysis. Values in parentheses indicate a duplicate run for that sample. ND = not determined.

Cl in mmol/l										
	Jun/Jul	**Jul/Aug**	**Aug/Sep**	**Sep/Oct**	**Oct/Nov**	**Nov/Jan**	**Jan/Feb**	**Feb/Mar**	**Mar/Apr**	**Apr/Jun**
Site 1	0.310	0.790	0.300 (0.290)	0.580	0.240	0.610	0.970	0.900 (0.870)	0.570	0.320
Site 2	0.410	0.730	0.330 (0.260)	0.610	0.230	0.360	0.670	0.620 (0.610)	0.680	0.390 (0.380)
Site 3	0.280	0.510	0.260	ND	0.170	0.280	0.790	0.860	0.540 (0.540)	0.320
Site 4	0.230	0.830	0.560	0.680	0.210	ND	1.000	0.510 (0.520)	1.010	0.540
Site 5	0.270	0.350	0.780	0.380 (0.360)	0.190	0.390	1.020	0.980	0.490 (0.500)	0.270 (0.280)

Table 3.4. Sodium concentrations rainwater samples expressed in mmol/l as determined by IC-PMS analysis. Values in parentheses indicate a duplicate run for that sample. ND = not determined.

Na in mmol/l										
	Jun/Jul	**Jul/Aug**	**Aug/Sep**	**Sep/Oct**	**Oct/Nov**	**Nov/Jan**	**Jan/Feb**	**Feb/Mar**	**Mar/Apr**	**Apr/Jun**
Site 1	0.160	0.430	0.250 (0.270)	0.420	0.200	0.380	0.750	0.522 (0.517)	0.430	0.270
Site 2	0.160	0.500	0.250 (0.250)	0.420	0.200	0.430	0.540	0.391 (0.300)	0.500	0.330 (0.320)
Site 3	0.130 (0.130)	0.370	0.230	ND	0.170	0.300	0.650	0.317	0.400 (0.400)	0.270
Site 4	0.150	0.500	0.410	0.510	0.190	0.250	0.790	0.343 (0.326)	0.680	0.430
Site 5	0.130	0.270	0.240	0.320 (0.320)	0.170	0.330	0.800	0.543	0.370 (0.380)	0.230 (0.190)

Table 3.5. Sulphate concentrations in rainwater samples expressed in mmol/l as determined by IC analysis. Values in parentheses indicate a duplicate run for that sample. ND = not determined

SO_4 in mmol/l										
	Jun/Jul	**Jul/Aug**	**Aug/Sep**	**Sep/Oct**	**Oct/Nov**	**Nov/Jan**	**Jan/Feb**	**Feb/Mar**	**Mar/Apr**	**Apr/Jun**
Site 1	0.030	0.320	0.110 (0.040)	0.070	0.030	0.140	0.540	0.084 (0.079)	0.060	0.040
Site 2	0.320	0.320	0.230 (0.050)	0.070	0.140	0.250	0.320	0.058 (0.040)	0.060	0.040 (0.030)
Site 3	0.300	0.160	0.090	ND	0.210	0.190	0.300	0.0930	0.050 (0.050)	0.020
Site 4	0.200	0.530	0.160	0.090	0.270	ND	0.550	0.0630 (0.060)	0.090	0.050
Site 5	0.280	0.060	0.510	0.050 (0.090)	0.280	0.310	0.520	0.070	0.040 (0.040)	0.020 (0.00)

Table 3.6. Magnesium concentrations in in rainwater samples expressed in mmol/l as determined by ICP-MS analysis. Values in parentheses indicate a duplicate run for that sample. ND = not determined

Mg in mmol/l (ICP-MS)										
	Jun/Jul	**Jul/Aug**	**Aug/Sep**	**Sep/Oct**	**Oct/Nov**	**Nov/Jan**	**Jan/Feb**	**Feb/Mar**	**Mar/Apr**	**Apr/Jun**
Site 1	0.054	0.051	0.029	0.012	0.024	0.027	0.078	0.059	0.063	0.029
Site 2	0.057	0.066	0.029	0.055	0.024	0.051	0.055	0.065	0.067	0.045
Site 3	0.057	0.045	0.024	ND	0.019	0.032	0.076	0.067	0.052	0.031
Site 4	0.012	0.037	0.049	0.051	0.035	0.028	0.099	0.048	0.097	0.053
Site 5	0.015	0.032	0.026	0.021	0.019	0.051	0.099	0.070	0.050	0.029

Table 3.7. Magnesium concentrations in in rainwater samples expressed in mmol/l as determined by IC analysis. Values in parentheses indicate a duplicate run for that sample. ND = not determined

Mg in mmol/l (IC)										
	Jun/Jul	**Jul/Aug**	**Aug/Sep**	**Sep/Oct**	**Oct/Nov**	**Nov/Jan**	**Jan/Feb**	**Feb/Mar**	**Mar/Apr**	**Apr/Jun**
Site 1	0.067	0.133	0.083	0.142	0.075	0.142	0.158	0.079 (0.079)	0.142	0.062
Site 2	0.058	0.175	0.092	0.142	0.067	0.067	0.117	0.061 (0.053)	0.151	0.080 (0.080)
Site 3	0.050	0.133	0.075	ND	0.058	0.058	0.150	0.057	0.124 (0.124)	0.062
Site 4	0.058	0.175	0.158	0.175	0.067	0.108	0.192	0.061 (0.057)	0.222	0.107
Site 5	0.050	0.100	0.092	0.117	0.058	0.075	0.183	0.083	0.124 (0.116)	0.062 (0.062)

Table 3.8. Calcium concentrations in rainwater samples expressed in mmol/l as determined by ICP-MS analysis. Values in parentheses indicate a duplicate run for that sample. ND = not determined

Ca in mmol/l (ICP-MS)										
	Jun/Jul	**Jul/Aug**	**Aug/Sep**	**Sep/Oct**	**Oct/Nov**	**Nov/Jan**	**Jan/Feb**	**Feb/Mar**	**Mar/Apr**	**Apr/Jun**
Site 1	0.010	0.029	0.010	0.007	0.012	0.012	0.014	0.027	0.009	0.005
Site 2	0.007	0.035	0.007	0.022	0.006	0.006	0.009	0.031	0.018	0.011
Site 3	0.035	0.024	0.005	ND	0.005	0.006	0.015	0.031	0.007	0.007
Site 4	0.008	0.019	0.011	0.016	0.020	0.015	0.021	0.021	0.047	0.021
Site 5	0.007	0.014	0.005	0.007	0.004	0.006	0.027	0.024	0.017	0.015

Table 3.9. Calcium concentrations in rainwater samples expressed in mmol/l as determined by IC analysis. Values in parentheses indicate a duplicate run for that sample. ND = not determined

Ca in mmol/l (IC)										
	Jun/Jul	**Jul/Aug**	**Aug/Sep**	**Sep/Oct**	**Oct/Nov**	**Nov/Jan**	**Jan/Feb**	**Feb/Mar**	**Mar/Apr**	**Apr/Jun**
Site 1	0.021	0.052	0.023	0.047	0.023	0.036	0.044	0.048 (0.043)	0.053	0.027
Site 2	0.018	0.049	0.031	0.042	0.018	0.023	0.036	0.037 (0.027)	0.075	0.032 (0.032)
Site 3	0.013	0.044	0.023	ND	0.016	0.026	0.039	0.027	0.053 (0.064)	0.027
Site 4	0.016	0.044	0.049	0.036	0.016	0.047	0.060	0.037 (0.037)	0.128	0.048
Site 5	0.016	0.023	0.031	0.029	0.013	0.026	0.057	0.045	0.069 (0.053)	0.032 (0.037)

Table 3.10. Potassium concentrations in rainwater samples expressed in mmol/l as determined by IC analysis. Values in parentheses indicate a duplicate run for that sample. ND = not determined

K in mmol/l										
	Jun/Jul	**Jul/Aug**	**Aug/Sep**	**Sep/Oct**	**Oct/Nov**	**Nov/Jan**	**Jan/Feb**	**Feb/Mar**	**Mar/Apr**	**Apr/Jun**
Site 1	0.023	0.035	0.008 (0.010)	0.117	0.064	0.018	0.020	0.015 (0.018)	0.041	0.010
Site 2	0.008	0.018	0.010 (0.010)	0.015	0.008	0.008	0.013	0.026 (0.015)	0.018	0.010 (0.010)
Site 3	0.005 (0.005)	0.013	0.008	ND	0.008	0.010	0.018	0.015	0.036 (0.033)	0.010
Site 4	0.005	0.015	0.013	0.015	0.008	0.010	0.020	0.015 (0.015)	0.018	0.015
Site 5	0.005	0.008	0.008	0.010 (0.010)	0.005	0.010	0.020	0.015	0.013 (0.013)	0.008 (0.005)

Table 3.11. Manganese concentrations in rainwater samples expressed in nmol/l as determined by ICPMS. Values in parentheses indicate a duplicate run for that sample. ND = not determined.

Mn in nmol/l										
	Jun/Jul	**Jul/Aug**	**Aug/Sep**	**Sep/Oct**	**Oct/Nov**	**Nov/Jan**	**Jan/Feb**	**Feb/Mar**	**Mar/Apr**	**Apr/Jun**
Site 1	175	45	6	15	16	74	81	204	111	2
Site 2	391	95	40	63	23	33	54	206	92	70
Site 3	69	138	44	ND	38	27	45	252	28	55
Site 4	68	167	50	117	428	42	66	199	222	66
Site 5	82	52	21	13	11	29	57	184	101	24

Table 3.12. Strontium concentrations in rainwater samples expressed in nmol/l as determined by ICP-MS. Values in parentheses indicate a duplicate run for that sample. ND = not determined.

Sr in nmol/l										
	Jun/Jul	**Jul/Aug**	**Aug/Sep**	**Sep/Oct**	**Oct/Nov**	**Nov/Jan**	**Jan/Feb**	**Feb/Mar**	**Mar/Apr**	**Apr/Jun**
Site 1	46	151	59	27	61	60	154	174	109	57
Site 2	43	150	61	121	50	29	121	183	148	76
Site 3	50	103	49	57	ND	26	142	184	97	59
Site 4	41	134	96	107	68	41	187	137	263	102
Site 5	37	65	52	48	39	41	187	163	106	60

3.3 Major and Trace Elements in Stream Waters and Soil Saturated Paste Extracts

Stream waters were sampled monthly and soils collected seasonally (winter – June 2010, spring – October 2010, summer – January 2011 and autumn – March 2011). Mountain seeps (str02 and str04) did not flow throughout the year and concentrations are omitted for periods when the seeps were dried up due to reduced rainfall.

Table 3.13. Chloride concentrations in streams and soil SPEs measured in mmol/l as determined by IC analysis. Values in parentheses indicate a duplicate run for that sample. DNF = did not flow. DNS = did not sample. ND = not determined.

Cl in mmol/l											
Streams	**17 Jun**	**15 Jul**	**17 Aug**	**22 Sep**	**22 Oct**	**23 Nov**	**11 Jan**	**10 Feb**	**25 Mar**	**29 Apr**	**1 Jun**
str01	0.649	0.748	0.942	0.843	0.801	0.654 (0.635)	0.739	0.815	0.843	0.818 (0.795)	0.705
str02	0.973	0.835	DNF	DNF	0.750	0.632 (0.598)	DNF	DNF	DNF	DNF	0.665 (0.663)
str03	0.725	0.883	1.331	1.142	0.671 (0.654)	0.654	0.618	0.316	0.733 (0.733)	0.680	0.578
str04	1.078	1.027	DNF	DNF	DNF	DNF	DNF	DNF	DNF	DNF	0.691 (0.683)
str05	1.072	1.111	0.945	0.776	0.824 (0.810)	0.671	0.663 (0.595)	0.671	0.736 (0.717)	0.835 (0.821)	0.705
str06	0.956	ND	0.894	0.894	0.776 (0.750)	0.671	0.370	0.460	0.747 (0.744)	0.846	0.708
str07	DNS	0.827	0.841	0.945	0.849	0.733	0.609	0.547	0.841	0.849 (0.846)	0.756 (0.742)
Soil Saturated Paste Extracts (SPEs)											
topsoil 1	0.288	-	-	-	0.310	-	0.358	-	0.900	-	-
subsoil 1	0.226	-	-	-	0.302	-	0.285	-	0.533	-	-
topsoil 2	0.457	-	-	-	0.265	-	0.567	-	0.925	-	-
subsoil 2	0.310	-	-	-	0.276	-	0.214	-	0.666	-	-
soil 3	0.288	-	-	-	0.260	-	0.313	-	0.748	-	-
soil 4	0.237	-	-	-	0.299	-	0.265	-	0.708	-	-
topsoil 5	0.186	-	-	-	0.220	-	0.279	-	0.564	-	-
subsoil 5	0.240	-	-	-	0.200	-	0.268	-	0.536	-	-

Table 3.14. Sodium concentrations in stream waters and soil SPEs measured in mmol/l as determined by IC analysis. Values in parentheses indicate a duplicate run for that sample. DNF = Did not flow. DNS = did not sample. ND = not determined.

Na in mmol/l											
Streams	**17 Jun**	**15 Jul**	**17 Aug**	**22 Sep**	**22 Oct**	**23 Nov**	**11 Jan**	**10 Feb**	**25 Mar**	**29 Apr**	**1 Jun**
str01	0.557	0.535	0.626	0.587	0.561	0.504	0.57	0.574	0.626	0.617 (0.622)	0.574
str02	0.626	0.552	DNF	DNF	0.565	0.483	DNF	DNF	DNF	DNF	0.522 (0.53)
str03	0.543	0.535	0.496	0.430	0.500	0.487	0.517	0.252	0.543 (0.548)	0.530	0.465
str04	0.817	0.743	DNF	DNF	DNF	DNF	DNF	DNF	DNF	DNF	0.596 (0.574)
str05	0.730	0.730	0.643	0.517	0.583	0.509	0.483	0.530	0.588 (0.548)	0.661 (0.643)	0.557
str06	0.691	ND	0.561	0.557	0.557	0.517	0.300	0.417	0.604 (0.600)	0.626	0.548
str07	DNS	0.613	0.591	0.587	0.622	0.539	0.491	0.378	0.635	0.648 (0.661)	0.582 (0.587)
Soil Saturated Paste Extracts (SPEs)											
topsoil 1	0.443	-	-	-	0.465	-	0.443	-	0.822	-	-
subsoil 1	0.348	-	-	-	0.478	-	0.413	-	0.457	-	-
topsoil 2	0.704	-	-	-	0.409	-	0.683	-	1.070	-	-
subsoil 2	0.478	-	-	-	0.426	-	0.383	-	0.857	-	-
soil 3	0.443	-	-	-	0.400	-	0.400	-	0.752	-	-
soil 4	0.365	-	-	-	0.461	-	0.322	-	0.809	-	-
topsoil 5	0.339	-	-	-	0.287	-	0.396	-	0.604	-	-
subsoil 5	0.309	-	-	-	0.370	-	0.322	-	0.522	-	-

Table 3.15. Sulphate concentrations in stream waters and soil SPEs measured in mmol/l as determined by IC analysis. Values in parentheses indicate a duplicate run for that sample. DNF = did not flow. DNS = did not sample. ND = Not determined.

SO_4 in mmol/l											
Streams	**17 Jun**	**15 Jul**	**17 Aug**	**22 Sep**	**22 Oct**	**23 Nov**	**11 Jan**	**10 Feb**	**25 Mar**	**29 Apr**	**1 Jun**
str01	0.247	0.310	0.242	0.216	0.190	0.119	0.125	0.118	0.036	0.072 (0.064)	0.040
str02	0.196	0.334	DNF	DNF	0.203	0.120	DNF	DNF	DNF	DNF	0.067 (0.075)
str03	0.208	0.283	0.332	0.358	0.133	0.133	0.034	0.080	0.049 (0.058)	0.056	0.048
str04	0.299	0.116	DNF	DNF	DNF	DNF	DNF	DNF	DNF	DNF	0.081 (0.092)
str05	0.291	0.270	0.245	0.217	0.199	0.147	0.090	0.144	0.067 (0.069)	0.096 (0.096)	0.097
str06	0.276	ND	0.130	0.255	0.066	0.150	0.086	0.116	DNF	0.083	0.104
str07	DNS	0.173	0.170	0.263	0.164	0.160	0.143	0.140	0.085	0.078 (0.079)	0.104 (0.043)
Soil Saturated Paste Extracts (SPEs)											
topsoil 1	0.041	-	-	-	0.057	-	0.048	-	0.157	-	-
subsoil 1	0.034	-	-	-	0.061	-	0.041	-	0.050	-	-
topsoil 2	0.108	-	-	-	0.064	-	0.121	-	0.164	-	-
subsoil 2	0.074	-	-	-	0.047	-	0.038	-	0.143	-	-
soil 3	0.085	-	-	-	0.059	-	0.049	-	0.078	-	-
soil 4	0.095	-	-	-	0.083	-	0.036	-	0.080	-	-
topsoil 5	0.038	-	-	-	0.058	-	0.045	-	0.093	-	-
subsoil 5	0.046	-	-	-	0.056	-	0.000	-	0.101	-	-

Table 3.16. Magnesium concentrations in stream waters and soil SPEs measured in mmol/l as determined by ICP-MS analysis. Values in parentheses indicate a duplicate run for that sample. DNF = did not flow. DNS = did not sample.

Mg in mmol/l (ICPMS)											
Streams	**17 Jun**	**15 Jul**	**17 Aug**	**22 Sep**	**22 Oct**	**23 Nov**	**11 Jan**	**10 Feb**	**25 Mar**	**29 Apr**	**1 Jun**
str01	0.093	0.064	0.059	0.073 (0.073)	0.012 (0.073)	0.065	0.063	0.065	0.067 (0.058)	0.081	0.083
str02	0.126	0.090	DNF	DNF	0.079 (0.041)	0.063	DNF	DNF	DNF	DNF	0.076
str03	0.064	0.053	0.080	0.060 (0.041)	0.048	0.064	0.058	0.064	0.060 (0.038)	0.062	0.063
str04	0.101	0.110 (0.062)	DNF	DNF	DNF	DNF	DNF	DNF	DNF	DNF	0.068
str05	0.090	0.079	0.076 (0.066)	0.070	0.078 (0.078)	0.065	0.053	0.062 (0.044)	0.067 (0.053)	0.086	0.081
str06	0.096 (0.062)	0.082 (0.062)	0.076	0.073	0.077	0.066	0.034	0.068	0.059 (0.066)	0.084	0.083
str07	DNS	0.069 (0.074)	0.073	0.073 (0.06)	0.079 (0.053)	0.071	0.054	0.061	0.700 (0.067)	0.075	0.086
Soil Saturated Paste Extracts (SPEs)											
topsoil 1	0.240	-	-	-	0.053	-	0.102 (0.66)	-	0.337	-	-
subsoil 1	0.108	-	-	-	0.028	-	0.046	-	0.086	-	-
topsoil 2	0.260	-	-	-	0.178	-	0.204 (0.201)	-	0.187	-	-
subsoil 2	0.219	-	-	-	0.069	-	0.047	-	0.443	-	-
soil 3	0.097	-	-	-	0.051	-	0.085	-	0.168	-	-
soil 4	0.134	-	-	-	0.068	-	0.044	-	0.124	-	-
topsoil 5	0.096	-	-	-	0.028	-	0.124	-	0.141	-	-
subsoil 5	0.063	-	-	-	0.023	-	0.039	-	0.134	-	-

Table 3.17. Magnesium concentrations in stream waters and soil SPEs measured in mmol/l as determined by IC analysis. Values in parentheses indicate a duplicate run for that sample. DNF = did not flow. DNS = did not sample. ND = not determined.

Mg in mmol/l (IC)											
Streams	**17 Jun**	**15 Jul**	**17 Aug**	**22 Sep**	**22 Oct**	**23 Nov**	**11 Jan**	**10 Feb**	**25 Mar**	**29 Apr**	**1 Jun**
str01	0.070	0.070	0.078	0.074	0.070	0.058	0.066	0.066	0.078	0.086 (0.086)	0.082
str02	0.082	0.066	DNF	DNF	0.070	0.053	DNF	DNF	DNF	DNF	0.078 (0.074)
str03	0.066	0.066	0.058	0.049	0.058	0.058	0.066	0.033	0.070 (0.070)	0.070	0.062
str04	0.099	0.090	DNF	DNF	DNF	DNF	DNF	DNF	DNF	DNF	0.066 (0.07)
str05	0.099	0.078	0.078	0.062	0.070	0.058	0.058	0.062	0.066 (0.062)	0.086 (0.082)	0.078
str06	0.099	ND	0.066	0.066	0.070	0.058	0.037	0.053	0.070 (0.066)	0.086	0.078
str07	DNS	0.078	0.070	0.070	0.070	0.066	0.058	0.045	0.070	0.074 (0.074)	0.082 (0.082)
Soil Saturated Paste Extracts (SPEs)											
topsoil 1	0.108	-	-	-	0.208	-	0.192	-	0.620	-	-
subsoil 1	0.067	-	-	-	0.083	-	0.067	-	0.160	-	-
topsoil 2	0.325	-	-	-	0.225	-	0.383	-	0.360	-	-
subsoil 2	0.133	-	-	-	0.100	-	0.092	-	0.830	-	-
soil 3	0.108	-	-	-	0.167	-	0.167	-	0.300	-	-
soil 4	0.100	-	-	-	0.142	-	0.092	-	0.230	-	-
topsoil 5	0.067	-	-	-	0.075	-	0.242	-	0.270	-	-
subsoil 5	0.058	-	-	-	0.158	-	0.075	-	0.280	-	-

Table 3.18. Calcium concentrations in stream waters and soil SPEs measured in mmol/l as determined by ICP-MS analysis. Values in parentheses indicate a duplicate run for that sample. DNF = did not flow. DNS = did not sample.

Ca in mmol/l (ICP-MS)											
Streams	**17 Jun**	**15 Jul**	**17 Aug**	**22 Sep**	**22 Oct**	**23 Nov**	**11 Jan**	**10 Feb**	**25 Mar**	**29 Apr**	**1 Jun**
str01	0.032	0.022 (0.022)	0.027	0.018 (0.022)	0.028 (0.029)	0.035	0.013	0.022	0.015 (0.02)	0.016	0.024
str02	0.044	0.017	DNF	DNF	0.029 (0.019)	0.034	DNF	DNF	DNF	DNF	0.027
str03	0.022	0.020	0.021	0.013 (0.012)	0.015	0.016	0.011	0.020	0.012 (0.008)	0.005	0.016
str04	0.027	0.022 (0.031)	DNF	DNF	DNF	DNF	DNF	DNF	DNF	DNF	0.017
str05	0.020	0.020	0.018	0.018	0.025	0.017	0.009	0.014	0.015 (0.012)	0.015	0.020
str06	0.027	0.021	0.020	0.015 (0.016)	0.031	0.015	0.009	0.017 (0.014)	0.015 (0.016)	0.024	0.021
str07	DNS	0.021 (0.035)	0.034	0.017	0.022 (0.013)	0.018	0.010	0.015	0.014 (0.024)	0.014	0.025
Soil Saturated Paste Extracts (SPEs)											
topsoil 1	0.125	-	-	-	0.035	-	0.064 (0.024)	-	0.205	-	-
subsoil 1	0.084	-	-	-	0.022	-	0.044	-	0.024	-	-
topsoil 2	0.216	-	-	-	0.095	-	0.123 (0.189)	-	0.075	-	-
subsoil 2	0.104	-	-	-	0.046	-	0.033	-	0.302	-	-
soil 3	0.094	-	-	-	0.041	-	0.048	-	0.091	-	-
soil 4	0.124	-	-	-	0.033	-	0.019	-	0.052	-	-
topsoil 5	0.088	-	-	-	0.017	-	0.048	-	0.052	-	-
subsoil 5	0.036	-	-	-	0.024	-	0.017	-	0.058	-	-

Table 3.19. Calcium concentrations in stream waters and soil SPEs measured in mmol/l as determined by IC analysis. Values in parentheses indicate a duplicate run for that sample. DNF = did not flow. DNS = did not sample. ND = Not determined.

Ca in mmol/l (IC)											
Streams	**17 Jun**	**15 Jul**	**17 Aug**	**22 Sep**	**22 Oct**	**23 Nov**	**11 Jan**	**10 Feb**	**25 Mar**	**29 Apr**	**1 Jun**
str01	0.040	0.040	0.052	0.047	0.027	0.030	0.025	0.035	0.045	0.065 (0.070)	0.080
str02	0.065	0.047	DNF	DNF	0.032	0.030	DNF	DNF	DNF	DNF	0.085 (0.110)
str03	0.040	0.040	0.035	0.020	0.022	0.022	0.022	0.012	0.041 (0.041)	0.050	0.050
str04	0.050	0.042	DNF	DNF	DNF	DNF	DNF	DNF	DNF	DNF	0.055 (0.055)
str05	0.052	0.042	0.042	0.027	0.025	0.022	0.022	0.025	0.041 (0.037)	0.060 (0.055)	0.070
str06	0.060	ND	0.027	0.025	0.025	0.022	0.015	0.025	0.053 (0.049)	0.065	0.060
str07	DNS	0.042	0.027	0.030	0.025	0.027	0.025	0.020	0.041	0.060 (0.065)	0.070 (0.070)
Soil Saturated Paste Extracts (SPEs)											
topsoil 1	0.090	-	-	-	0.190	-	0.500	-	0.200	-	-
subsoil 1	0.050	-	-	-	0.075	-	0.080	-	0.070	-	-
topsoil 2	0.230	-	-	-	0.205	-	0.210	-	0.350	-	-
subsoil 2	0.090	-	-	-	0.080	-	0.710	-	0.090	-	-
soil 3	0.070	-	-	-	0.130	-	0.240	-	0.140	-	-
soil 4	0.055	-	-	-	0.095	-	0.140	-	0.060	-	-
topsoil 5	0.040	-	-	-	0.050	-	0.150	-	0.150	-	-
subsoil 5	0.040	-	-	-	0.105	-	0.190	-	0.060	-	-

Table 3.20. Potassium concentrations in stream waters and soil SPEs measured in mmol/l as determined by IC analysis. Values in parentheses indicate a duplicate run for that sample. DNF = did not flow. DNS = did not sample. ND = not determined.

K in mmol/l											
Streams	**17 Jun**	**15 Jul**	**17 Aug**	**22 Sep**	**22 Oct**	**23 Nov**	**11 Jan**	**10 Feb**	**25 Mar**	**29 Apr**	**1 Jun**
str01	0.062	0.062	0.051	0.051	0.059	0.062 (0.062)	0.041	0.038	0.031	0.044 (0.044)	0.033
str02	0.054	0.069	DNF	DNF	0.074	0.069 (0.069)	DNF	DNF	DNF	DNF	0.041 (0.041)
str03	0.023	0.026	0.021	0.023	0.028	0.031	0.028	0.015	0.023 (0.023)	0.023	0.021
str04	0.036	0.085	DNF	DNF	DNF	DNF	DNF	DNF	DNF	DNF	0.054 (0.054)
str05	0.049	0.054	0.046	0.046	0.054 (0.056)	0.056	0.036 (0.036)	0.036	0.031 (0.031)	0.041 (0.044)	0.036
str06	0.044	ND	0.044	0.046	0.049 (0.051)	0.049	0.023	0.033	0.028 (0.028)	0.038	0.036
str07	DNS	0.044	0.036	0.041	0.044	0.051	0.036	0.023	0.038	0.041 (0.038)	0.038 (0.038)
Soil Saturated Paste Extracts (SPEs)											
topsoil 1	0.113	-	-	-	0.128	-	0.103	-	0.167	-	-
subsoil 1	0.095	-	-	-	0.118	-	0.095	-	0.123	-	-
topsoil 2	0.190	-	-	-	0.115	-	0.177	-	0.292	-	-
subsoil 2	0.108	-	-	-	0.110	-	0.095	-	0.213	-	-
soil 3	0.126	-	-	-	0.113	-	0.103	-	0.187	-	-
soil 4	0.118	-	-	-	0.169	-	0.097	-	0.144	-	-
topsoil 5	0.072	-	-	-	0.113	-	0.095	-	0.154	-	-
subsoil 5	0.103	-	-	-	0.090	-	0.087	-	0.167	-	-

Table 3.21. Manganese concentrations in stream waters and soil SPEs measured in nmol/l as determined by ICP-MS analysis. DNF = did not flow. DNS = did not sample.

Mn in nmol/l											
Streams	**17 Jun**	**15 Jul**	**17 Aug**	**22 Sep**	**22 Oct**	**23 Nov**	**11 Jan**	**10 Feb**	**25 Mar**	**29 Apr**	**1 Jun**
str01	1324	855	1582	1127	200	2018	1345	1818	1545	2236	1473
str02	331	545	DNF	DNF	600	1182	DNF	DNF	DNF	DNF	436
str03	331	455	200	1000	364	291	1350	3036	55	<2	655
str04	331	127	DNF	DNF	DNF	DNF	DNF	DNF	DNF	DNF	109
str05	662	600	909	1636	1091	455	109	473	473	673	800
str06	2316	1691	2400	1873	1982	1564	1345	218	4036	3473	2091
str07	DNS	327	473	218	345	327	73	3291	109	200	491
Soil Saturated Paste Extracts (SPEs)											
topsoil 1	6949	-	-	-	135	-	2455	-	8873	-	-
subsoil 1	6287	-	-	-	23	-	418	-	4145	-	-
topsoil 2	20187	-	-	-	139	-	2527	-	982	-	-
subsoil 2	4633	-	-	-	45	-	818	-	21182	-	-
soil 3	14231	-	-	-	109	-	1982	-	1745	-	-
soil 4	28460	-	-	-	185	-	3364	-	10855	-	-
topsoil 5	18864	-	-	-	174	-	3164	-	11000	-	-
subsoil 5	4964	-	-	-	113	-	2055	-	24218	-	-

Table 3.22. Strontium concentrations in stream waters and soil SPEs measured in nmol/l as determined by ICP-MS analysis. DNF = did not flow.

Sr in nmol/l										
Streams	**17 Jun**	**15 Jul**	**17 Aug**	**22 Sep**	**22 Oct**	**23 Nov**	**11 Jan**	**10 Feb**	**25 Mar**	**29 Apr**
str01	169	176	169	31	186	64	157	141	175	197
str02	186	DNF	DNF	198	190	DNF	DNF	DNF	DNF	210
str03	150	171	134	109	145	56	147	123	122	138
str04	213	DNF	DNF	DNF	DNF	DNF	DNF	DNF	DNF	167
str05	166	175	160	178	152	55	140	131	168	175
str06	168	171	157	169	150	38	155	136	174	182
str07	173	173	165	176	168	55	142	142	156	188
Soil Saturated Paste Extracts (SPEs)										
topsoil 1	-	-	-	-	13.8	-	158	-	825	-
subsoil 1	-	-	-	-	7.54	-	86	-	184	-
topsoil 2	-	-	-	-	39.0	-	446	-	395	-
subsoil 2	-	-	-	-	15.8	-	181	-	1269	-
soil 3	-	-	-	-	13.7	-	156	-	487	-
soil 4	-	-	-	-	20.2	-	230	-	284	-
topsoil 5	-	-	-	-	6.57	-	75	-	350	-
subsoil 5	-	-	-	-	6.58	-	75	-	356	-

3.4 Bedrock mineralogy

Petrographic observations of thin sections and XRF analysis revealed the quartz-rich nature of the Peninsula sandsone bedrock. Thin sections were made from bedrock samples from all five sites.

3.4.1 Petrography

Sandstone from site 1 showed a more deformed texture with a quartz ribbon or vein running through it (Figure 3.1 and Figure 3.2). The quartz vein had smaller grain sizes of up to 0.1 μm. The surrounding quartz grains increased to a size of up to 3 μm. Bladed micas were observed distributed along grain boundaries and as inclusions within the quartz. The larger quartz grains were stained in a yellow tinted colour. Few opaque minerals were observed in plane polarized light (ppl). Iron oxides are distributed along grain boundaries.

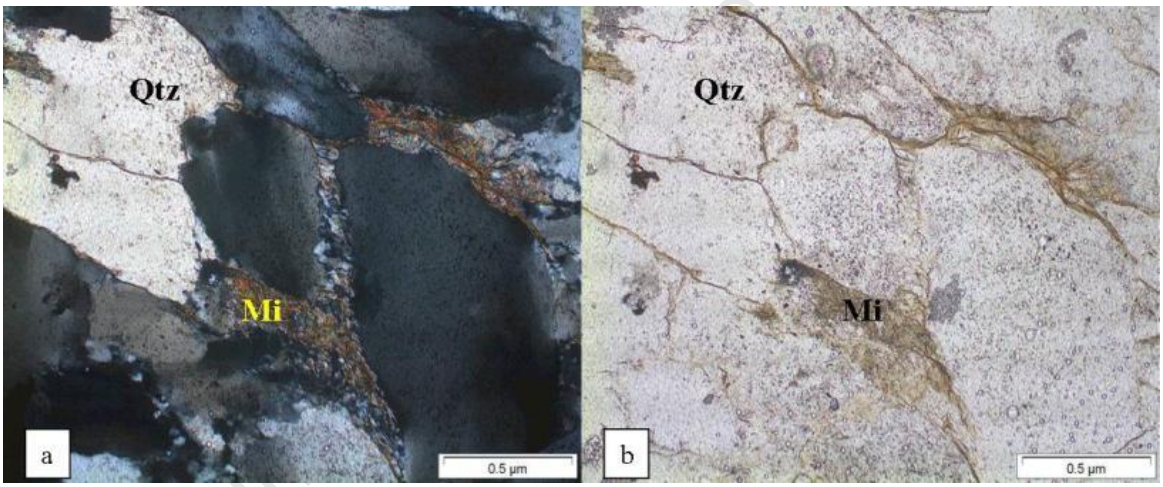

Figure 3.1. Photomicrographs of sandstone from site 1 under a petrographic microscope in a) cross polarised light and b) plane polarised light wih a magnification of 10x. Mi = Mica. Qtz = Quartz.

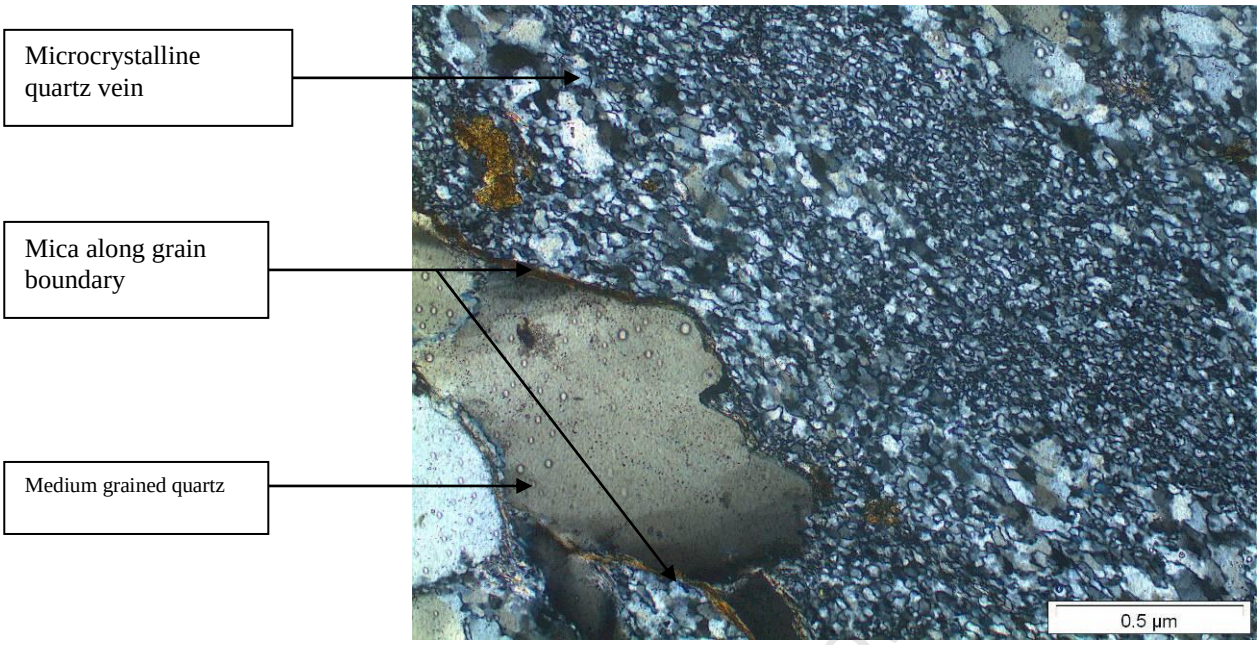

Figure 3.2. Photomicrograph of sandstone from site 1 in the HPNBG showing the boundary between the smaller fused grains of a quartz vein and the larger dominant grains found in the rock (magnification of 10x).

Sandstone from site 2 consists of fine to medium sand size quartz grains cemented by quartz (Figure 3.3). Quartz grain sizes range from <0.1 µm to 1 µm. Opaque minerals occur as inclusions or along grain boundaries with grain sizes of less than 0.1 µm. Bladed mica minerals were distributed along grain boundaries.

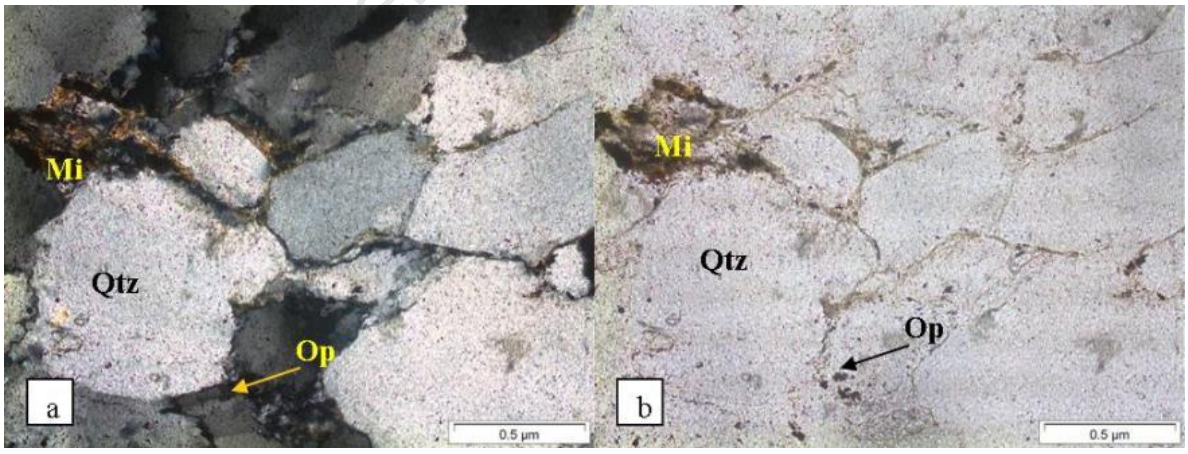

Figure 3.3. Photomicrographs of sandstone from site 2 under petrographic microscope in a) cross polarised light and b) plane polarised light with a magnification of 10x. Mi = Mica. Qtz = Quartz. Op = Opaque minerals.

Sandstone from site 3 in the HPNBG showed a more well sorted texture than other samples in this study (Figure 3.4). Grains reached a size of ~0.5 µm. Quartz grain boundaries were

also more sutured and pressure solution surfaces were present. Micas were observed on grain boundaries between the quartz grains, but in decreased amounts. They were also not as bladed as in other samples. Biotite was also observed and had larger grain sizes than other mica minerals (~0.5 μm). Opaque minerals were less abundant.

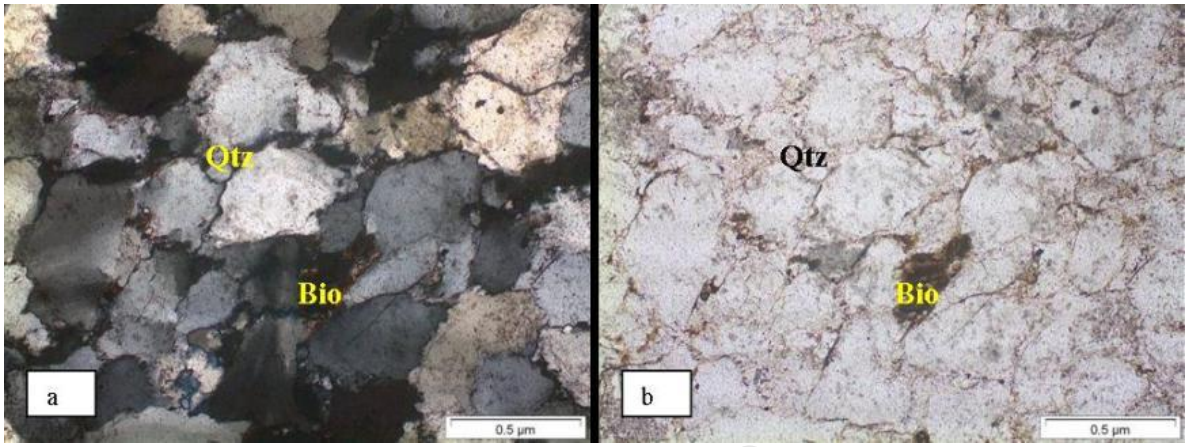

Figure 3.4. Photomicrographs of sandstone from site 3 under petrographic microscope in a) cross polarised light and b) plane polarised light with a magnification of 10x. Qtz = Quartz. Bio = Biotite.

Sandstone from site 4 appeared more deformed than site 3 (Figure 3.5). Quartz grains were stained yellow in places and ranged in size from 0.1 μm to 3 μm. Boundaries between quartz grains appeared sutured and pressure solution surfaces were apparent. Fused quartz grains and overgrowths were present. Less mica and fewer opaque minerals were observed in the sample from site 4 than in other samples.

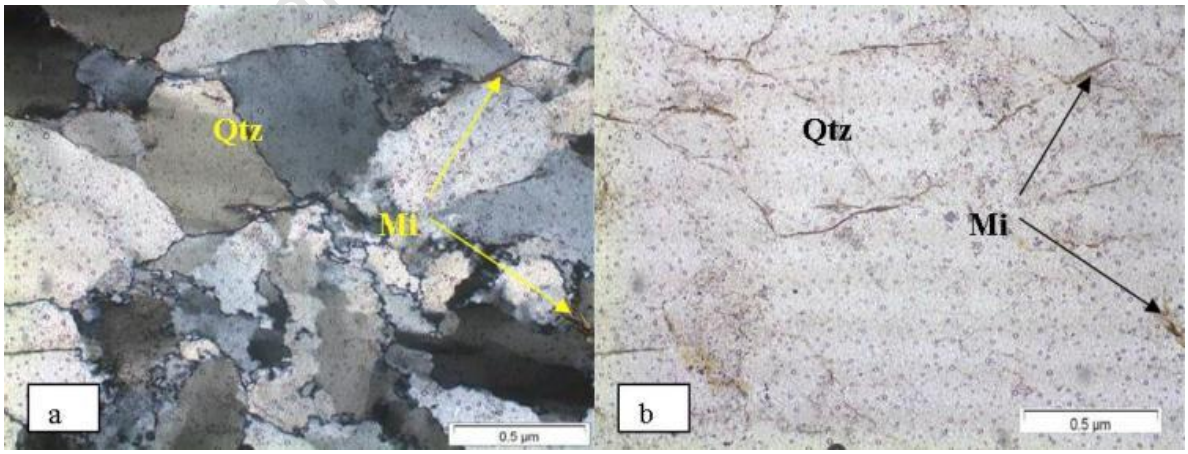

Figure 3.5. Photomicrographs of sandstone from site 4 under petrographic microscope in a) cross polarised light and b) plane polarised light with a magnification of 10x. Qtz = Quartz. Mi = Mica minerals.

Quartz grains for sandstone at site 5 (KBR) reached sizes of ~0.5 μm. Pockets of coalesced smaller grained quartz (<0.1 μm) were also observed. Micas were more concentrated along grain boundaries than in other samples and showed preferred orientation (Figure 3.6).

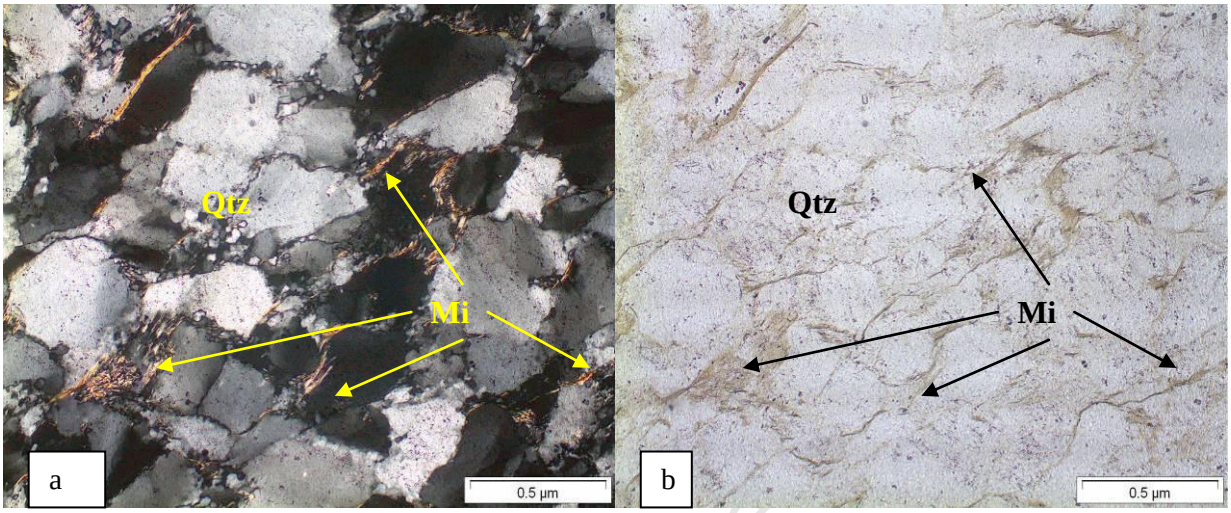

Figure 3.6. Photomicrographs of sandstone from site 5 under petrographic microscope in a) cross polarized light and b) plane polarized light with a magnification of 10x. Qtz = Quartz. Mi = Mica.

3.4.2 Major Oxides and Trace Elements in Bedrock

The powdered bedrock samples were analysed for major oxides (Table 3.23) and trace element compositions (Table 3.24).

Table 3.23. Major oxides in Peninsula Formation sandstone sampled from the HPNBG and KBR.

	Site 1 (HPNBG)	Site 2 (HPNBG)	Site 3 (HPNBG)	Site 4 (HPNBG)	Site 5 (KBR)
Major Oxides in wt%					
SiO_2	97.996	97.621	98.733	98.805	97.990
TiO_2	0.121	0.128	0.117	0.037	0.368
Al_2O_3	0.799	1.296	0.309	0.430	0.956
Fe_2O_3	0.133	0.155	0.158	0.108	0.171
MnO	0.011	0.012	0.010	0.011	0.012
MgO	0.047	0.035	0.049	0.057	0.001
CaO	0.004	0.008	0.011	0.011	0.006
Na_2O	0.026	0.031	0.036	0.044	0.064
K_2O	0.193	0.344	0.076	0.100	0.265
P_2O_5	0.014	0.016	0.009	0.032	0.011
SO_3	0.035	0.033	0.030	0.033	0.031
Cr_2O_3	0.001	0.001	0.001	0.002	0.001
NiO	0.001	0.001	0.001	0.003	0.001
H_2O-	0.021	0.012	0.017	0.003	0.012
LOI	0.129	0.224	0.106	0.071	0.200
Total	99.529	99.916	99.662	99.747	100.089

Table 3.24. Trace element concentrations (in ppm) of Peninsula Formation sandstone sampled in the HPNBG and KBR.

Trace elements in ppm	**Site 1 (HPNBG)**	**Site 2 (HPNBG)**	**Site 3 (HPNBG)**	**Site 4 (HPNBG)**	**Site 5 (KBR)**
Mo	<0.3	<0.3	<0.3	<0.3	<0.3
Nb	<0.3	<0.3	<0.3	<0.3	4.3
Zr	65.1	59.7	66.7	36.5	290.8
Y	10.4	10.6	9.2	11.4	14.7
Sr	8.3	13.2	5.7	9.6	6.2
Rb	8.4	14.4	5.9	6.6	11.6
U	<0.7	<0.7	<0.7	<0.7	<0.7
Th	5.7	6.2	5.2	4.8	8.3
Pb	12.4	12.5	10.9	11.2	11.4
Zn	2.9	2.7	2.7	1.9	2.7
Cu	<0.6	<0.6	<0.6	<0.6	<0.6
Ni	<0.8	<0.8	<0.8	<0.8	<0.8
Co	<2.2	<2.2	<2.2	<2.2	<2.2
Mn	22.7	18.6	24.4	25.9	19.2
Cr	16.3	13.7	14.7	15.8	16.3
V	9.2	13.5	8.7	8.3	15.1
Sc	<1.5	3.2	2.4	<1.5	3.5
Ba	71.3	93.9	54.7	67.4	100.3
S	<1.0	<1.0	<1.0	<1.0	<1.0

3.5 Soil Texture and Mineralogy

The soil texture was found to be sandy with <2 wt% clay content (Table 3.25 and Table 3.26). Gravel components were disregarded and non-gravel sized fractions were used for XRF and organic carbon analysis. The clay sized fractions were used for XRD analysis.

Table 3.25. Grain size distribution (in wt%) of the soils collected from the HPNBG and KBR. Soils from sites 3 and 4 were too thin to separate into top and sub soil.

	Gravel (>2mm)	Sand (2mm - 63 μm)	Silt (63 - 2 μm)	Clay (<2 μm)	Sum
Site 1 (HP) Topsoil	18.52	73.99	6.22	1.27	100
Site 1 (HP) Subsoil	20.7	72.88	5.15	1.27	100
Site 2 (HP) Topsoil	27.18	67.36	4.83	0.63	100
Site 2 (HP) Subsoil	32	60.47	6.44	1.09	100
Site 3 (HP) Total soil	19.53	77.11	2.89	0.47	100
Site 4 (HP) Total soil	37.52	58.68	3.21	0.59	100
Site 5 (KBR) Topsoil	16.65	76.37	5.86	1.12	100
Site 5 (KBR) Subsoil	19.17	72.03	7.47	1.33	100

Table 3.26. Normalised grain size distribution (in wt%) of the soils studied in this thesis to exclude gravel components. Soils from sites 3 and 4 were too thin to separate into top and sub soil.

	Sand (2mm - 63 μm)	Silt (63 - 2 μm)	Clay (<2 μm)	Sum
Site 1 (HP) Topsoil	90.81	7.63	1.56	100
Site 1 (HP) Subsoil	91.9	6.49	1.6	99.99
Site 2 (HP) Topsoil	92.5	6.63	0.87	100
Site 2 (HP) Subsoil	88.93	9.47	1.6	100
Site 3 (HP) Total soil	95.82	3.59	0.58	99.99
Site 4 (HP) Total soil	93.92	5.14	0.94	100
Site 5 (KBR) Topsoil	91.63	7.03	1.34	100
Site 5 (KBR) Subsoil	89.11	9.24	1.65	100

3.5.1 Major Oxides and Trace Elements in Soil Samples

The powdered sand size fractions (<2 mm) were analysed for major oxides and trace element compositions. The results from XRF analysis are displayed in Table 3.27 and Table 3.28, respectively.

Table 3.27. Major oxides (in wt%) of soil samples collected from the HPNBG and KBR.

Major Oxides in wt%	Site 1 topsoil HPNBG	Site 1 subsoil HPNBG	Site 2 topsoil HPNBG	Site 2 subsoil HPNBG	Site 3 total soil HPNBG	Site 4 total soil HPNBG	Site 5 topsoil KBR	Site 5 subsoil KBR
SiO_2	81.168	88.663	71.848	82.162	83.460	72.089	87.728	91.069
TiO_2	0.167	0.146	0.194	0.232	0.133	0.075	0.494	0.539
Al_2O_3	0.228	0.157	0.410	0.389	0.149	0.248	0.543	0.472
Fe_2O_3	0.049	0.107	0.031	0.083	0.045	0.015	0.082	0.100
MnO	0.009	0.012	0.007	0.011	0.008	0.008	0.012	0.010
MgO	0.036	0.002	0.109	0.048	0.020	0.054	0.003	0.013
CaO	0.260	0.088	0.440	0.176	0.129	0.196	0.058	0.024
Na_2O	0.004	0.021	0.002	0.023	0.031	0.001	0.051	0.046
K_2O	0.036	0.025	0.074	0.075	0.014	0.037	0.087	0.073
P_2O_5	0.026	0.016	0.037	0.023	0.018	0.023	0.017	0.018
SO_3	0.002	0.026	0.001	0.020	0.021	0.017	0.027	0.031
Cr_2O_3	0.001	0.002	0.001	0.001	0.001	0.001	0.001	0.003
NiO	0.001	0.001	0.001	0.001	0.001	0.001	0.002	0.001
H_2O-	1.885	1.025	3.165	1.851	1.475	2.765	0.910	0.645
LOI	15.568	9.599	23.001	14.725	13.999	23.743	9.403	6.696
Total	99.440	99.889	99.321	99.820	99.504	99.273	99.418	99.739

Table 3.28. Trace element concentrations (in ppm) of soil samples collected from the HPNBG and KBR.

Trace elements in ppm	Site 1 topsoil HPNBG	Site 1 subsoil HPNBG	Site 2 topsoil HPNBG	Site 2 subsoil HPNBG	Site 3 total soil HPNBG	Site 4 total soil HPNBG	Site 5 topsoil KBR	Site 5 subsoil KBR
Mo	<0.3	<0.3	<0.3	<0.3	<0.3	<0.3	<0.3	1.8
Nb	<0.3	<0.3	1.2	2.4	<0.3	<0.3	8.6	13.3
Zr	131.3	117.4	132.9	152.8	141.3	57.9	411.8	681.5
Y	11.4	9.1	10.4	11.7	10.0	12.7	17.2	20.0
Sr	21.3	12.5	38.8	22.0	15.6	25.5	11.0	8.6
Rb	3.9	3.5	5.6	5.2	3.1	3.3	5.2	5.3
U	<0.7	<0.7	<0.7	<0.7	<0.7	<0.7	<0.7	<0.7
Th	4.7	4.4	4.9	4.2	4.5	3.6	5.8	6.2
Pb	11.8	10.6	13.8	10.6	11.7	11.7	11.6	11.2
Zn	5.1	2.4	8.4	3.3	4.8	4.6	5.4	4.4
Cu	<0.6	<0.6	<0.6	<0.6	<0.6	<0.6	<0.6	<0.6
Ni	<0.8	<0.8	<0.8	<0.8	<0.8	<0.8	<0.8	<0.8
Co	<2.2	<2.2	<2.2	<2.2	<2.2	<2.2	<2.2	<2.2
Mn	36.1	26.6	44.7	26.3	45.2	48.5	37.9	32.2
Cr	20.4	21.4	18.4	19.7	25.6	31.9	23.3	21.4
V	10.5	8.4	16.4	15.7	11.9	10.4	17.1	15.4
Sc	2.6	2.1	3.3	3.3	<1.5	3.0	<1.5	2.5
Ba	65.9	49.2	116.1	81.5	69.1	78.9	82.9	72.1
S	1130.4	448.3	1893.3	1170.2	958.8	1570.9	449.1	288.9

3.5.2 X-ray Diffraction Results

X-ray diffractograms for the bulk (< 2 mm) and clay (< 2 μm) fractions of all soil samples are presented in Appendix B. The mineralogy as indicated by the x-ray diffraction patterns of the soil samples is dominated by quartz. The X-ray diffractograms show minor peaks for clay minerals such as smectite, mica minerals, illite and kaolinite.

3.5.3 Organic Carbon

The non-gravel size fraction (<2 mm) of topsoil and subsoil samples from all sites discussed in this study were analysed for organic carbon content. Three soil samples from sites 1, 3 and 5 were selected for duplicate analysis. The results are displayed in Table 3.29. Sites 2 and 4 recorded the highest organic carbon content and site 5 the lowest.

Table 3.29. Organic carbon content and carbon isotope data for the sand size fraction (<2 mm) of soil samples collected from the HPNBG and KBR. Dup = Duplicate samples.

Sample	%C	$\delta^{13}C$	Std corrected $\delta^{13}C$
Site 1 topsoil (HPNBG)	9.21	-26.73	-27.96
Dup-Site 1 topsoil (HPNBG)	9.36	-26.74	-27.96
Site 1 subsoil (HPNBG)	5.55	-26.18	-27.36
Site 2 topsoil (HPNBG)	19.91	-27.08	-28.33
Site 2 subsoil (HPNBG)	9.48	-26.06	-27.22
Site 3 total soil (HPNBG)	7.82	-26.46	-27.66
Dup-Site 3 total soil (HPNBG)	8.80	-26.38	-27.58
Site 4 total soil (HPNBG)	18.78	-26.12	-27.29
Site 5 topsoil (KBR)	5.29	-27.68	-28.99
Dup-Site 5 topsoil (KBR)	5.81	-27.60	-28.90
Site 5 subsoil (KBR)	3.65	-26.92	-28.16

Chapter 4 : Discussion

The main objectives of this study are to investigate the chemical composition of different components (rainfall, streams, mountain seeps, bedrock and soil) in a fynbos ecosystem adapted to nutrient-poor sandstone-derived soils and to assess the significance of marine and mineral aerosol input to the ecosystem. The study area is a mountainous region with strong gradients in elevation directly adjacent to the coast. Two fire events during the course of this study may help to shed some light on the role of fire in the fynbos ecosystem. The fire of 3 June 2010 burnt through most of the study area wiping out 90% of nearly 20 years worth of above ground vegetation growth. The fire did not appear to be hot enough to burn much of the subsurface vegetation as evidenced by incompletely burnt litter and intact root mats in the uppermost 4 cm of the soil profile. This is consistent with the observation, made while walking through the study area two weeks before the fire, that the vegetation did not appear to be dried out but was green with abundant moisture both in the plant cover and in soils. The fire event of 16 March 2011 affected areas to the north and east of the Kogelberg Biosphere Reserve. Although the fire event of 16 March did not burn through the area, the regional fallout of ash from the fire may have overlapped with the study area. Soderberg (2003) outlines the atmosphere, vegetation, soil, bedrock, groundwater and stream water as forming the major chemical reservoirs of the fynbos ecosystem. Ions may be transferred into and out of the ecosystem, as well as from one reservoir to another through the interaction with water and wind (Figure 4.1). Plants gain their nutrients primarily from the soil which may contain elements delivered as marine aerosols, as mineral aerosols from windblown dust or derived from bedrock weathering (Soderberg and Compton, 2007). Clay minerals within the soils may further break down into constituent elements providing additional nutrients to plants. Soils on Peninsula Formation bedrock are thin (2 to 20 cm thick) and quartz rich and therefore additional aerosol inputs into the ecosystem are important in contributing to the availability of nutrients to the plants.

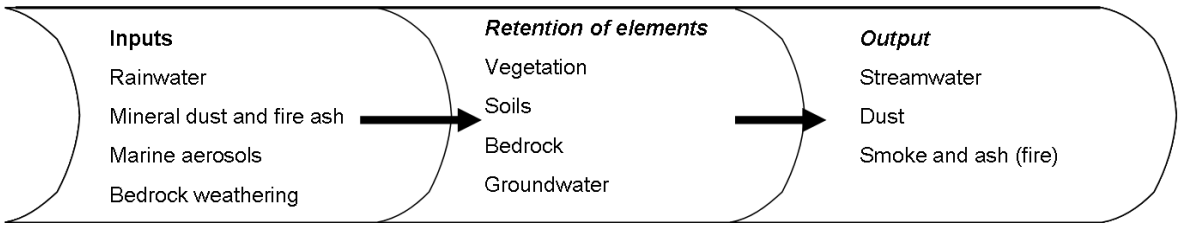

Figure 4.1. Flow diagram outlining the major inputs, retention and output of elements within an ecosystem.

Soils may retain some of the minerals delivered by wind or rainout. Bedrock can exchange ions with groundwater as it percolates through cracks and pores within the bedrock. Groundwater may exit bedrock as mountain seeps to feed into streams. Vegetation, streams, soils and bedrock are all influenced by rainfall and rainwater chemistry.

4.1 Rainfall and Rainwater Chemistry

Rainfall plays an important role in the transfer of elements from the atmosphere to other ecosystem components such as vegetation, soil, bedrock and stream water outflow. A large component of the biologically important elements in a Peninsula Formation sandstone ecosystem such as Mg, Ca and K that are retained in the vegetation and soil may come from atmospheric deposition (Soderberg, 2003). Wet deposition involves rainfall whereas dry deposition excludes any water content. The sum of wet and dry deposition can be termed total or bulk deposition. In this study, rainwater also incorporates dry deposition by rinsing off the surfaces of the rainwater collectors and therefore measures total deposition.

4.1.1 Rainfall

Total rainfall varied among the collection sites and throughout the year (Figure 4.2). There were large variations in mean total rainfall across the sites for most sampling periods. Total rainfall at sites 3 and 5 remained above the mean total rainfall for most of the year. Winter and spring months had a mix of wet and dry periods with the Jul/Aug sampling period unseasonably dry and the Oct/Nov sampling period unseasonably wet. An increase in mean total rainfall was recorded from February (summer) to June 2011 (winter).

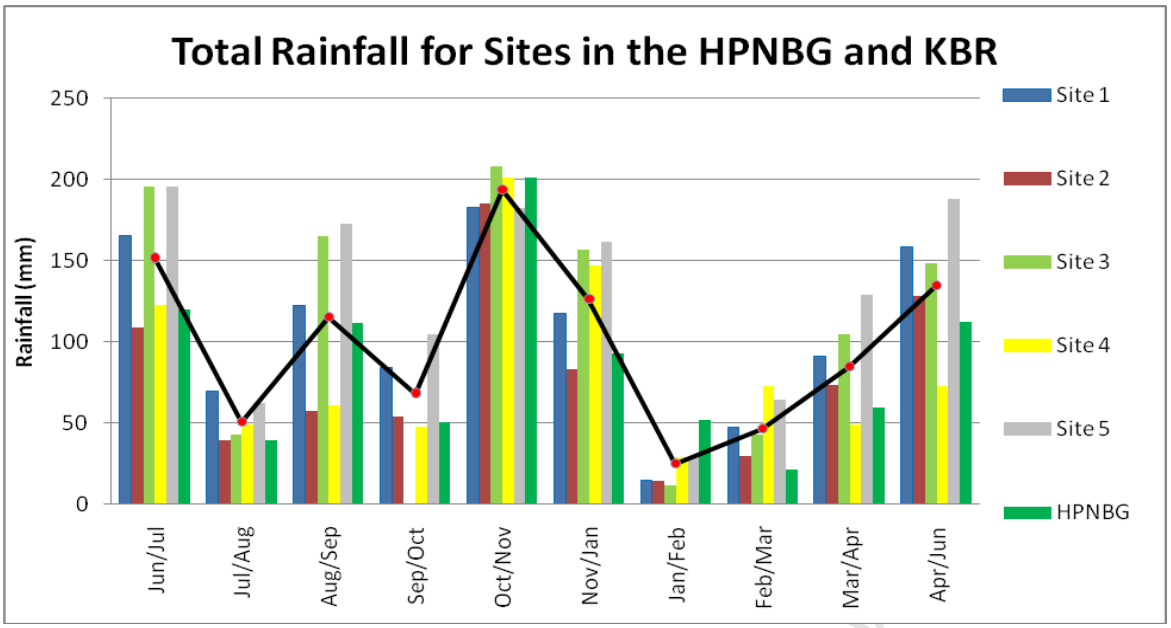

Figure 4.2. Total rainfall recorded at the five sites studied in this thesis as well as rainfall recorded by the office at the Harold Porter National Botanical Gardens (HPNBG) over the different collection periods. The red points and black line show the mean rainfall amounts among the 6 sites combined.

The rainfall distribution is characteristic of a Mediterranean type climate with cool wet winter months and dry warm and windy summer months (Figure 4.3). Rainfall is a minimum during the summer months and increases in the transition to spring. The seasonal variation is as expected but with rainfall in Jul/Aug unusually low and Oct/Nov unusually high for an area with a Mediterranean type climate. The unusually high rainfall during the Oct/Nov period seems to be a regular feature in the HPNBG as noticed from records dating back to 2002 (Figure A. 11 in appendix A).

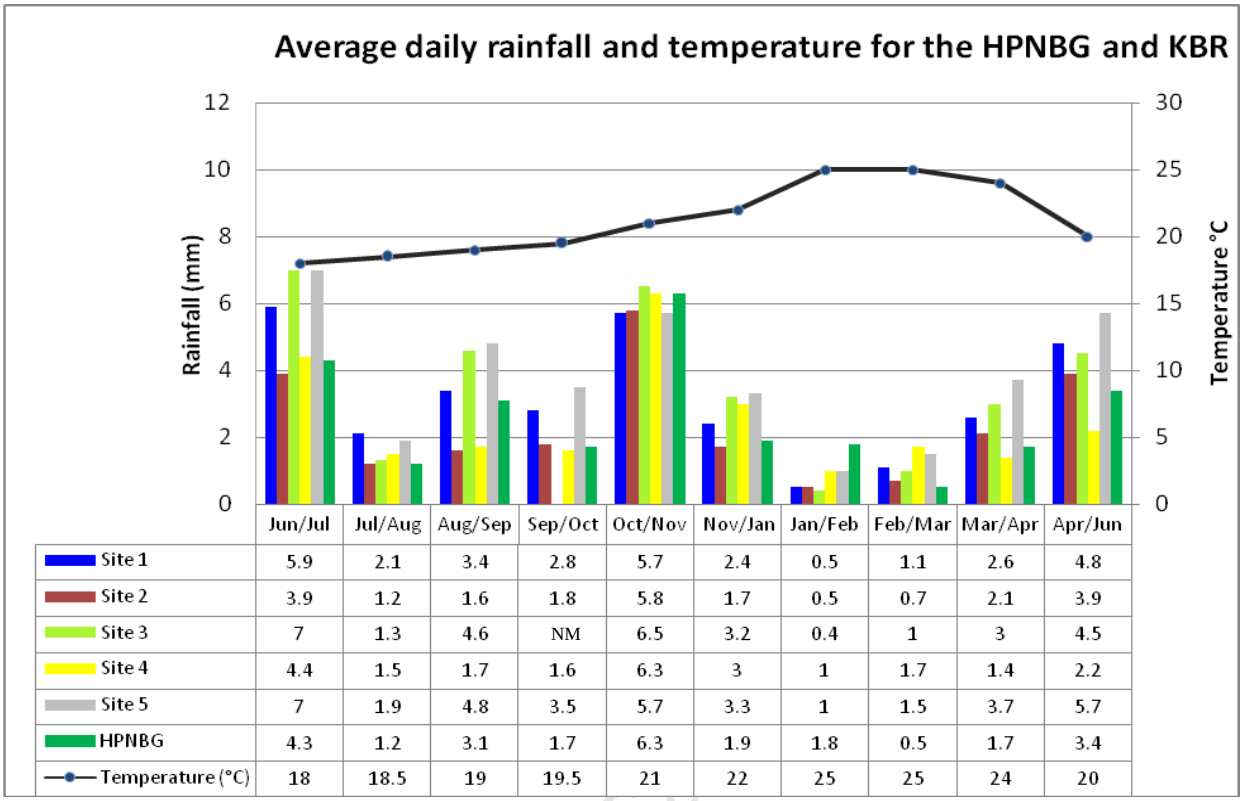

	Jun/Jul	Jul/Aug	Aug/Sep	Sep/Oct	Oct/Nov	Nov/Jan	Jan/Feb	Feb/Mar	Mar/Apr	Apr/Jun
Site 1	5.9	2.1	3.4	2.8	5.7	2.4	0.5	1.1	2.6	4.8
Site 2	3.9	1.2	1.6	1.8	5.8	1.7	0.5	0.7	2.1	3.9
Site 3	7	1.3	4.6	NM	6.5	3.2	0.4	1	3	4.5
Site 4	4.4	1.5	1.7	1.6	6.3	3	1	1.7	1.4	2.2
Site 5	7	1.9	4.8	3.5	5.7	3.3	1	1.5	3.7	5.7
HPNBG	4.3	1.2	3.1	1.7	6.3	1.9	1.8	0.5	1.7	3.4
Temperature (°C)	18	18.5	19	19.5	21	22	25	25	24	20

Figure 4.3. Average daily rainfall (mm/day) recorded at the five sites studied in this thesis as well as rainfall recorded by the office at the Harold Porter National Botanical Gardens (HPNBG). The blue points and connected black line denote the mean monthly temperature as recorded by the office of the Harold Porter National Botanical Gardens (HPNBG). NM = not measured.

It can be expected that areas to the west of the study area would show a stronger seasonal difference in rainfall. Zandvlei, a wetland close to Cape Town and northwest of the study area (Figure 4.4), was identified as an area to compare rainfall data with in order to determine regional variations in rainfall (Figure 4.5). Eight sites at Zandvlei are monitored for rainfall daily (http://www.zandvleitrust.org.za/art-ZIMP%20abiotic-rainfall.html). Zandvlei falls within a catchment drained by a number of rivers and streams. The catchment is bordered by the Muizenberg Mountain, Constantiaberg and Wynberg Hill to the west. The mouth of Zandvlei opens up into False Bay at Muizenberg (Jackson *et al*., 2010). The eight sites monitored around Zandvlei are scattered on the western and eastern sides of the wetland. Two sites are monitored on the western side (labeled Mountain side), two on the northwestern side (labeled MdG (NE)), one site on the eastern side labeled MdG (E) and three sites on the southeastern side labeled MdG (SE). Sites in Zandvlei are located at roughly equal elevation.

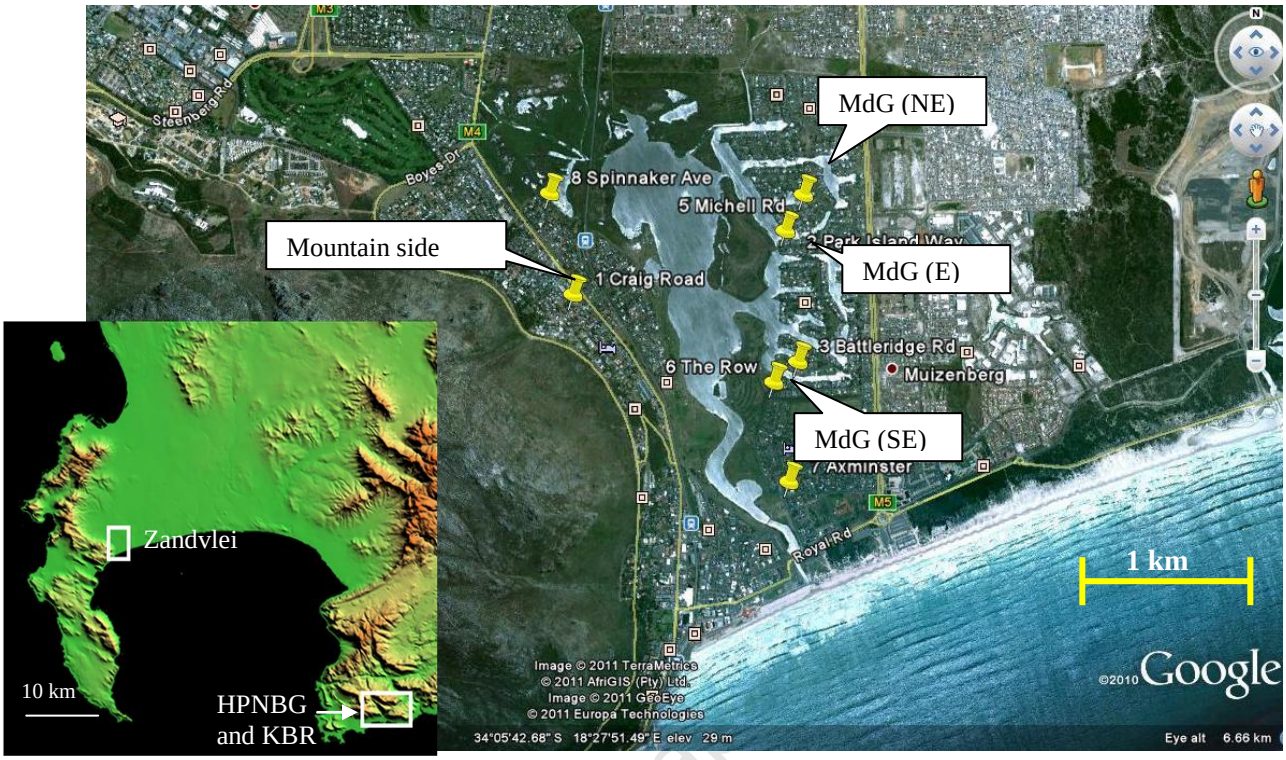

Figure 4.4. Location map of Zandvlei relative to the study area discussed in this thesis with a Google satellite image indicating the stations monitored for rainfall. MdG (E) = Marina da Gama (East). MdG (SE) = Marina da Gama (southeast). MdG (NE) = Marina da Gama (northeast).

Average rainfall was significantly higher in the study area as opposed to that of Zandvlei for the same period with the exception of July/August 2010 (Figure 4.5). Total average annual rainfall for the period of this study was calculated to be 404 mm at Zandvlei and 997 mm for the study area in the Kogelberg region (HPNBG and KBR). Seasonal rainfall decreases eastward and results from this study suggest that rainfall in the study area occurs throughout the year, although in decreased amounts during summer. The Zandvlei record is thus more typical of a winter rainfall region whereas sites from this study show less seasonality in rainfall. This is supported by field observations where the weather for Cape Town was clear on certain days, but the study area had isolated rain showers. The rainfall data suggest that the study area falls on the boundary between the winter seasonal rainfall area to the west and the transition eastward to areas of year round rainfall along the South Coast.

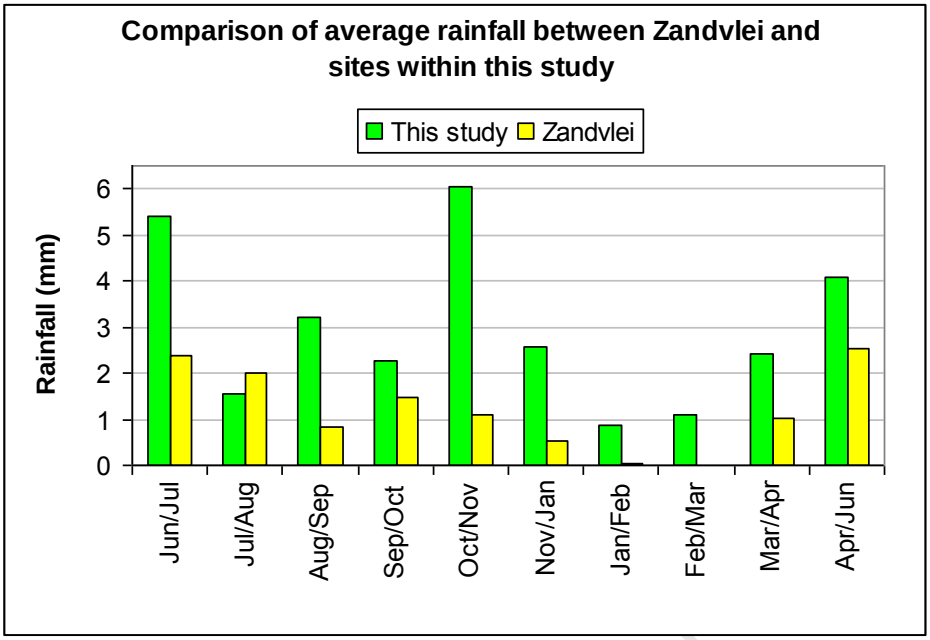

Figure 4.5. Average daily rainfall (in mm) from measured stations in the HPNBG and KBR compared to the same period as measured at Zandvlei in Cape Town.

Mucina and Rutherford (2006) comment that the Kogelberg region usually receives higher rainfall than other areas in the Cape Region. The greater variability in the rainfall of the HPNBG and KBR may be attributed to an increased orographic effect in the Kogelberg Mountains. The orographic effect at Zandvlei is limited to the west of the area, whereas the sites in this study have large elevation differences and are located on a more complex and rugged topography (Figure 1.5). Sites 1, 2 and 5 of this study are located at lower elevation and received more precipitation during autumn and winter, whilst during the summer months these sites received less precipitation than the more elevated sites 3 and 4. This seasonal difference in rainfall may also be a function of wind direction.

Northwesterly winds prevail during the passage of winter storm events while southeasterly winds prevail during the summer months. Jury (1991) attributes the predominant NW-SE wind axis as being influenced by the Hottentots-Holland Mountains. Southwesterly winds are rare and were recorded for two days during the November to January period. Figure 4.6 illustrates how the dominant southeasterly and northwesterly winds may influence the movement of storm events. Southeasterly winds may drive rain events from the south in a northwesterly direction across False Bay striking the study area first and then reaching

Zandvlei. Northwesterly winds may have the opposite effect with rain first falling at Zandvlei and then in the Kogelberg region.

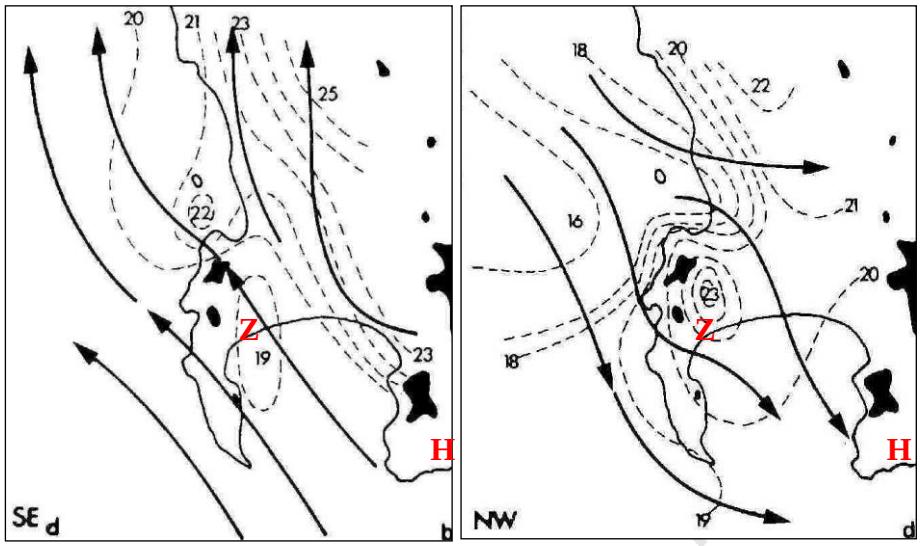

Figure 4.6. Mesoscale wind streamline patterns and air temperatures at 150 m for the dominant SE and NW weather phases. The dark shaded regions indicate elevations above 600 m and the dashed lines indicate air temperature at an elevation of 150 m. Z = Zandvlei. H = Harold Porter National Botanical Gardens (adapted from Jury, 1991).

A comparative look at the rainfall distribution between Zandvlei and the HPNBG and KBR suggests that orographic and frontal influences cause variations in the distribution of rainfall among the different sites. Rainfall in the HPNBG and KBR was less seasonal than that of Zandvlei, with peak rainfall in the spring months of Oct/Nov. Rainfall is not pure H_2O, but contains a variety of ions, particles and gases. The next section will explore the nature of major ions in the rainwater collected and what factors may have been important in determining their concentrations and distributions.

4.1.2 Rainwater Chemistry

Rainwater chemistry is influenced by different processes involving particle scavenging by cloud and rainwater. The composition of rainfall may further be influenced by the strength of emission sources, atmospheric chemical reactions and scavenging mechanisms by moving air masses (Avila and Alarcón, 1999). Kohfeld and Harrison (2001) noted that rainfall is important in the chemical composition of the climate system and provides nutrients to terrestrial and marine ecosystems.

The major ions Cl, Na, SO_4, Mg, K and Ca in rainfall were measured for this study. Two methods (ICP-MS and IC) were used to analyse Mg and Ca concentrations. The two methods should ideally give the same results and reflect a 1:1 ratio, but this was not the case. Ion concentrations from IC analysis were mostly higher than ion concentrations determined by ICP-MS (Figure 4.7). Correlation values (r) between the two methods were calculated to be 0.55 for Mg and 0.57 for Ca. Correlation between the two methods was shown not to be significant (Table 4.1). The difference between the two methods has been noted by previous workers (Soderberg, 2003). IC data for Mg and Ca are used in the discussion section of this thesis because the IC results show better reproducibility and concentrations for SO_4 and K were determined by IC only.

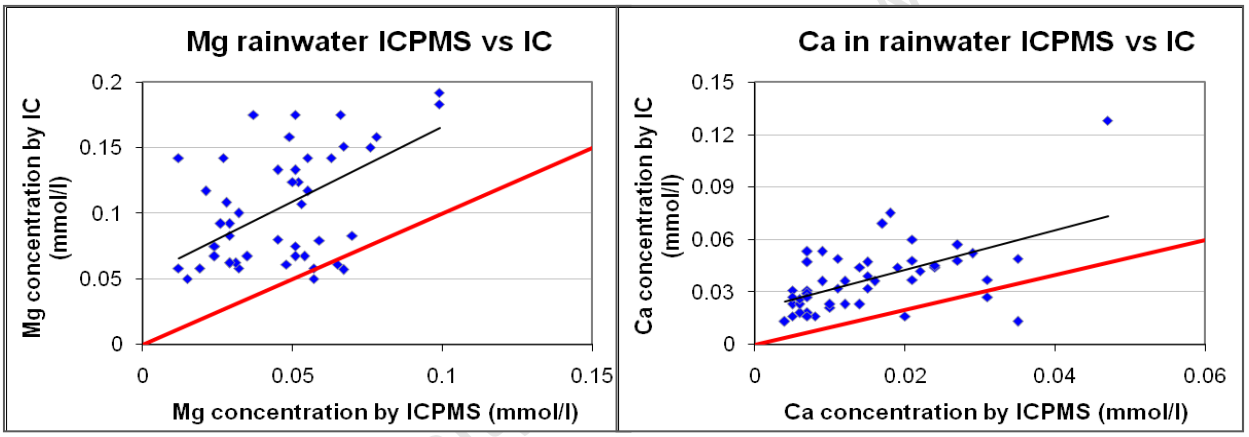

Figure 4.7. XY scatter plots for Mg and Ca concentrations as determined by ICP-MS and IC. The black line indicates the trend of the data. The red line indicates a 1:1 ratio.

Table 4.1. Statistical information for correlation and regression between ICP-MS and IC methods for Mg and Ca.

	Mg	**Ca**
R	0.55	0.57
p-value	<0.001	<0.001
df	47	47
Equation of the regression line	y= 1.382x + 0.0355	y = 1.5x + 0.017

Mean ion concentrations among the five sites are plotted as column charts with green and blue lines indicating the range in data (minimum concentration and maximum concentration) for the particular sampling period. Average Cl concentrations in the rainwater samples collected vary by up to a factor of four (Figure 4.8). Chloride is expected to be sourced primarily from marine aerosols (Gorham, 1958) and to be most concentrated during low rainfall periods and this is what is generally observed. Average Cl ion concentrations were highest during summer months with the lowest rainfall because of greater evaporation and less dilution by rainfall of washed out ions.

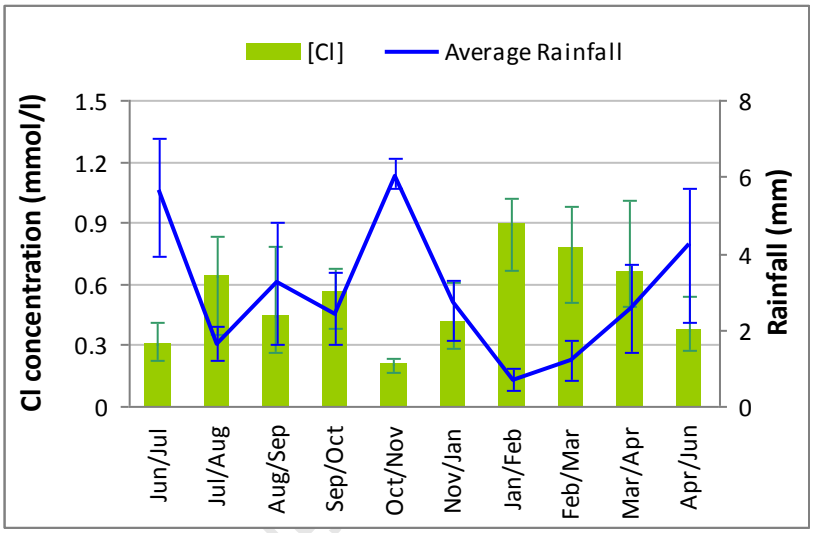

Figure 4.8. Mean Cl concentrations in rainwater for all five sites combined and average daily rainfall (mm/day) for sites measured in this study. The blue lines on the rainfall curve and the green lines on the Cl concentration bars indicate the range in data among the five sites.

Sodium showed a similar trend to chloride (Figure 4.9) with the mean Na concentration in rainwater increasing with a decrease in rainfall amount. A similar trend shared by Cl suggests the same strong marine influence.

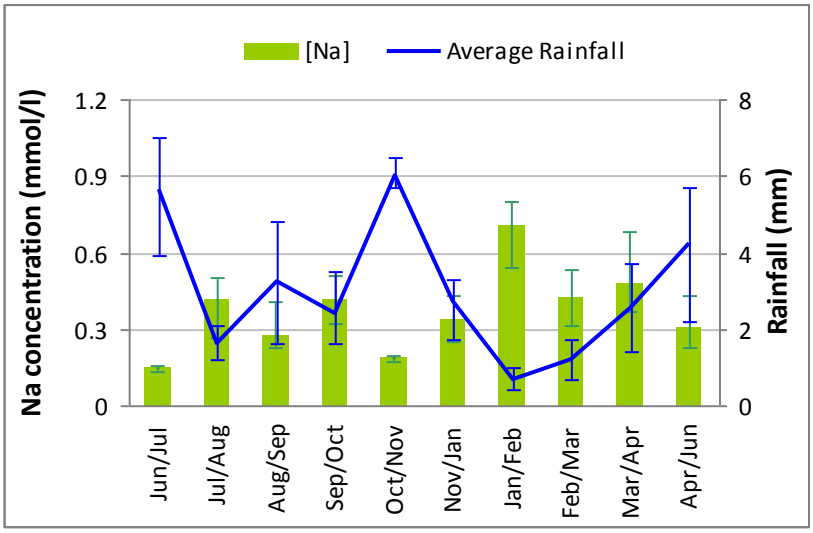

Figure 4.9. Mean Na concentrations in rainwater for all five sites combined and average daily rainfall (mm/day) for sites measured in this study. The blue lines on the rainfall curve and the green lines on the Na concentration bars indicate the range in data among the five sites.

Sulphate ion is also expected to have a strong marine influence, but does not show a pattern similar to that of Cl and Na. Sulphate shows an inverse relationship with rainfall amount for most of the sampling period (Figure 4.10). This relationship weakens from October to January. Sulphate concentration in rainwater is at its maximum during the Jan/Feb period when average rainfall was at its minimum. Autumn SO_4 concentrations decreased to their lowest levels when precipitation increased. These results indicate that there are other more significant sources of sulphate ion to the rainwater than marine aerosols.

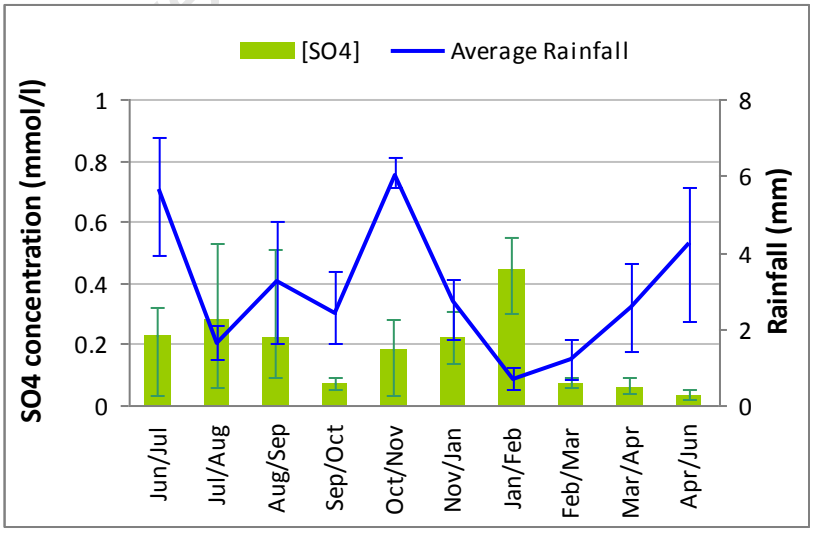

Figure 4.10. Mean SO4 concentrations in rainwater for all five sites combined and average daily rainfall (mm/day) for sites measured in this study. The blue lines on the rainfall curve and the green lines on the SO4 concentration bars indicate the range in data among the five sites.

Magnesium ion differs from the patterns displayed by Cl, Na and SO_4 and shows a weak marine influence with varied patterns through the seasons. Magnesium shows an inverse relationship to rainfall amount for much of the year (Figure 4.11).

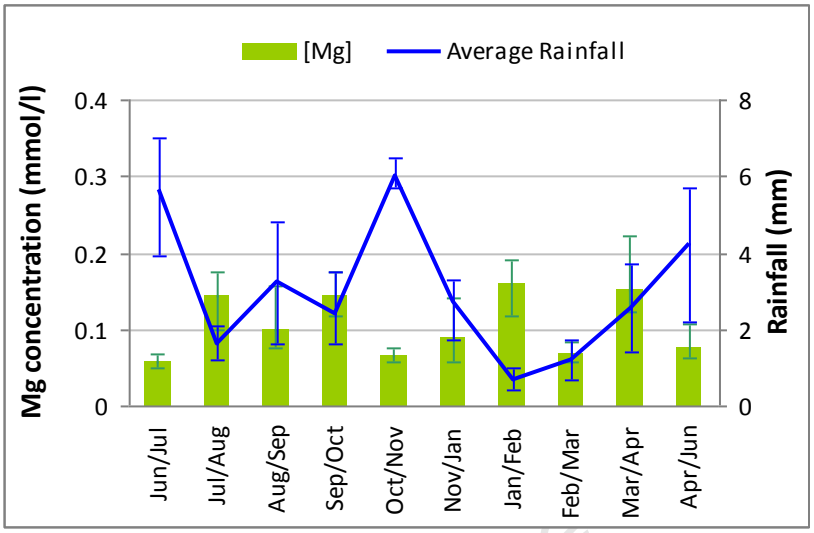

Figure 4.11. Mean Mg concentrations in rainwater for all five sites combined and average daily rainfall (mm/day) for sites measured in this study. The blue lines on the rainfall curve and the green lines on the Mg concentration bars indicate the range in data among the five sites.

Calcium shows a similar trend to Mg which suggests a mixed source of marine and mineral dust for these elements in rainfall. Figure 4.12 illustrates a moderate inverse relationship between Ca concentration and rainfall amount. Calcium concentrations peak in autumn as rainfall increases. The lowest Ca concentration was during the Oct/Nov period, much like Cl, Na and Mg, when rainfall was at its highest.

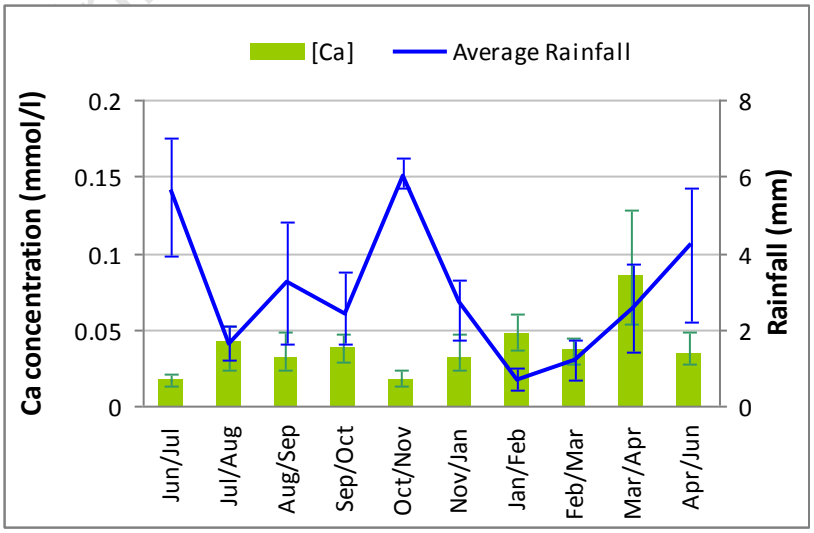

Figure 4.12. Mean Ca concentrations in rainwater for all five sites combined and average daily rainfall (mm/day) for sites measured in this study. The blue lines on the rainfall curve and the green lines on the Ca concentration bars indicate the range in data among the five sites.

Average K concentrations show a similar pattern to that of Ca and Mg (Figure 4.13). Winter and spring months indicate a decrease in K with an increase in rainfall whereas the K increases with rainfall amount during late summer to autumn.

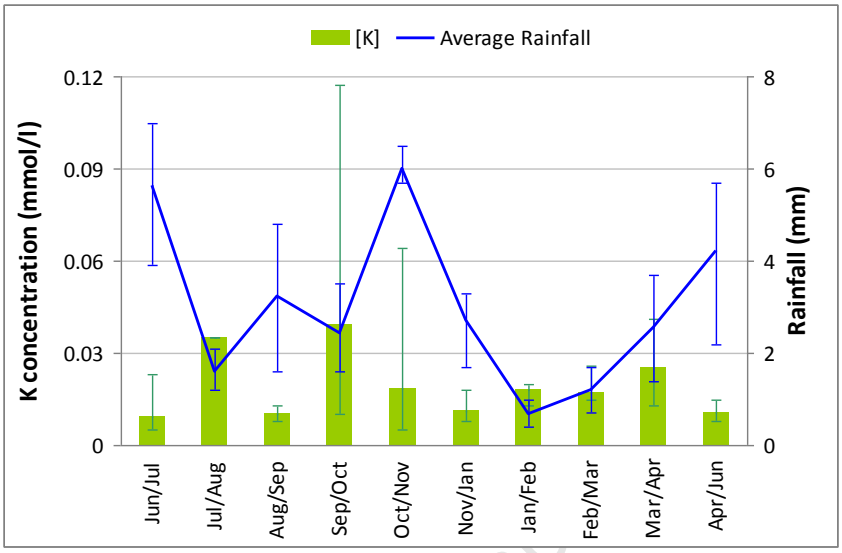

Figure 4.13. Mean K concentrations in rainwater for all five sites combined and average daily rainfall (mm/day) for sites measured in this study. The blue lines on the rainfall curve and the green lines on the K concentration bars indicate the range in data among the five sites.

All major ions measured in this study show an inverse relationship with rainfall to varying degrees among the different sites. All sites show a negative correlation between rainfall amount and the concentration of the major ions Cl, Na and Mg and to a lesser extent SO_4 (Table 4.2). The negative correlation of rainfall to Cl and Na concentrations is greatest at site 1 near the coast and tends to decrease at sites further away from the coast suggesting a rapid rain out of marine aerosols across the study area. Site 1, the closest site to the coast, also has the highest negative correlation to rainfall for all the ions measured except K. Chloride and sodium concentrations show the strongest negative correlation to rainfall amount. Magnesium and calcium share a more moderate inverse correlation between concentration and rainfall amount. Correlation values (r) for K closest to the coast indicate a weak correlation between ion concentration and rainfall amount. The correlation between K concentration in rainwater and rainfall amount becomes stronger and negative for sites further away from the coast. Graphs and calculated correlation values in this study thus support the idea that Cl and Na concentrations and rainfall have a consistent strong negative correlation whereas SO_4, Mg, Ca and K show only episodic weak correlations with rainfall amount.

Table 4.2. Correlation values (r) for the relationship between major ions (Na, Cl, Mg and SO4) and rainfall amount across the 5 sites discussed in this study. The numbers in parentheses indicate p-values for the correlation values at 9 degrees of freedom.

	Site 1	Site 2	Site 3	Site 4	Site 5
Cl	-0.90 (<0.001)	-0.78 (<0.005)	-0.83 (<0.001)	-0.71 (<0.02)	-0.68 (<0.05)
Na	-0.93 (<0.001)	-0.84 (<0.002)	-0.84 (<0.001)	-0.73 (<0.02)	-0.79 (0.005)
SO_4	-0.69 (<0.02)	-0.13 (<0.8)	-0.02 (<0.8)	-0.45 (<0.2)	0.01 (<0.8)
Mg	-0.68 (<0.02)	-0.51 (<0.2)	-0.65 (<0.02)	-0.57 (<0.1)	-0.75 (<0.01)
Ca	-0.82 (<0.002)	-0.53 (<0.2)	-0.69 (<0.02)	-0.42 (<0.2)	-0.63 (<0.05)
K	0.10 (<0.8)	-0.57 (<0.2)	-0.50 (<0.2)	-0.65 (<0.02)	-0.90 (<0.001)

The dominance of Cl, Na and SO_4 is also reflected in rainfall collected further inland in the Olifants River Valley where Cl and Na ions showed the highest concentrations at ratios similar to seawater. This suggests that marine aerosols are a major source for the ions Cl, Na, SO_4 and Mg in rainwater in the Olifants River Valley (Soderberg 2003; Soderberg and Compton, 2007). Van Wyk *et al*. (1992) also concluded that a dominant marine source exists for Cl, Na, SO_4 and Mg in the Swartboskloof. The study area of Van Wyk *et al*. (1992) is 20 km north and that of Soderberg (2003) lies 70km north of the study area of this thesis (Figure 4.14). It is expected that concentrations for ions sourced from marine aerosols decrease further inland as marine salts are rapidly rained out as fronts move inland and a continental influence on rainfall increases.

Figure 4.14.Google Earth image of the Western Cape showing locations for previous and current studies discussed in this chapter. Locations for the Swartboskloof (Van Wyk *et al*., 1992), the Olifants River Catchment (Soderberg, 2003) and the study area for this thesis are indicated by the yellow pins.

A comparison between the mean major ion concentrations of the three studies indicates a significant decrease further inland (Figure 4.15). Major ion concentrations in rainwater are the highest for the Kogelberg region and drops off substantially towards the interior. The higher mean Cl, Na, SO_4 and Mg concentrations in the HPNBG and KBR suggest that coastal areas may have a greater marine aerosol influence compared to areas further inland. This result may be exaggerated by the fact that the rainwater samples in Soderberg (2003) were collected during rain events in pre-cleaned collectors. Only wet deposition was thus collected in the study of Soderberg (2003) and no dry deposition.

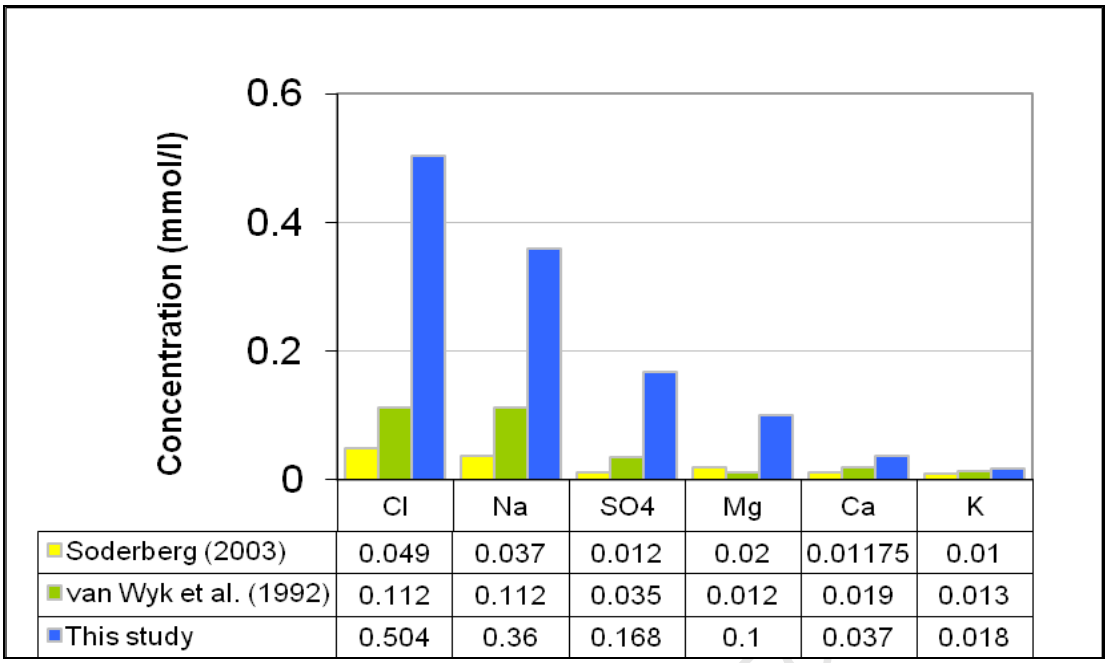

Figure 4.15. A comparison between macronutrient (Cl, Na, SO_4, Mg, Ca and K) concentrations of the Elandskloof subcatchment area (Soderberg, 2003), the Swartboskloof (van Wyk et al., 1992) and the study area discussed in this study.

A method to determine how dependent ion concentration is on a marine source involves comparing ion-chloride molar ratios within rainwater to ion-chloride molar ratios of seawater. The assumption with ion-chloride ratios is that Cl is the most conservative ion with no other sources of Cl besides seawater and therefore ratios to Cl should give an indication of the significance of marine aerosols.

Molar ratios for Na/Cl plot relatively close to the seawater line (Figure 4.16) and indicate a predominantly marine source for Na. However, Na in rainwater is relatively depleted compared to seawater for certain periods of the year. It may be possible that the presence of other minerals and particles in the rainwater will have an affect on Na. The removal of Na by adsorption to particle surfaces may change the molar ratios to values less than the seawater signature line. Van Wyk *et al.* (1992) suggested a marine influence for Na in their study as well, but a stronger continental influence for SO_4.

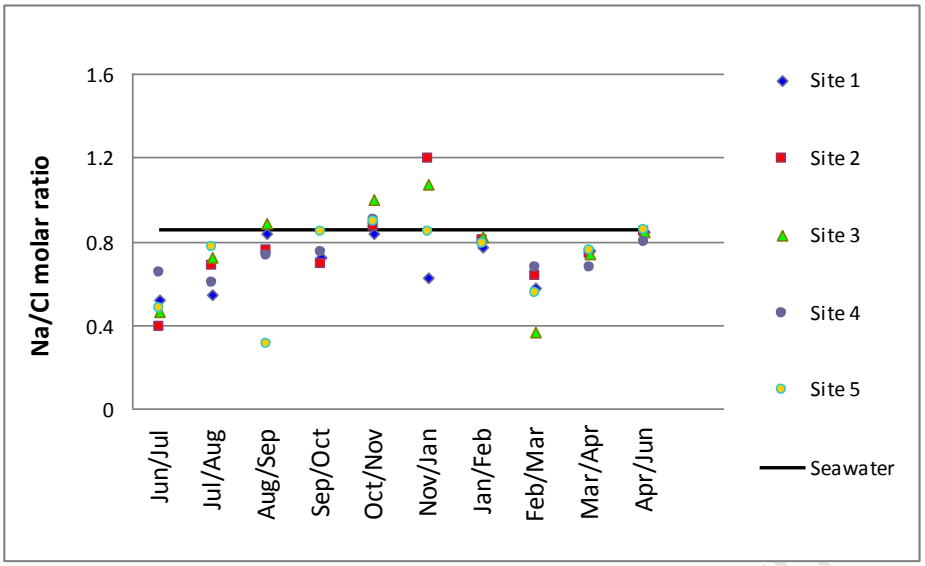

Figure 4.16. Na/Cl molar ratios for rainwater collected at all five sites discussed in this study. The molar ratio for seawater (0.85) is plotted as a black solid line for comparison.

A large amount of scatter is observed in results obtained for SO_4/Cl molar ratios in this study (Figure 4.17). Sulphur is relatively enriched in rainwater compared to seawater. This suggests additional inputs from the atmosphere besides marine aerosols. The large amount of scatter in the data may also be related to the uncertainty of the data. Some duplicate samples for SO_4 revealed a difference of more than 10% whereas most duplicates had differences of below 10%. Van Wyk *et al.* (1992) mention that the rainwater chemistry may not reflect any changes brought on by a fire event. It should however be noted that large amounts of biomass were burnt during the two fire events relevant to this study. Ash, plant debris and subsequent erosion may increase after fire. Burnt plant material and fine ash were observed on the collectors and in the samples during fieldwork. Burnt plant material and ash particles remain in the ecosystem as the ecosystem is gradually reestablished after the fire event.

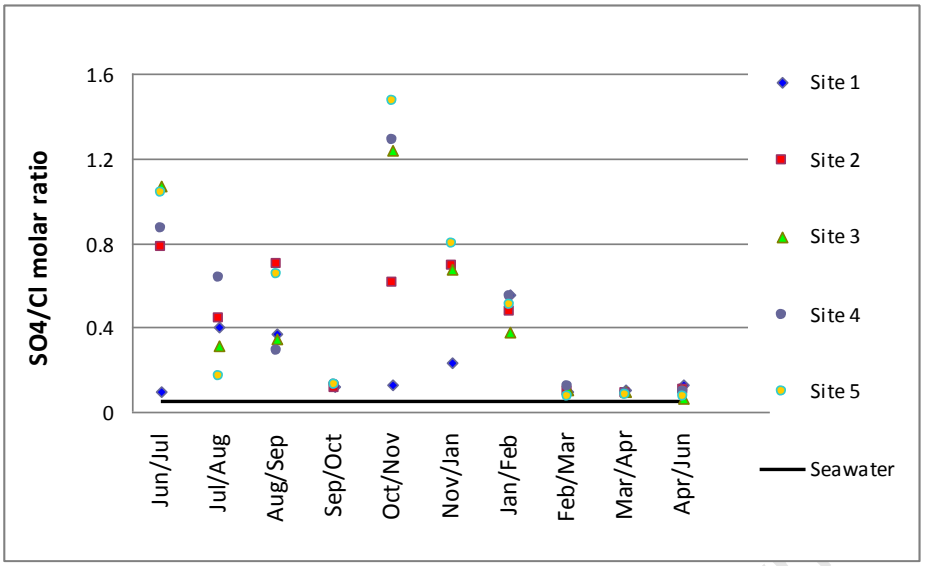

Figure 4.17. SO_4/Cl molar ratios for rainwater collected at all five sites discussed in this study. The molar ratio for seawater (0.05) is plotted as a black solid line for comparison.

Chloride molar ratios for sulphate during the periods Jun/Jul, Oct/Nov and Nov/Jan increase with distance from the ocean. Site 1 plots closest to the seawater line and sites 3 to 5 furthest. This indicates a decreasing marine influence further away from the ocean. The reasons for the sulphate distributions and variations may become complex and a range of factors need to be considered.

Faloona (2009) describes sulphur compounds as playing an integral part of coastal atmospheric budgets due to the vast source pool of sulphate in the ocean. Sulphur may be released into the atmosphere through human activities and natural processes (Figure 4.18). Anthropogenic activities emitting SO_2 into the atmosphere include industrial processes (Gorham, 1958), fuel combustion, ore processing and biomass burning (Mihajlidi-Zelić *et al*., 2006; Faloona, 2009). It can be assumed that these effects are minimal in and around the study area as it is far from industrial or urban development areas. The release of SO_2 from volcanic activity can be ruled out in this study. Dimethyl sulfide (DMS) and H_2S are released through primary productivity in the oceans as a result of assimilatory reduction through phytoplankton (Eckardt, 2001). Bathmann *et al.* (1997) describe phytoplankton blooms as playing an important role in the transport of biogenic elements from the surface layer to coastal areas and inland. The aforementioned compounds are transformed (oxidized) into SO_4 in a matter of days (Gorham, 1958; Eckardt and Spiro, 1999; Faloona, 2009; Lana *et al*., 2011) and ultimately aid in the formation of cloud condensation nuclei

(CCN). Sulphate then forms part of marine aerosols and may wash out during rain events (Kwint and Kramer, 1996; Eckardt, 2001; Faloona 2009).

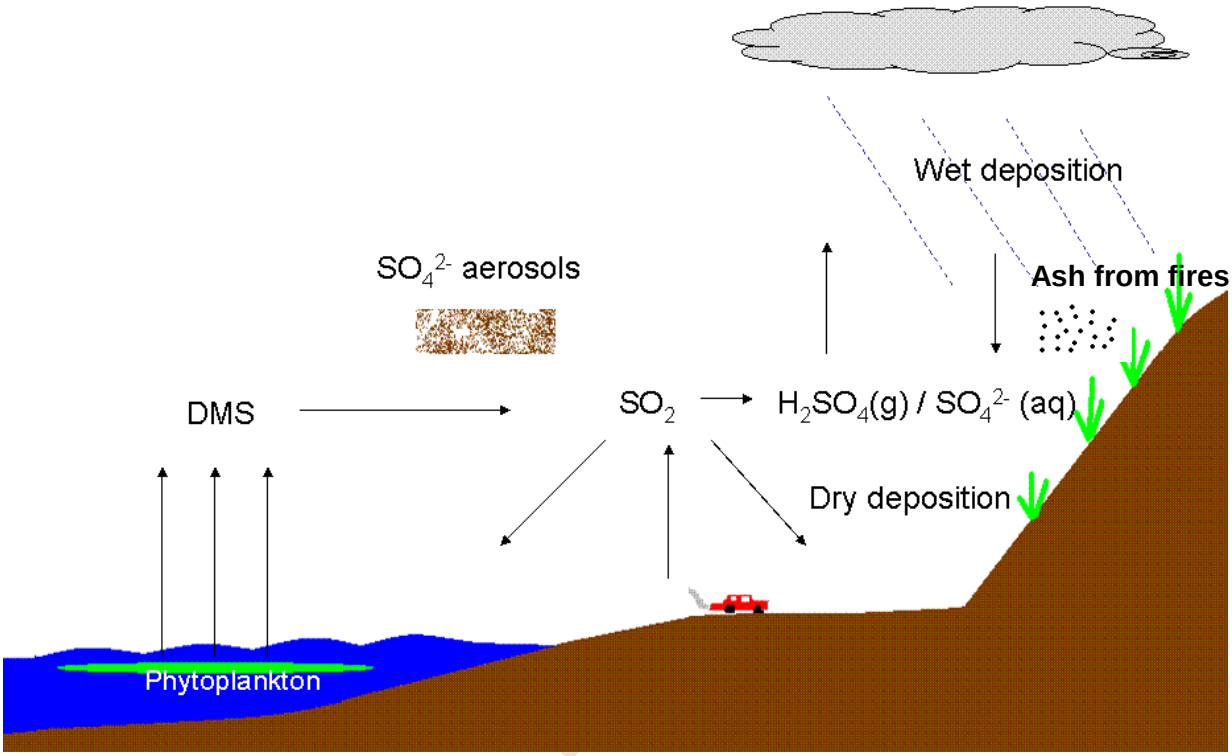

Figure 4.18. Simplified diagram of inputs and outputs into the sulphur cycle as described by Faloona (2009).

Bathmann *et al.* (1997) identify the seasonality of phytoplankton blooms forming mostly in spring. Lana *et al.* (2011) suggest maximum DMS production from phytoplankton blooms off the southwestern coast of South Africa to occur during summer months (November to March). This may support the occurrence of unusually high sulphate levels in the rainwater samples during October and November 2010 that then decreased with time. It may also be the case that sulphate from ash particles in the atmosphere gradually dropped, but DMS-derived sulphate coupled with SO_4 leached from ash particles may have contributed to the high SO_4/Cl molar ratios during Oct/Nov 2011. However, the reason why DMS-derived sulphate is least abundant at site 1, which is closest to the ocean, is not clear. Dry particles in the form of mineral S and SO_4 compounds as well as ash from fires, may impact on the surface or be incorporated into rain droplets. The high SO_4/Cl molar ratios of Jun/Jul 2010 that dropped off rapidly to Sep/Oct 2010 may reflect the rainout of ash material following the fire event of 3 June 2010. In contrast the fire event of 16 March 2011 to the northeast of the study area did not appear to have impacted the SO_4/Cl molar ratios which remained at

near marine values from Feb/Mar to Apr/Jun 2011. Clearly a large number of complex factors can influence the varying patterns displayed by sulphate in this study.

Molar ratios for Mg/Cl indicate the strongest marine signature during February/March 2011 (Figure 4.19). The highest molar ratios were recorded during the period of highest rainfall (Oct/Nov). The lowest molar ratios were recorded during the driest period (Feb/Mar). Results suggest an increasing marine influence from Oct/Nov to Feb/Mar as rainfall decreases.

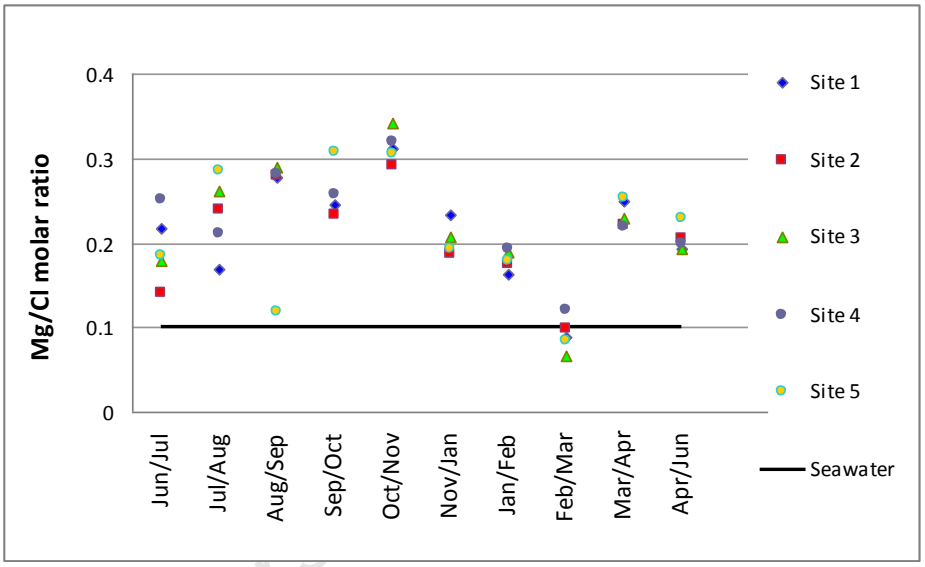

Figure 4.19. Mg/Cl molar ratios for rainwater collected at all 5 sites discussed in this study. The molar ratio for seawater (0.1) is plotted as a black solid line for comparison.

Results for Ca/Cl molar ratios indicate similar trends to that of Mg/Cl molar ratios (Figure 4.20), although the greatest continental influence was during the Mar/Apr period perhaps associated with the fire event of 16 March 2011 that swept through the northeastern part of the Kogelberg Biosphere Reserve. Minerals may be remobilized and distributed via wind in the form of windblown dust and ash. Molar ratios for Ca/Cl show a positive correlation with rainfall amount during the period Jul/Aug 2010 to Feb/Mar 2011. Similar to Mg/Cl molar ratios the lowest Ca/Cl molar ratios were recorded during the driest period (Feb/Mar).Van Wyk *et al.* (1992) found that Mg and Ca concentrations had a greater continental influence. Results in this study suggest a mixture of marine aerosols and mineral dust for Mg and Ca.

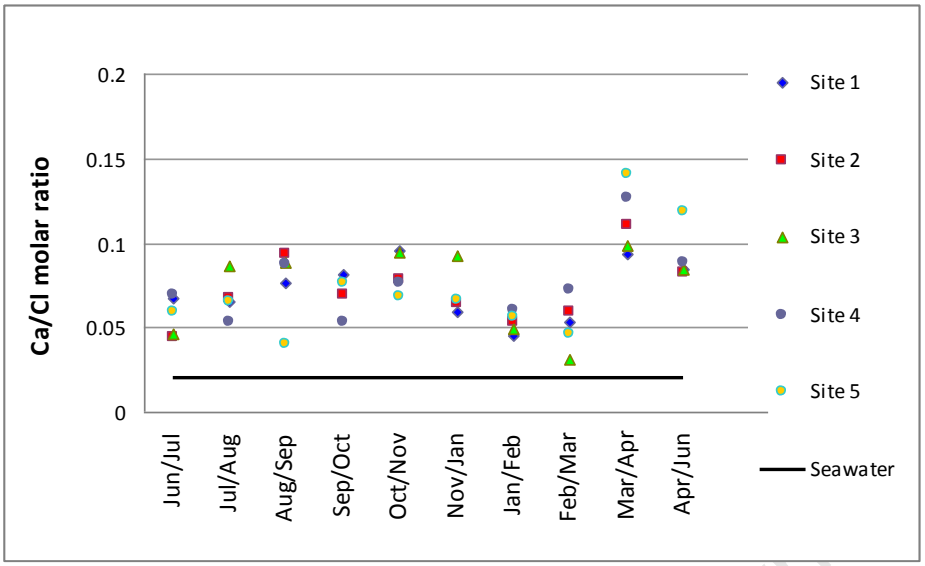

Figure 4.20. Ca/Cl molar ratios for rainwater collected at all five sites discussed in this study. The molar ratio for seawater (0.02) is plotted as a black solid line for comparison.

Potassium-chloride molar ratios largely show a positive correlation to rainfall amount. Molar ratios for K/Cl increase during periods of higher rainfall and decrease during drier periods. Molar ratios for K/Cl are similar to seawater or only deviate to somewhat higher values and indicate a larger marine influence for K than for either Mg or Ca (Figure 4.21). Chemical constituents within the rainwater may not only be derived from the diffusion of soluble particles into liquid molecules, but may also be derived from dry fallout. Particles may be collected or fall in the rain sampler through dry atmospheric processes and later incorporated into the collected rain. The fallout of dry particles may also be accelerated through rain events. Potassium associated with mineral or organic particles in the rainwater may be less easily dissolved into the rainwater than Ca and Mg especially if Ca and Mg are associated with highly soluble carbonate minerals such as calcite or dolomite.

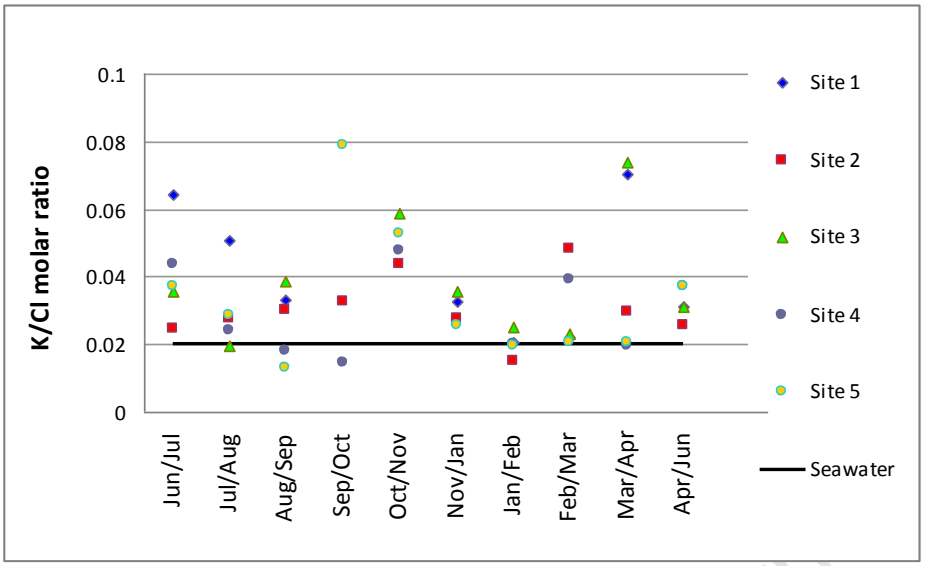

Figure 4.21. K/Cl molar ratios for rainwater collected at all five sites discussed in this study. The molar ratio for seawater (0.02) is plotted as a black solid line for comparison.

Molar ratios for Ca/Cl in rainwater are up to 7 times the seawater ratio and Mg/Cl and K/Cl up to 3 times the seawater ratio. This reflects additional sources to marine aerosols and may come from mineral dust and ash. Dust particles from the interior may arrive through any northerly wind (Figure 4.22). Northwester winds dominated during winter months. This coincides with higher Mg/Cl and Ca/Cl molar ratios during the periods Mar/Apr and Apr/Jun. The wind may carry mineral dust and terrestrial dust particles from further inland and into the study area, contributing to a higher continental influence during the autumn and winter months. Conversely, any southerly summer winds should contribute marine aerosols to the study area. The lower Mg/Cl and Ca/Cl molar ratios during the summer period Feb/Mar corresponds with a dominant SE wind direction which would favour marine over continental dust aerosols.

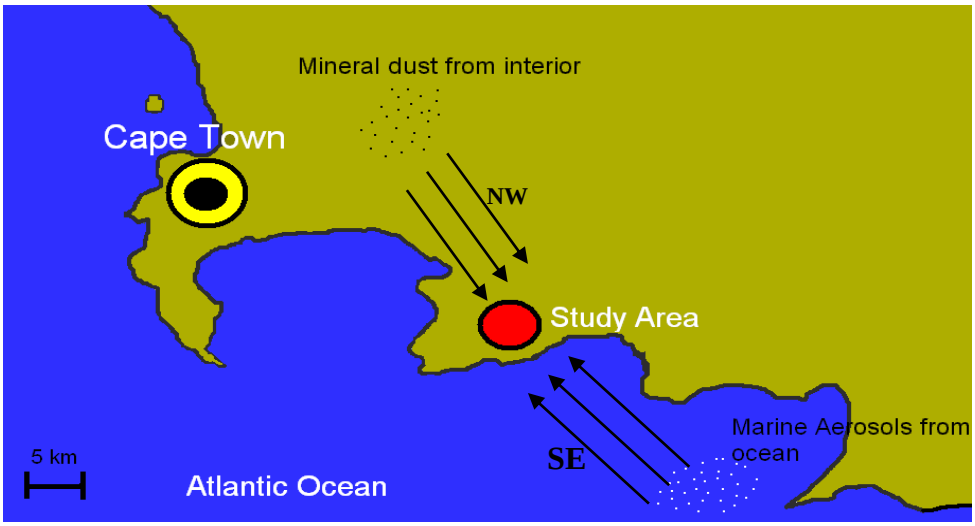

Figure 4.22. Illustration showing how mineral dust and marine aerosols are delivered to the study area driven by the dominant seasonal wind directions (NW in winter and SE in summer). This figure can be read in conjunction with Figure 4.6.

Galloway (1978) identified Na, K, Ca and Mg as the most common elements that are present in precipitation that are derived from soils through dry deposition. Another reason for the variation in chloride molar ratios of Ca, Mg and K may be in their ability to be released from the mineral dust into rainwater. The rainwater pH measured in this study is slightly acidic ranging from 5.3 to 5.9 (Table 4.3). These pH values indicate an acidity which would favour the leaching of these elements, for example Ca may be released from calcite more rapidly than K would be released from clay minerals. This would increase the Ca/Cl ratio in rainwater more readily than the K/Cl ratio.

Graphical representations of rainfall data and rainwater chemistry suggest an inverse correlation between the two. Chloride and sodium show the strongest negative correlation with rainfall amount. Low rainfall can cause high salt (Cl and Na) content within precipitation. Magnesium and calcium concentrations also show a negative correlation with rainfall amount, but to a weaker degree. Potassium showed almost no correlation between ion concentration and rainfall amount. Chloride-ion molar ratios for this study suggest a strong marine influence for major ions, but to varying degrees between major ions. Sodium shows a strong marine influence. Molar ratios for SO_4/Cl indicate a mixture of marine (DMS production) and terrestrial (ash from fires, mineral dust, etc.) sources. Magnesium and calcium show a stronger continental influence than other ions. Potassium had a stronger marine influence than Mg and Ca. Major ion contents in rainfall may further be influenced by a range of atmospheric processes such as wind direction, rainfall amount and

temperature variations. Macronutrients, as they are washed out by rainfall onto the land surface, may ultimately be transported through a network of ecosystem components such as vegetation interception, soils, streams and bedrock infiltration (Gibbs, 1970).

4.2 Streams and Mountain Seeps

Rainfall introduces water to the land surface where it will pass over vegetation and soils and eventually infiltrate into the bedrock and flow by seeps into streams and exit the study area to the sea by means of rivers. Stream and mountain seep waters can act as both a source and pathway for the transport of ions. Streams provide habitat for various vertebrate and invertebrate fauna and provide a source of nutrients to plants. Soderberg (2003) describes a river catchment as a large continuous and selective deposition collector. The transport of ions and cycling of nutrients within the streams never cease and this provides an invaluable link to other components within the ecosystem. This process may in turn depend on various factors and characteristics of the stream water. The chemistry of seep and stream waters are compared here to the chemistry of the rainfall and what these differences imply about nutrient cycling within the study area.

The stream waters and mountain seeps in the HPNBG and KBR are light to dark brown in colour and vegetation is most concentrated along river banks (Figure 4.23). The predominantly afromontane vegetation within the deep gorges along streams 5, 6 and 7 was largely unaffected by the June 2010 fire event and was not burnt. Fynbos vegetation around other streams and mountain seeps steadily returned during the course of this study and did not fully recover at the conclusion of fieldwork (Appendix D). However, the vegetation regrowth around the streams was faster than on the mountain slopes. Rundel (1983) and van Wyk *et al.* (1992) mention the maturity of a fynbos ecosystem to be approximately 20 years. The last fire event before the 2010 fire was in 1991. All of the above ground vegetation was removed by the fire of 3 June 2010 and was slow to recover. Therefore, the above ground vegetation is absent and a more direct relation of rainout to stream water chemistry can be anticipated.

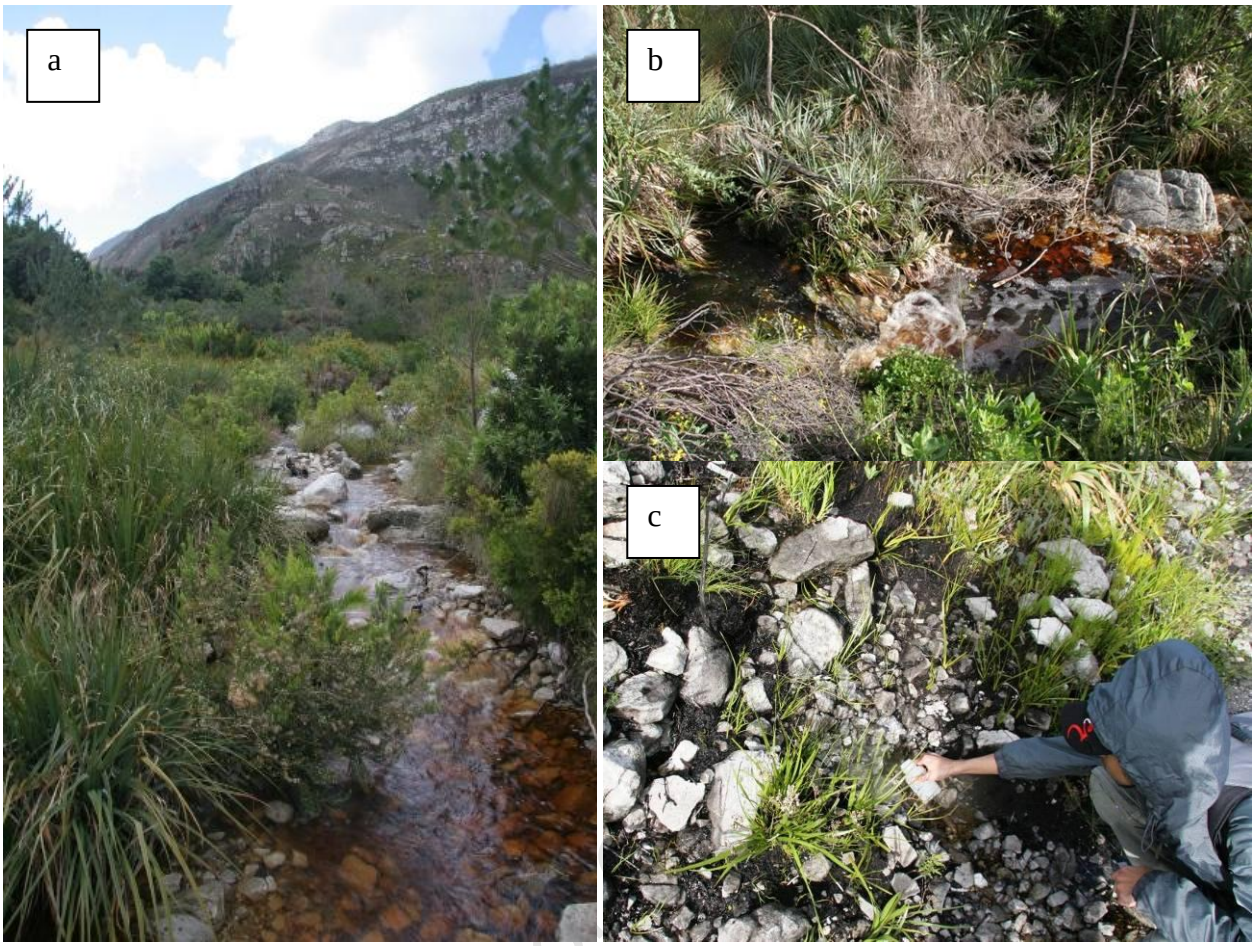

Figure 4.23. Some of the streams sampled in this study include a) the Dawidskraal River in the HPNBG (str06), b) the Oudebosch River in the KBR (str01) and c) a mountain seep feeding into the Oudebosch River (str02). Pictures by John Compton.

King and Day (1979) mentioned stream waters of the fynbos biome to be low in nutrients with low total dissolved salts (TDS), to be poorly buffered and to have low sediment loads with pH levels as low as 4.3. Smit (2003) reported pH values of 3.7 to 4.2 for selected streams in the HPNBG. The temperature and pH of streams sampled in this study measured on 17 August 2010 (Table 4.3) had pH values lower than that of King and Day (1979) and similar to values measured by Smit (2003).

Table 4.3. A comparison between the pH values of rain, stream and mountain seep waters as measured on 17 August 2010.

	Sampling site	pH in standing water	Temperature of standing water (in °C)	pH in flowing water	Temperature of flowing water (in °C)
Rainwater	Site 1 (HPNBG)	5.8	13.4	-	-
	Site 2 (HPNBG)	5.9	11.9	-	-
	Site 3 (HPNBG)	5.3	14.3	-	-
	Site 4 (HPNBG)	5.4	14.1	-	-
	Site 5 (KBR)	5.3	11.1	-	-
Stream water	Str01 (KBR)	4.2	11	4.1	11
	Str02 (KBR)	4.2	14.4	4.15	14
	Str03 (KBR)	4.39	16.4	4.32	16.2
	Str04 (HPNBG)	4.08	14	4.02	14
	Str05 (HPNBG)	4.05	11.4	4	11.2
	Str06 (HPNBG)	4.1	11	4.04	11
	Str07 (HPNBG)	4.2	13.3	4.01	13.2

Rainwater samples recorded higher pH values (5.3 to 5.9) compared to stream water samples which ranged from 4 to 4.3 in flowing stream water and 4.1 to 4.4 in standing water. The pH of rainwater in this study agrees with the upper limits of the pH in rainwater (4.6 to 5.8) found by Soderberg (2003) and Soderberg and Compton (2007) in the Olifants River Valley. The lower pH of stream waters relative to rainwater can be ascribed to interactions with soil organic matter and a lack of carbonate buffering from the sandstone bedrock (Smit, 2003). The low pH of stream waters may have further implications on the chemistry of stream and seep waters. Major ions in stream waters include Cl, SO_4, Na, Mg, K and Ca (with descending concentrations in that order). This is consistent across all streams and mountain seeps during the entire sampling period. The major ion chemistry of the streams was similar to that observed in the rainwater chemistry except for certain periods and sites during the year. Ions within the streams come from a variety of sources and interactions between different components of the ecosystem.

4.2.1 Stream Water Chemistry

Stream waters derive their dissolved salts and nutrients from a variety of sources. Dry fallout of particles on stream surfaces (Galloway, 1978), rainout of particles (Galloway, 1978; Lovett, 1994), through the decomposition of plant material (Mitchell, *et al*., 1986) and groundwater interaction with soil and bedrock and the subsequent outflow of seeps into rivers, streams and tributaries can all contribute to the chemical composition of stream waters.

Rainfall can have a direct influence on stream water and plays an important role in stream flow and capacity. Certain ions within stream water may reflect a similar source as rainfall. This is expected of the dissolved salts such as Cl and Na. Results here indicate that concentrations of these salts do not show a direct relationship with rainfall amount. It would be expected that evaporation during drier summer months would lead to increased concentrations, but results suggest otherwise. Chloride concentrations in streams and mountain seeps are higher during winter and spring months (June to October 2010) than during summer months (November 2010 to February 2011) (Figure 4.24).

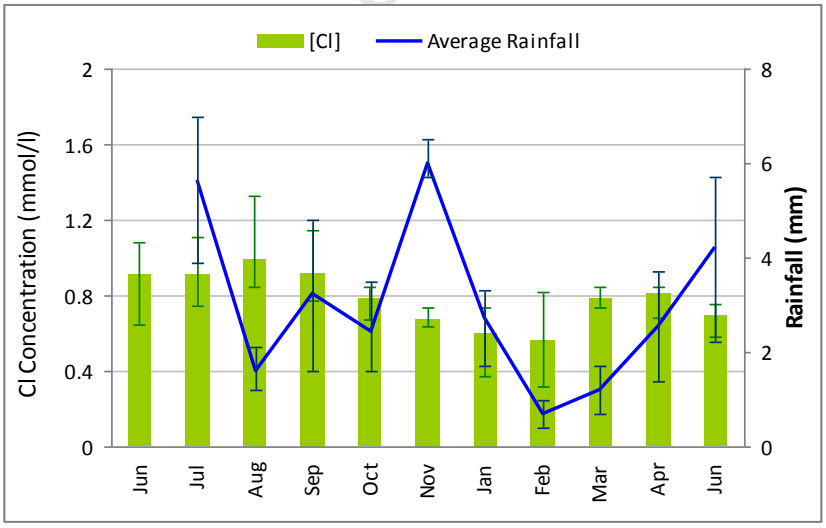

Figure 4.24. Mean Cl concentrations in all of the main streams and mountain seeps sampled in this study with average daily rainfall (mm/day) on the secondary y-axis. The blue lines on the rainfall curve and the green lines on the Cl concentration bars indicate the range in the data among the sampling sites.

A decreasing rainfall rate coupled with higher temperatures during summer months increase evaporation and retention of salts on the surface rather than being washed into streams during the dry summer months. Chloride concentrations increase during periods of higher

rainfall indicating salts being washed into streams during winter months. Results from the rainwater chemistry indicate chloride to be less concentrated in rainwater compared to stream water. This may indicate accumulation of Cl in stream waters by evaporation. Mean Cl concentration across all sites in rainwater is 0.5 mmol/l (Figure 4.8 and Figure 4.15) compared to 0.8 in stream waters (Figure 4.24) suggesting an evaporative water loss of 38%.

The mean Na concentrations show less variability and differ from Cl during winter, but show similar trends during summer and autumn (Figure 4.25). Sodium increases with a decrease in rainfall during winter and spring months. The mean Na concentrations show a similar trend as rainfall indicating that Na is dependent on rainfall amount during summer and autumn months. The mean Na concentration in stream waters show less variation compared to Na in rainwater.

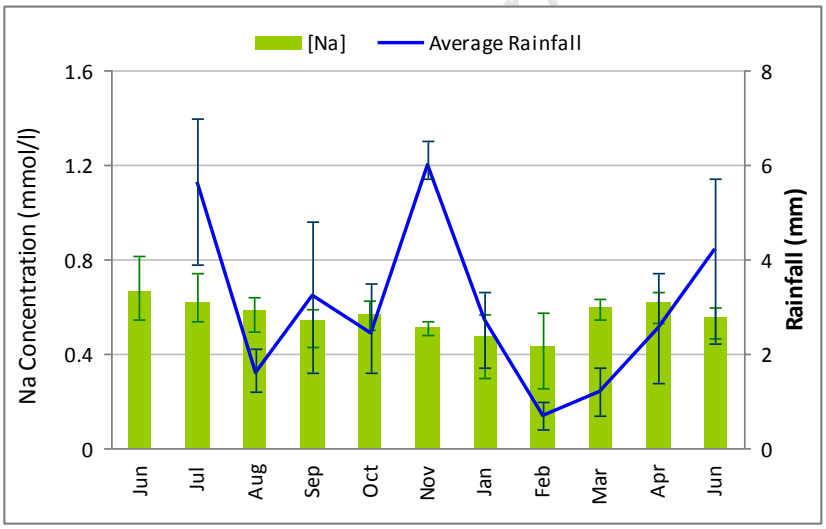

Figure 4.25. Mean Na concentrations for all the main streams and mountain seeps sampled in this study with average daily rainfall (mm/day) on the secondary y-axis. The blue lines on the rainfall curve and the green lines on the Na concentration bars indicate the range in the data among the sampling sites.

Similar to Cl, Na is more concentrated in stream water compared to rainwater. The mean Na concentration in rainwater is less than 0.4 mmol/l (Figure 4.9 and Figure 4.15) compared to 0.6 (Figure 4.25) in stream waters suggesting an evaporative water loss of 33%.

Sulphate behaves differently to Na and Cl. The sulphate data show more variability and results indicate that there is no clear relation between SO_4 and rainfall amount (Figure 4.26). Sulphate in stream waters shows higher concentrations following the fire event of June

2010. Concentrations remain high until September and then decrease and show no consistent correlation to rainfall. A decrease in sulphate during drier periods may indicate evaporative retention by salts in soils during periods of higher temperatures and lower rainfall. The decline in sulphate from September 2010 to June 2011 may reflect the gradual leaching out of soluble sulphate from ash deposited during the fire event over time. The pattern for mean SO_4 concentrations in stream water differs to that in rainwater, but still shows a major decline in concentration after March 2011. This indicates different source controls on rainwater and stream water. Accumulation of salts during dry periods coupled with decreased stream capacity and flow and stream-soil and stream-bedrock interaction may have additional effects on SO_4 concentrations in stream water and mountain seeps outside of rainwater and dry fallout.

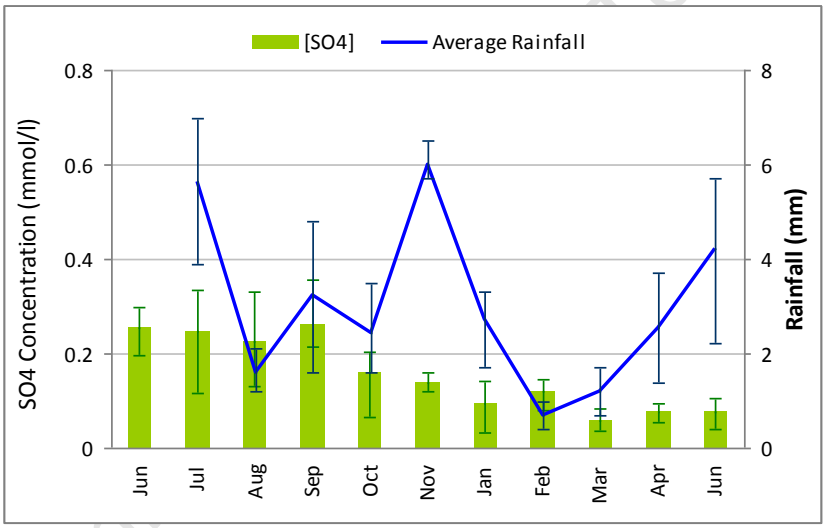

Figure 4.26. Mean SO_4 concentrations for all the main streams and mountain seeps sampled in this study with average daily rainfall (mm/day) on the secondary y-axis. The blue lines on the rainfall curve and the green lines on the SO_4 concentration bars indicate the range in data among the sampling sites.

The mean SO_4 concentration in rainwater is 0.17 mmol/l (Figure 4.10 and Figure 4.15) compared to 0.18 (Figure 4.26) in stream waters suggesting that SO_4 may be leaving the system or retained in the soil when evaporation is taken into consideration.

Both Mg and Ca average concentrations in stream waters show high values after the June 2010 fire event and then progressively decrease until March 2011 when both ions increase sharply until June 2011. The sharp increase in concentrations after March 2011 (Figure 4.27) may be related to the fire event to the northeast of the study area on 16 March 2011. Sampling of stream water took place 9 days after the 16 March 2011 fire event. Ash and

burnt plant material may have blown into the area and leached into stream waters. Wind direction data obtained from the offices of the HPNBG indicate a northwesterly wind blowing through the area one week prior to sampling the stream water. Northwesterly winds would have been capable of blowing some fire ash over and into the study area. There is less variation in the mean Mg concentrations in stream water than in rainwater suggesting additional inputs of Mg to stream water such as mineral aerosols.

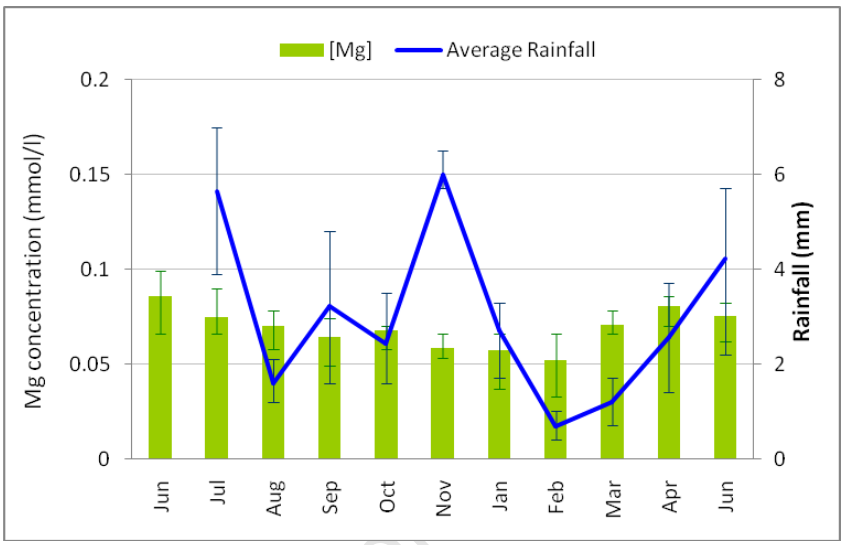

Figure 4.27. Mean Mg concentration for all the main streams and mountain seeps sampled in this study with average daily rainfall (mm/day) on the secondary y-axis. The blue lines on the rainfall curve and the green lines on the Mg concentration bars indicate the range in data among the sampling sites.

The mean Mg concentration in rainwater is 0.1 mmol/l (Figure 4.11 and Figure 4.15) compared to 0.07 (Figure 4.27) in stream waters. If an average evaporative water loss of 35% between Cl (38%) and Na (33%) can be taken as the minimum, then approximately half of the rainwater Mg input is retained by the soils.

Mean Ca concentrations in stream water show the same pattern as Mg. The highest mean Ca concentrations were found to be after the March 2011 fire event (Figure 4.28). The lowest Ca concentrations were during periods of both high and low rainfall. The summer months show low mean Ca concentrations indicating accumulation on surfaces. Accumulated Ca ions are being washed into streams during winter. Calcium in stream waters shows a more consistent pattern in stream waters than in rainwater. This suggests additional inputs into the streams such as increased dry deposition from the atmosphere. Similar to Mg, increased Ca concentrations in the streams are noticed after the March 2011 fire event.

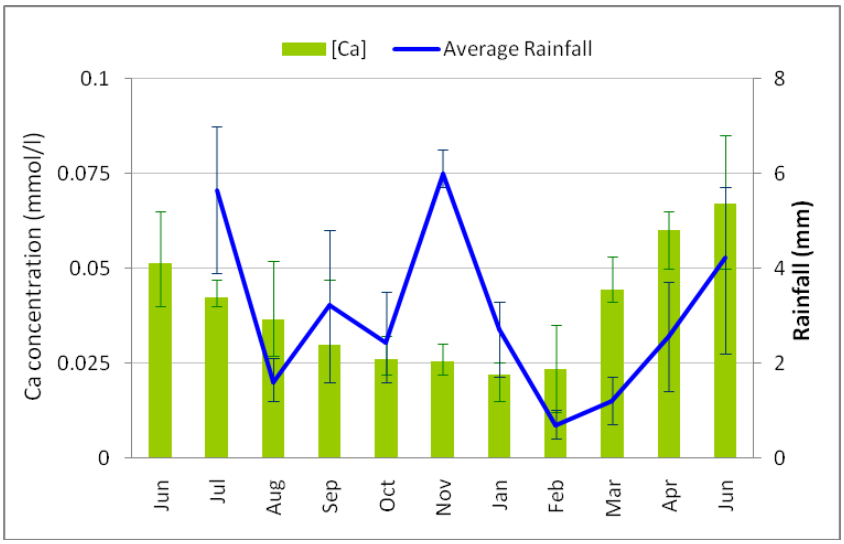

Figure 4.28. Mean Ca concentrations for all the main streams and mountain seeps sampled in this study with average daily rainfall (mm/day) on the secondary y-axis. The blue lines on the rainfall curve and the green lines on the Ca concentration bars indicate the range in data among sampling sites.

The mean Ca concentration in rainwater (Figure 4.12 and Figure 4.15) is the same as that in stream water (Figure 4.28). A mean Ca concentration of 0.04 mmol/l in both rainwater and stream water suggests that Ca is retained in soil when evaporation is taken into account.

Potassium in stream water shows a strong positive correlation with rainfall amount (Figure 4.29). Mean K concentration increases with an increase in rainfall amount. This may indicate a dependency on rainfall, but other variables should also be taken into account such as nutrient uptake by plants, nutrient input through vegetation decomposition and K contributions through bedrock weathering and inputs from soil.

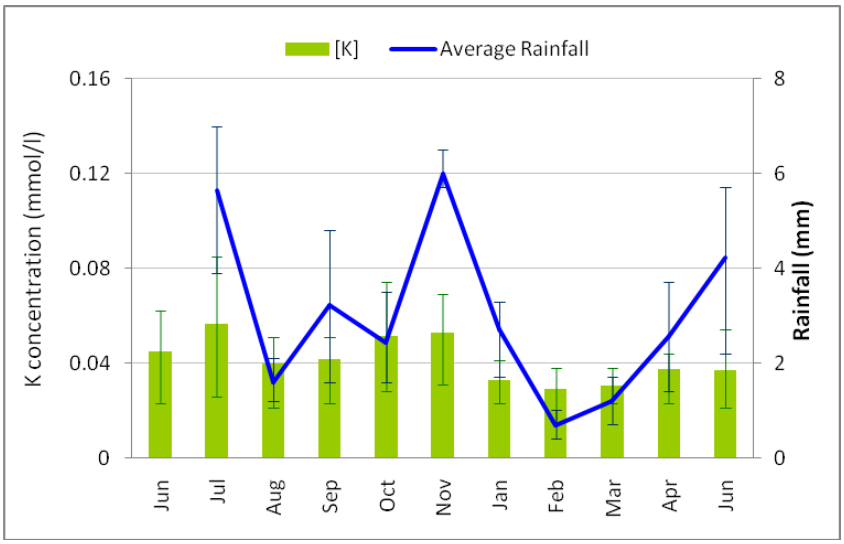

Figure 4.29. Mean K concentrations for all the main streams and mountain seeps sampled in this study with average daily rainfall (mm/day) on the secondary y-axis. The blue lines on the rainfall curve and the green lines on the K concentrations bars indicate the range in data among the sampling sites.

The concentration of K in stream water is higher than in rainwater. The mean K concentration in rainwater is 0.2 mmol/l (Figure 4.13 and Figure 4.15) compared to 0.4 (Figure 4.29) in stream water. Assuming an evaporative water loss of 35% there is an approximate 33% additional K input from the soils into streams. The output of K in stream water is however proportional to rainfall amount. Potassium is a major plant nutrient and its loss from streams indicates that plant regrowth is not rapid enough to take up all the available K and that nutrients other than K may be limiting the regrowth of vegetation after the fire.

Major ions in stream water and mountain seeps do not show the same relationship between rainfall amount and ion concentration as rainwater. This implies additional inputs into streams which may include, but not limited to, the decomposition of plant material, bedrock weathering and soil leaching, ash from fires and dry fallout from the atmosphere that does not dissolve in rainwater but only later in soils. Mean stream water concentrations for K, Cl and Na show the highest correlation to rainfall amount. Sulphate concentrations reflected a range of inputs into rainfall discussed in Section 4.1, but other factors such as inputs through soil, bedrock weathering and the washout of sulphur compounds into streams will now also play a role in controlling sulphate concentrations in stream waters and mountain seeps. Bedrock and soil weathering may also play a role in Mg and Ca concentrations, but this will be further explored in Section 4.3. It is uncertain whether fire can have such a significant role in increasing concentrations of Mg and Ca, but windblown dust and ash can

increase after such events and leaching of dust and ash in soils may provide additional sources of these ions to stream waters. The strong correlation shared between marine inputs and ion concentration discussed in Section 4.1 may also be reflected in stream water chemistry. Ion-chloride molar ratios for stream water and mountain seeps were calculated and plotted against the seawater ratio to determine the significance of marine aerosols in stream water chemistry.

Smit (2003) identifies Na as an essential plant nutrient and Soderberg (2003) found Na to be preferentially taken up by fynbos plants. Streams are slightly depleted in Na compared to seawater, but do not deviate far from the seawater Na/Cl molar ratio suggesting a strong marine aerosol source (Figure 4.30). A marine signature for Na is weaker during winter months and starts to follow the seawater molar ratio during summer months. Molar ratios for Na/Cl indicate that stream water is slightly more depleted in Na relative to rainwater. Stream water Na/Cl molar ratios follow rainwater ratios indicating a direct correlation between rainwater and stream water and suggests that there are not many reactions in bedrock and soil involving Na.

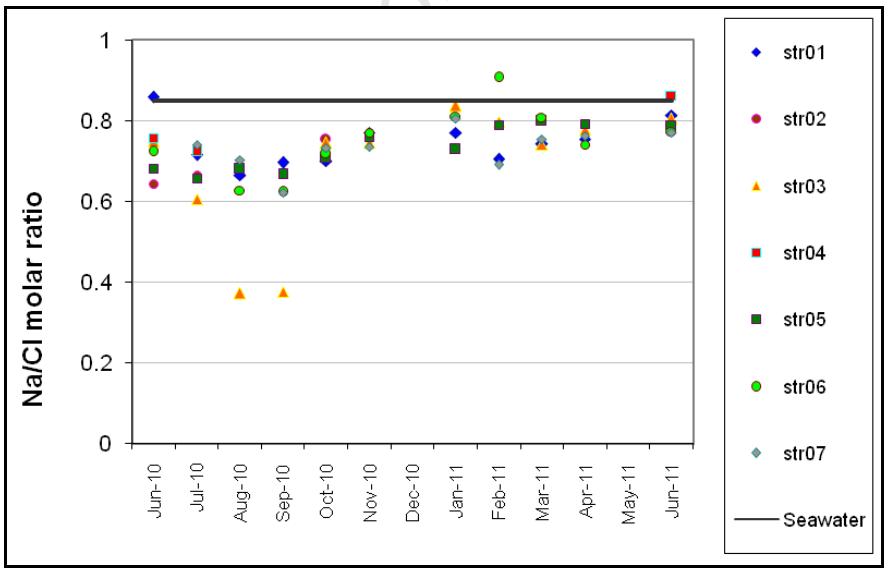

Figure 4.30. Na/Cl molar ratios for all streams and mountain seeps discussed in this study. The Na/Cl molar ratio for seawater (0.85) is indicated by the solid black line for comparison.

This study does not incorporate all streams sampled by Smit (2003) who collected stream water samples in August 2002. A comparative assessment indicates similar Na/Cl molar ratios between the two studies (Figure 4.31). The range in Na/Cl molar ratios measured on stream samples collected in one day by Smit (2003) falls within the broader range of values

measured in this study over a one year period. Both studies show an overall strong marine signature, but with some samples showing minor to fairly large depletion of Na relative to seawater particularly in August and September 2010.

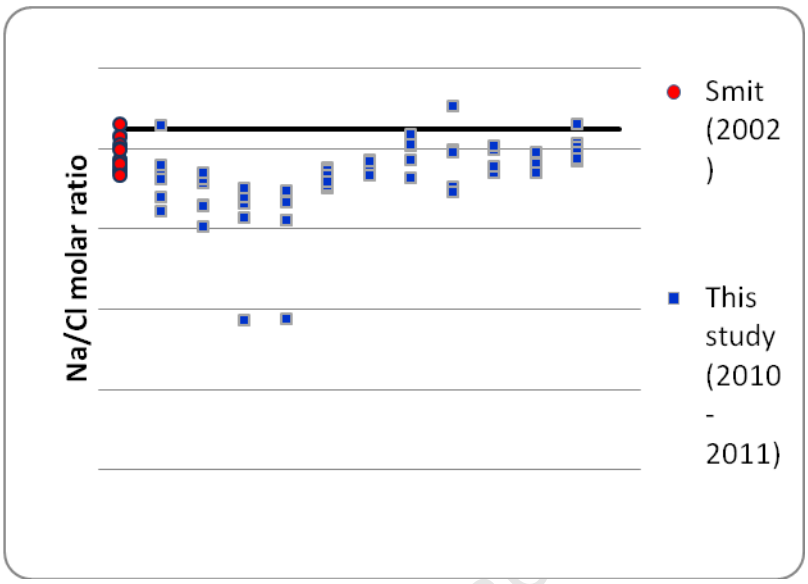

Figure 4.31. A comparison of Na/Cl molar ratios between stream waters sampled by Smit (2003) (red circles) and those sampled for this study (blue squares).

Sulphate is another ion important to plants (Smit, 2003; Soderberg, 2003) and is expected to exhibit a strong marine influence as sulphate is the second most abundant anion in seawater after Cl (Howarth and Cole, 1985; Marino *et al*., 2003). Chloride molar ratios for SO_4 plot above the seawater line (Figure 4.32) indicating an additional source of sulfate besides marine aerosols to streams and mountain seeps. The high concentrations following the June 2010 fire event suggest that sulphate may have been derived from the leaching of this ion from ash deposited after the fire. Molar ratios for SO_4/Cl start to decrease over time, suggesting a return to the pre-fire state.

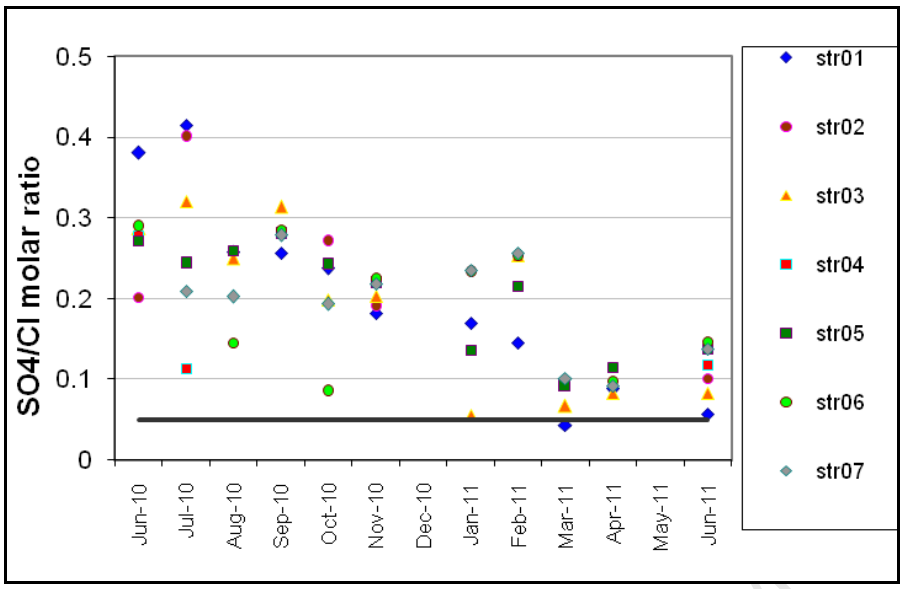

Figure 4.32. SO_4/Cl molar ratios for all streams and mountain seeps discussed in this study. The SO_4/Cl molar ratio for seawater (0.05) is indicated by the black solid line for comparison.

Sulphate concentrations in rainwater had similar trends to the sulphate in stream water where concentrations dropped after March 2011 and showed a strong marine influence in the March to June 2011 period. Molar ratios for SO_4/Cl in stream waters show a slight increase from March to June 2011 perhaps reflecting ash fallout from the March 2011 fire event. Input from this fire event was not substantial enough to elevate molar ratios to the extent of the June 2010 event. This is due to a direct influence of the June 2010 fire where the study area was burnt. The March 2011 fire event did not reach the study area and thus input was more limited during the March to June 2011 period. The deposition of excess SO_4 in the form of fire ash starts to flush out of the ecosystem after a period of time following the fire event. Smit (2003) found SO_4/Cl molar ratios in stream waters to be slightly depleted relative to seawater in the study prior to the fire event (Figure 4.33).

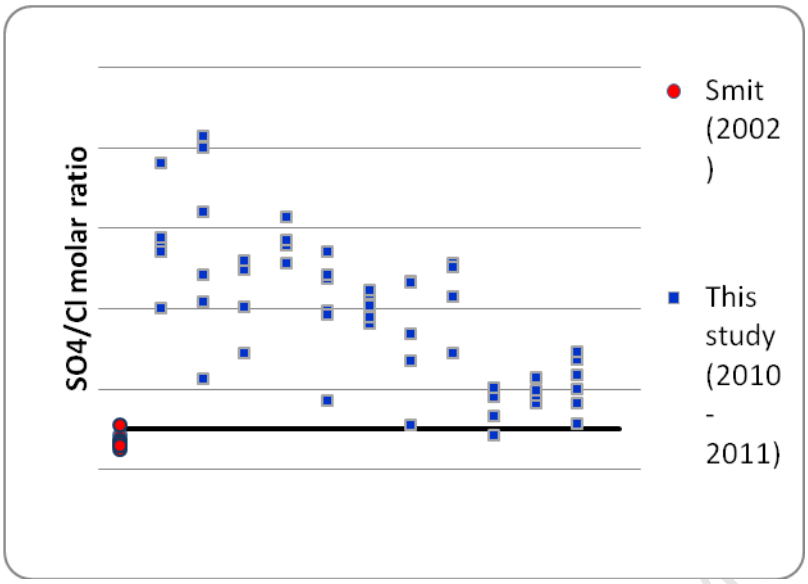

Figure 4.33. A comparison of SO_4/Cl molar ratios between stream waters sampled by Smit (2003) (red circles) and those sampled for this study (blue squares).

Most data points for Mg/Cl molar ratios plot on or slightly below the seawater line (Figure 4.34). Results suggest that Mg has a stronger influence from marine sources and mimics the pattern seen for Na/Cl molar ratios with Mg being five times more concentrated in seawater than Ca (Henderson and Henderson, 2009). In addition, Mg is not taken up by plants to the same extent as Ca and K (Soderberg, 2003; Soderberg and Compton, 2007). Molar ratios for Mg/Cl in stream water are more depleted than in rainwater relative to seawater. This indicates a loss of Mg in stream water through outflow or plant nutrient take up.

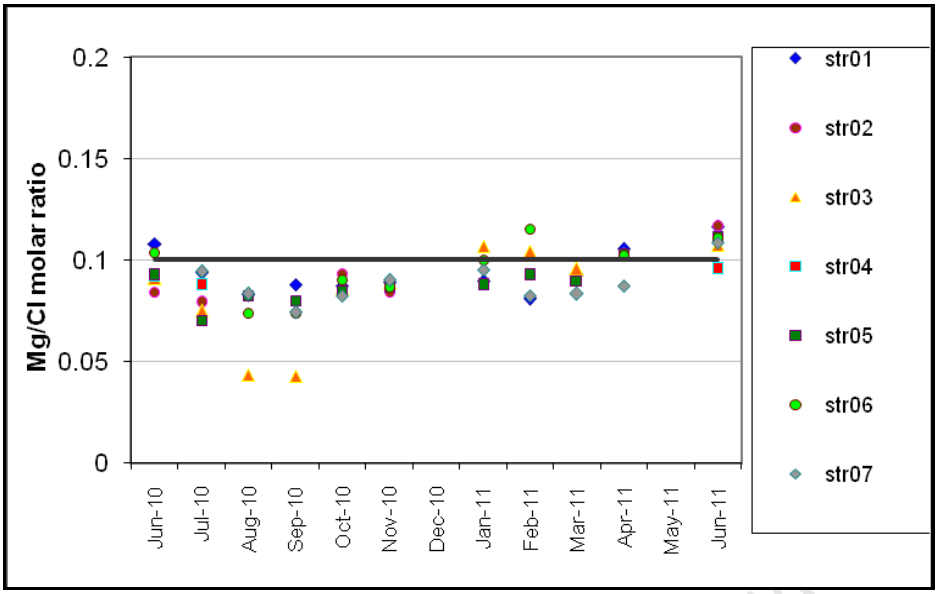

Figure 4.34. Mg/Cl molar ratios for all streams and mountain seeps discussed in this study. The Mg/Cl molar ratio for seawater (0.1) is indicated by the black solid line for comparison.

Magnesium-chloride molar ratios for this study support that of Smit (2003) (Figure 4.35). Magnesium depletion relative to seawater may result from nutrient uptake by vegetation, decreasing mineral content in major stream waters relative to seawater and mountain seep waters.

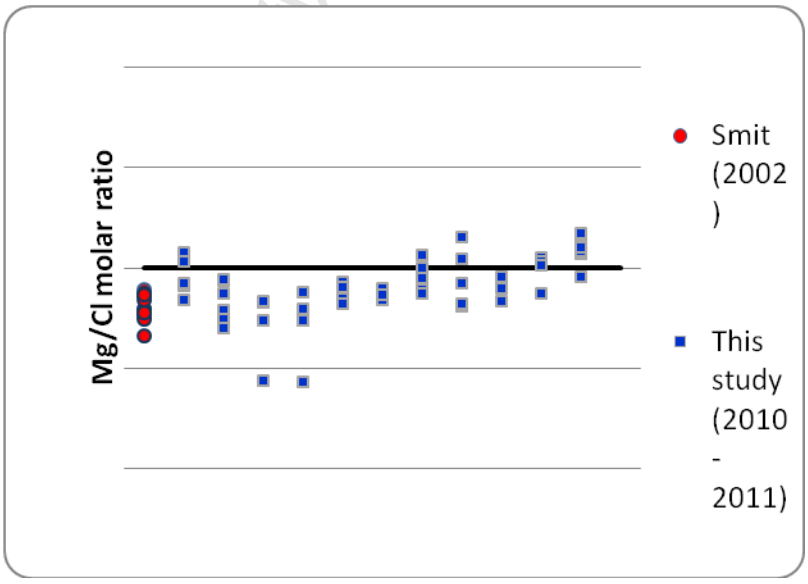

Figure 4.35. A comparison of Mg/Cl molar ratios between stream waters sampled by Smit (2003) (red circles) and those sampled for this study (blue squares).

Values for Ca/Cl molar ratios in stream water suggest a weaker marine influence than Mg. Molar ratios for Ca/Cl in stream water show a decrease from after the June 2010 fire until spring and then a steady increase from summer to winter 2011. The Ca/Cl molar ratios then

rise rapidly going into autumn and winter (Figure 4.36). The gradual trend of decreasing Ca/Cl molar ratios may represent the progressive leaching of deposited ash by throughflow waters feeding into the streams. The rapid rise in stream Ca/Cl molar ratios from January to June 2011 may reflect a greater deposition of mineral to marine aerosols as the rains increase and the seasonal wind direction shifts from predominantly SE to NW.

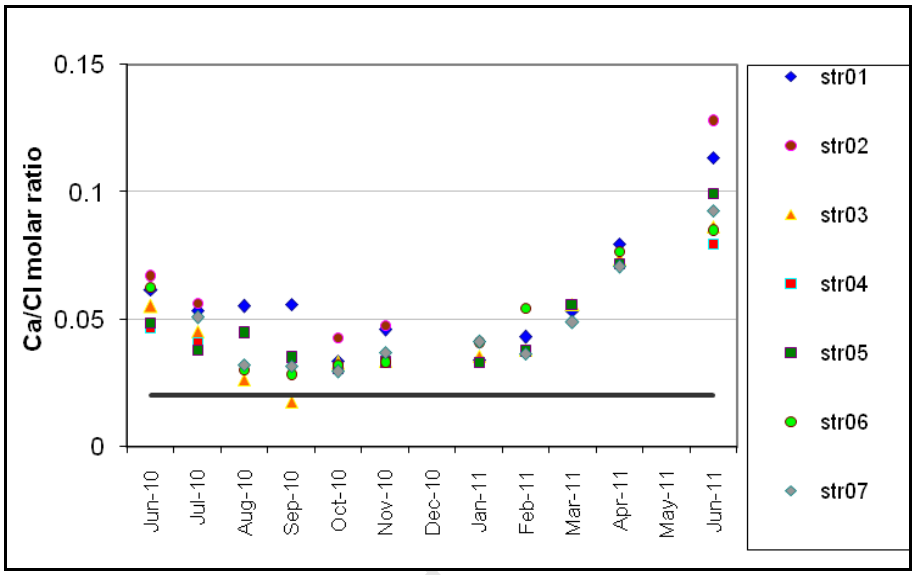

Figure 4.36. Ca/Cl molar ratios for all streams and mountain seeps discussed in this study. The Ca/Cl molar ratio for seawater (0.02) is indicated by the black solid line for comparison.

Results for this study suggest a strong continental source for Ca during winter months coinciding with a shift from the dominant SE winds during summer to NW winds during winter. The marine influence on Ca weakened 8 months after the fire. This pattern was evident in the Ca/Cl molar ratios of the rainwater as well (Figure 4.20). There is a greater elevation of Ca/Cl molar ratios in rainwater than in stream water. This suggests that there is a loss of Ca in stream waters relative to rainwater. Stream 2 (str02, a mountain seep leading into str01) had the lowest marine influence. This may indicate the effects of groundwater interaction with bedrock and soils at a site relatively distant from the ocean.

Smit (2003) also found Ca/Cl molar ratios to be elevated above the seawater value (Figure 4.37). Plant nutrient take up, bedrock weathering and atmospheric dust sources may influence the distribution of Ca in the ecosystem. Smit (2003) cited the cycling of plant litter mass and decomposition of plants returning nutrients to the soil and stream waters as important in regulating the movement of Ca through streams. There are a number of possible reasons for the elevation of Ca relative to seawater. Apart from windblown dust

and the deposition of ash after a fire event, Ca can also increase by the washing through of salts and dry deposition which accumulated during the summer months. Mineral aerosols may also accumulate during dry summer months and be leached from soils by acidic throughflow into streams with the onset of winter rains. Smit (2003) suggests that Ca enters the ecosystem mostly in winter months through dry Berg wind events transporting mineral aerosols from further inland into the study area. Soderberg (2003) concluded that additional Ca may be derived from the washout of dry particles in the atmosphere. Vegetation has also not recovered in sufficient amounts to take up appreciable Ca. Bedrock weathering will have a limited contribution to stream water Ca concentrations as bedrock contains only small amounts of Ca, but this will be explored further in Section 4.3.

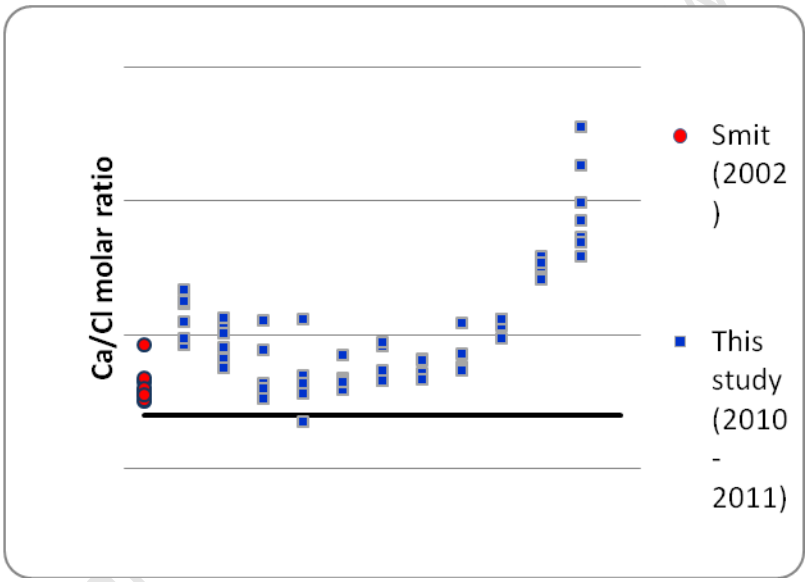

Figure 4.37. A comparison of Ca/Cl molar ratios between stream waters sampled by Smit (2003) (red circles) and those sampled for this study (blue squares).

Smit (2003) and Soderberg (2003) outline Ca and K as essential nutrients for fynbos vegetation. Stream water molar ratios for K/Cl show a different trend to Ca and follow a similar pattern to rainfall (Figure 4.38). The amount of scatter reflected in the data points may indicate variable sources for K. Molar ratios for K/Cl in stream waters are highest during times of increased precipitation. Potassium concentration in seawater is only 1/5 as much as Mg (Henderson and Henderson, 2009). Increased K/Cl molar ratios may result from the washing through of marine aerosols. Stream 3 (str03) had the closest relationship to the seawater molar ratio of K/Cl. Vegetation returned faster around site 3 than other sites. Streams 5 and 7 drain large catchment areas that include non-burned areas. Together these

observations with the low K/Cl molar ratios before the fire (Smit, 2003) may suggest that plant nutrient take up plays an important role in the distribution of K. The similar pattern shown by rainfall amount and stream water K/Cl molar ratios may indicate that the excess K is being derived from soil leaching associated with the amount of rainfall. Rainwater infiltration into soils may flush out K into streams and be taken up by plants. The ecosystem may not be able to hold on to K that has accumulated in above ground biomass which is released after a fire event and may need to regain K gradually over time from marine and mineral aerosols as the vegetation is reestablished.

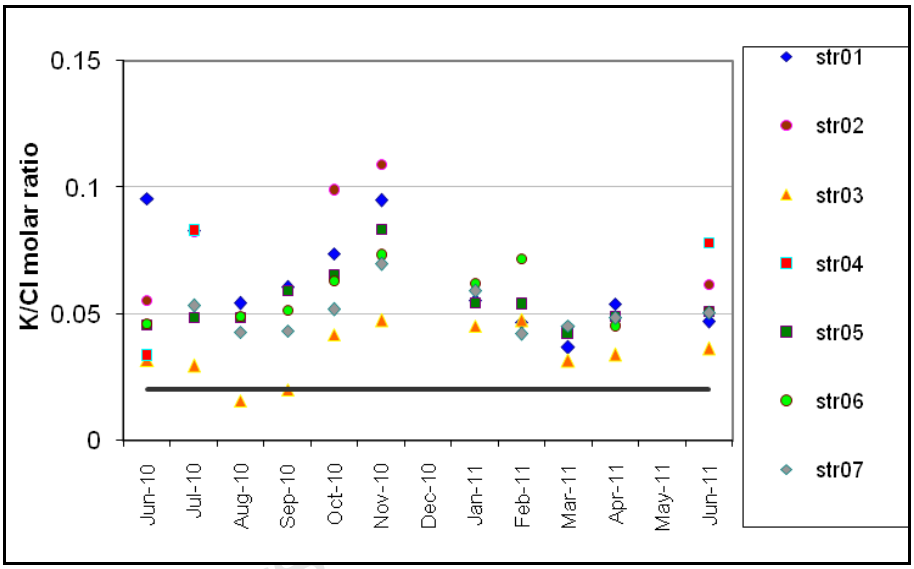

Figure 4.38. K/Cl molar ratios for all streams and mountain seeps discussed in this study. The K/Cl ratio for seawater (0.02) is indicated by the black line for comparison.

A plot of K/Cl molar ratios indicates a difference between K/Cl molar ratios from the study of Smit (2003) and this study (Figure 4.39). Potassium can enter the system through rainwater and windblown dust. Vegetation may also selectively take up K. It is unclear how big a role a fire event can play in concentrating K in streams and mountain seeps, but it may be possible that vegetation has not recovered sufficiently to counteract an excess of K in the study area released after the fire event in June 2010.

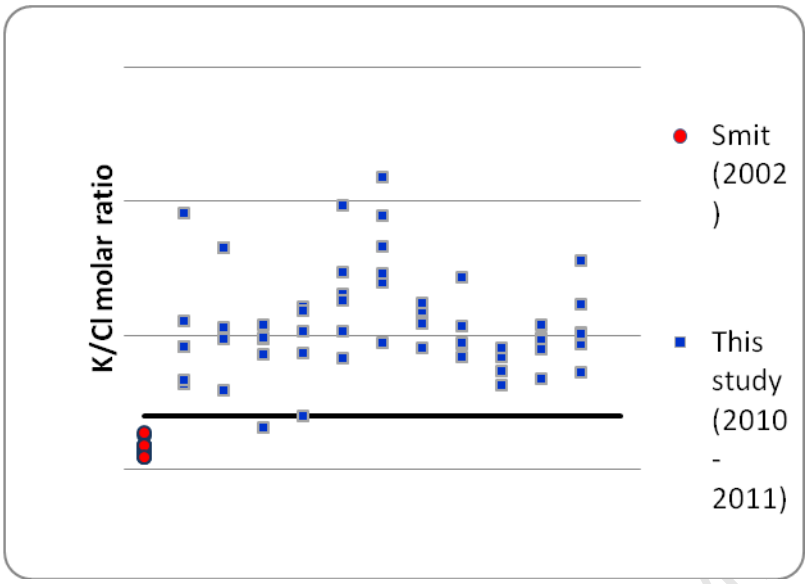

Figure 4.39. A comparison of K/Cl molar ratios between stream waters sampled by Smit (2003) (red circles) and those samples for this study (blue squares).

Smit (2003) had the same study area for his thesis. Concentrations of major ions in stream waters were compared to that of the values obtained by Smit (2003) from two of the same sample locations. The location of samples from str05 matches with site W11 in Smit (2003) and str07 matches with W4 in Smit (2003). Stream water chemistry does not seem to have changed significantly in a matter of 8 years with the exceptions of SO_4 and K (Table 4.4). There is a larger difference between Cl concentrations in stream water before (Smit, 2003) and after (this study) at str05 than at str07.

Table 4.4. Comparative concentrations (in mmol/l) of major ions in stream waters from the same sampling location in Smit (2003) and this study. Values from this study are mean concentrations.

	Cl	Na	SO_4	Mg	K	Ca
str05 (this study)	0.82	0.59	0.17	0.072	0.044	0.039
W11 (Smit, 2002)	0.67	0.6	0.03	0.062	0.005	0.022
str07 (this study)	0.78	0.57	0.15	0.068	0.039	0.037
W4 (Smit, 2002)	0.77	0.57	0.03	0.071	0.005	0.025

A t-test was conducted to determine whether the mean concentrations before a fire (Smit, 2003) and after a fire (this study) are significantly different. The following equation was used to determine the t-value for each major ion measured in stream water:

$$t* = \frac{(\bar{X}_1 - \bar{X}_2) - (\mu_1 - \mu_2)}{\sqrt{\left(\frac{s_1^2}{n_1}\right) + \left(\frac{s_2^2}{n_2}\right)}}$$

Where: n is the degrees of freedom calculated as n_1+n_2-2

$\bar{X}$ is the sample mean

μ is the population mean (in this case set to 0)

s^2 is the sample variance

The hypothesis tested whether mean ion concentrations differ significantly before and after a fire event at the 95% significance level.

n = 17

95% significance level for $t_{17} = 2.11$

The null hypothesis is rejected when the calculated t-statistic is less than -2.11 or greater than 2.11 (within the rejection region).

Ion	**Calculated t-statistic**	**Null hypothesis rejected/accepted**
Cl	2.49	Rejected
Na	-0.76	Accepted
SO_4	5.68	Rejected
Mg	1.62	Accepted
Ca	2.79	Rejected
K	6.38	Rejected

The t-statistic values calculated for the ions Cl, SO_4, Ca and K all fall within the rejection region. This means that there is a significant difference in the concentration means of these ions before and after a fire. The null hypothesis for the ions Na and Mg were accepted and it is concluded that the mean Na and Mg concentrations in stream water do not differ significantly before and after a fire event. The calculated t-statistic values suggest that a fire

event will have a more marked effect on stream ion concentrations for Cl, SO_4, Ca and K than what it would have on Na and Mg.

The stream water concentrations for Na and Mg in two identical sites measured in this study and in Smit (2003) agree with each other. The calculated t-statistic values for mean Na and Mg concentrations measured in the study of Smit (2003) and in this study support the ion-chloride molar ratio plots. There is a significant difference between ions Cl, SO_4, Ca and K from the two studies. Sulphate concentrations determined in this study increased by as much as five times and K by eight times when compared to that of Smit (2003). This implies that ions such as Cl, Na and Mg are not influenced as much by additional factors outside of a marine source. Sulphate, calcium and potassium may have been influenced by the remobilization of minerals (Rundel, 1983) following the fire event of June 2010. The last fire prior to the 2010 fire event was in 1991. Smit (2003) thus had a study area with vegetation growth of at least 10 years. Above ground vegetation loss followed by a steady but slow recovery (Appendix D) were important factors in elevating SO_4, Ca and K concentrations in the present study implying that the supply of nutrients after the fire was greater than what was needed by the regrowth of plants at least within the first year.

Humic acids (tannins) are also present in stream waters in addition to the nutrients available to plants. The brown colour of the stream waters can be ascribed to the presence of these acids, which result from decaying vegetation. Leaching of humic acids from decaying plants increase with an increase in water amount (King and Day, 1979). This may lead to lower pH values. Orographic effects on steep seaward facing slopes and the seasonality of rainfall may also influence the leaching of humic substances from decaying plants. Humic acids in stream water can be measured as dissolved organic carbon (DOC). DOC can be defined as the fraction of organic carbon compounds that can pass through a 0.45 μm filter, whereas particulate organic carbon (POC) cannot pass through a 0.45 μm filter (Smit, 2003). DOC was not measured in this study, but Smit (2003) reported values to be well over 10 mg/l at all stream waters sampled from the study area. The high DOC content can also be related to the soil organic carbon content. Soil saturated paste extracts (SPEs) were of similar colour to that of the stream waters and mountain seep samples (str02 and str04). Plant nutrient cycling in the form of litterfall and decomposition is also an important factor in DOC content (Mitchell *et al*., 1986). Dissolved organic carbon compounds may find their way

through groundwater flow and bedrock fractures and into an outlet in the form of mountain seeps or as part of larger streams. Oxidation and remineralisation of DOC and POC can release ions into the stream waters such as SO_4, Ca and K.

This study suggests that stream water chemistry is not entirely dependent on rainfall. Additional factors need to be considered, such as temperature, rainfall quantity, accumulation of salts during dry seasons and their flushing into streams during wetter periods, dry fallout, vegetation re-establishment and growth and deposition of ash from fire events. Another particularly relevant component to consider is bedrock and soil interaction with groundwater. Bedrock weathering provides mineral content to soils. Minerals which occur in the bedrock such as mica minerals or are deposited in soils as mineral aerosols may weather in the low pH soils to produce K ions for nutrient take up by plants or the rinsing through by rainwater and soil throughflow to streams. Magnesium may not be as leachable as other minerals such as Ca and K. This is reflected in the relatively depleted Mg/Cl molar ratios in stream water compared to rain water when measured against the seawater molar ratios. Results from the stream water chemistry measured in this study suggest that the balance between uptake by plants and the release of ions through bedrock or soil or mineral input via marine and terrestrial dust sources were not reached after one year of the June 2010 fire event. Vegetation growth did not reach sufficient levels during the one year sampling period of this study to take up maximum nutrients from the ecosystem. When vegetation is well established and growth has returned to levels similar to before the fire, nutrients such as SO_4, Mg, Ca and K are removed more efficiently and stream export is small. The relation of bedrock and soil geochemistry to stream water chemistry is explored in the next section.

4.3 Bedrock and Soils

Rainwater percolates through soils (throughflow) and feeds into bedrock as groundwater. The water may react or exchange with minerals in soils and bedrock and nutrients may be taken up or released by plants. These water-rock, -soil and –plant interactions may have a strong influence on the chemical composition of stream waters. The study area was purposefully selected to limit the immediate bedrock to the Peninsula Formation which is a rock formation composed of quartz arenite sandstone. The Peninsula Formation sandstones

sampled for this study have homogeneous and simple chemical compositions dominated by SiO_2 (>97 wt% SiO_2). This leaves less than 3 wt% of other major oxides in the bedrock that may interact with soil and stream waters. Beyond the immediate sample sites, the bedrock geology of the stream catchments includes Pakhuis Formation tillite, Cedarberg Formation siltstone and shale and sandstone of the Goudini and Skurweberg formations (Figure 1.5). Many of these other rock formations are dominated by quartz but not to the same extent as the Peninsula Formation. Weathering of bedrock is typically one of the key sources of elements to soils, groundwater and streams. However, the hard, resistant sandstone bedrock of the study area is slow to weather and is therefore unlikely to provide a significant source of elements besides silicon. Soils on the Peninsula Formation bedrock are typically thin and composed of quartz sand and organic matter (Soderberg and Compton, 2007).

Mitchell *et al*. (1986) noted that decomposition of vegetation and the subsequent return of nutrients to the soil is an important link in the fynbos ecosystem. Their study indicated that decomposition of leaf litter causes an increase in Ca, Mg and K within the soil. Several other factors may also influence an increased soil nutrient concentration such as soil microbial activity (Lamont, 1983; Read and Mitchell, 1983; Slabbert *et al*., 2010), retention of nutrients in leaf litter and absorption through atmospheric processes. Mitchell *et al*. (1986) concluded that periodic fires may provide a quicker method than decomposition of leaf litter for the release of nutrients into the soil. The mineralogy and chemistry of the bedrock and overlying soils was determined in order to evaluate their impact on the composition of waters in the study area.

4.3.1 Bedrock Description

Petrography reveals the quartz-rich nature of the Peninsula formation bedrock and supports results from XRF analysis showing that the bedrock sandstone has high SiO_2 content (Table 3.23). Fine to coarse sand quartz grains are angular to subrounded and together with interstitial quartz cement account for over 95 wt% of the rock. The thin sections that were analysed suggest that the sandstone is moderately to poorly sorted. The few mica and opaque minerals present occur along grain boundaries. Mica minerals likely contain the bulk of the Al, K, Mg and Na oxides measured by XRF as no feldspar minerals were observed in the thin sections. Trace amounts of opaque minerals may represent iron (<0.2 wt%) and manganese oxides (~0.01 wt%). Titanium oxide (TiO_2) may occur in detrital

rutile (0.04 to 0.13 wt% TiO_2) and Ca (0.004 to 0.011 wt%) and P (0.01 to 0.03 wt%) in detrital apatite grains. Minerals present within the bedrock may weather to constituent elements and nutrients to become part of the soil chemistry.

The Peninsula Formation proved to be the most arenaceous of all formations in the TMG (Figure 1.5) in comparison to rock formations discussed in previous studies. Young *et al*. (2004) found the SiO_2 content of the overlying Pakhuis Formation to be between 52 and 66 wt%. The Pakhuis Formation formed through glacial processes incorporating weathered material picked up from underlying formations. Rocks from the Pakhuis Formation have higher Al_2O_3 (13 wt% to 23 wt%) and Fe_2O_3 (5 wt% to 9 wt%) than other TMG formations. The Peninsula Formation studied in this thesis recorded an Al_2O_3 content of between 0.3 and 1.3 wt%. Young *et al*. (2004) found Pakhuis Formation rocks to be depleted in Na and Ca. The basal member of the Cedarberg Formation was found to be enriched in Mo, U and other trace elements (Young *et al*., 2004). Smit (2003) describes the Cedarberg Formation to be easily weathered and kaolinite rich. Soils overlying the Cedarberg Formation were found to have strong X-ray diffraction (XRD) peaks for kaolinite possibly related to the bedrock. The Cedarberg Formation was found to be higher in Al, Mg and K than other sandstone formations of the TMG due to the presence of aluminosilicate clays (Smit, 2003). According to Smit (2003) the Goudini Formation of the Silurian aged Nardouw Subgroup have higher Fe and Ca content in the bedrock relative to the soil cover.

4.3.2 Soil Description and Mineralogy

The soils of the HPNBG and KBR can be described as grey to dark grey (2.5YR 6/1 to 2.5YR 3/1). Soil horizons overlying the fractured bedrock are thin and range from 2 to 20 cm thick. Top soils occupy the uppermost 2 to 4 cm and have a tough, tightly interwoven fine root network and contain charcoal as well as partially burnt plant material from the June 2010 fire. Sub soils occur 2 to 4 cm below the surface and are generally more quartzitic, less organic rich (including fewer roots) and lighter in colour than the overlying top soils. Quartz pebbles and rock fragments are also common in the soil profiles, particularly below the topsoil.

Grain size analysis revealed that the subsoil of sites 1, 2 and 5 have greater gravel components than the top soil (Table 3.25). This reflects the increase of gravel rock

fragments with depth in the soil. The sandstone rock fragments increase the weight percentage of the gravel sized fraction. Analyses on the soil samples did not include the gravel component. For these reasons, the grain size distribution was normalized to reflect a gravel-free soil (Figure 4.40). Topsoil from sites 2 and 5 were sandier than the sub soils. Soil from site 3 was sandier than all the other sites. Clay size fractions are low (0.6 to 1.7 wt%) and tend to be slightly higher in the subsoil than the topsoil.

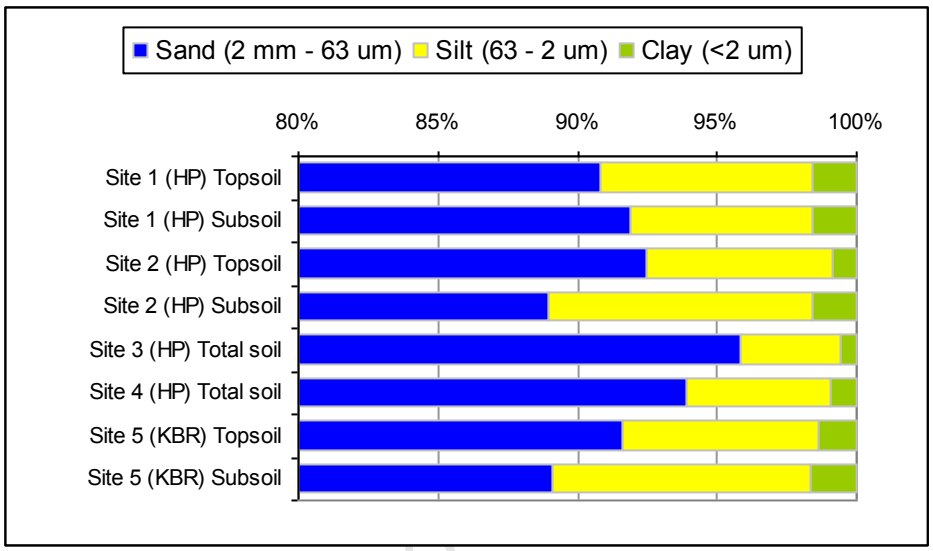

Figure 4.40. The normalised grain size distribution to reflect gravel-free components of soils discussed in this study.

X-ray fluorescence (XRF) data of powdered sand to clay sized fractions determined quantitative amounts of major oxides within the soil. Subsoil samples showed enriched quartz content compared to the topsoil at sites 1, 2 and 5. SiO_2, TiO_2, Al_2O_3, Fe_2O_3 and CaO are the dominant oxides in the soil. Oxides such as Al_2O_3, MgO and CaO are higher in the topsoil than in the subsoil. The Fe_2O_3 content is higher in the subsoil than in the topsoil at sites 1, 2 and 5. MnO is higher in the subsoil at site 1 and 2, but lower than the topsoil at site 5. These elements can enter the soil through a variety of pathways such as weathering of bedrock, through decomposition of organic material and as windblown dust.

X-ray diffraction analysis carried out on the clay size fraction revealed strong intensity peaks for quartz (Figure 4.41, Figure 4.42 and Appendix B) consistent with the high SiO_2 content in the soil determined by XRF. The XRD profiles of the preferred orientated clay size fractions had a 10 angstrom (Å) peak at a 2 theta angle of 9 indicating the presence of mica and illite minerals. Smaller peaks for smectite (16-20 Å at a 2 theta angle of 3),

kaolinite (7.1 Å at a 2 theta angle of 12) and feldspars (3.2 Å at a 2 theta angle of 27) were also detected in some of the soil XRD profiles. In addition to these minerals, three broad peaks of moderate intensity corresponding to d-spacings of 5.2 Å (2 theta angle 14), 6.3 Å (2 theta angle 17) and 3.9 Å (2 theta angle 26) occurred in all the soil clay size fraction XRD patterns. The d-spacings of these peaks did not match any oxides or clay minerals, but the search-match programme identified the peaks as corresponding to hydrocarbons. The hydrocarbons that are present within the soils may result from the leaching of organic horizons following a fire event (Doerr *et al.*, 2000; Horne and McIntosh, 2000; González-Pérez *et al*., 2004). It may also be possible that the hydrocarbons are associated with the soil organic matter and formed a partially crystalline substance to appear in the XRD analysis. The XRD pattern for randomly orientated packed powder mounts of the clay size fraction had strong quartz peaks, but more reduced mica/illite peaks and none of the three hydrocarbon peaks seen in the preferred orientation mounted sample (Figure 4.42).

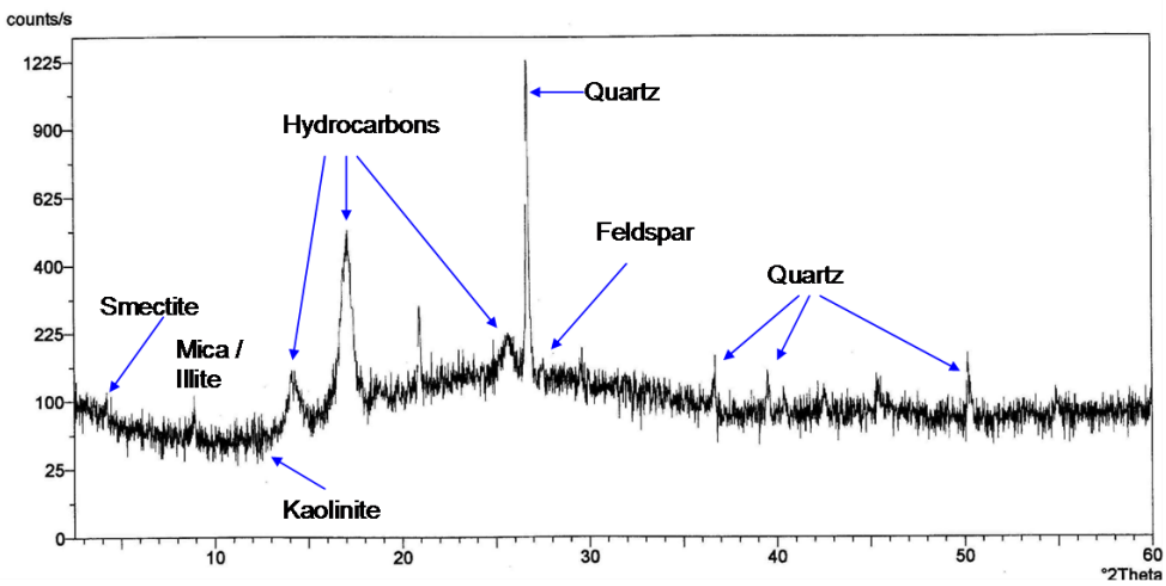

Figure 4.41. The XRD profile for preferred orientated dried suspension of the clay fraction (<2 μm) from the topsoil of site 1.

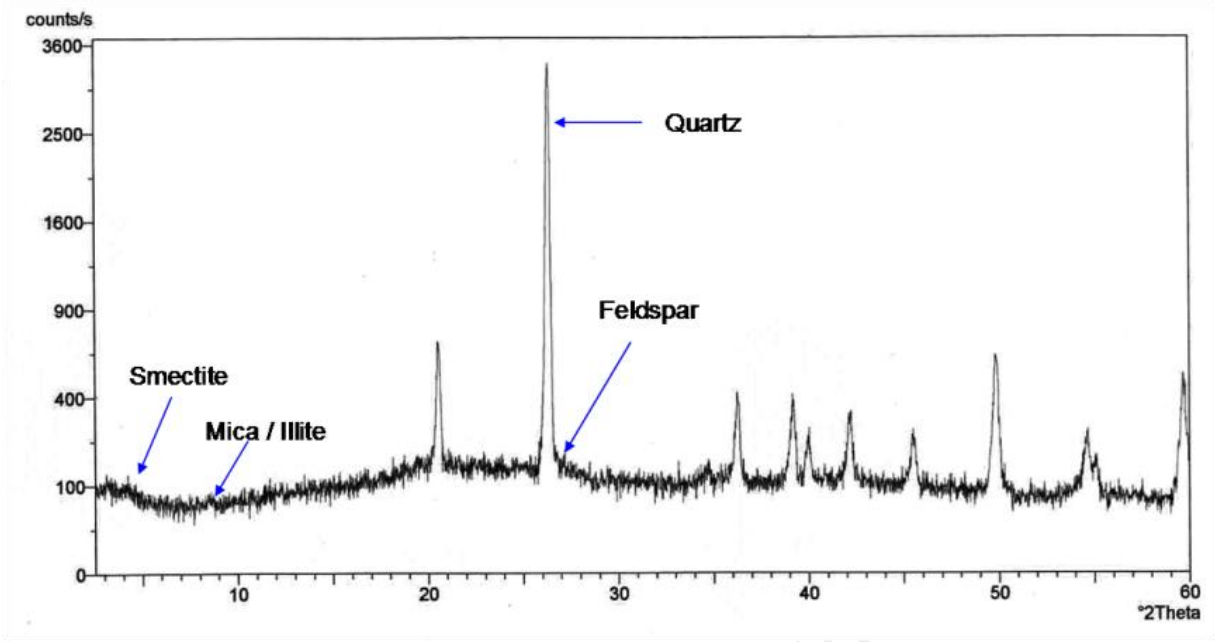

Figure 4.42. The XRD profile for the randomly packed dried clay (<2 µm) fraction powder of the topsoil from site 1. The peaks identified as hydrocarbons in Figure 4.41 are no longer present.

Feldspars may weather to kaolinite through the following reaction:

$2KAlSi_3O_8 + 3H_2O \rightarrow Al_2Si_2O_5(OH)_4 + 4SiO_2 + 2K(OH)$

The low amounts of kaolinite ($Al_4[Si_4O_{10}](OH)_8$) present in the soils are consistent with the lack of feldspar minerals observed in the bedrock and in the small XRD peak intensities indicating few feldspar minerals in the soil samples. Kaolinite may also form through the weathering of mica or illite minerals and along with weathering of minor amounts of feldspar may account for the small amounts of kaolinite detected in certain samples. Mica/illite, feldspar and kaolinite minerals may be transported into the study area via windblown dust. Soderberg (2003) found more abundant kaolinite in the Elandskloof catchment area to the north (Figure 4.14). Kaolinite is however not an important source of nutrients to plants as it is an aluminosilicate whereas illite or mica minerals contain K, an important nutrient for plants. Illite is a clay mineral ($K_{1.5\text{-}1.0}Al_4[Si_{6.5\text{-}7.0}Al_{1.5\text{-}1.0}O_{20}](OH)_4$) structurally related to mica minerals where the principal interlayer cation is K (Deer *et al.*, 1992). The occurrence of illite within the soil may be derived from the weathering of small amounts of mica minerals in the bedrock observed in thin sections. The breakdown of these minerals may provide additional sources of K and Al to the soil. Illite composition can be more complex and may also include interlayers of the expandable clay mineral smectite, although XRD profiles indicate that smectite interlayers were not abundant in the soil

samples. Weathering of mica and illite minerals may also provide a source of other cations besides K such as Mg, Ca and Fe.

It is not clear what the exact source for the clay minerals may be. Soderberg and Compton (2007) suggest that clay minerals in quartz rich fynbos soils may be derived from an external source through the deposition of mineral aerosols. Most of the elements occurring within minerals present in the soil may not be available to plants. Elements bonded to crystal structures must first be chemically weathered and released before they can be taken up by plants.

Saturated paste extracts (SPEs) for soils provide a means to determine the concentration of ions that are readily soluble in water and are most available for take up by plants. Most ions measured in this study with the exception of anions (Na, Cl and SO_4) showed higher concentrations in soil SPE than in stream waters. The soil SPE concentrations suggest a highly soluble and readily available nutrient pool in soils for plants. Subsoils show a decrease in SPE concentrations suggesting that the bulk of SPE nutrients occur in the topsoil focused there because of deposition from the atmosphere or from the degradation of plant material concentrating elements in the topsoil. With time, these elements may percolate through the soil profile and become part of the groundwater reservoir if not taken up and retained by the vegetation. The flow of groundwater to streams and eventually reaching the ocean would represent the exit of these nutrients from the ecosystem.

All major soluble ions in soil SPE, with the exception of Ca, show fairly uniform concentrations between June 2010 and January 2011 and then increase between January and March 2011 (Figure 4.43). This pattern is consistent with the buildup of salts by dry deposition over the dry, windy summer months. Soil SPE for site 2 had the highest major ion content across all sampling periods. Sites 1 and 2 are situated closer to the ocean than site 5 and consistently had higher SPE ion concentrations than site 5 suggesting that proximity to the ocean may influence the distribution of marine aerosol deposition. Sodium is the dominant ion in soil saturated paste extracts suggesting that Na is being retained in the soil and may explain why stream waters have Na/Cl molar ratios less than seawater (Figure 4.30). Topsoil in most cases has higher SPE concentrations than subsoil, particularly in the case of Ca and Mg. The increase in major ion concentrations in March 2011 indicates an

accumulation of salts during the dry summer period (January – March). The accumulation of salts is evident in top soils and this is expected if salts are accumulating by dry deposition on the soil surface. Because the fire removed nearly all above ground vegetation, deposition was directly on the soil surface with no significant above ground plant intercept. Sulphate shows consistently low concentrations relative to the concentration in rainwater and stream waters across all sampling periods and suggests that the high concentrations of SO_4 noted in rainwater and streams are not retained as soluble ions in the soils. Calcium and potassium are least like the other ions and suggest that soil SPE of these two ions is not as strongly related to marine aerosol deposition during summer but to dust deposition.

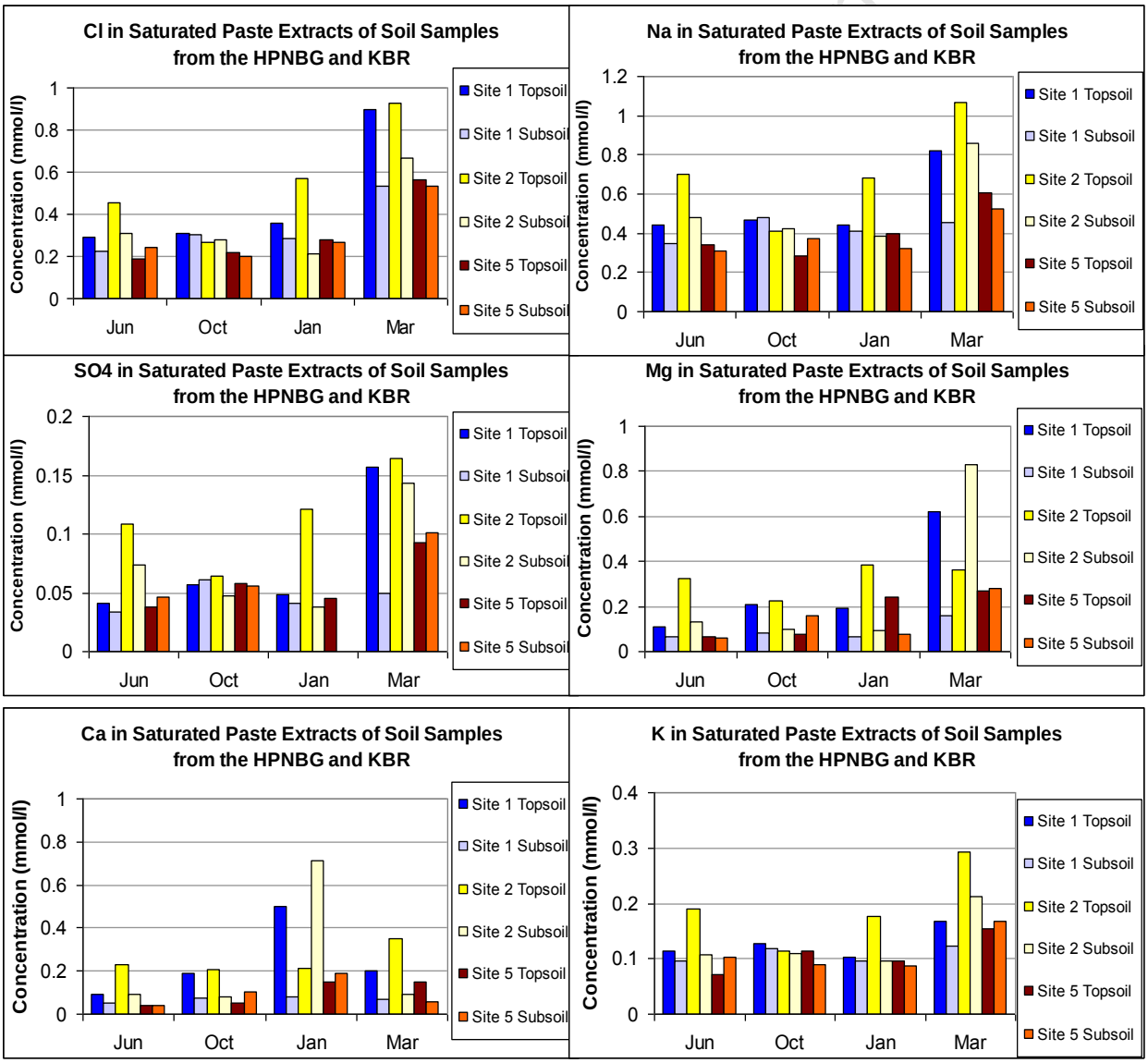

Figure 4.43. Major ion concentrations (in mmol/l) in saturated soil paste extracts of top soils and sub soils at sites 1, 2 and 5.

A representative bulk (total) soil sample was taken at sites 3 and 4 for SPE analysis, because soils at these sites were too thin to differentiate between top and sub soil. The pattern in SPE concentrations of the major ions at sites 3 and 4 are similar to those seen at sites 1, 2 and 5.

Sites 2 and 3 had similar major ion compositions with little deviation for all sampling periods, although Mg and Ca were slightly higher for site 3 (Figure 4.44). Site 3 is situated on the slopes of a valley whereas site 4 is located at a higher elevation closer to the ocean. Sulphate had its lowest concentration in January 2011 where it increased towards March again. This may represent an accumulation of this ion in the soil during a drier period.

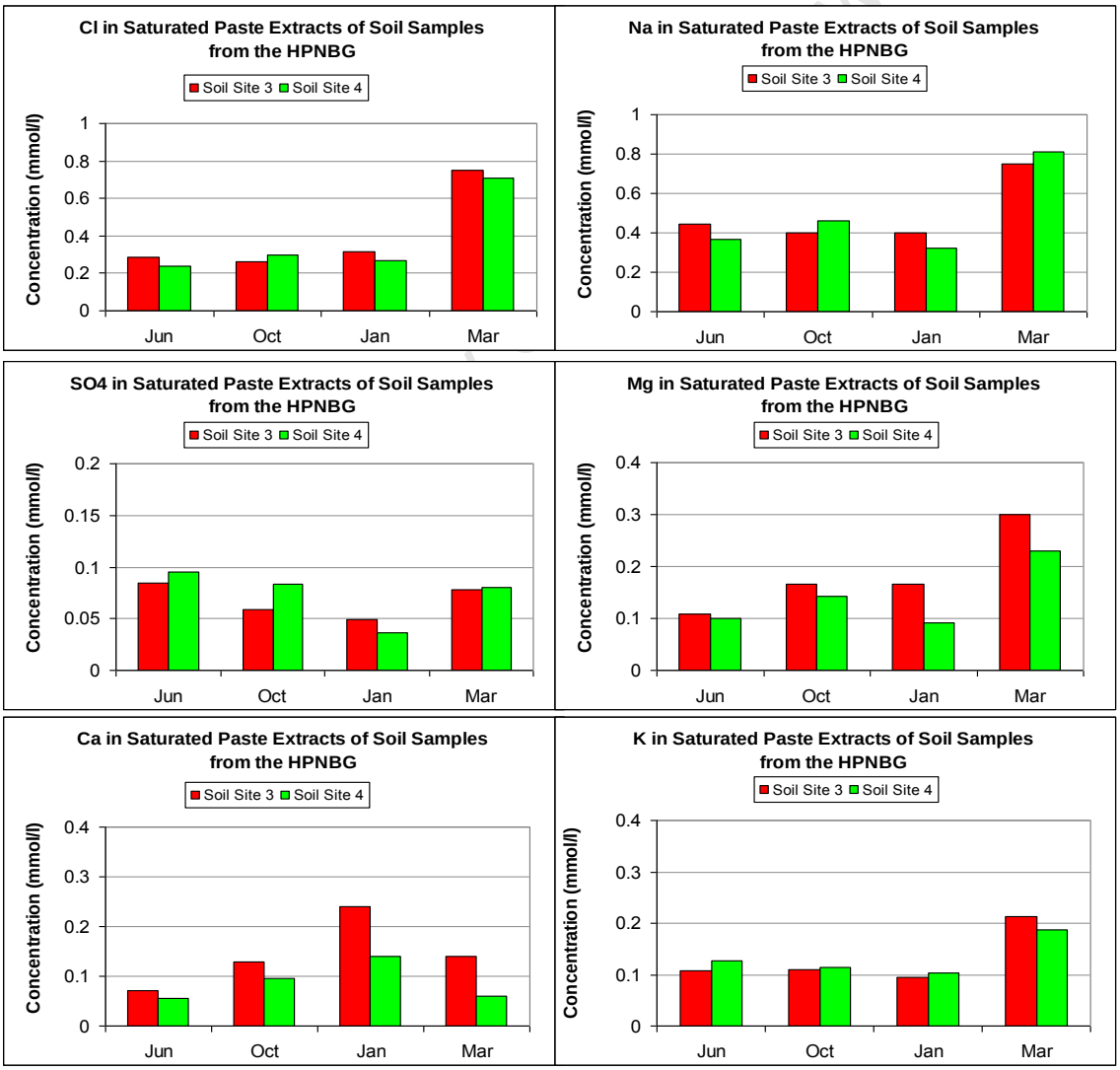

Figure 4.44. Major ion concentrations (in mmol/l) in soil saturated paste extracts of bulk soils at sites 3 and 4 in the HPNBG.

A comparison between ion concentrations in stream water and in soil SPE reveals some interesting trends. Where sulphate concentrations and SO_4/Cl molar ratios in stream waters decreased after March 2011 (Figure 4.26 and Figure 4.32), SPE concentrations increased by March 2011(Figure 4.43 and Figure 4.44), thus indicating sulphate retention in soils from March 2011. Potassium showed decreased stream water concentrations (Figure 4.29) and had the lowest K/Cl molar ratios during March 2011 (Figure 4.38) corresponding with the highest soil saturated paste extract concentrations for K during the same period (Figure 4.43 and Figure 4.44). Calcium showed the reverse of sulphate during this period. Where Ca concentrations and Ca/Cl molar ratios in stream waters increased (Figure 4.28 and Figure 4.36), Ca concentrations in soil SPE decreased for this period (Figure 4.43 and Figure 4.44) indicating flushing of Ca from soils into streams. The opposite happened during January 2011 where Ca concentrations and Ca/Cl molar ratios in stream waters were lower and SPE concentrations for Ca were at its highest. Soil SPE concentrations for SO_4, K and Ca thus indicate the retention of these ions in the soil during periods when stream water concentrations are lower and the flushing of ions when concentrations in stream waters are higher.

Sodium, magnesium and potassium concentrations are usually higher in mountain fynbos soils than in coastal fynbos soils (Herppich *et al*., 2002) (Table 4.5). Soil SPE concentrations recorded in this study for most macronutrients (Mg, Ca and K) show significantly lower concentrations than those found by Herppich *et al*. (2002), Smit (2003) and Soderberg (2003). Results from Smit (2003) agrees with the major ion concentrations in Herppich *et al*. (2002) with the exception of Na. Sodium in this study showed the same concentrations outlined by Herppich *et al*. (2002) for mountain fynbos soils, but were significantly lower than that of Soderberg (2003) and Smit (2003). The higher soil macronutrient SPE concentrations suggested by previous studies may reflect bulk soil sampling which included plant litter. Soil SPE concentrations from Smit (2003) were found to be higher than that of Soderberg (2003) suggesting a decrease in soil macronutrient content further inland. The comparison between this study and previous studies suggests that soluble macronutrients are removed from soils following a fire event. Herppich *et al*. (2002) suggest Na to be the least concentrated in both mountain and coastal fynbos soils. It may be possible that the relatively close proximity to the ocean allow for the high concentration of Na in hillslope soils within the study area. Nitrogen was not measured in

this study or in Smit (2003). Herppich *et al*. (2002) suggest that N concentrations in mountain fynbos soils are higher than in coastal fynbos soils. The occurrence of high levels of N within the soil may be due to the N-fixation through nitrogen fixers in the soil roots (Lamont, 1983; van Reenen *et al*., 1992).

Table 4.5. Comparison of macronutrients (Na, Mg, Ca and K) in soil SPE (in mmol/l) between four studies for mountain and coastal fynbos soils.

	This study - mountain fynbos	**Soderberg (2003) mountain fynbos**	**Smit (2003) mountain fynbos**	**Herppich *et al*. (2002) mountain fynbos**	**Herppich *et al*. (2002) coastal fynbos**
Na	0.5	5.63	7.9	0.5 ± 0.3	0.4 ± 0.1
Mg	0.2	0.93	3.03	4.1 ± 3.3	1.9 ± 1.1
Ca	0.15	0.67	1.35	2.4 ± 1.9	6 ± 3.7
K	0.13	0.45	0.97	1.4 ± 1.1	0.5 ± 0.2

Analyses into the chemistry and composition of the soils reveal a sandy quartzitic soil profile for the study area. Oxides such as Al_2O_3, MgO and CaO are higher in the top soils than in the sub soils suggesting nutrient uptake by plants possibly coupled with mineral dust and ash deposition. Clay fractions revealed the presence of illite with minor kaolinite arriving through windblown dust into the ecosystem and through bedrock weathering. Soil saturated paste extracts show an accumulation of salts during drier periods, supporting XRF analysis. The results provide a glimpse into the movement and possible processes of these ions in the soil profile. Drever (1997) mentions the movement of ions into the soil as being driven by the interaction between rain and bedrock. This interaction may provide additional elements and ions to the soil. Above soil and bedrock interaction, external sources are important in contributing to the mineral and elemental composition of soil. Processes and inputs may include nutrient recycling through vegetation, microbial activity in the soil, bedrock weathering, atmospheric inputs in the form of washout and dryfall, rainwater percolation and groundwater flow.

Vegetation may take up nutrients and add to soil chemistry through decomposition of plant material. Microbes within the soil may chemically breakdown and recycle nutrients. Mineral dust and ash may be deposited onto soil surfaces through dryfall or washout.

Rainwater percolation aid in the transport of these ions and may flow as groundwater through the bedrock and exit as mountain seeps. These processes act as an interlinked network reflecting various sources for the nutrient budget in soils outlining the important links between bedrock and soil (Figure 4.45).

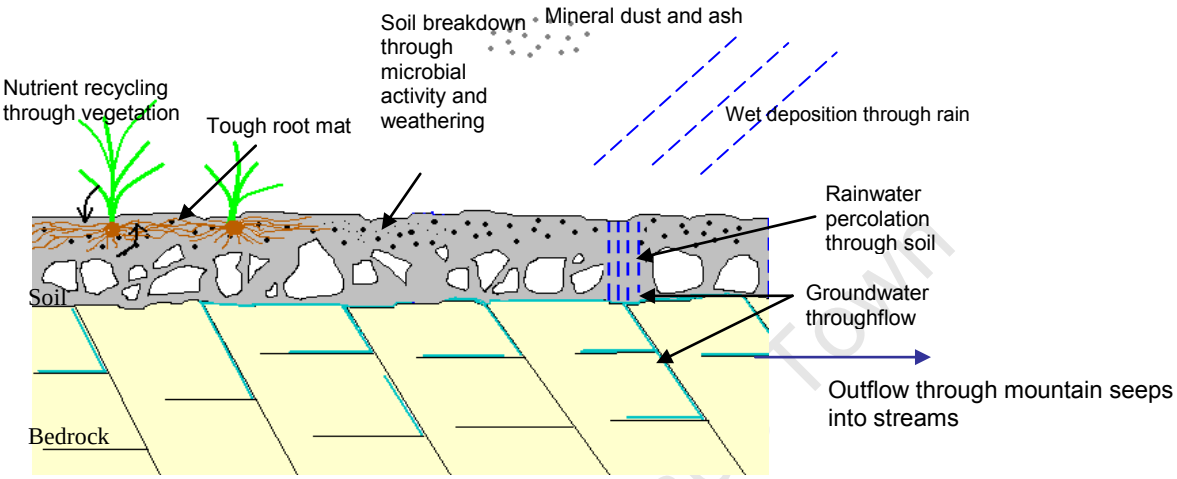

Figure 4.45. Inputs into a soil profile and pathway for ions to flow through a soil-bedrock profile.

There is a strong positive correlation between sulphur content and organic carbon (Figure 4.46 and Table 4.6) with the organic matter containing around 1 wt% sulphur. The increased occurrence of S in the soil relative to bedrock means additional inputs of sulphur such as marine aerosols and DMS production offshore. Sulphur oxidizes to sulphate in the atmosphere where soils are able to adsorb sulphates and retain it by soil organic matter together with hydrous iron and aluminum oxides. Murphy (1980) estimates total S in soils to be more than 90% organic derived from plant residues which are further decomposed by micro-organisms. This results in only a portion of the sulphur being converted to sulphate. Sulphates may be soluble only in small amounts and accumulate under conditions of increased hydrous iron and aluminum oxides as well as kaolinite clay. Accumulations of this nature may be beneficial to the local flora. Plants may take up S through their roots in the sulphate form and through their leaves as sulphur dioxide. These compounds are then reduced to supply protein sulphur in the form of amino acids and vitamins (Murphy, 1980).

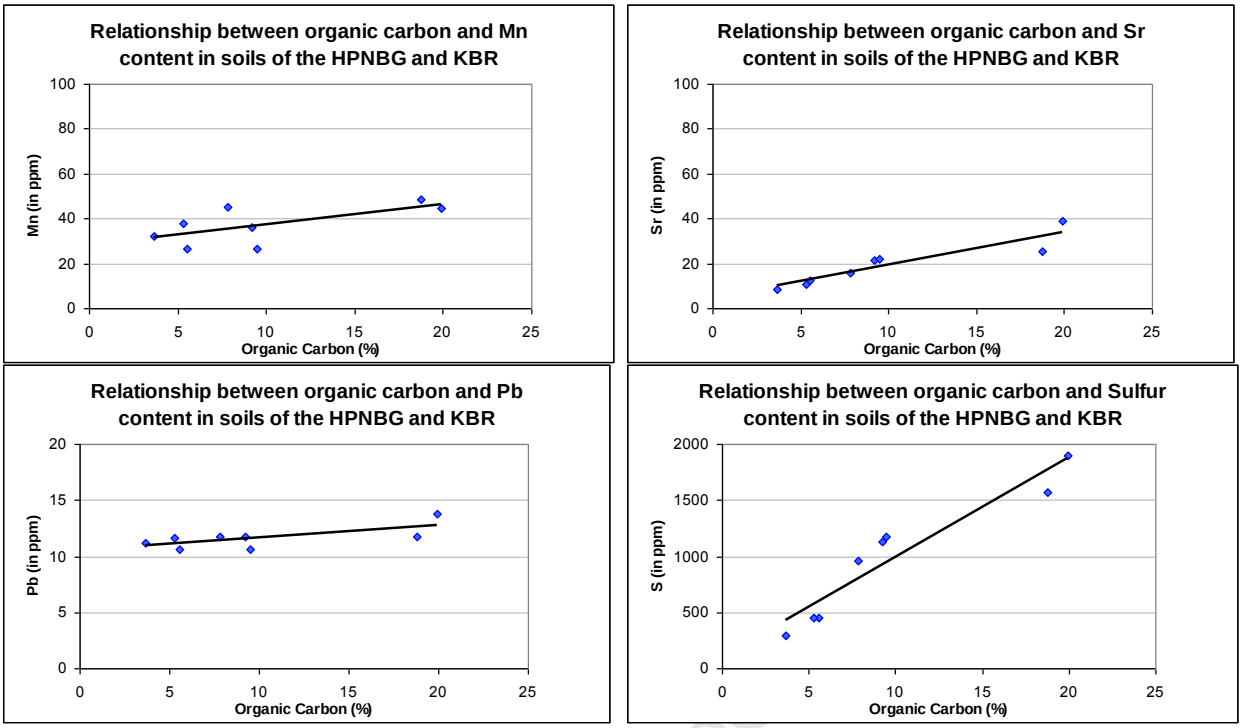

Figure 4.46. Correlation plots between soil organic carbon and selected trace elements (Mn, Sr, Pb and S).

Table 4.6. Correlation values (r), degrees of freedom (df), the p-value and equations for the regression line between soil organic carbon and selected trace elements discussed in this study.

	Manganese (Mn)	Strontium (Sr)	Lead (Pb)	Sulphur (S)
r	0.65	0.93	0.69	0.95
df	6	6	6	6
p-value	<0.05	<0.001	<0.05	<0.001
Equation of regression line	y=0.905x+28.172	y=1.482x+4.651	y=0.113x+10.497	y=88.608x+106.09

Sulphur and strontium show the strongest correlation with correlation coefficients of 0.95 and 0.93, respectively. The trace elements Pb and Mn have lower correlation coefficients of 0.69 and 0.65. These positive correlations suggest that these elements are associated with soil organic carbon either within organic compounds or adsorbed to organic particles.

Buringh (1984) lists organic matter as live or dead plant remains, partially decomposed plant remains, colloidal organic matter, microorganisms such as bacteria, fungi and protozoans, macroorganisms (worms, ants or termites) and burnt vegetation and ash. Most soil organic carbon is present in the upper 1 to 20 cm of the soil profile, with organic carbon content increasing at the uppermost layers (Buringh, 1984). This supports data analysed in this study where topsoils (upper 1 to 4 cm) show an increased organic carbon content

relative to subsoils (Table 3.29). The organic carbon content of soils in this study falls within the broader range of soil organic carbon content results found by Smit (2003). Organic carbon values for this study range from 4 to 20 wt% C whereas soils in Smit (2003) recorded values between 7 and 36 wt% C. The isotopic composition of the soil organic carbon indicates the fynbos vegetation is C3.

4.3.3 A Comparative Look at Bedrock and Soil

The mineral composition of the soil may broadly reflect the mineral composition of the underlying bedrock, but may also include minerals and ions that have precipitated from the soil solution or entered the soil through atmospheric processes (Soderberg, 2003). Clay minerals present in the soil samples of this study as discussed in Section 4.4.2 are suggested to come from an external source such as windblown dust. Thin section analysis reveals the distribution of minor mica minerals along grain boundaries in the bedrock sandstone. Illite may be derived from the breakdown of these minerals, but also enter the ecosystem through windblown dust. Kaolinite may result from the weathering of feldspar or mica/illite minerals. The absence of feldspar in thin section may mean that feldspar and its alteration to kaolinite reaches the soil through windblown dust. It is however mica or illite and feldspar minerals that provide nutrients to plants as kaolinite is composed of only Al and Si oxides.

Bedrock weathering may be enhanced by groundwater processes. Weathering of sandstone may thus give a more siliceous nature to the soil. XRF analysis of the soil samples revealed a more quartzitic nature (higher SiO_2 content) for the soil than the bedrock at all sites with the exception of site 4. The high SiO_2 contents in the soils are derived from the bedrock. The soils and bedrock of sites 3 and 4 are more quartzitic than other sites. The relatively small difference in composition between the soil and bedrock at sites 3 and 4 may be explained by their relatively thin soils. The remaining oxides show decreased compositions in the subsoil.

The oxides such as Fe_2O_3, Al_2O_3, MnO, MgO, Na_2O and K_2O are higher in bedrock than in the soil samples (Figure 4.47). Higher Fe_2O_3 and Al_2O_3 in the bedrock may be caused by bedrock not releasing Fe and Al through weathering but retaining these as insoluble oxides. It is also possible that Fe and Al in soils may be soluble in acidic soil waters and washed into streams perhaps as metal complexed to DOC and POC. Soderberg (2003) and

Soderberg and Compton (2007) found Al_2O_3 in the soils of the Olifants River Catchment to be higher than the Al_2O_3 contents in the sandstone bedrock. Similarly, Smit (2003) also found the Al_2O_3 contents of the soils of the same area as this study to be higher than the sandstone bedrock. Thus the results regarding Al_2O_3 content in the soils relative to the bedrock substrate in this study do not support previous studies that could not include a post-fire analysis. It is possible that certain minerals may have been removed from the soil layer and taken up as ash in windblown dust and/or removed through increased runoff and erosion following the fire event.

The Na_2O content decreases from bedrock to subsoil to topsoil suggesting a progressive loss of Na by leaching. Bedrock weathering may not account for the total Na_2O in soil. Sodium delivered by marine aerosols may infiltrate into soils through rain which percolates down the soil profile and accumulates in the sub soil. Groundwater throughflow may carry Na out through seeps into streams. Stream water Na/Cl molar ratios however suggest that Na delivered to streams are not enough to elevate the molar ratios to above the seawater average (Figure 4.30) and most Na delivered by rainout accumulates on and within the topsoil.

The higher K_2O contents in the bedrock may reflect the presence of mica minerals observed in thin section. The lower K content of soils to bedrock may reflect preferential uptake of K by plants which were largely removed by the fire and flushed out by rain into streams. Oxides such as MnO and MgO also show higher contents in the bedrock indicating plant take up causing a decrease in the soil composition. Soderberg (2003) suggests K is taken up by plants more efficiently than Mg and Ca. The low CaO contents in bedrock agree with the lack of feldspar observed in thin sections. Calcium may be elevated in soils relative to bedrock due to windblown dust, the retention of Ca by plants (including roots and soil organic matter) and the release of Ca through the decomposition of leaf litter. The accumulation of TiO_2 in the soils relative to the bedrock can be attributed to plants not taking up as much TiO_2 in relation to other elements and the insolubility of Ti-rich minerals such as rutile.

Figure 4.47. Comparison between sandstone bedrock and gravel-free sub soil and top soil major oxide compositions at sites discussed in this study. Soil data were renormalized to 100 wt% after excluding LOI (organic matter).

Trace element concentrations for Rb, Th, Pb and V are higher in bedrock than in the overlying soil. Results for Mo, Nb, Cu, Ni and Co could not be established as their concentrations were too low to be measured. Trace element concentrations in soil for S, Zr, Ba, Mn, Cr, Y and Zn were higher than bedrock concentrations and indicate that these elements are retained by the soil. Additional inputs of these elements and increased availability to vegetation may also explain the enrichment in soil relative to bedrock. Bedrock weathering combined with rainout and windblown dust may add to these elements. The fire event also released elements and nutrients into the ecosystem. Many of the trace elements (Sr, Zn, Mn, Ba and S) show depletion in the subsoil relative to the topsoil and may indicate their take up by the vegetation and enrichment in the organic-rich topsoil. Soil sampling in the field revealed the extensive root network in the topsoil. Zr, Y, Rb and Th concentrations are higher in the subsoil than in the topsoil at sites 2 and 5. Cr concentrations are elevated in the subsoil relative to the topsoil at site 1.

Bedrock chemistry is not as open to changes from external sources as soil. The underlying bedrock may be altered through deformational processes and mineralogy changed through groundwater interaction, whereas soil chemistry is more exchangeable and open to external inputs. XRF analysis has shown that soils are more quartzitic, possibly through the uptake of nutrients of plants and washout of ions. Certain trace elements in the soil are enriched relative to the bedrock. These elements may arrive through windblown dust or weather from the bedrock and accumulate in the soil. The positive correlation between trace elements and soil organic carbon (Table 4.6 and Figure 4.46) suggests trace element remobilization after the fire event of June 2010. Analyses undertaken in this study show a complex interlinked ecosystem through which nutrients and ions are constantly introduced into the ecosystem, recycled and eliminated from the system.

Chapter 5 : Synthesis

This study emphasizes the interlinked network of different components in a mountain fynbos ecosystem. The different elements show different behaviour in the different components. Determining differences in element concentrations over a one year period following a fire event has allowed insight into the dynamics of the fynbos ecosystem on seasonal timescales. This chapter estimates the flux of elements into and out of the ecosystem and explores how major ions move through the fynbos ecosystem synthesising earlier discussions from the preceding chapter.

5.1 Transport of Elements through the Ecosystem

Elements are supplied to the fynbos ecosystem from above through atmospheric deposition and from below or laterally through weathering of bedrock (Figure 5.1). Atmospheric deposition includes marine aerosols consisting mostly of seawater salts and dust which includes minerals, organic matter and fire ash. Airborne particles may be deposited directly on surfaces or washed out and incorporated into rainwater through droplet formation. In this study, the total wet and dry deposition were collected and measured in the rainwater samples. Marine aerosols enter the study area predominantly through southerly winds off the ocean. Mineral dust from the interior arrives mostly from northerly winds from the interior.

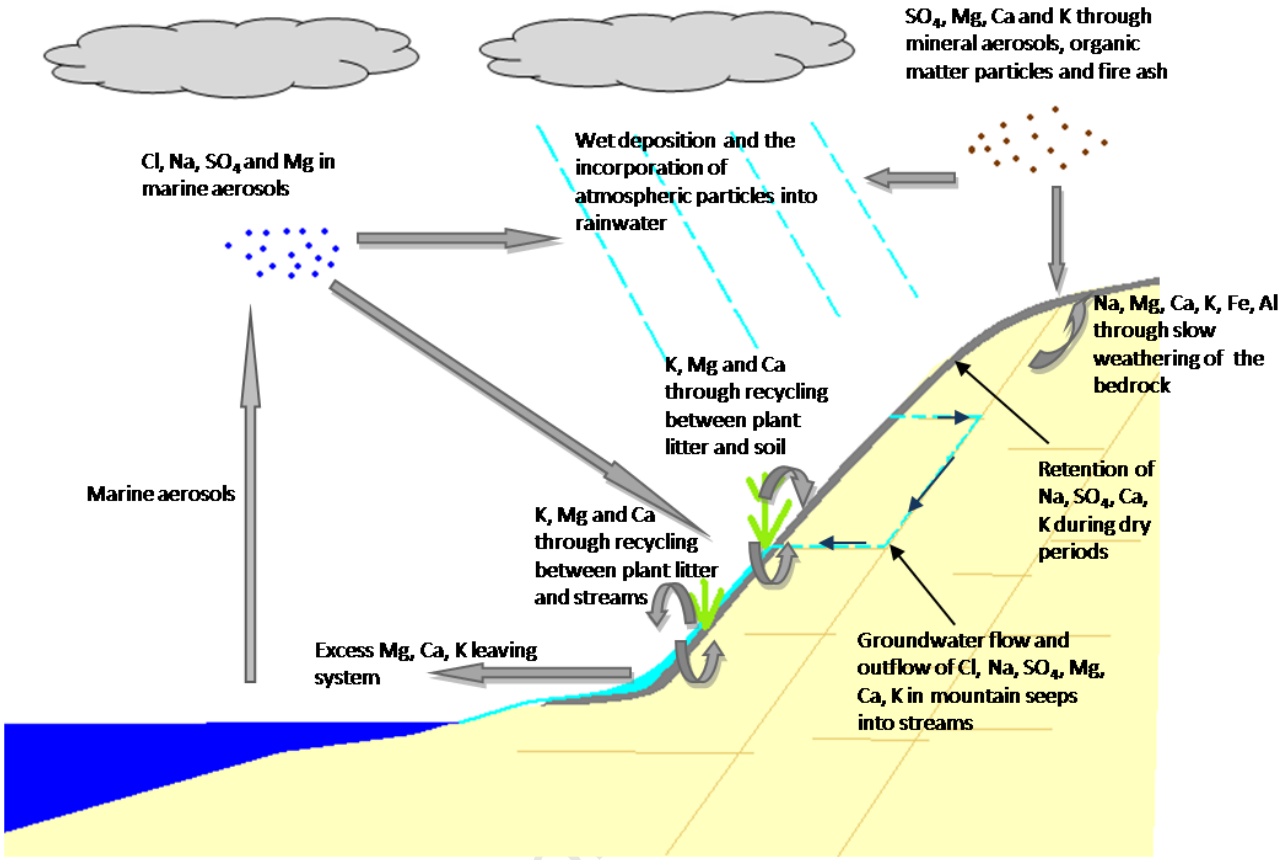

Figure 5.1. The movement of major ions through the different components of the ecosystem as outlined in this study.

Chloride is almost exclusively derived from marine aerosols as the bedrock minerals do not contain Cl. Chloride therefore provides a useful nonreactive tracer of marine aerosol sources to the ecosystem. Chloride is most concentrated in rainwater during periods of lower rainfall (Figure 4.8). The lowest average Cl concentration occurs in Oct/Nov 2010 during increased precipitation which dilutes the Cl concentration of the rainwater. Chloride in streams is higher during spring and winter months than during summer months (Figure 4.24). Chloride accumulates on the soil surface during the dry warm windy summer months and is washed through the soils and into streams with the onset of rain in the spring and winter months.

Sodium concentrations in rainwater increase with a decrease in rainfall amount (Figure 4.9). Molar ratios for Na/Cl indicate a strong marine source for Na (Figure 4.16 and Figure 4.30). Sodium is slightly depleted in rainwater and stream water relative to average seawater indicating possible adsorption of Na by particles and uptake of Na by vegetation. The dominant ion in soil SPE is Na explaining why this ion is depleted in stream water. Sodium

is thus primarily derived from marine aerosols but is generally not strongly retained in the soil relative to Cl. X-ray fluorescence (XRF) analysis indicates that Na_2O decreases from bedrock to subsoil to topsoil and suggests that bedrock weathering is an additional source of Na. However, sodium sourced from the weathering of bedrock is not significant relative to the amount of Na deposited as marine aerosols

Chloride molar ratios of sulphate, magnesium, calcium and potassium in rain and stream waters indicate that these elements have a mixture of marine and mineral aerosol sources. In addition to mineral sources, rainfall may incorporate SO_4 particles in the atmosphere derived from DMS released through primary production offshore. Sulphate may also have been derived from fire ash during the 3 June 2010 event. The highest SO_4 concentration in rainwater is during the driest period of this study (Jan/Feb) indicating increased DMS production during this period. Lana *et al.* (2011) suggest that maximum DMS production off the coast closest to the study area occurs during the drier summer months. SO_4/Cl molar ratios in rainwater and stream water show relative enrichment compared to seawater for most of the study period and decrease towards the seawater SO_4/Cl molar ratio line after the March 2011 fire event (Figure 4.17 and Figure 4.32). The decrease in average stream water SO_4 concentrations during drier periods indicates retention of this ion in soils. The highest SO_4 concentrations in soils were measured during March 2011 when rainfall was relatively low. Little sulphate can be derived from the bedrock as sulphur levels in the sandstone bedrock were shown to be negligible (Table 3.24). The sulphur content of soils correlates strongly with organic carbon contents and suggests that most sulphur in the ecosystem is associated with organic matter. Therefore sulphate has a number of sources including marine aerosols, rainout of atmospheric DMS, organic particles and the deposition and leaching of fire ash. Sulphate from marine primary production of DMS may provide a significant additional source of S, as well as acidity because the conversion of DMS to sulphate is by way of hydrogen sulphide and sulphuric acid, to fynbos ecosystems adjacent to productive coastal environments on the south and west coast of South Africa.

The highest average concentration for Mg in rainwater was found to be during the driest period of the study (Jan/Feb 2011) (Figure 4.11). Overall Mg shows no distinctive seasonal trends. Molar ratios for rainwater and stream water Mg/Cl show enrichment of Mg relative to the seawater Mg/Cl molar ratio (Figure 4.19 and Figure 4.27). It is unclear whether the

increase in Mg/Cl molar ratios from March to June 2011 may be a seasonal effect or a response to the fire event of March 2011 northeast of the study area. Approximately half of rainfall Mg may be retained in soils or possibly taken up by vegetation. Topsoil samples showed higher MgO contents than subsoil samples. In addition to rainwater and dust fallout from the atmosphere, Mg in soils may also be derived through the weathering of mica minerals from the sandstone bedrock. However, the bedrock source of Mg is probably negligible given the low concentration and slow weathering rate of the bedrock, compared to the input of Mg associated with marine aerosols.

In comparison to Mg, Ca is less abundant in the bedrock and five times less abundant in seawater, thus mineral dust (particularly carbonate minerals) and organic matter are likely to be important sources of Ca to the fynbos ecosystem. Whatever the source, Ca appears to be available in excess to the ecosystem as indicated by the net loss of Ca by streams. Calcium concentrations in rainwater showed a moderate inverse correlation with rainfall amount (Figure 4.12 and Table 4.2). More pronounced than Mg, Ca also showed an increase in rainfall and stream water concentration as well as Ca/Cl molar ratios following the March 2011 fire event (Figure 4.11, Figure 4.19, Figure 4.27 and Figure 4.34). Calcium concentrations in soil SPE indicate the flushing of Ca into streams from March to June 2011 when it is lost in the soils through runoff during increased precipitation. Ash releases mainly SO_4, Mg, Ca and K (Groves, 1983; Rundel, 1983). Ash deposited from the March 2011 fire may have caused an increase in topsoil deposition of these ions. Calcium carbonate is more soluble than mica or feldspar sources of K in acidic rainwater and soil/groundwater. Calcium accumulated on surfaces during dry periods and washed into streams during periods of increased precipitation. The excess of Ca and subsequent loss of this ion from the system was also noted by Smit (2003). The export of Ca may also be coupled with possible uptake by the vegetation. The small amount of CaO in the bedrock (Table 3.23) corresponds with the absence of feldspar in the bedrock. The calcium in the soils may thus be derived from rainout of atmospheric Ca-rich particles in the atmosphere (carbonate minerals and organic matter) and mineral weathering within these acidic soils. Calcium is retained in soils during the driest period (January 2011) and shows lower stream concentrations during this period.

Potassium in rainwater and stream water was found to be elevated above the K/Cl seawater molar ratio (Figure 4.21 and Figure 4.38) reflecting additions from mineral dust, fire ash, decomposition of plant material and chemical weathering of clay minerals in the soil. Potassium is retained in soils during dry periods (March 2011). The retention of K in soils correlates with periods of decreased stream water concentrations. Clay minerals within the soil included illite and mica minerals with smaller amounts of smectite, feldspar and kaolinite. Illite and mica minerals are the most beneficial to the plants as they can release K during chemical weathering. Kaolinite is an aluminosilicate clay mineral and will not provide the plants with vital nutrients. The clay minerals may be derived from weathering of mica in the bedrock (Figure 3.1 to Figure 3.6) supported by a higher K_2O contents in the bedrock relative to soil (Figure 4.47). Additional sources of K may be derived from dust containing clay, feldspar and mica minerals as well as organic matter. The dissolution of minerals delivered by windblown dust or degradation of organic matter would contribute macronutrients K, Ca, Mg as well as trace metals such as Fe and Mn to the soil and vegetation. Potassium has a similar concentration in seawater as Ca but appears to cycle more slowly through the fynbos ecosystem perhaps influenced by the greater uptake by plants and the slower chemical weathering of K-rich mica and feldspar in comparison to Ca-rich carbonate minerals delivered as dust to the acidic soils.

5.2 Fluxes and Reservoirs

In this section the flux of elements into and out of the study area and the reservoir size of elements in the soil and bedrock are estimated from the data collected in order to assess the net flux of elements in the ecosystem (influx - outflux). The fluxes of elements into the study area (influx) were calculated from the element concentrations in the rain water samples (total deposition) collected and the amount of rainfall averaged over the sample sites for each collection period. The fluxes of elements out of the study area (outflux) were calculated from the element concentration of the stream waters and from a stream discharge estimated by assuming 38 to 42% of stream water evaporate within the catchment area upstream of the stream sampling points. Streamflow was not measured directly in the field, but precipitation amounts multiplied by the catchment areas adjusted to 38 to 42% evaporative loss were used to estimate total streamflow. Precipitation amounts in samplers closest to the streams were used. Catchment areas were calculated using an ArcView GIS program. The catchment areas are given in Appendix C.

An evaporative loss in this study of 38% was estimated through calculations described in Section 4.2.1. An average evaporative loss after fire in three TMG subcatchment areas of Zachariashoek near Stellenbosch was determined to be 42% (Lindley *et al.*, 1988). Here it is assumed that evaporative loss ranges between 38 and 42% with an average of 40%. Calculations of soil and bedrock reservoirs require estimates of porosity (ϕ) and density (ρ in g/cm^3). The bulk air dried soil density was determined by measuring the weight of a volume of soil. The top and sub soil densities ranged from 0.9 to 1.1 g/cm^3. The bulk density of the quartz arenite bedrock was estimated based on the mean particle density of quartz of 2.65 g/cm^3 (Deer *et al.* 1992) and 10% porosity, present mainly as fracture porosity. The mean depth (d) for both top- and subsoils was taken as 5 cm. The mean depth for bedrock was also taken as 5 cm to allow for comparison with the top and sub soil reservoirs. Reservoir size was calculated using the following equation (Soderberg, 2003):

$$M = C \times A \times d \times \rho \times (1 - \phi)$$

with, M = amount of an element on a spatial basis (kg/ha or mol/ha)

C = mean concentration of an element for the specified area on a dry mass basis (g/kg or mmol/kg)

A = area for which the calculation is based (in m^2)

The following quantities were taken,

C = the concentration of the element in the soil or bedrock sample

A = 10000 m^2 (1 ha)

d = 0.05 m

ρ = average of 1.1 g/cm^3 for soils, 2.65 g/cm^3; the mean particle density for quartz (Deer *et al.* 1992)

ϕ = 0.1 for bedrock

Site 1 received the highest influx for all major ions measured in the study, except for SO_4 (Figure 5.2). Site 2 received the lowest influx for all ions and the second lowest SO_4 influx. The low influx rates of site 2 may result from the rainout of aerosols towards the west. Site 5 recorded the highest SO_4 influx suggesting that the source for the increased SO_4 influx may predominantly come from the northern interior areas rather than from marine sources to the south. Sites with high Cl influx have low SO_4 influxes and the reverse applies for sites with high SO_4 influxes.

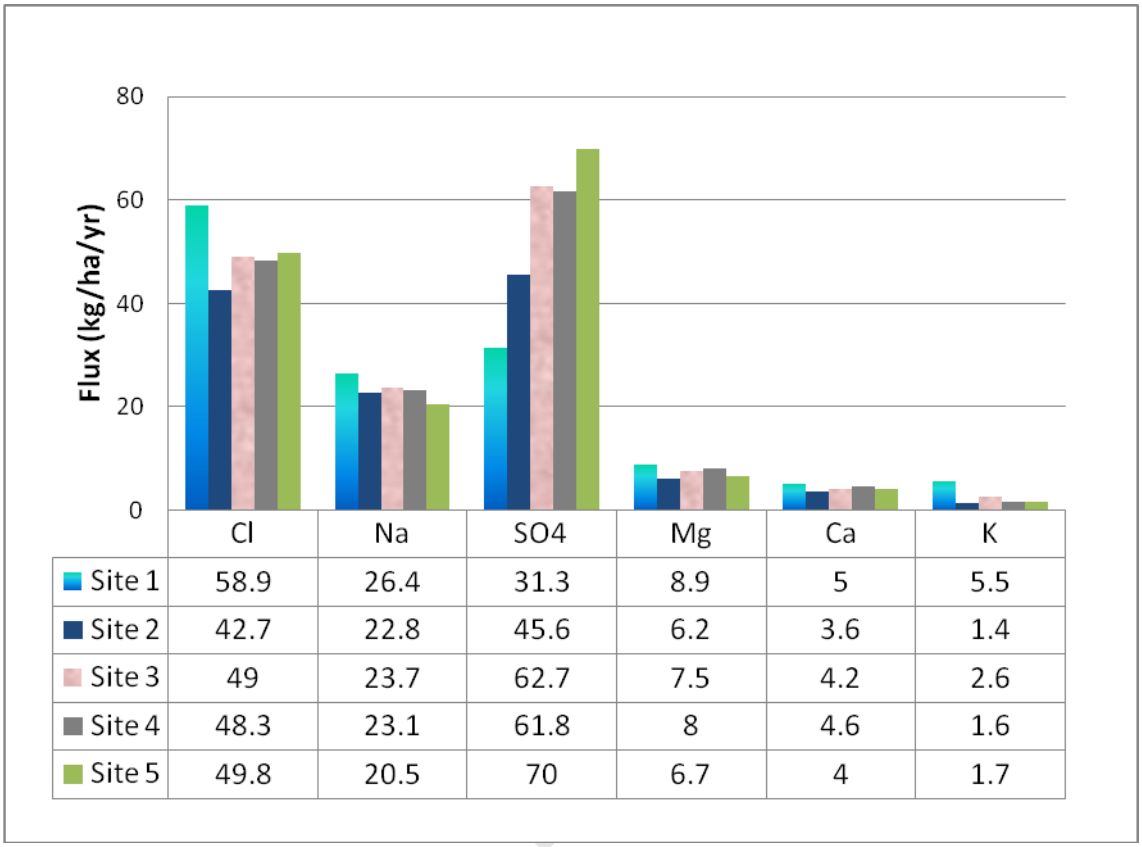

	Cl	Na	SO4	Mg	Ca	K
Site 1	58.9	26.4	31.3	8.9	5	5.5
Site 2	42.7	22.8	45.6	6.2	3.6	1.4
Site 3	49	23.7	62.7	7.5	4.2	2.6
Site 4	48.3	23.1	61.8	8	4.6	1.6
Site 5	49.8	20.5	70	6.7	4	1.7

Figure 5.2 Total influx rates (in kg/ha/yr) for the different major ions measured in this study.

The outflux of ions Cl, Na and SO_4 is highest at site 1 (corresponding to stream 5) (Figure 5.3). The outflux of ions Mg, Ca and K is highest at site 5 (corresponding to stream 1). Stream 4 (str04), closest to site 4 recorded the lowest outflow of ions due to the mountain seep flowing only during periods of high rainfall. There is thus an accumulation and net gain of ions at site 4 throughout the sampling period.

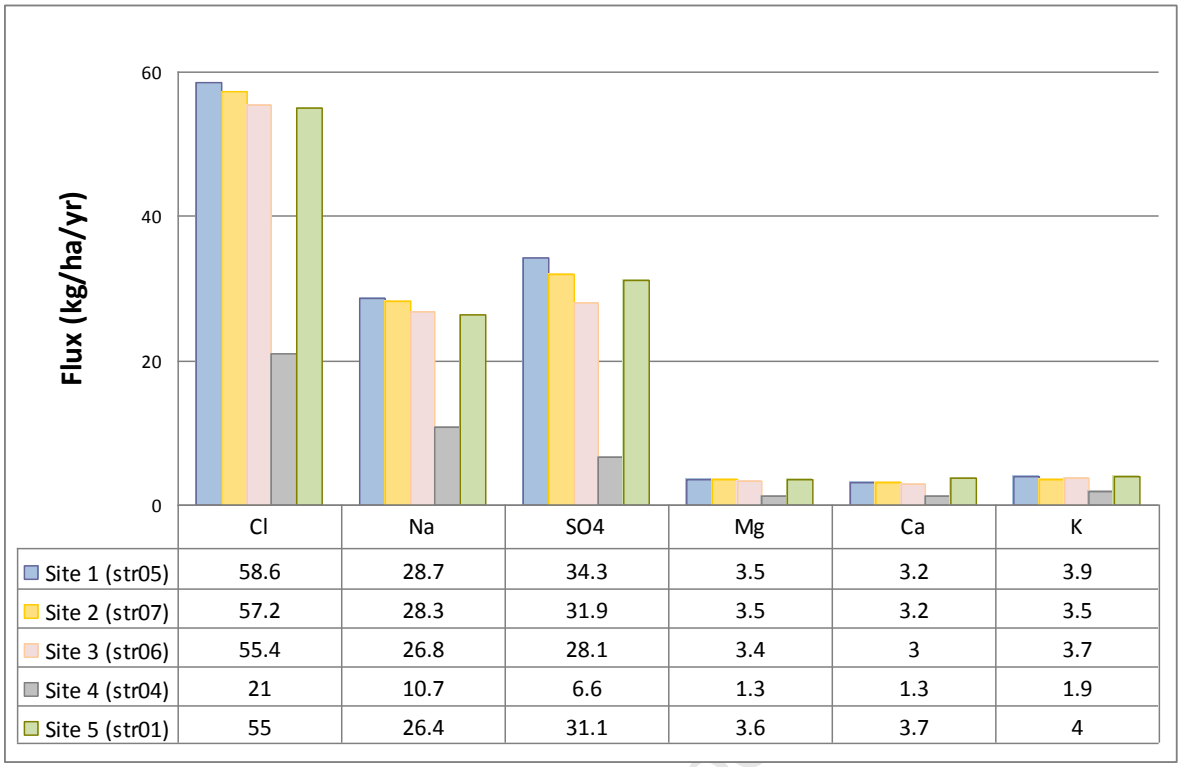

	Cl	Na	SO4	Mg	Ca	K
Site 1 (str05)	58.6	28.7	34.3	3.5	3.2	3.9
Site 2 (str07)	57.2	28.3	31.9	3.5	3.2	3.5
Site 3 (str06)	55.4	26.8	28.1	3.4	3	3.7
Site 4 (str04)	21	10.7	6.6	1.3	1.3	1.9
Site 5 (str01)	55	26.4	31.1	3.6	3.7	4

Figure 5.3. Outflux rates (in kg/ha/yr) for all major ions at the different sampling points. Streams closest to the sites are indicated in parentheses.

Figure 5.4 shows the total influx and outflux of ions in the entire study area as well as reservoir size and fluxes of top and sub soil and bedrock reservoirs. The calculation of fluxes in rainfall (influx) and streams (outflux) allow for the net flux to be determined. Chloride, sodium and potassium ions record a net loss, whilst sulphate, magnesium and calcium record net gains for the ecosystem. The net loss of Na and K suggests that these ions are not retained and that the total influx is supplemented by loss from the soil reservoir when averaged over the entire sample period. The large net gain in SO_4 suggests that SO_4 ions are retained in the soil. Soderberg (2003) noted that SO_4 is taken up by plants and the analyses of soil in this study included plant roots. The retention of SO_4 may also be related to the washout and redistribution of SO_4 ions after fire in the form of ash.

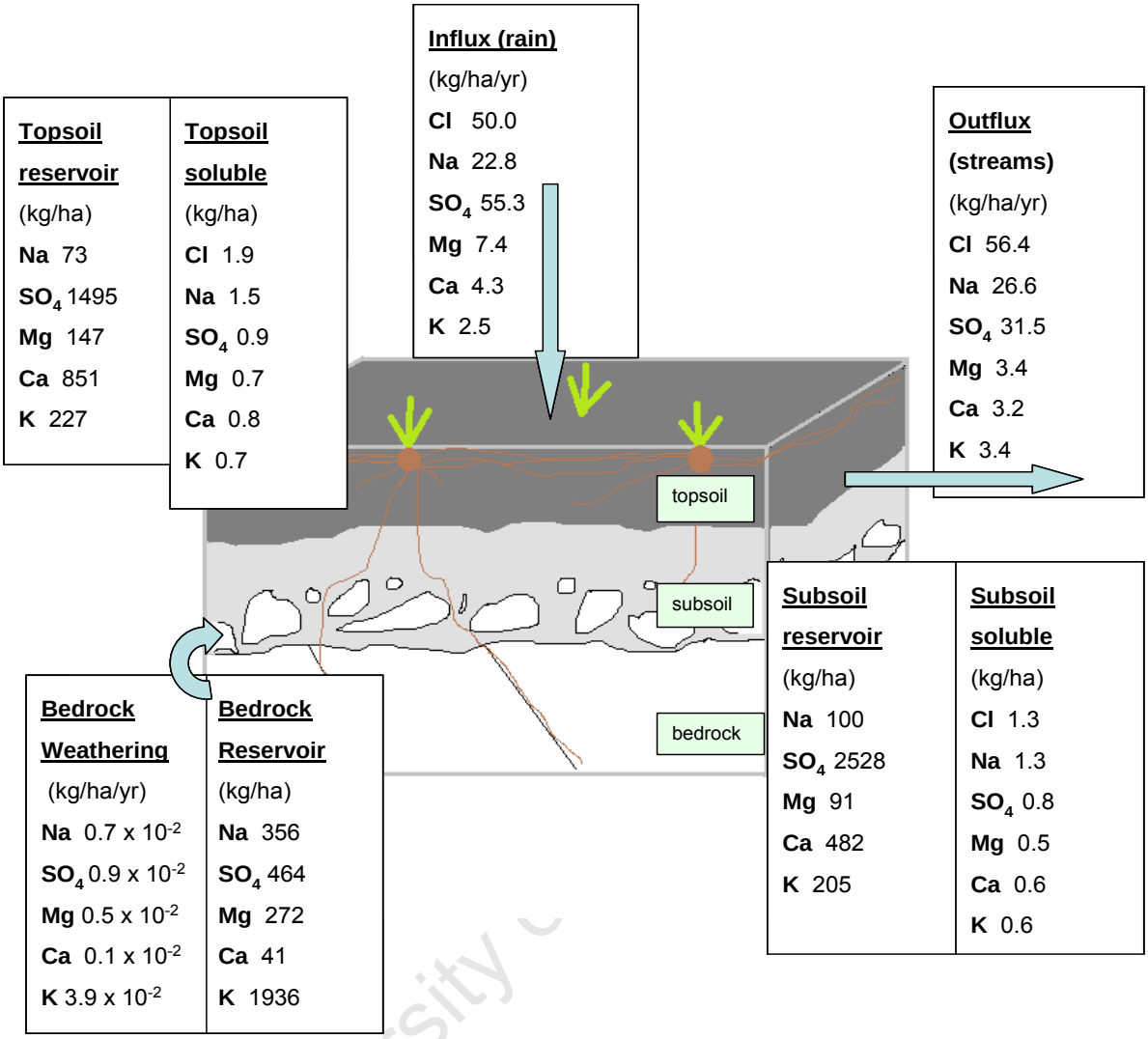

Figure 5.4. Diagram showing the total fluxes and soil-bedrock reservoirs for the entire study area as well as contributions to the soil reservoir from the underlying bedrock. The sub and top soil as well as bedrock depths are 5 cm.

Soderberg (2003) does not record the same net loss in Cl and Na (Figure 5.5) indicating that fire has an effect on these ions. Soderberg (2003) indicated similar Cl and Na influxes, but it should be noted that a proportion of this was estimated to be dry deposition (more than 50%) added to the wet deposition measured in the study. Sulphate was not measured in the study of Soderberg (2003). The influx of ions decreases from K to Ca to Mg. Magnesium recorded a higher influx than K and Ca in this study. The higher influx of K and Ca in Soderberg (2003) may result from more dust input as the study area is closer to inland dust sources. The outflux of ions reported in Soderberg (2003) was almost negligible compared to the influx and decreased from Mg (0.6 kg/ha/yr) to K (0.4 kg/ha/yr) to Ca (0.3 kg/ha/yr). The low outflux recorded in Soderberg (2003) reflects the uptake of these nutrients by plants, the above ground portion of which were removed by the fire in this study.

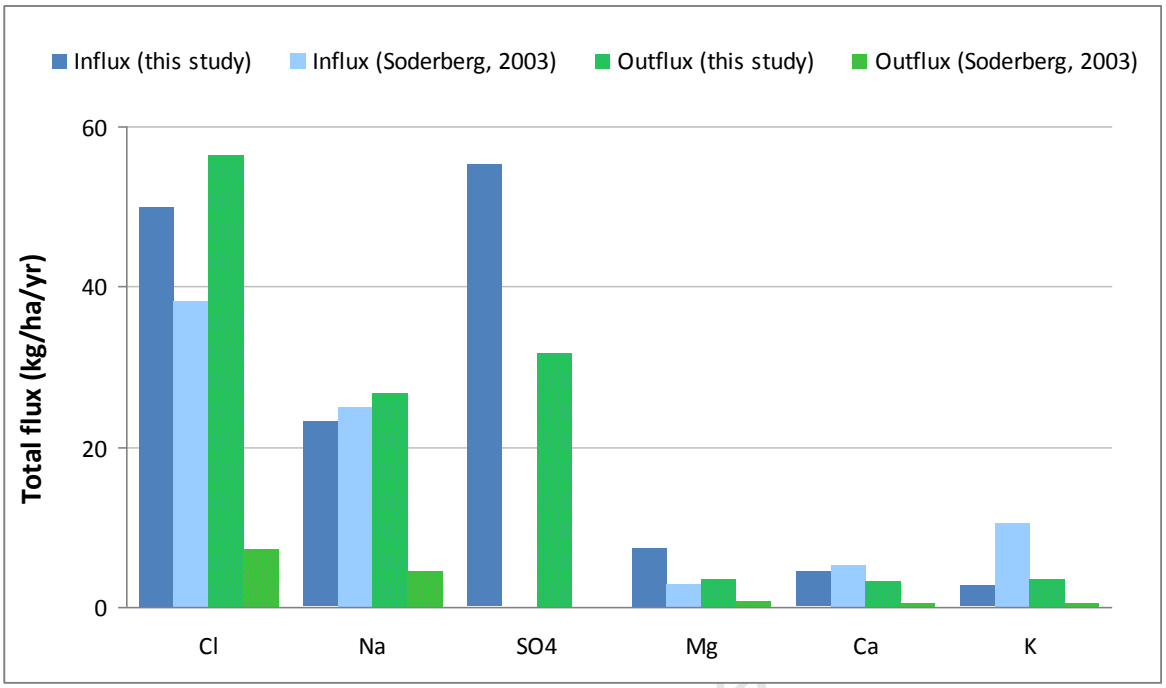

Figure 5.5. Comparison between influx and outflux as determined in this study and in Soderberg (2003).

The soluble fraction of the soil accounts for a small proportion of the total soil reservoir, but is readily available to the plants for nutrient uptake. Ions retained as the soluble fraction during dry periods are most easily flushed out of the soil during a rain event (Soderberg, 2003). The large net difference between the total outflux and influx of SO_4 is reflected in the large total soil reservoirs of SO_4. Sodium and sulphate have greater reservoirs in the subsoil compared with the topsoil whereas magnesium, calcium and potassium have greater topsoil reservoirs. Soderberg (2003) noted that Mg, Ca and K are more readily recycled and taken up by plants. The greater root and organic matter content of topsoil may explain the larger topsoil reservoirs of Mg, Ca and K.

Bedrock weathering contributions to the soil were based on the slow weathering rate of TMG sandstone assumed to be between 1 and 10 m/Myr (Kounov *et al.*, 2007). An average of 5 m/Myr was taken to calculate the bedrock contribution of ions to the overlying soil. The contribution of bedrock weathering to soil is slow and minute compared to the influx of ions through rainfall and rainout (Figure 5.4). Potassium has the largest bedrock reservoir and has the greatest weathering flux to soil. Calcium and magnesium have relatively small bedrock reservoirs and lower bedrock weathering fluxes to the soil than potassium. This is

consistent with observations made in thin section where mica minerals were more abundant than feldspar minerals in the quartz arenite sandstone.

5.3 The Role of Hydrology and Topography in the Biodiversity of a Mountain Fynbos Ecosystem

The preceding sections of this chapter have outlined the effectiveness of rainwater and stream water in delivering ions to the ecosystem which are taken up by the vegetation. Precipitation and stream capacity can affect the moisture contents of soil. Beard (1983) outlines the importance of moisture and hydrology in Mediterranean-type ecosystems. Ions are taken up more effectively in areas with increased moisture. Soil moisture can also determine the vegetation type (Miller, 1983). Tall forest vegetation is confined to sheltered ravines and stream banks (Manders, 1990) whereas fynbos vegetation is more adapted to unsheltered higher slopes. The afromontane forests in the study area were largely unburnt during the 3 June 2010 fire event. Ions and organic debris will filter down slopes into valleys and ravines and feed into the stream chemistry where the vegetation can utilize the available nutrients. Steeper slopes will have less opportunity to make use of the water and the ions it carries as the water rapidly flows through the highly permeable thin soils during rain events. Rainwater may filter through or run off steeper slopes more rapidly than on more gentle gradients. Soil thickness and moisture content thus increase close to stream banks. The water that is made available to the regrowth and already established growth contain essential elements to the plants. Plant regrowth was slower on higher slopes and ridges than in the valleys or near streams (Appendix D). Water takes up ions and transports them through the soils making them available for plants. This allows the opportunity for plant nutrient recycling whereas little or no nutrient recycling can take place on burnt steep rocky slopes. The accumulation of nutrients along streams and river valleys as noted by the wash down of ions during wetter periods may also hold an advantage to vegetation regrowth. Bedrock is highly fractured and soils are thin and permeable which means rainwater will rapidly flow through and out of thin soils on steep slopes and only slow down when it reaches less steep slopes of valley floors containing relatively thick soils. Nutrients are therefore rapidly flushed from upper slopes and transported to lower slopes such that

outside of seeps and stream paths, fynbos struggles to build up much biomass or soil. The tough root mat is critical in this respect to retain the thin soil that exists on the steep slopes.

5.4 Possible Effects of Fire on the Ecosystem

The effects of fire are poorly understood and not well documented in the fynbos ecosystem (Kruger, 1979a; van Wilgen *et al*., 1985). This was the case four decades ago and is still today. It was fortuitous that this study incorporated a fire component. There have been attempts at understanding what role fire plays in the fynbos biome and van Wyk, *et al.* (1992) emphasized the importance of the role that fire plays in affecting nutrient budgets in ecosystems. Ions may volatize, be released or concentrate on lower slopes. There is a rapid and permanent loss of nutrients through stream outflow and wind transport immediately after the fire. Nutrients may be trapped in organic burnt plant debris and accumulate on lower slopes.

The ash released by the fire may be taken up as windblown dust and as such change the chemistry of rainwater. Fire ash is a rich source of nutrients playing a role in the cycling of ions post-fire (Lamont, 1983; Franco-Vizcafno and Sosa-Ramirez, 1997; González-Pérez *et al.*, 2004). Much of the fire ash is carried by wind to neighbouring unburnt areas and not retained in the burnt areas. The broader redistribution of nutrients is perhaps just as well since the regrowth is too slow to take up all the nutrients made available after a fire and these nutrients are likely better put to use in areas with established biomass in place. Ions such as SO_4, Mg and Ca showed increased concentrations in rainwater after the fire events relevant to this study. The rainwater feeds into stream water and can determine the ion content of the stream water and mountain seeps. Molar ratios for SO_4/Cl and K/Cl in rainwater and stream water were found to be higher than molar ratios for seawater. The higher molar ratios for SO_4/Cl and K/Cl compared to the seawater molar ratios suggest that there is an additional source other than marine aerosols to the ecosystem. One possibility is that the fire released and remobilized these ions enriching rainwater and stream water in SO_4 and K relative to seawater. Other non-marine inputs include atmospheric dust entering the ecosystem from the north. Results from the study area prior to the fire (Smit, 2003) indicate SO_4/Cl and K/Cl molar ratios were depleted compared to the seawater molar ratios. After the June 2010 fire, sulphate showed decreasing concentrations and SO_4/Cl molar

ratios in rainwater and stream water for a period of 8 months post fire. This may indicate that SO_4 will return to a pre-fire equilibrium after approximately one year following a fire event. Potassium concentrations may also decrease with time and attain pre-fire concentrations when vegetation growth has reached levels sufficient for all K to be taken up by plants in the ecosystem. Molar ratios for Mg/Cl in this study and in Smit (2003) generally agree, but with more scatter in the data for this study. Both studies show that Mg/Cl molar ratios are depleted relative to the seawater molar ratios. Molar ratios for Ca/Cl between the two studies also agree in that Ca/Cl molar ratios show relative enrichment compared to the seawater molar ratios, but with the enrichment significantly higher in this study. A comparison between the two studies regarding ion-Cl molar ratios thus indicates that SO_4 and K are the most affected by the fire event, while Mg and Ca are less affected.

Rundel (1983) and Scott and van Wyk (1992) outline the fact that fire can have different effects on hydrology. Factors influencing the response of hydrology to fire include the season of the burn, the intensity of the fire, soil characteristics (Trabaud, 1983), basin morphology, vegetation type and climate. A uniform response of hydrology to fire is thus unlikely (Oechel and Hastings, 1983; Scott and van Wyk, 1992; Pérez-Cabello, 2009). The consequences of fire to hydrology in Mediterranean-type ecosystems show an overall increase in total water yield, peak discharge and streamflow following a fire (Scott and van Wyk *et al.*, 1992). The response of water yield, peak discharge and sediment erosion are all related to hydrophobicity or water repellency (Scott and van Wyk, 1992; Scott, 1993; DeBano, 2000; Pérez-Cabello, 2009). Water repellency increases due to the coating of soil particles with hydrophobic organic substances produced by the fire. A hydrophobic layer will form which inhibits rainwater infiltration and percolation. The result is that overland flow into streams will occur (Richardson and van Wilgen, 1992). The hydrophobic layer and removal of large amounts of biomass will lead to increased soil erosion (Scott, 1993). This was evident during fieldwork when dry partially burnt organic plant debris was washed down slope to accumulate on the lower slopes. The plant debris is of much lower density than the rock components of the soil and is easily separated by running water. Many of the seeds that sprouted after the fire were focused within debris-rich patches of litter that had accumulated within small downslope surface depressions or up against prominent rock exposures to act as natural compost. Streamflow will subsequently increase as well. The removal of plant biomass will also increase streamflow as transpiration and rainfall

interception is reduced. Lindley *et al*. (1988) mention that the response of streamflow increasing after a fire event is small and short-lived. Fire counteracts the unequal downslope distribution of nutrients by redistributing them as airborne fine ash where the wind can distribute them more equally over an area.

A tough interwoven root network remained in place after the fire. The root mat was a mixture of both dead and live roots. This suggests that the fire was not intense enough to burn significantly through the soil. Rundel (1983) estimates fynbos fires to be approximately 300ºC and dramatically decreases within the first few centimeters of the soil profile. The tough root mat plays an important role in holding the thin soil layer in place. The dead organic plant debris may hold nutrients that could have added to the nutrient pool for vegetation regrowth, but this is eventually lost as leaching of these nutrients outstrips the plants regrowth rate. Regrowth may however be more dependent on the nutrients that are stored in the roots of resprouters and the seeds of non-sprouters.

This study did not include N in the analyses, but the little work done on fynbos nutrient dynamics included N deposition in their studies. Nitrogen largely relies on the cycling of plant material (Read and Mitchell, 1983), but the main sources of N come from atmospheric deposition and N fixation (Ellis *et al*., 1983). Studies in areas with little anthropogenic influences concluded N inputs from the atmosphere to be approximately 2 kg/ha/yr (Stock and Lewis, 1986; van Wyk, *et* al., 1992). Wilson *et al.* (2009) outline the dangers of increasing N inputs into the ecosystem. An increase in N inputs may lead to biodiversity loss. Fynbos vegetation has relatively slower decomposition rates than other Mediterranean-type ecosystems such as the Californian chaparral and Australian heathlands. Fire can thus play an important role in releasing and remobilizing essential nutrients to the fynbos ecosystem (Read and Mitchell, 1983; Rundel, 1983; Herppich *et al*., 2002). Fire may increase nitrogen levels in the soil surface in the short-term (Trabaud, 1983; Stock and Lewis, 1986). However, high intensity fires can volatilize N reducing rather that increasing the soil nitrogen (Ellis *et al*., 1983; Rundel, 1983; van Wyk *et al*., 1992; Herppich *et al*., 2002). The usual processes may still be active in the ecosystem after a fire event, but denitrification and volatilization of ions will have an additional affect in that it will limit plant regrowth (Figure 5.6). Biological N fixation may still be active in plants where the

roots have not been destroyed playing a role in the regrowth of these plants (Rundel, 1983). Any excess in ions will leave the soil through stream outflow and as sediment loss.

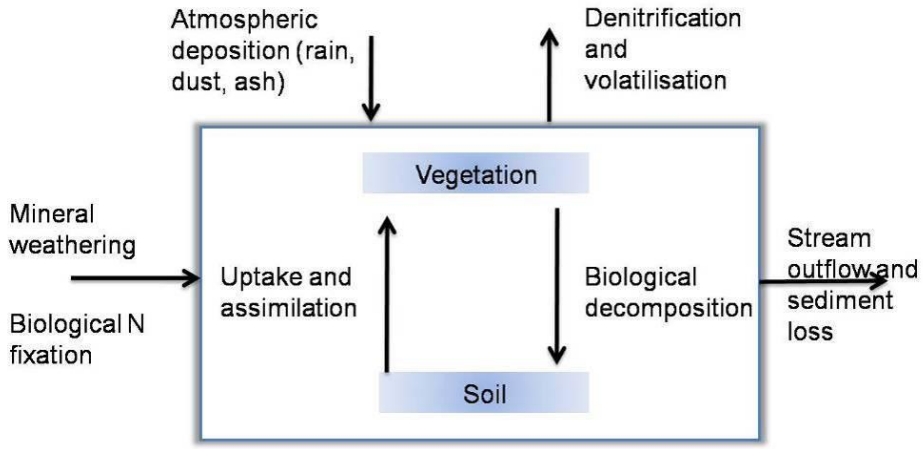

Figure 5.6. Diagram showing the main processes in an ecosystem following a fire event (modified from van Wyk *et al*., 1992).

Plant regrowth depends on the availability of nutrients. This study suggests that the inputs of major ions do not limit plant regrowth as most are being exported by streams from the study area. The possible depletion and slow return of N may prove to be limiting plant regrowth (Read and Mitchell, 1983; Vitousek, *et al*., 2010).

The soils of the southwestern Cape account for some of the most phosphorus deficient in the world (Kruger, 1979a; Specht and Moll, 1983; Bond, 2010). A fire event may deplete the soil more of any available P for plant regrowth. Phosphorus may be remobilized as part of the ash, but the surge of P in soils may be short-lived as an increase in fertility reaches its peak close after the fire. Thereafter plant regrowth slows down as P deposition decreases (Pérez-Cabello *et al*., 2009). After a fire, additional P can be derived from bedrock weathering or mineral aerosol deposition (Witkowski and Mitchell, 1987). The bedrock contains only a trace amount of P and weathers too slowly to likely be a significant source of P. The winter northerly winds transporting dust from the interior are the most probable source of additional P to the ecosystem.

This study emphasizes that a mountain fynbos ecosystem is reliant on a variety of factors and that quartz rich and slow weathering bedrock generally plays a very limited role in the supply of nutrients. The different components of the ecosystem provide a source pathway

for elements to be transported and made available to the plants. The components within the ecosystem are further influenced by aspects such as rainfall variation, topography, slope aspect and hydrology. Fire events on an average of one per every one or two decades add an additional component to the ecosystem, redistributing the uneven build up of plant nutrients a product of the focus of water and nutrients on plant biomass in downslope valleys to spread them more equably over the entire ecosystem.

Chapter 6 : **Conclusions**

The mountain slopes of the Harold Porter National Botanical Gardens and Kogelberg Biosphere Reserve are home to more than 1600 plant species, of which 77 species occur nowhere else forming one of the most diverse ecosystems in the Cape Floristic Region. The fynbos vegetation in the study area grows on thin, acidic soils derived from sandstone bedrock with low nutrient status. Nutrients supplied to the ecosystem are thus derived from a range of sources other than the bedrock substrate. Fire is critical to the fynbos biome. Fynbos vegetation relies on fire for the redistribution of nutrients, the release of their seeds and hence fire forms part of their reproductive strategy. The fire event of 3 June 2010 provided a unique opportunity to assess what influence a fire may have on the behaviour of elements within the various components of the ecosystem.

This study set out to measure the chemistry and mineralogy of different components of a mountain fynbos ecosystem over a one year period in a mountainous near-coastal setting to gain a better understanding into the dynamics of nutrient sources into the ecosystem. The macronutrients Cl, Na, SO_4, Mg, Ca and K were measured in rainwater, stream water (including two mountain seeps) and soil saturated paste extracts. Bedrock and soil mineralogy were analysed through XRF and XRD techniques.

Major ions enter the system primarily through two components, namely the atmosphere and through bedrock weathering. The weathering of bedrock provides nutrients to the ecosystem at a much slower rate than inputs from the atmosphere. Atmospheric deposition comprises both wet and dry deposition. Total deposition in the form of rainout and rainwater were considered in this study. Rainwater includes both marine aerosols and windblown mineral and organic matter dust. The fire event added an additional input component to the system in the form of ash particles. The ash will form part of windblown dust and can also be deposited through rain events. An excess of SO_4, Mg, Ca and K compared to their seawater chlorinity ratios indicate a mixed source from marine and dust aerosols. The removal of above ground biomass through fire allows for two pathways of fire ash. Elements forming part of the fire ash may either be removed from the area through wind or be deposited onto and eventually into the soil allowing for the accumulation of elements through fire ash in the top soil. Chloride and sodium are elements that are the least affected by the fire and

showed the strongest marine influence concentrating more during periods of low rainfall. The rainwater will filter into other components such as the stream water and soils.

Rainwater infiltrates soil and reaches the bedrock-soil interface where it flows as groundwater and may exit into streams as mountain seeps. A fraction of the rainwater would be intercepted by vegetation in an ecosystem unaffected by fire, but it was possible to rule this out in this study. A comparison with two previous studies in the Swartboskloof (van Wyk *et al*., 1992) and in the Elandskloof subcatchment area near Citrusdal (Soderberg, 2003; Soderberg and Compton, 2007) revealed that major ions, especially those of predominantly marine origin (Cl, Na and SO_4) decreased significantly further away from the coast.

Rainwater feeds directly into streams by runoff and throughflow. The stream water chemistry showed similar trends to the rainwater with an excess of SO_4, Mg and Ca recorded and Cl and Na were more concentrated during drier periods. Chloride, sodium and potassium recorded a net loss (higher outflux than influx). Sulphate, magnesium and calcium showed a net gain with a large proportion of the sulphate being stored in the soil reservoir. The slight depletion of Na relative to the seawater chlorinity ratio reflects possible adsorption to particles and nutrient uptake by plants. A comparison of SO_4/Cl molar ratios in stream waters between this study and that of Smit (2003) reveals that pre-fire sulphate is depleted relative to seawater but that after the fire event the SO_4/Cl ratios increased. These sulphate enriched stream waters tended towards the seawater SO_4/Cl molar ratios after 8 months following the fire event. The decrease after 8 months suggests that SO_4 returns to pre-fire levels within one year following a fire event. The source for sulphate reflects a range of inputs into the ecosystem. Phytoplankton produces dimethyl sulphide (DMS) offshore particularly during the summer months which is oxidised to sulphur dioxide and sulphate in the atmosphere. Sulphate aerosols reach the study area through mainly southeasterly winds and enter the ecosystem as rainout and dry fallout. Magnesium and calcium showed mineral dust inputs into the ecosystem and may arrive through northwesterly winds mainly during winter. Ash deposition associated with nearby fires may also be a source of Mg, Ca, SO_4 and K. Potassium, similar to sulphate, showed enrichment post-fire whereas Smit (2003) showed that potassium is depleted relative to seawater in a pre-fire state. The excess K in the system suggests that plant regrowth was not sufficient

within one year following the fire event to take up all bioavailable K. Potassium, calcium and magnesium are usually recycled between decomposing plant litter and stream water and similarly between plant litter and soil. The removal of above ground vegetation and plant litter provided the opportunity to analyse elements without the possibility of nutrient cycling by litter degradation.

It was found that elements are retained within the soil during dry summer months and washed into streams during wetter winter months. The lower Mg concentrations in streams compared to rainwater indicates the retention of Mg in soil and possible uptake by vegetation. Calcium is retained in soils during the driest period (January 2011) and shows lower stream concentrations during this period. Magnesium and calcium concentrations are higher in the topsoil compared to the subsoil suggesting they are sourced from ash or dust deposition and taken up by vegetation. Potassium is retained in soils during dry periods (March 2011) which correlate with periods of decreased stream water concentrations.

Clay minerals within the soil include illite and mica minerals with smaller amounts of smectite, feldspar and kaolinite. Illite and mica minerals are the most potentially beneficial to the plants as they can release K during chemical weathering. Kaolinite is an aluminosilicate clay mineral and will not provide the plants with vital nutrients. The clay minerals may be derived from bedrock weathering as well as through windblown dust. Mica minerals identified in thin section were supported by a higher K_2O contents and K reservoir in the bedrock relative to soil. Potassium showed the highest bedrock reservoir of all the ions measured in this study. The contribution of K to the overlying soil through bedrock weathering was higher than the other ions. Feldspar minerals were absent in the bedrock and support the low CaO content of the bedrock. Calcium recorded the lowest bedrock reservoir of all ions measured in the study. Mineral dust may deliver certain clay, feldspar and carbonate minerals the dissolution of which in these acidic fynbos soils would contribute the macronutrients K, Ca, Mg as well as trace metals such as Fe and Mn.

Plant regrowth was initially fast following the fire event with sprouting vegetation growing back first followed by seeder vegetation germinating 4 months after the June 2010 fire event. The rapid growth following the fire event can be attributed to the remobilization of nutrients through dissolution of ash rich in nutrients. Growth of the vegetation slows down

with time as nutrients are flushed from the ecosystem and no longer available to sustain rapid regrowth. Nitrogen may be the limiting nutrient as it volatilises during the fire. Phosphorus is lost as ash blows beyond the burnt area. A fraction of N and P may be left after the fire event, but these ions must first build up to sufficient levels to constantly supply new as well as established growth. Nitrogen increases through soil microbial activities and phosphorus is mostly supplied through plant litter decomposition and recycling. The plant regrowth must then wait for the delivery of P, N and other nutrients derived from marine and dust aerosol sources, gradually rebuilding plant biomass and living as well as litter nutrient pools.

This project outlines the complex interaction of different components in a mountain fynbos ecosystem to sustain a species rich floral community. A supply of macronutrients is continuously supplied through atmospheric processes and the slow weathering of bedrock. The one-year post-fire record of macronutrients measured in this study reflects seasonal influences as well as effects from the two fire events of 2010 and 2011. The role that fire plays on the behaviour and cycling of ions in the ecosystem may not be entirely understood, but this study suggests that fire plays a critical role in the dynamics of the ecosystem. This study forms only a small part of essential research still needed for future fynbos related studies.

Reference List

Abanda, P.A; Compton, J.S and Hannigan, R.E. 2011. Soil nutrient content, above-ground biomass and litter in a semi-arid shrubland, South Africa. *Geoderma*, **164,** 128-137.

Anderson, J.M; Anderson, H.M; Afichangelsky, S; Bamford, M; Chandra, S; Dettmann, M; Hill, R; McLoughlin, S and Rösler, O. 1999. Patterns of Gondwana plant colonisation and diversification. *Journal of African Earth Sciences*, **28** (1), 145-167.

Avila, A and Alarcón, M. 1999. Relationship between precipitation chemistry and meteorological situations at a rural site in NE Spain. *Atmospheric Environment*, **33,** 1663-1677.

Bathmann, U.V; Scharek, R; Klaas, C; Dubischar, C.D and Smetacek, V. 1997. Spring development of phytoplankton biomass and composition in major water masses of the Atlantic sector of the Southern Ocean. *Deep-Sea Research II*, **44** (1-2), 51-67.

Beard, J.S. 1983. Ecological control of the vegetation of Southwestern Australia: moisture versus nutrients. In: Kruger, F.J; Mitchell, D.T and Jarvis, J.U.M (Ed.) *Mediterranean-Type Ecosystems: The Role of Nutrients*, Ecological Studies 43, Springer-Verlag, Heidelberg, 66-73.

Bond, W.J. 2010. Do nutrient-poor soils inhibit development of forests? A nutrient stock analysis. *Plant Soil*, **334**, 47-60.

Bond, W.J and Keeley, J.E. 2005. Fire as a global 'herbivore': the ecology and evolution of flammable ecosystems. *Trends in Ecology and Evolution*, **20** (7), 387-394.

Born, J; Linder, H.P and Desmet, P. 2007. The Greater Cape Floristic Region. *Journal of Biogeography*, **34**, 147-162.

Brown, G; Mitchell, D.T and Stock, W.D. 1984. Atmospheric deposition of phosphorus in a coastal fynbos ecosystem of the Southwestern Cape, South Africa. *Journal of Ecology*, **72,** 547-551.

Brown, N.A.C. 1993. Promotion of germination of fynbos seeds by plant-derived smoke. *New Phytologist*, **123** (3), 575-583.

Burgoyne, P.M; van Wyk, A.E; Anderson, J.M and Schrire, B.D. 2005. Phanerozoic evolution of plants on the African plate. *Journal of African Earth Sciences*, **43**, 13-52.

Buringh, P. 1984. Organic carbon in soils of the world. In: Woodwell, G.M (Ed.) *The role of terrestrial vegetation in the global carbon cycle: Measurement by remote sensing*, John Wiley and Sons, 91-108.

Campbell, B.M. 1986. Montane plant communities of the fynbos biome. *Vegetatio*, **66** (1), 3-16.

Carlson, J.E; Holsinger, K.E and Prunier, R. 2010. Plant responses to climate in the Cape Floristic Region of South Africa: evidence for adaptive differentiation in the *Proteaceae*. *Evolution*, **65**, 108-124.

Certini, G. 2005. Effects of fire on properties of forest soils: a review. *Oecologia*, **143**, 1-10

Chadwick, O.A; Derry, L.A; Vitousek, P.M; Huebert, D.A and Hedin, L.O. 1999. Changing sources of nutrients during four million years of ecosystem development. *Nature*, **397,** 491-497.

Chen, L; Arimoto, R and Duce, R.A. 1985. The sources and forms of phosphorus in marine aerosol particles and rain from northern New Zealand. *Atmospheric Environment*, **19** (5), 779-787.

Compton, J.S. 2004. *The rocks and mountains of Cape Town*. Double Storey Books, Cape Town, 112pp.

Cornell, S.E. 2010. Atmospheric nitrogen deposition: Revisiting the question of the importance of the organic component. *Environmental Pollution*, **159** (10), 2214-2222.

Cornell, S.E; Jickells, T.D; Cape, J.N; Rowland, A.P and Duce, R.A. 2003. Organic nitrogen deposition on land and coastal environments: a review of methods and data. *Atmospheric Environment*, **37**, 2173-2191.

Cowling, R.M. 1992. The Ecology of Fynbos: *Nutrients, Fire and Diversity.* Oxford University Press, Cape Town. 411pp.

Cowling, R.M. 1995. *Fynbos: South African unique floral kingdom*. Fernwood Press. 156pp.

Cowling, R.M and Heijnis, C.E. 2001. The identification of Broad Habitat Units as biodiversity entities for systematic conservation planning in the Cape Floristic Region. *South African Journal of Botany*. **67**, 15-38.

Cowling, R.M; Procheş, Ş and Partridge, T.C. 2009. Explaining the uniqueness of the Cape flora: Incorporating geomorphic evolution as a factor for explaining its diversification. *Molecular Phylogenetics and Evolution*, **51,** 64-74.

Cowling, R.M; Rundel, P.W; Desmet, P.G and Esler, K.J. 1998. Extraordinary high regional-scale plant diversity in Southern African arid lands: Subcontinental and global comparisons. *Diversity and Distributions*, **4** (1), 27-36.

Cowling, R.M; Rundel, P.W; Lamont, B.B; Arrojo, M.K and Arianoutsou, M. 1996. Plant diversity in Mediterranean-climate regions, *Trends in Ecology and Evolution*, **11** (9), 362-366.

Cox, R.L and Underwood, E.C. 2011. The importance of conserving biodiversity outside of protected areas in Mediterranean ecosystems. *Mediterranean Conservation*, **6** (1), 1-6.

Crosti, R; Ladd, P.G; Dixon, K.W and Piotto, B. 2006. Post-fire germination: The effect of smoke on seeds of selected species from the central Mediterranean basin. *Forest Ecology and Management*, **221,** 306-312.

Day, J.A; Dallas, H.F and Wackernagel, A. 1998. Delineation of management regions for South African rivers based on water chemistry. *Aquatic Ecosystem Health and Management*, **1**, 183-197.

De Klerk, H.M; Wilson, A.M and Steenkamp, K. 2011. Evaluation of satellite-derived burned area products for the fynbos, a Mediterranean shrubland. *International Journal of Wildland Fire*, **21** (1), 36-47.

Deacon, H.J. 1979. Palaeoecology. In: Day, J., Siegfried, W.R., Louw, G.N and Jarman, M.L (Ed.) *Fynbos ecology: a preliminary synthesis*, Cooperative Scientific Programmes, CSIR, 58-69.

Deacon, H.J. 1983. The comparative evolution of Mediterranean-type ecosystems: a southern perspective. In: Kruger, F.J; Mitchell, D.T and Jarvis, J.U.M (Ed.) *Mediterranean-Type Ecosystems: The Role of Nutrients*, Ecological Studies 43, Springer-Verlag, Heidelberg, 3-40.

DeBano, L.F. 2000. The role of fire and soil heating on water repellency in wildland environments: a review. *Journal of Hydrology*, **231-232**, 195-206.

Deer, W.A; Howie, R.A and Zussman, J. 1992. *An Introduction to the Rock-forming Minerals*. Prentice Hall, Edinburgh, 695 pp.

Doerr, S.H; Shakesby, R.A and Walsh, R.P.D. 2000. Soil water repellence: its causes, characteristics and hydro-geomorphological significance. *Earth Science Reviews*, **51**, 33-65.

Drever, J.I. 1997. *The geochemistry of natural waters: surface and groundwater environments*, 3rd Edition, Prentice Hall, New Jersey, 436 pp.

Eckardt, F.D. 2001. The origin of sulphates: an example of sulphur isotopic applications. *Progress in Physical Geography*, **25** (4), 512-519.

Eckardt, F.D and Spiro, B. 1999. The origin of sulphur in gypsum and dissolved sulphate in the central Namib Desert, Namibia. *Sediment Geology*, **123** (3-4), 255-273.

Ellis, B.A; Verfaillie, J.R and Kummerow, J. 1983. Nutrient gain from wet and dry atmospheric deposition and rainfall acidity in Southern California Chaparral. *Oecologia*, **60** (1) 118-121.

Faloona, I. 2009. Sulfur processing in the marine atmospheric boundary layer: A review and critical assessment of modeling uncertainties. *Atmospheric Environment*, **43**, 2841-2854.

Fillion, N; Probst, A and Probst, J.L. 1999. Dissolved organic matter contribution to rain water, throughfall and soil solution chemistry. *Analusis*, **27** (5), 409-413.

Franco-Vizcafno, E and Sosa-Ramirez, J. 1997. Soil properties and nutrient relations in burned and unburned Mediterrenean-climate shrublands of Baja California, Mexico, *Acta Ecologica***, 18** (4), 503-517.

Fuggle, R.F and Ashton, E.R. 1979. Climate. In: Day, J., Siegfried, W.R., Louw, G.N and Jarman, M.L (Ed.) *Fynbos ecology: a preliminary synthesis*, Cooperative Scientific Programmes, CSIR, 7-15.

Galloway, J.N. 1978. The collection of precipitation for chemical analysis. *Tellus*, **30**, 71-82.

Gartley, K.L. 2009. Recommended soluble salts tests. IN: Recommended soil testing procedures for the Northeastern United States, 3rd edition. Northeastern regional publication no. 493, 70-75

Germs, W.J. 2004. *Geochemical investigation into the occurrence and fate of Nitrogen and Phosphorus in the lower Olifants River, Western Cape*. Master's thesis, Department of Geological Sciences, University of Cape Town, 85pp.

Gibbs, R.J. 1970. Mechanisms controlling world water chemistry, *Science*, **170** (3962), 1088-1090.

Goldblatt, P. 1978. An analysis of the Flora of Southern Africa: Its characteristics, relationships and origins. *Annals of the Missouri Botanical Garden*, **65** (2), 369-436.

Goldblatt, P. 1997. Floristic diversity in the Cape Flora of South Africa. *Biodiversity and Conservation*, **6,** 359-377.

Goldblatt, P and Manning, J.C. 2002. Plant diversity of the Cape region of Southern Africa. *Annals of the Missouri Botanical Garden*, **89** (2), 281-302.

Goldstein, H.L; Reynolds, R.L; Reheis, M.C; Yount, J.C and Neff, J.C. 2008. Compositional trends in aeolian dust along a transect across the southwestern United States. *Journal of Geophysical Research*, **113,** 1-15

González-Pérez, J.A; González-Vila, F.J, Gonzalo, A and Knicker, H. 2004. The effect of fire on soil organic matter – a review. *Environment International*, **30**, 855-870.

Gorham, E. 1958. The influence and importance of daily weather conditions in the supply of chloride, sulphate and other ions to fresh waters from atmospheric precipitation. *Philosophical Transactions of the Royal Society of London. Series B. Biological Sciences*, **241** (679), 147-178.

Graham, W.F and Duce, R.A. 1979. Atmospheric pathways of the phosphorus cycle. *Geochimica et Cosmochimica Acta*, **43**, 1195-1208.

Groves, R.H. 1983. Nutrient cycling in Australian heath and South African fynbos. In: Kruger, F.J; Mitchell, D.T and Jarvis, J.U.M (Ed.) *Mediterranean-Type Ecosystems: The Role of Nutrients*, Ecological Studies 43, Springer-Verlag, Heidelberg, 179-191.

Henderson, P and Henderson, G.M. 2009. *The Cambridge Handbook of Earth Science Data*. Cambridge University Press, New York, 277 pp.

Herppich, M; Herppich, W and von Willert, D.J. 2002. Leaf nitrogen content and photosynthetic activity in relation to soil nutrient availability in coastal and mountain fynbos plants (South Africa). *Basic and Applied Ecology*, **3**, 329-337.

Higgins, S.I; Turpie, J.K; Costanza, R; Cowling, R.M; Le Maitre, D.C; Marais, C and Midgley, G.F. 1997. Analysis: An ecological economic simulation model of mountain fynbos ecosystems: dynamics, valuation and management. *Ecological Economics*, **22**, 155-169.

Horne, D.J and McIntosh, J.C. 2000. Hydrophobic compounds in sands in New Zealand-extraction, characterization and proposed mechanisms for repellence expression. *Journal of Hydrology*, **231**, 35-46.

Howarth, R.W and Cole, J.J. 1985. Molybdenum availability, nitrogen limitation and phytoplankton growth in natural waters. *Science*, **229** (4714), 653-655.

Jackson, L; Conrad, J and Carstens, M. 2010. Cape Estuaries Programme: Situation assessment for the Zandvlei Estuary, *Coastal and Environmental Consulting*, 89 pp.

Johns, A. and Johns, M. (2001) *Kogelberg Biosphere Reserve: Heart of the Cape Flora*. Struik Publishers, Cape Town. 56pp.

Jongens-Roberts, S.M and Mitchell, D.T. 1986. The distribution of dry mass and phosphorus in an evergreen fynbos shrub species, *Leucospermum parile* (Salisb. Ex. J. Knight) Sweet *(Proteaceae)*, at different stages of development. *New Phytologist*, **103** (4) 669-683.

Jury, M. 1991. The weather of False Bay. *Transactions of the Royal Society of South Africa*, **4-5**, 401-417.

King, J.M and Day, J.A. 1979. Hydrology and hydrobiology. In: Day, J., Siegfried, W.R., Louw, G.N and Jarman, M.L (Ed.) *Fynbos ecology: a preliminary synthesis*, Cooperative Scientific Programmes, CSIR, 27-42.

Klausmeyer, K.R and Shaw, M.R. 2009. Climate change, habitat loss, protected areas and the climate adaptation potential of species in Mediterranean ecosystems worldwide. *Mediterranean Climate Change*, **4** (7), 1-9.

Kohfeld, K.E and Harrison, S.P. 2001. DIRTMAP: The geological record of dust. *Earth Science Reviews*, **54**, 81-114.

Kounov, A; Niedermann, S; de Wit, M.J; Viola, G; Andreoli, M and Erzinger, J. 2007. Present denudation rates at selected sections of the South African escarpment and the elevated continental interior based on cosmogenic ^{3}He and ^{21}Ne. *South African Journal of Geology*, **110** (2-3), 235-248.

Kruger, F.J. 1979a. Fire. In: Day, J., Siegfried, W.R., Louw, G.N and Jarman, M.L (Ed.) *Fynbos ecology: a preliminary synthesis*, Cooperative Scientific Programmes, CSIR, 43-57.

Kruger, F.J. 1979b. Plant ecology. In: Day, J., Siegfried, W.R., Louw, G.N and Jarman, M.L (Ed.) *Fynbos ecology: a preliminary synthesis*, Cooperative Scientific Programmes, CSIR, 88-126.

Kruger, F.J. 1983. Plant community diversity and dynamics in relation to fire. In: Kruger, F.J; Mitchell, D.T and Jarvis, J.U.M (Ed.) *Mediterranean-Type Ecosystems: The Role of Nutrients*, Ecological Studies 43, Springer-Verlag, Heidelberg, 446-472.

Kwint, R.L.J and Kramer, K.J.M. 1996. The annual cycle of the production and fate of DMS and DMSP in a marine coastal system. *Marine Ecology Progress Series*, **134,** 217-224.

Lambrechts, J.J.N. 1979. Geology, geomorphology and soils. In: Day, J., Siegfried, W.R., Louw, G.N and Jarman, M.L (Ed.) *Fynbos ecology: a preliminary synthesis*, Cooperative Scientific Programmes, CSIR, 16-26.

Lamont, B.B. 1982. Mechanisms for enhancing nutrient uptake in plants, with particular reference to Mediterranean South Africa and Western Australia. *Botanical Review*, **48** (3), 597-689.

Lamont, B.B. 1983. Strategies for maximizing nutrient uptake in two Mediterranean ecosystems of low nutrient status. In: Kruger, F.J; Mitchell, D.T and Jarvis, J.U.M (Ed.) *Mediterranean-Type Ecosystems: The Role of Nutrients*, Ecological Studies 43, Springer-Verlag, Heidelberg, 246-273.

Lana, A; Bell, T.G; Simó, R; Vallina, S.M; Ballabrera-Poy, J; Kettle, A.J; Dachs, J; Bopp, L; Saltzman, E.S; Stefels, J; Johnson, J.E and Liss, P.S. 2011. An updated climatology of surface dimethylsulfide concentrations and emission fluxes in the global ocean. *Global Biogeochemical* Cycles, **25**, 1-17.

Le Maitre, D.C. 1992. The relative advantages of seeding and sprouting in fire-prone environments: a comparison of life histories of *Protea neriifolia* and *Protea nitida*. In: van Wilgen, B.W; Richardson, D.M; Kruger, F.J and van Hersbergen, H.J (Ed.) *Fire in South African Mountain Fynbos: Ecosystem, Community and Species Response at Swartboskloof*, Springer-Verlag, 123-144.

Le Maitre, D.C and Brown, P.J. 1992. Life cycles and fire-stimulating flowering in geophytes. In: van Wilgen, B.W; Richardson, D.M; Kruger, F.J and van Hensbergen, H.J (Ed.) *Fire in South African Mountain Fynbos: Ecosystem, Community and Species Response at Swartboskloof*, Springer-Verlag, 145-160.

Linder, H.P. 1991. Environmental correlates of patterns of species richness in the South-Western Cape Province of South Africa. *Journal of Biogeography*, **18** (5), 509-518.

Linder, H.P. 2001. Plant diversity and endemism in sub-Saharan tropical Africa. *Journal of Biogeography*, **28**, 169-182.

Linder, H.P and Hardy, C.R. 2004. Evolution of the Species-rich Cape Flora. *Philosophical Transactions: Biological Sciences*, **359** (1450), 1623-1632.

Lindley, A.J; Bosch, J.M and van Wyk, D.B. 1988. Changes in water yield after fire in fynbos catchments. *Water SA*, **14** (1), 7-12.

Liodakis, S; Katsigiannis, G and Kakali, G. 2005. Ash properties of some dominant Greek forest species. *Thermochimica Acta*, **437**, 158-167.

Louw, G.N. 1979. Conclusions and recommendations. In: Day, J., Siegfried, W.R., Louw, G.N and Jarman, M.L (Ed.) *Fynbos ecology: a preliminary synthesis*, Cooperative Scientific Programmes, CSIR, 158-162.

Lovett, G.M. 1994. Atmospheric deposition of nutrients and pollutants in North America: An ecological perspective. *Ecological Applications*, **4** (4), 629-650.

Manders, P.T. 1990. Fire and other variables as determinants of forest / fynbos boundaries in the Cape Province. *Journal of Vegetation Science*, **1**, 483-490.

Manders, P.T; Richardson, D.M and Masson, P.H. 1992. Is fynbos a stage in succession to forest? Analysis of the perceived ecological distinction between two communities. In: van Wilgen, B.W; Richardson, D.M; Kruger, F.J and van Hensbergen, H.J (Ed.) *Fire in South African Mountain Fynbos: Ecosystem, Community and Species Response at Swartboskloof*, Springer-Verlag, 81-107.

Manry, D.E and Knight, R.S. 1986. Lightning density and burning frequency in South African vegetation. *Vegetatio*, **66** (2), 67-76.

Marino, R; Howarth, R.W; Chan, F; Cole, J.J and Likens, G.E. 2003. Sulfate inhibition of molybdenum-dependent nitrogen fixation by planktonic cyanobacteria under seawater conditions: a non-reversible effect. *Hydrobiologia*, **500**, 277-293.

Midgley, J.J; Kruger, L.M and Skelton, R. 2011. How do fires kill plants? The hydraulic death hypothesis and Cape Proteaceae "fire-resisters". *South African Journal of Botany*, **77** (2), 381-386.

Midgley, J.J and Rebelo, A.G. 2008. Life-history evolution as an explanation for the absence of the tree life-form in Cape fynbos. *South African Journal of Science*, **104**, 89-90.

Mihajlidi-Zelić, A; Deršek-Timotić, I; Relić, D; Popović, A and Đorđević, D. 2006. Contribution of marine and continental aerosols to the content of major ions in the precipitation of the central Mediterranean. *Science of the Total Environment*, **370,** 441-451.

Miller, P.C. 1983. Canopy structure of Mediterrenean-type shrubs in relation to heat and moisture. In: Kruger, F.J; Mitchell, D.T and Jarvis, J.U.M (Ed.) *Mediterranean-Type Ecosystems: The Role of Nutrients*, Ecological Studies 43, Springer-Verlag, Heidelberg, 133-166.

Mitchell, D.T; Coley, P.G.F; Webb, S and Alsopp, N. 1986. Litterfall and decomposition processes in the coastal fynbos vegetation, south-western Cape, South Africa. *Journal of Ecology*, **74** (4), 977-993.

Moll, E.J; Campbell, B.M; Cowling, R.M; Bossi, L; Jarman, M.L and Boucher, C. 1984. A description of major vegetation categories in and adjacent to the Fynbos biome. *South African National Scientific Programmes Report no. 83*, 1-35.

Mooney, H.A. 1983. Carbon-gaining capacity and allocation patterns of Mediterranean-climate plants. In: Kruger, F.J; Mitchell, D.T and Jarvis, J.U.M (Ed.) *Mediterranean-Type Ecosystems: The Role of Nutrients*, Ecological Studies 43, Springer-Verlag, Heidelberg, 103-119.

Mouillot, F, Rambant, S and Joffre, R. 2002. Simulating climate change impacts on fire frequency and vegetation dynamics in a Mediterranean-type ecosystem. *Global Change Biology*, **8**, 423-437.

Mucina, L and Rutherford, M.C. 2006. *The vegetation of South Africa, Lesotho and Swaziland*. South African National Biodiversity Institute, 807pp.

Murphy, M.D. 1980. Essential micronutrients III: Sulphur. In: Davies, B.E (Ed.) *Applied Soil Trace Elements*, John Wiley and Sons, Chichester, New York, Brisbane, Toronto, 235-258.

Neary, D.G; Klopatek, C.C; De Bano, F and Ffolliott, P.F. 1999. Fire effects on belowground sustainability: a review and synthesis. *Forest Ecology and Management*, **122**, 51-71.

Neff, J.C; Reynolds, R.L; Sanford, R.L; Fernandez, D and Lamothe, P. 2006. Controls of bedrock geochemistry on soil and plant nutrients in Southeastern Utah. *Ecosystems*, **9,** 879-893.

Ochoa-Hueso, R; Allen, E.B; Branquinho, C; Cruz, C; Dias, T; Fenn, M.E; Manrique, E; Pérez-Corona, M.E; Sheppard, L.J and Stock, W.D. 2011. Nitrogen deposition effects on Mediterranean-type ecosystems: An ecological assessment. *Environmental Pollution*, 1-15.

O'Dowd, C.D; Smith, M.H; Consterdine, I.E and Lowe, J.A. 1997. Marine aerosol, sea-salt, and the marine sulphur cycle: A short review. *Atmospheric Environment*, **31** (1), 73-80.

Oechel, W.C and Hastings, S.J. 1983. The effects of fire on photosynthesis in chaparral resprouts. In: Kruger, F.J; Mitchell, D.T and Jarvis, J.U.M (Ed.) *Mediterranean-Type Ecosystems: The Role of Nutrients*, Ecological Studies 43, Springer-Verlag, Heidelberg, 274-285.

Orshan, G. 1983. Approaches to the definition of Mediterranean growth forms. In: Kruger, F.J; Mitchell, D.T and Jarvis, J.U.M (Ed.) *Mediterranean-Type Ecosystems: The Role of Nutrients*, Ecological Studies 43, Springer-Verlag, Heidelberg, 86-102.

Paterson-Jones, C and Manning, J. 2007. Ecoguide: *Fynbos*. Briza Publications, Pretoria. 184pp.

Pausas, J.G; Carbó, E; Caturla, R; Gil, J.M and Vallejo, R. 1999. Post-fire regeneration patterns in the eastern Iberian Peninsula. *Acta Oecologica*, **20** (5), 499-508.

Pérez-Cabello, F; Echverría, M.T; Ibarra, P and de la Riva, J. 2009. Effects of fire on vegetation, soil and hydrogeomorphological behaviour in Mediterranean ecosystems. In: Chuvieco, E (Ed.) *Earth Observation of Wildland Fires in Mediterranean Ecosystems*, Springer-Verlag, Berlin Heidelberg, 111-129.

Piketh, S.J; Swap, R.J; Maenhaut, W; Annegarn, H.J and Formenti, P. 2002. Chemical evidence of long-range atmospheric transport over Southern Africa. *Journal of Geophysical Research*, **107,** 1-13.

Pryor, S.C and Barthelmie, R.J. 2000. Particle dry deposition to water surfaces: Processes and consequences. *Marine Pollution Bulletin*, **41**, 220-231.

Rambal, S. 2001. Hierarchy and productivity of Mediterranean-type ecosystems. In: Roy, J; Saugier, B and Mooney, H.A (Ed.) *Terrestrial Global Productivity*. Academic Press, London, 315-344.

Read, D.J and Mitchell, D.T. 1983. Decomposition and mineralization processes in Mediterranean-type ecosystems and in heathlands of similar structure. In: Kruger, F.J; Mitchell, D.T and Jarvis, J.U.M (Ed.) *Mediterranean-Type Ecosystems: The Role of Nutrients*, Ecological Studies 43, Springer-Verlag, Heidelberg, 208-232.

Reheis, M.C; Budahn, J.R and Lamothe, P.J. 2002. Geochemical evidence for diversity of dust sources in the southwestern United States. *Geochimica et Cosmochimica Acta*, **66** (9) 1569-1587.

Reynolds, R.L; Neff, J; Reheis, M and Lamothe, P. 2006a. Atmospheric dust in modern soil on aeolian sandstone, Colorado Plateau (USA): Variation with landscape position and contribution to potential plant nutrients. *Geoderma*, **130,** 108-123.

Reynolds, R.L; Reheis, M.C; Neff, J.C; Goldstein and Yount, J.C. 2006b. Late Quaternary eolian dust in surficial deposits of a Colorado Plateau grassland: Controls on distribution and ecological effects. *Catena*, **66,** 251-266

Reynolds, R.L; Reheis, M.C; Yount, J. and Lamonthe, P. 2006c. Composition of aeolian dust in natural traps on isolated surfaces of the central Mojave Desert (USA) – insights to mixing, sources and nutrient inputs. *Journal of Arid Environment*, **66,** 42-61.

Richardson, D.M and van Wilgen, B.W. 1992. Ecosystem, community and species response of fire in mountain fynbos: conclusions from the Swartboskloof experiment. In: van Wilgen, B.W; Richardson, D.M; Kruger, F.J and van Hensbergen, H.J (Ed.) *Fire in South African Mountain Fynbos: Ecosystem, Community and Species Response at Swartboskloof*, Springer-Verlag, 273-284.

Richardson, J.E; Weitz, F.M; Fay, M.F; Cronk, Q.C; Linder, H.P; Reeves, G and Chase, M.W. 2001. Rapid and recent origin of species richness in the Cape flora of South Africa. *Nature*, **412**, 181-183.

Rouget, M; Richardson, D.M and Cowling, R.M. 2003. The current configuration of protected areas in the Cape Floristic Region, South Africa – reservation bias and representation of biodiversity patterns and processes. *Biological Conservation*, **112**, 129-145.

Rouget, M; Richardson, D.M; Cowling, R.M; Lloyd, J.W and Lombard, A.M. 2003. Current patterns of habitat transformation and future threats to biodiversity in terrestrial ecosystems of the Cape Floristic Region, South Africa. *Biological Conservation*, **112**, 63-85.

Rundel, P.W. 1983. Impact of fire on nutrient cycles in Mediterranean-type ecosystems with reference to chaparral. In: Kruger, F.J; Mitchell, D.T and Jarvis, J.U.M (Ed.) *Mediterranean-Type Ecosystems: The Role of Nutrients*, Ecological Studies 43, Springer-Verlag, Heidelberg, 192-207.

Russell-Smith, J; Ryan, P.G and Cheal, D.C. 2002. Fire regimes and the conservation of sandstone heath in monsoonal northern Australia: frequency, interval, patchiness. *Biological Conservation*, **104**, 91-106.

Rutherford, M.C; Powrie, L.W; Husted, L.B and Turner, R.C. 2011. Early post-fire plant succession in Peninsula Sandstone Fynbos: The first three years after disturbance.*South African Journal of Botany*, **77** (3), 665-674.

Scott, D.F. 1993. The hydrological effects of fire in South African mountain catchments. *Journal of Hydrology*, **150**, 409-432.

Scott, D.F and van Wyk D.B. 1992. The effects of fire on soil water repellency, catchment sediment yields and streamflow. In: van Wilgen, B.W; Richardson, D.M; Kruger, F.J and van Hensbergen, H.J (Ed.) *Fire in South African Mountain Fynbos: Ecosystem, Community and Species Response at Swartboskloof*, Springer-Verlag, 216-239.

Siegfried, W.R. 1979. Climate. In: Day, J., Siegfried, W.R., Louw, G.N and Jarman, M.L (Ed.) *Fynbos ecology: a preliminary synthesis*, Cooperative Scientific Programmes, CSIR, 127-132.

Siegfried, W.R and Crowe, T.M, 1983. Distribution and species diversity of birds and plants in fynbos vegetation of Mediterranean-climate zone. In: Kruger, F.J; Mitchell, D.T and Jarvis, J.U.M (Ed.) *Mediterranean-Type Ecosystems: The Role of Nutrients*, Ecological Studies 43, Springer-Verlag, Heidelberg, 403-416.

Slabbert, E; Kongor, R.Y; Esler, K.J and Jacobs, K. 2010. Microbial diversity and community structure in fynbos soil. *Molecular Ecology*, **19**, 1031-1041.

Smit, A.K. 2003. G*eochemistry of a pristine fynbos ecosystem in the Harold Porter National Botanical Gardens and Kogelberg Biosphere Reserve.* Master's thesis, Department of Geological Sciences, University of Cape Town, 100pp.

Smith, R.E; van Wilgen, B.W; Forsyth, G.G and Richardson, D.M. 1992. Coexistence of seeders and sprouters in a fire-prone environment: the role of ecophysiology and soil moisture. In: van Wilgen, B.W; Richardson, D.M; Kruger, F.J and van Hensbergen, H.J (Ed.) *Fire in South African Mountain Fynbos: Ecosystem, Community and Species Response at Swartboskloof*, Springer-Verlag, 108-122.

Soderberg, K. 2003. *Geochemistry of the fynbos ecosystem in a Table Mountain Group sub-catchment of the Olifants River, Western Cape, South Africa.* Master's thesis, Department of Geological Sciences, University of Cape Town, 147pp.

Soderberg, K and Compton, J.S. 2007. Dust as a nutrient source for Fynbos ecosystems, South Africa. *Ecosystems*, **10,** 550-561.

Söhnge, A.P.G. 1984. Glacial diamictite in the Peninsula Formation near Cape Hangklip. *Transactions of the Geological Society of South Africa*, **87,** 199-210.

Specht, R.L and Moll, E.J. 1983. Mediterranean-type heathlands and sclerophyllous shrublands of the world: An overview. In: Kruger, F.J; Mitchell, D.T and Jarvis, J.U.M (Ed.) *Mediterranean-Type Ecosystems: The Role of Nutrients*, Ecological Studies 43, Springer-Verlag, Heidelberg, 41-65.

Specht, R.L; Moll, E.J; Pressinger, F and Sommerville, J. 1983. Moisture regime and nutrient control of seasonal growth in Mediterranean ecosystems. In: Kruger, F.J; Mitchell, D.T and Jarvis, J.U.M (Ed.) *Mediterranean-Type Ecosystems: The Role of Nutrients*, Ecological Studies 43, Springer-Verlag, Heidelberg, 120-132.

Stock, W.D and Lewis, O.A.M. 1986. Soil nitrogen and the role of fire as a mineralizing agent in a South African coastal Fynbos ecosystem. *Journal of Ecology*, **74** (2), 317-328.

Stumm, W. 1981. *Aquatic chemistry*, 2nd edition. Wiley Interscience, New York, 780pp.

Swap, R; Garstang, M; Macko, S.A; Tyson, P.D; Maenhaut, W; Artaxo, P; Kållberg, P and Talbot, R. 1996. The long-range transport of southern African aerosols to the tropical South Atlantic. *Journal of Geophysical Research,* **101,** 23 777-23 791.

Taylor, H.C. 1979. Phytogeography. In: Day, J., Siegfried, W.R., Louw, G.N and Jarman, M.L (Ed.) *Fynbos ecology: a preliminary synthesis*, Cooperative Scientific Programmes, CSIR, 70-81.

Taylor, J.E; Lee, S and Crous, P.W. 2001. Biodiversity in the Cape Floral Kingdom: fungi occurring on *Proteaceae*. *Mycological Research*, **105** (12), 1480-1484.

Trabaud, L. 1983. The effects of different fire regimes on soil nutrient levels in *Quercus coccifera* Garrigue. In: Kruger, F.J; Mitchell, D.T and Jarvis, J.U.M (Ed.) *Mediterranean-Type Ecosystems: The Role of Nutrients*, Ecological Studies 43, Springer-Verlag, Heidelberg, 233-245.

Tyson, P; Odada, E; Schulze, R and Vogel, C. 2002. Regional-global change linkages: Southern Africa. In: Tyson, P; Fuchs, R; Fu, C; Lebel, L; Mitra, A.P; Odada, E; Perry, J; Steffen, W and Virja, H (Ed.) *Global-Regional Linkages in the Earth System*, Springer, Berlin, 3-73.

Van der Niet, T and Johnson, S.D. 2009. Patterns of plant speciation in the Cape floristic region. *Molecular Phylogenetics and Evolution*, **51**, 85-93.

Van Reenen, C.A; Visser, G.J and Loos, M.A. 1992. Soil microorganisms and activities in relation to season, soil factors and fire. In: van Wilgen, B.W; Richardson, D.M; Kruger, F.J and van Hensbergen, H.J (Ed.) *Fire in South African Mountain Fynbos: Ecosystem, Community and Species Response at Swartboskloof*, Springer-Verlag, 258-272.

Van Wilgen, B.W and Forsyth, G.G. 1992. Regeneration strategies in fynbos plants and their influence on the stability of community boundaries after fire. In: van Wilgen, B.W; Richardson, D.M; Kruger, F.J and van Hensbergen, H.J (Ed.) *Fire in South African Mountain Fynbos: Ecosystem, Community and Species Response at Swartboskloof*, Springer-Verlag, 54-80.

Van Wilgen, B.W and McDonald, D.J. 1992. The Swartboskloof experimental site. In: van Wilgen, B.W; Richardson, D.M; Kruger, F.J and van Hensbergen, H.J (Ed.) *Fire in South African Mountain Fynbos: Ecosystem, Community and Species Response at Swartboskloof*, Springer-Verlag, 1-20.

Van Wilgen, B.W and van Hensbergen, H.J. 1992. Fuel properties of vegetation in Swartboskloof. In: van Wilgen, B.W; Richardson, D.M; Kruger, F.J and van Hensbergen, H.J (Ed.) *Fire in South African Mountain Fynbos: Ecosystem, Community and Species Response at Swartboskloof*, Springer-Verlag, 37-53.

Van Wilgen, B.W; le Maitre, D.C and Kruger, F.J. 1985. Fire behaviour in South African fynbos (macchia) vegetation and predictions from Rothermel's Fire Model. *Journal of Applied Ecology*, **22** (1), 207-216.

Van Wyk, D.B; Lesch, W and Stock, W.D. 1992. Fire and catchment chemical budgets. In: van Wilgen, B.W; Richardson, D.M; Kruger, F.J and van Hensbergen, H.J (Ed.) *Fire in South African Mountain Fynbos: Ecosystem, Community and Species Response at Swartboskloof*, Springer-Verlag, 240-257.

Versfeld, D.B; Richardson, D.M; van Wilgen, B.W; Chapman, R.A and Forsyth, G.G. 1992. The climate of Swartboskloof. In: van Wilgen, B.W; Richardson, D.M; Kruger, F.J and van Hensbergen, H.J (Ed.) *Fire in South African Mountain Fynbos: Ecosystem, Community and Species Response at Swartboskloof*, Springer-Verlag, 21-36.

Vitousek, P.M; Porder, S; Houlton, B.Z and Chadwick, O.A. 2010. Terrestrial phosphorus limitation: mechanisms, implications, and nitrogen-phosphorus interactions. *Ecological Applications*, **20** (1), 5-15.

Wessels, K.J; Prince, S.D; Malherbe, J; Small, J; Frost, P.E and Van Zyl, D. 2007. Can human-induced land degradation be distinguished from the effects of rainfall variability? *Journal of Arid Environments*, **68,** 271-297.

Westman, W.E. 1983. Plant community structure – spatial partitioning of resources. In: Kruger, F.J; Mitchell, D.T and Jarvis, J.U.M (Ed.) *Mediterranean-Type Ecosystems: The Role of Nutrients*, Ecological Studies 43, Springer-Verlag, Heidelberg, 417-445.

Wilson, D; Stock, W.D and Hedderson, T. 2009. Historical nitrogen content of bryophyte tissue as an indicator of increased nitrogen deposition in the Cape Metropolitan Area, South Africa. *Environmental Polluion*, **154** (3), 938-945.

Witkowski, E.T.F and Mitchell, D.T. 1987. Variations in soil phosphorus in the Fynbos Biome, South Africa. *Journal of Ecology*, **75** (4), 1159-1171.

Young, G.M; Minter, W.E.L and Theron, J.N. 2004. Geochemistry and palaeogeography of upper Ordovician glaciogenic sedimentary rocks in the Table Mountain Group, South Africa. *Palaeogeography, Palaeoclimatology, Palaeoecology*, **214** (4), 1146-1151.

Zhang, H; Schroder, J.L; Pittman, J.J; Wang, J.J and Payton, M.E. 2005. Soil salinity using saturated paste and 1:1 soil to water extracts. *Soil Science Society of America Journal*, **69,** 1146-1151.

Website Reference

[http://www.zandvleitrust.org.za/art-ZIMP%20abiotic-rainfall.html] accessed on 26 September 2011.

Appendix A: Rainfall data from HPNBG

Table A. 1 Rainfall data (in mm) from the office of the HPNBG. Gray shaded blocks indicate days outside of the sampling period. Black shaded blocks indicate days that do not exist.

	Jun	Jul	Aug	Sep	Oct	Nov	Dec	Jan	Feb	Mar	Apr	May	June
1													2
2					3.0		14.5						
3						5.5	17.5				1.0	11.0	
4						50.0	1.5						
5						5.5	3.0						
6		8.5		14.5		3.5						12.0	
7												0.7	
8	13.5		8.0		2.5			8.0				1.0	
9	9.0		16.0			23.0		16.0					
10	1.5	9.6	3.5			4.0		3.5					
11		41.0			20.0				4.5				
12		4.0			7.5	9.5							
13	12.5												
14	13.0	1.5											
15	29.0	19.5		15.5	10.0								
16	10.0			9.0									
17									6.5				
18									8.5				
19			13.0					13.0					
20													
21					13.0	3.5					5.0		
22	2.5		24.0		1.5	35.0	0.5	24.0					
23		3.0	7.5		8.0			7.5				6.5	
24		5.0	1.5				1.0	1.5				12.0	
25					6.5		1.3		2.5			6.5	
26		1.0	5.5			1.5		5.5			28.0		
27				3.5							11.0		
28						24.5					3.0		
29			2.0				3.0	2.0				10.0	
30	33.5				30.0							11.0	
31					0.5					13		40.5	

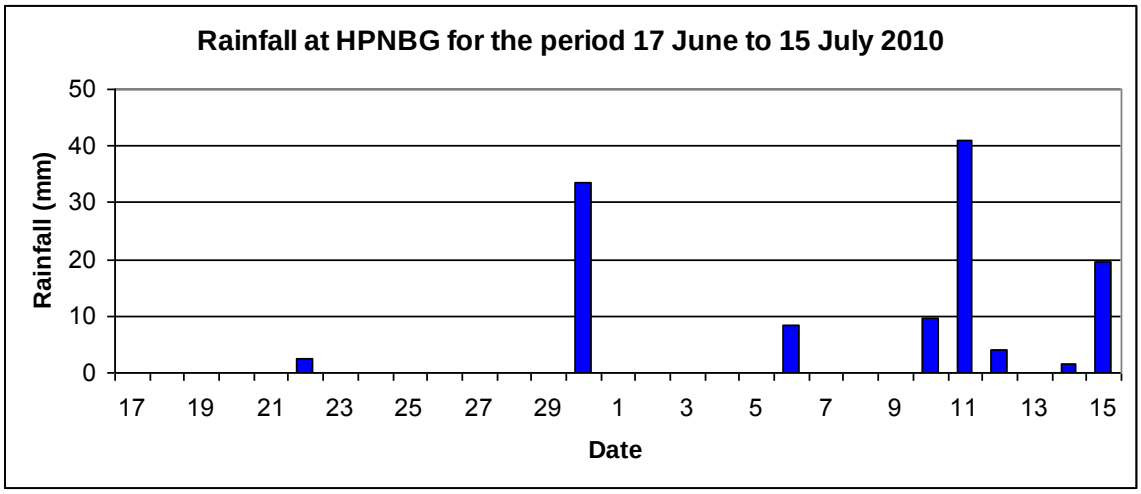

Figure A. 1. Rainfall for the period 17 June to 15 July 2010 as recorded by the office of the HPNBG.

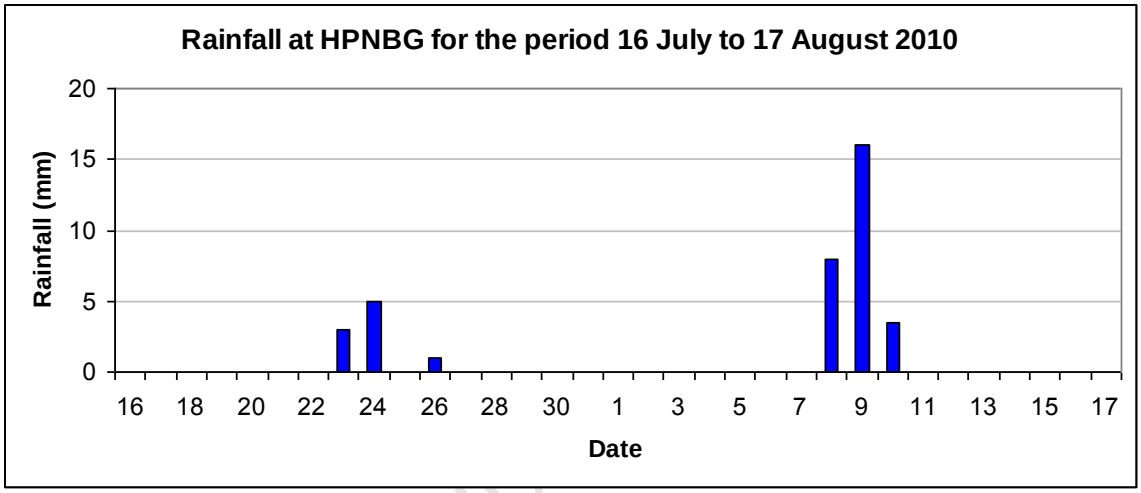

Figure A. 2. Rainfall for the period 16 July to 17 August 2010 as recorded by the office of the HPNBG.

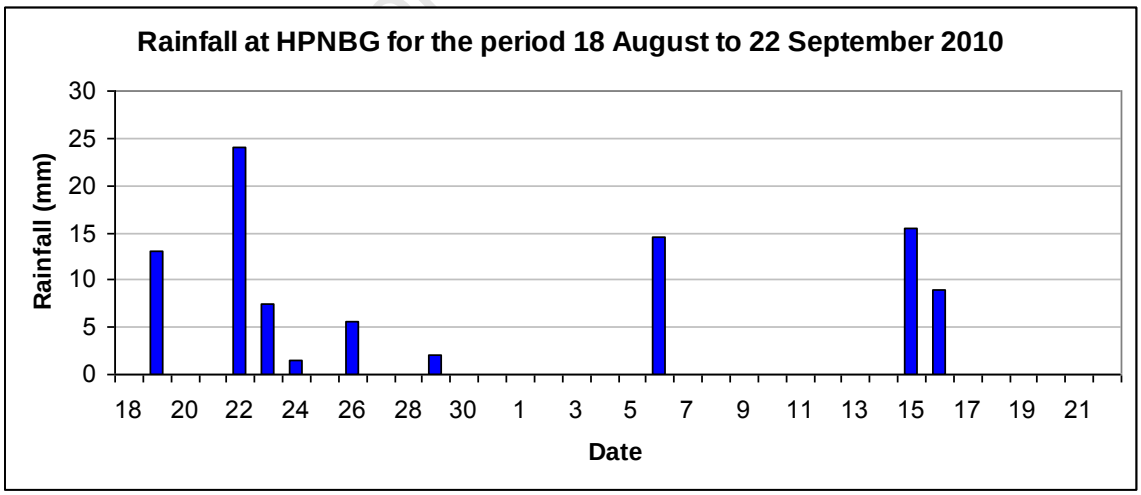

Figure A. 3. Rainfall for the period 18 August to 22 September 2010 as recorded by the office of the HPNBG.

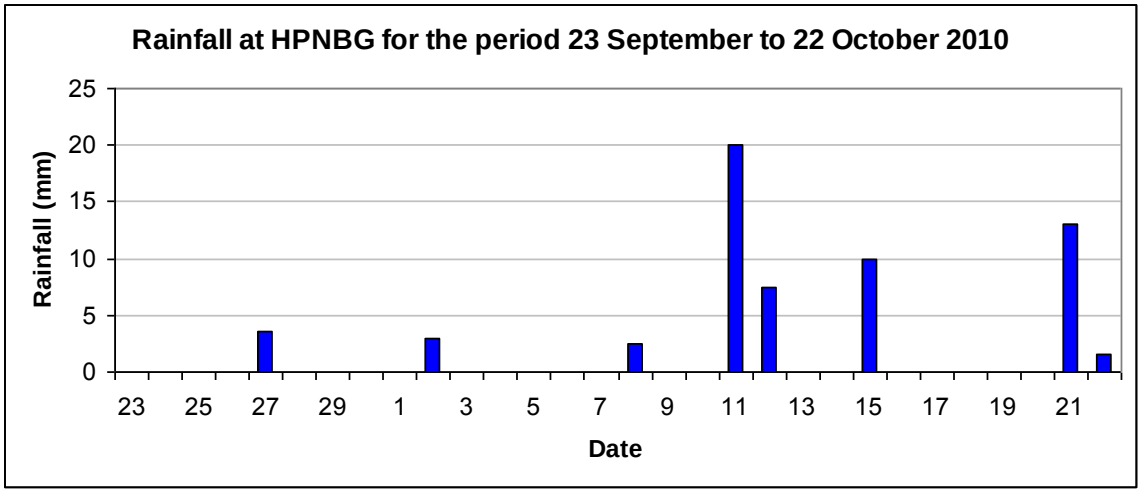

Figure A. 4. Rainfall for the period 23 September to 22 October 2010 as recorded by the office of the HPNBG.

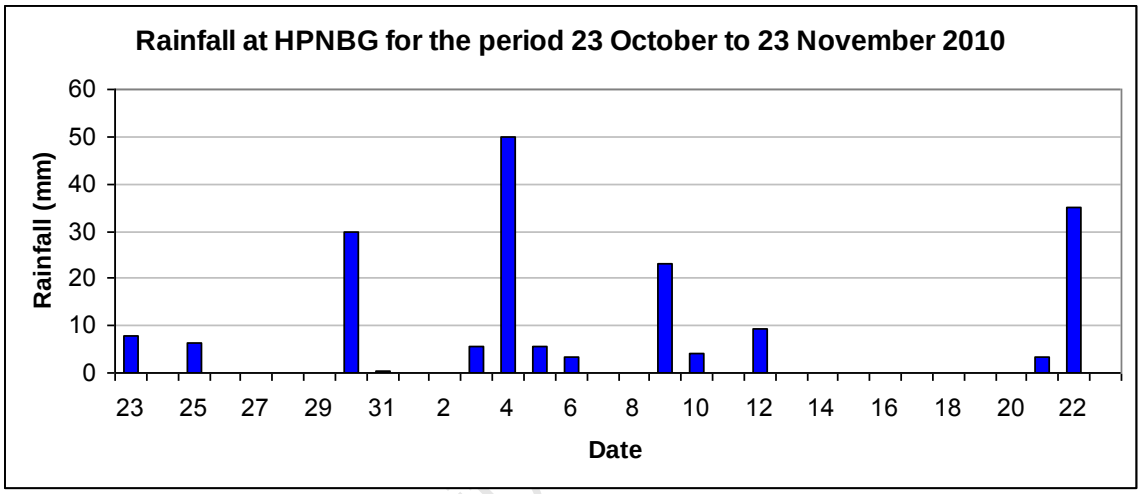

Figure A. 5. Rainfall for the period 23 October to 23 November 2010 as recorded by the office of the HPNBG.

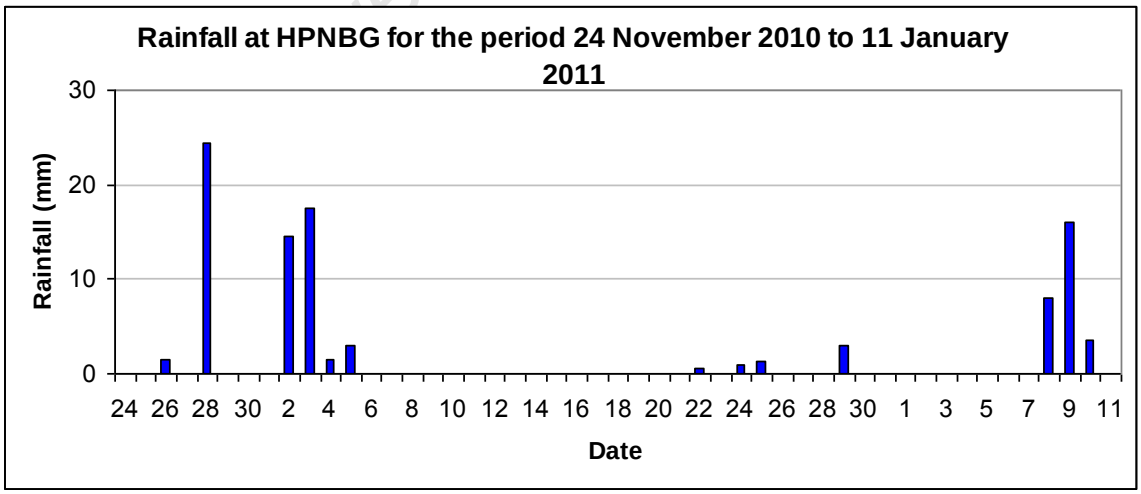

Figure A. 6. Rainfall for the period 24 November 2010 to 11 January 2011 as recorded by the office of the HPNBG.

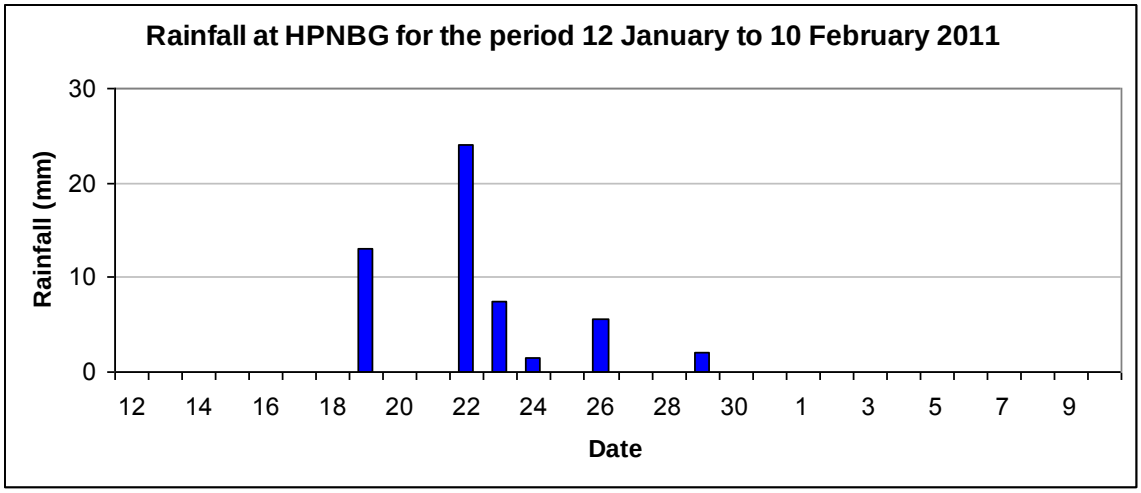

Figure A. 7. Rainfall for the period 12 January to 10 February 2011 as recorded by the office of the HPNBG.

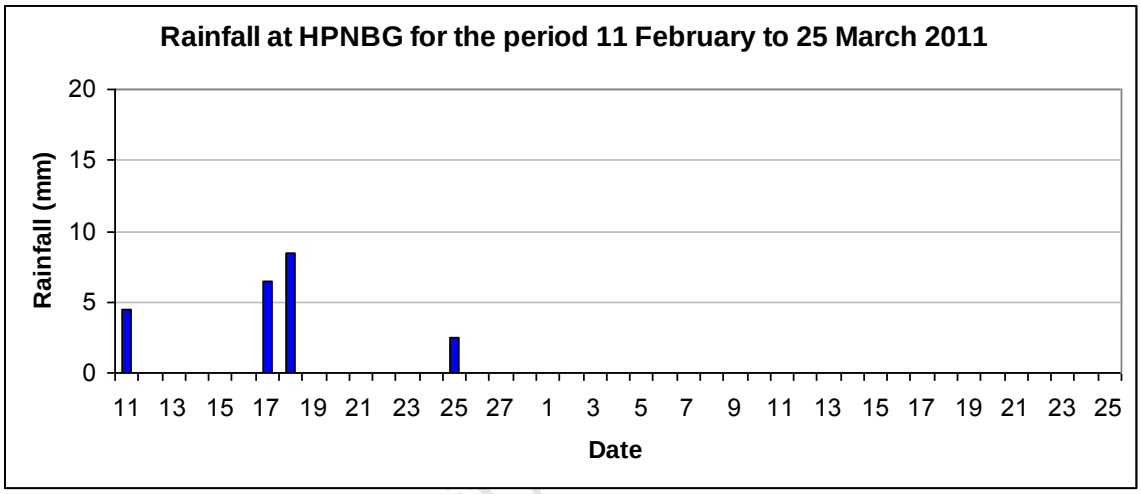

Figure A. 8. Rainfall for the period 11 February to 25 March 2011 as recorded by the office of the HPNBG.

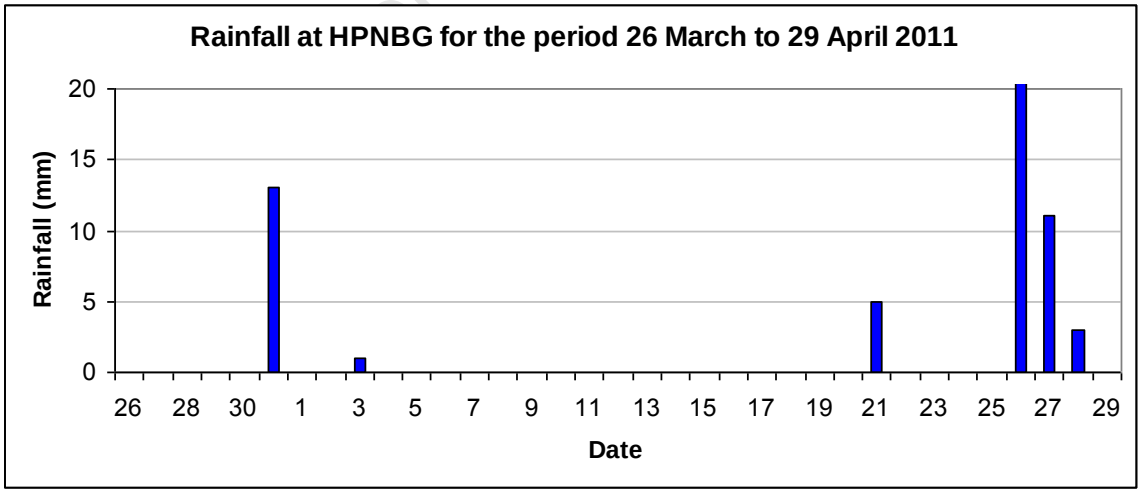

Figure A. 9. Rainfall for the period 26 March to 29 April 2011 as recorded by the office of the HPNBG.

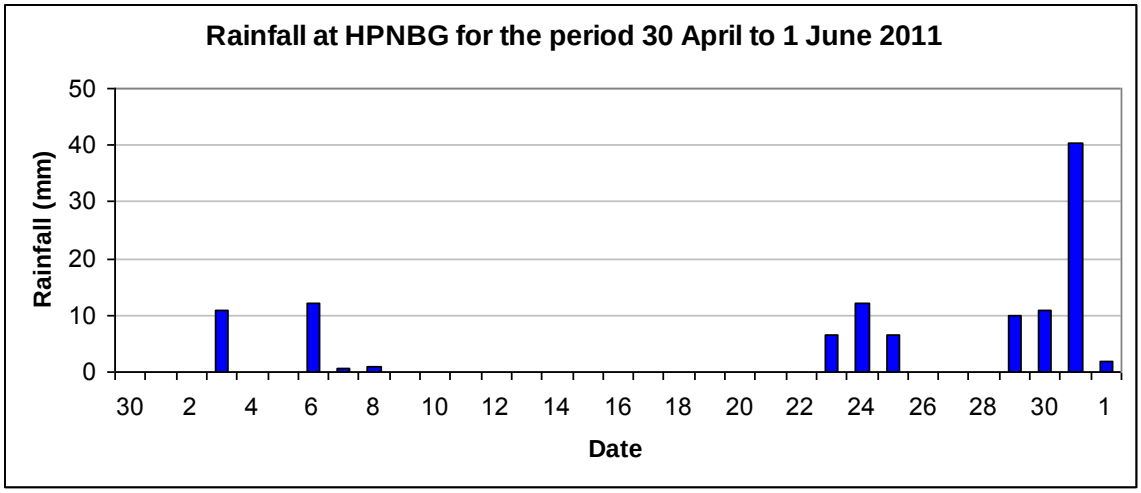

Figure A. 10. Rainfall for the period 30 April to 1 June 2011 as recorded by the office of the HPNBG.

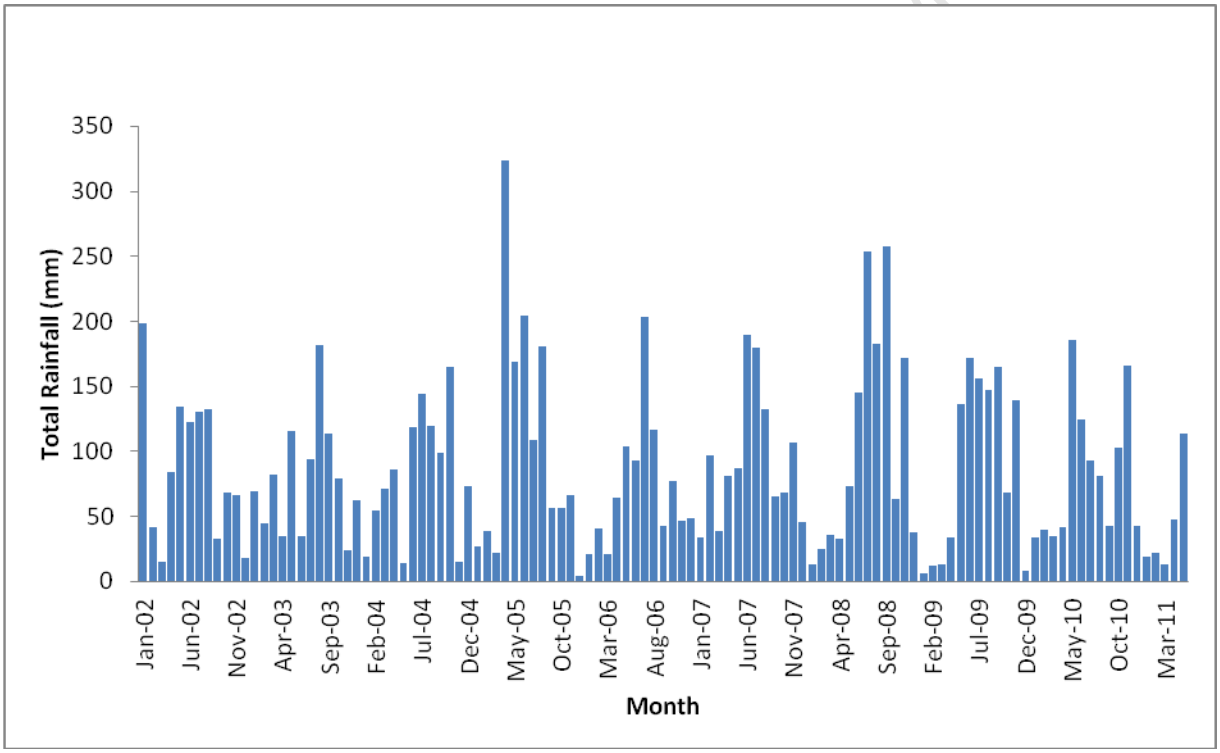

Figure A. 11 : Total rainfall as recorded by the offices of the HPNBG from January 2002 until May 2011.

Appendix B: XRD Results

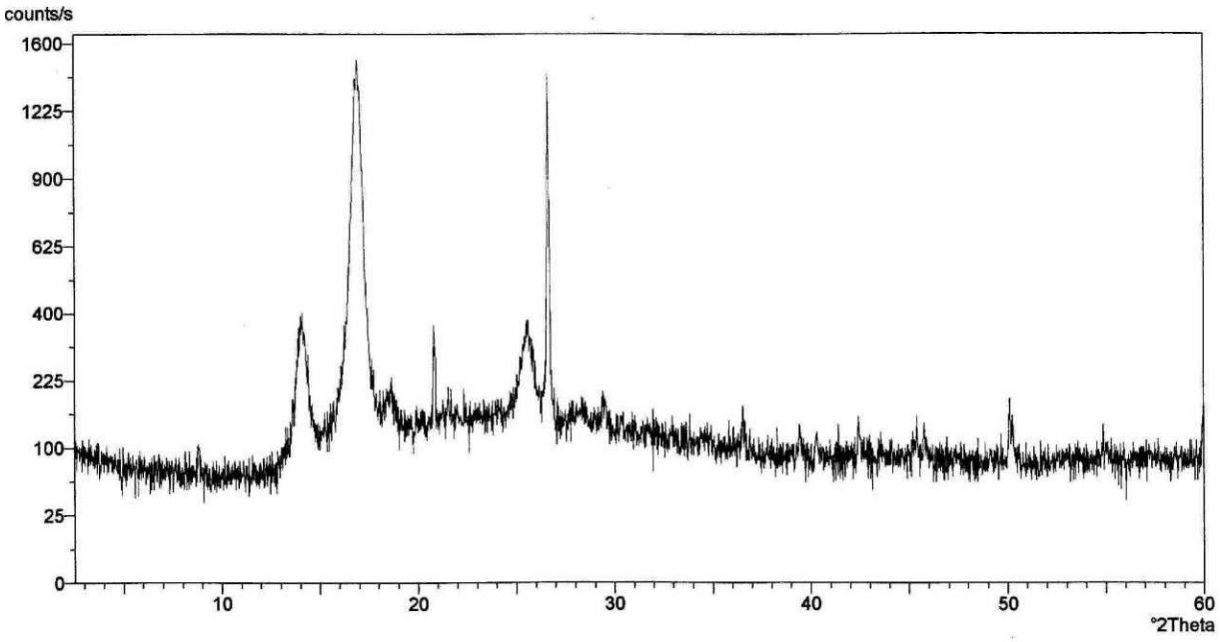

Figure B. 1. XRD profile of the dried suspension for the clay fraction (<2 μm) of the subsoil at site 1 in the HPNBG.

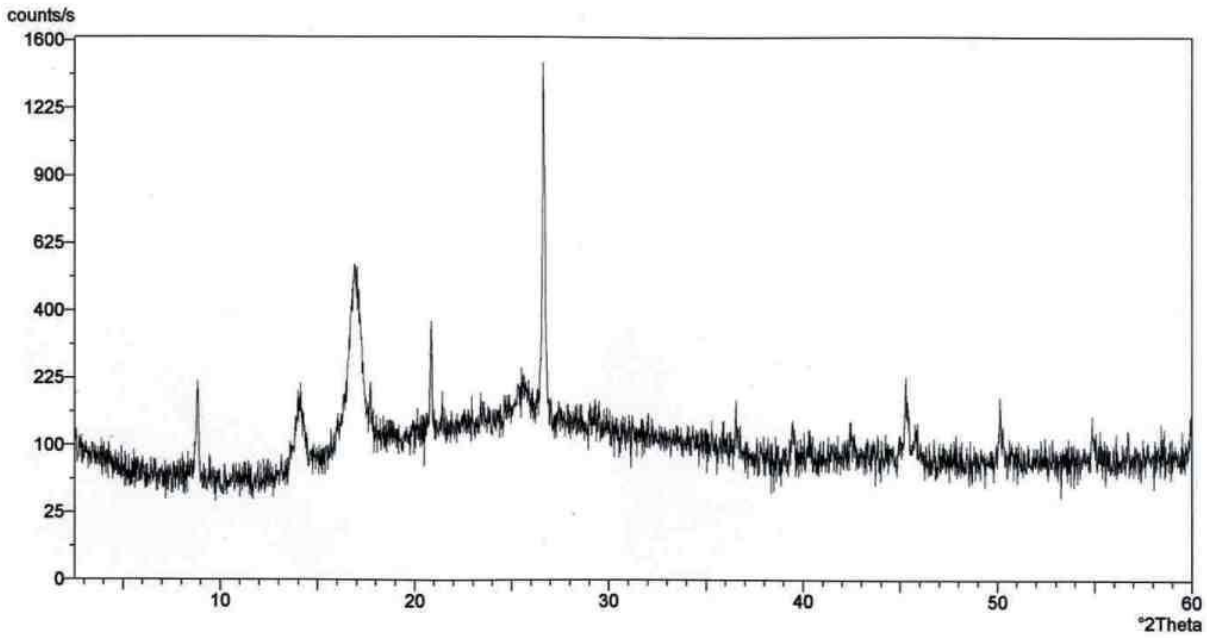

Figure B. 2. XRD profile of the dried suspension for the clay fraction (<2 μm) of the topsoil at site 2 in the HPNBG.

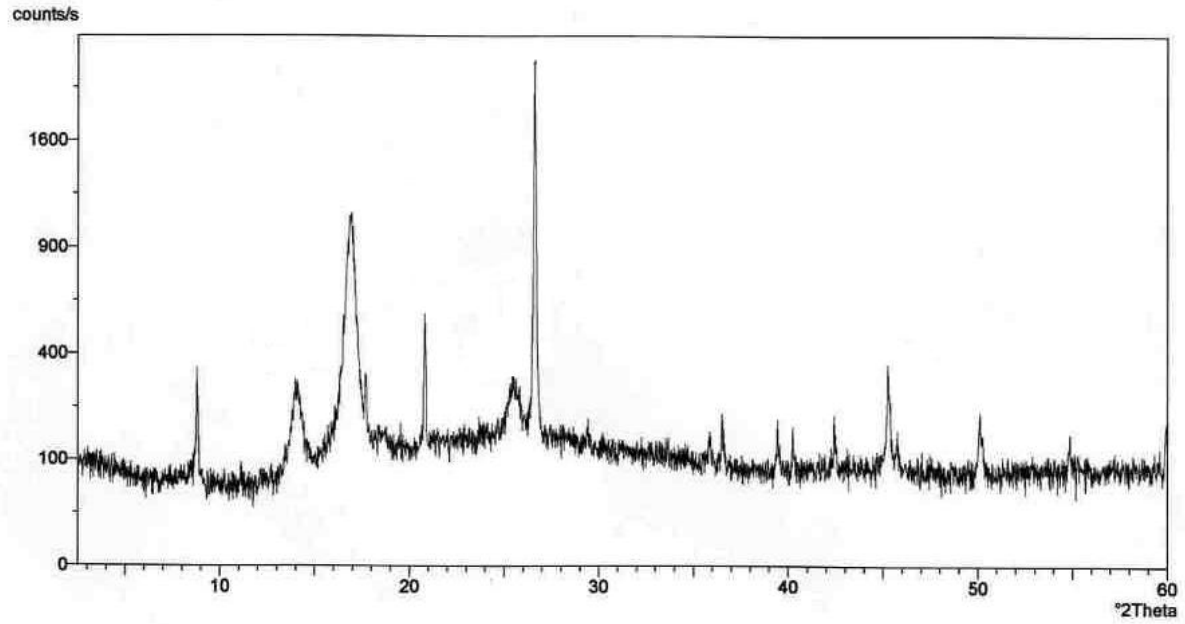

Figure B. 3. XRD profile of the dried suspension for the clay fraction (<2 μm) of the subsoil at site 2 in the HPNBG.

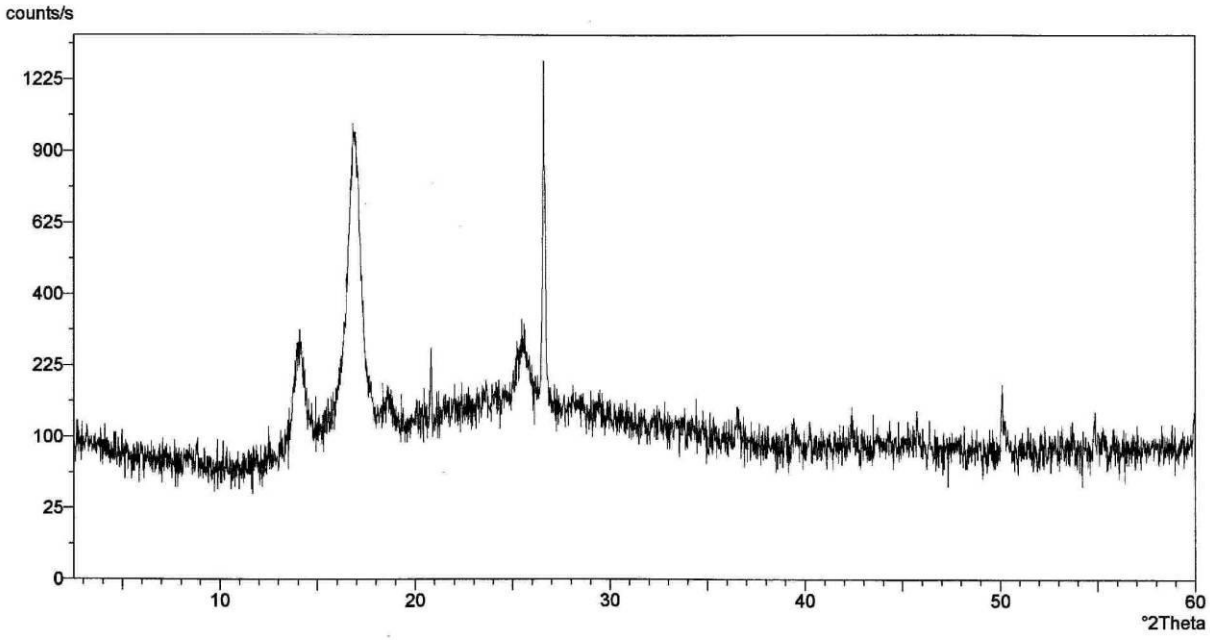

Figure B. 4. XRD profile of the dried suspension for the clay fraction (<2 μm) of the bulk soil at site 3 in the HPNBG.

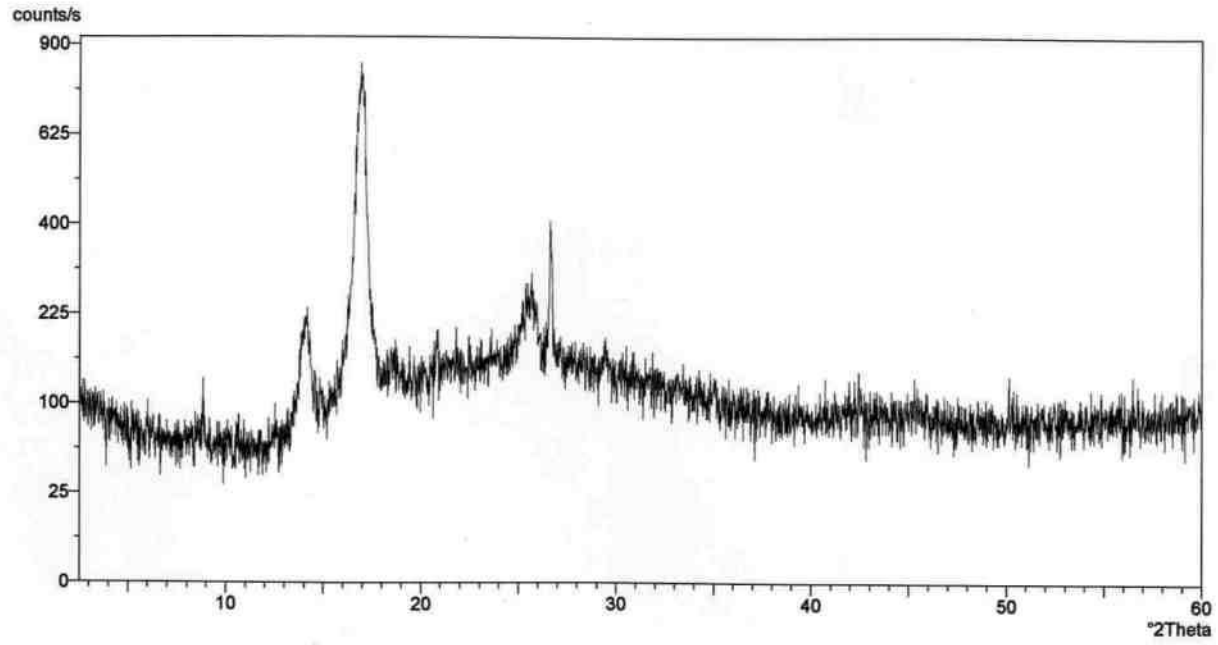

Figure B. 5. XRD profile of the dried suspension for the clay fraction (<2 μm) of the bulk soil at site 4 in the HPNBG.

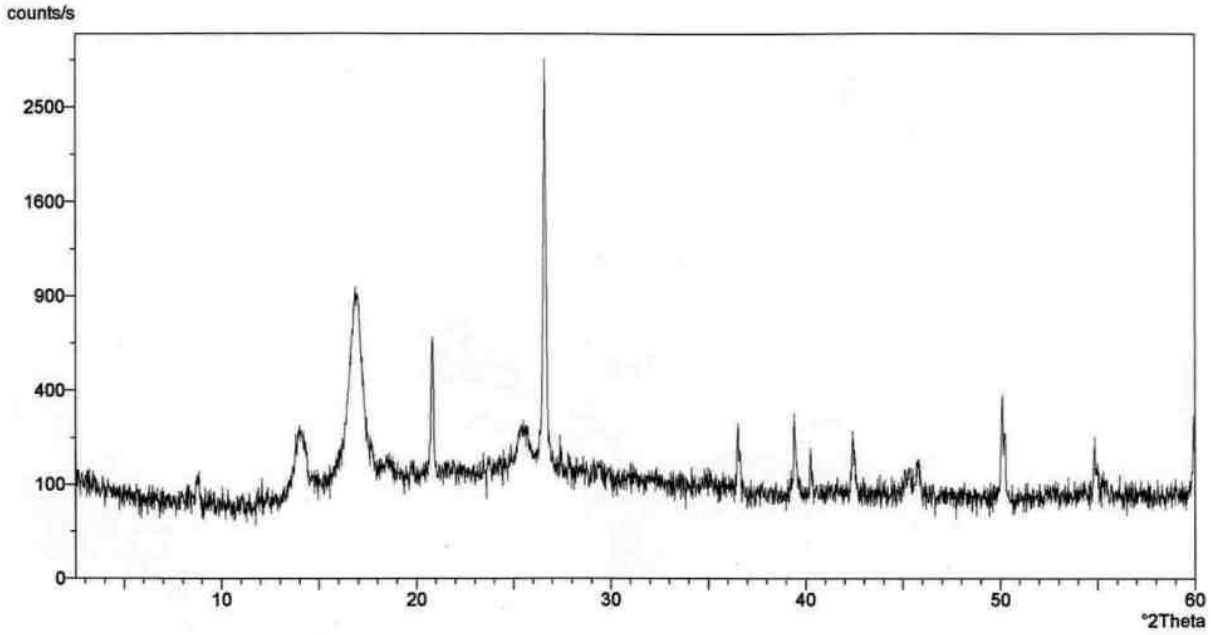

Figure B. 6. XRD profile of the dried suspension for the clay fraction (<2 μm) of the topsoil at site 5 in the KBR.

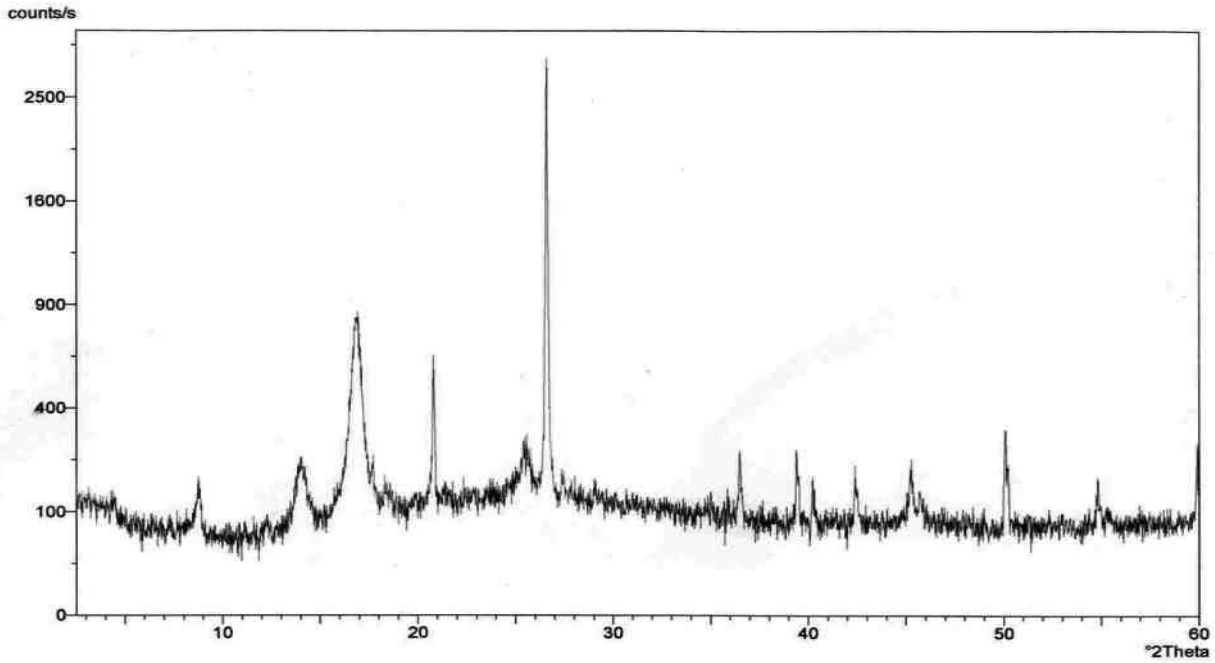

Figure B. 7. XRD profile of the dried suspension for the clay fraction (<2 μm) of the subsoil at site 5 in the KBR.

Appendix C: Stream Catchments

Table C 1. Stream catchment areas as determined through a 3-dimensional DEM application on ArcView GIS.

Stream	Area (in ha)
Str01	346
Str02	15
Str03	35
Str04	3.3
Str05	446
Str06	1447
Str07	88

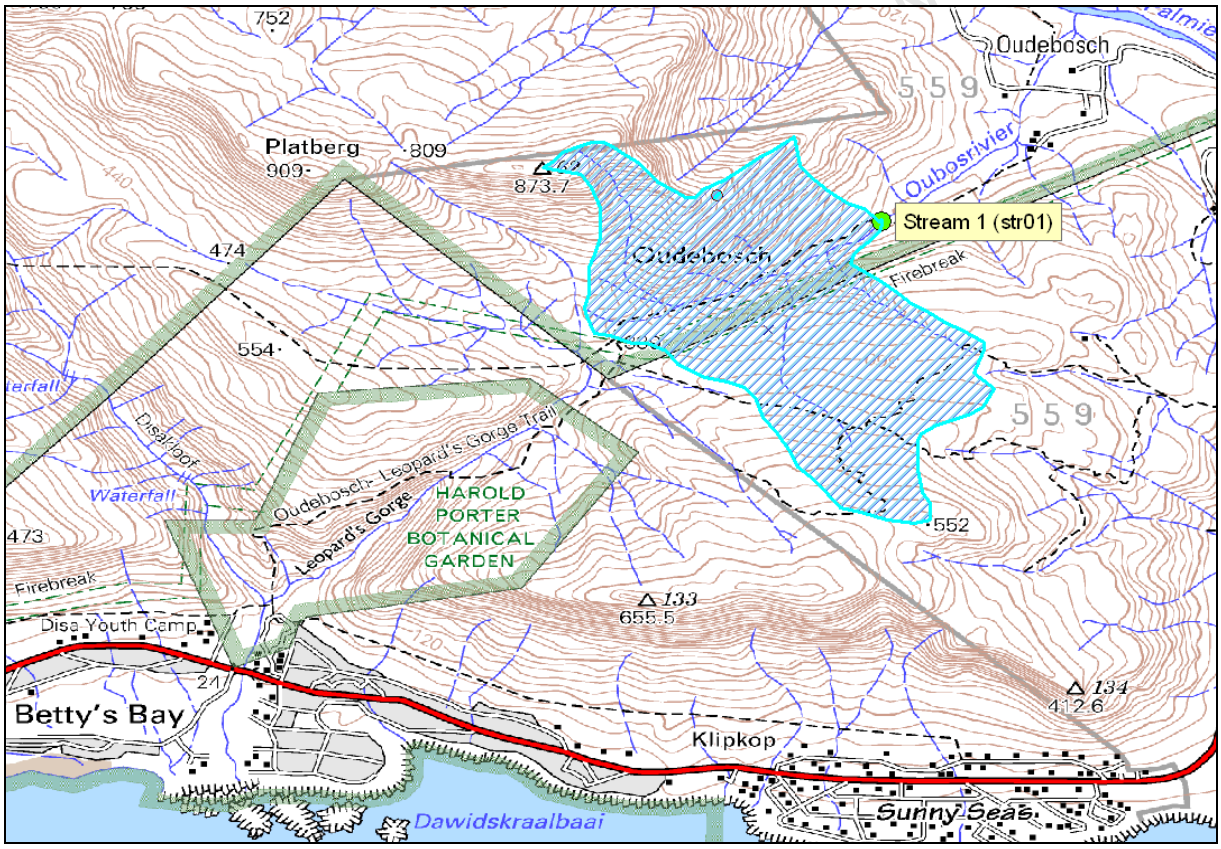

Figure C. 1. A topographic map of the study area overlain by the stream catchment area of stream 1. The green filled circle denotes the sampling point.

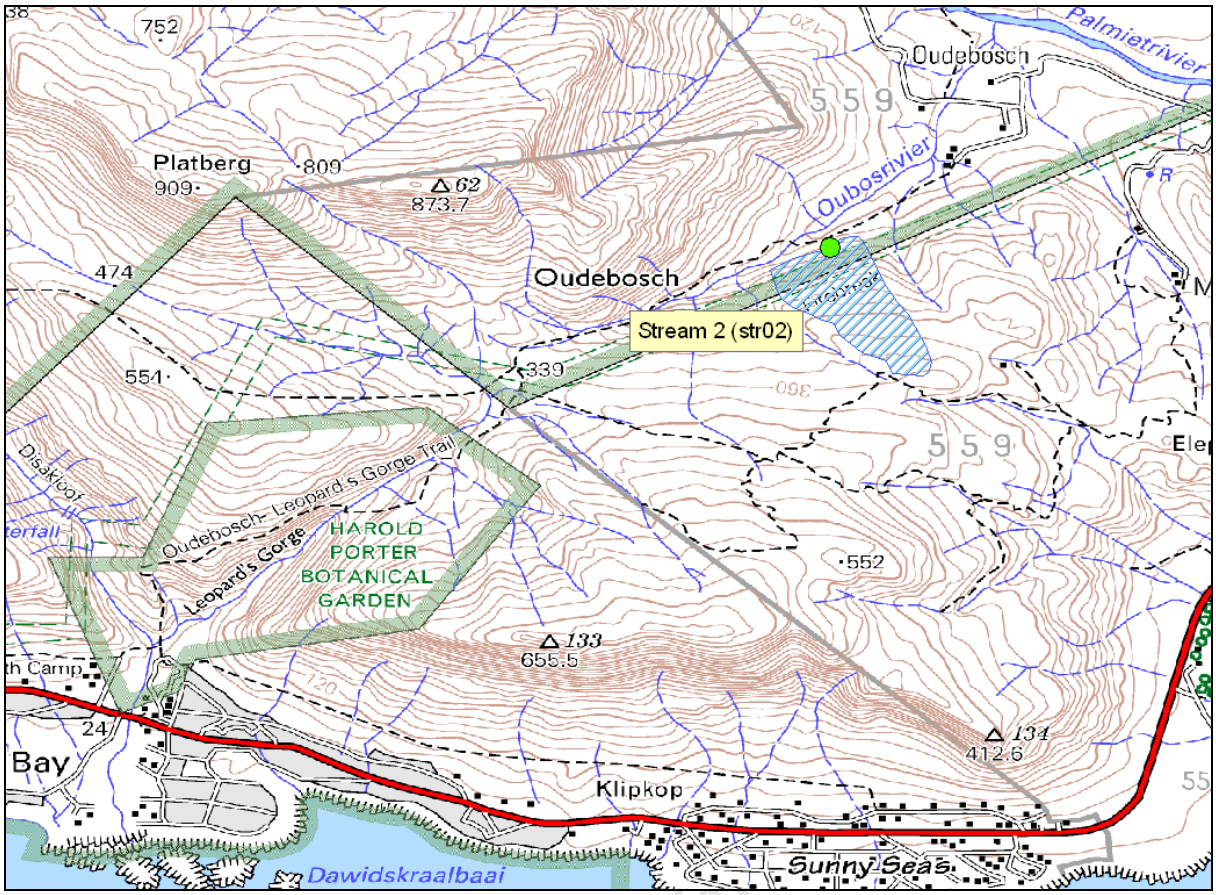

Figure C. 2. A topographic map of the study area overlain by the stream catchment area of stream 2 (mountain seep). The green filled circle denotes the sampling point.

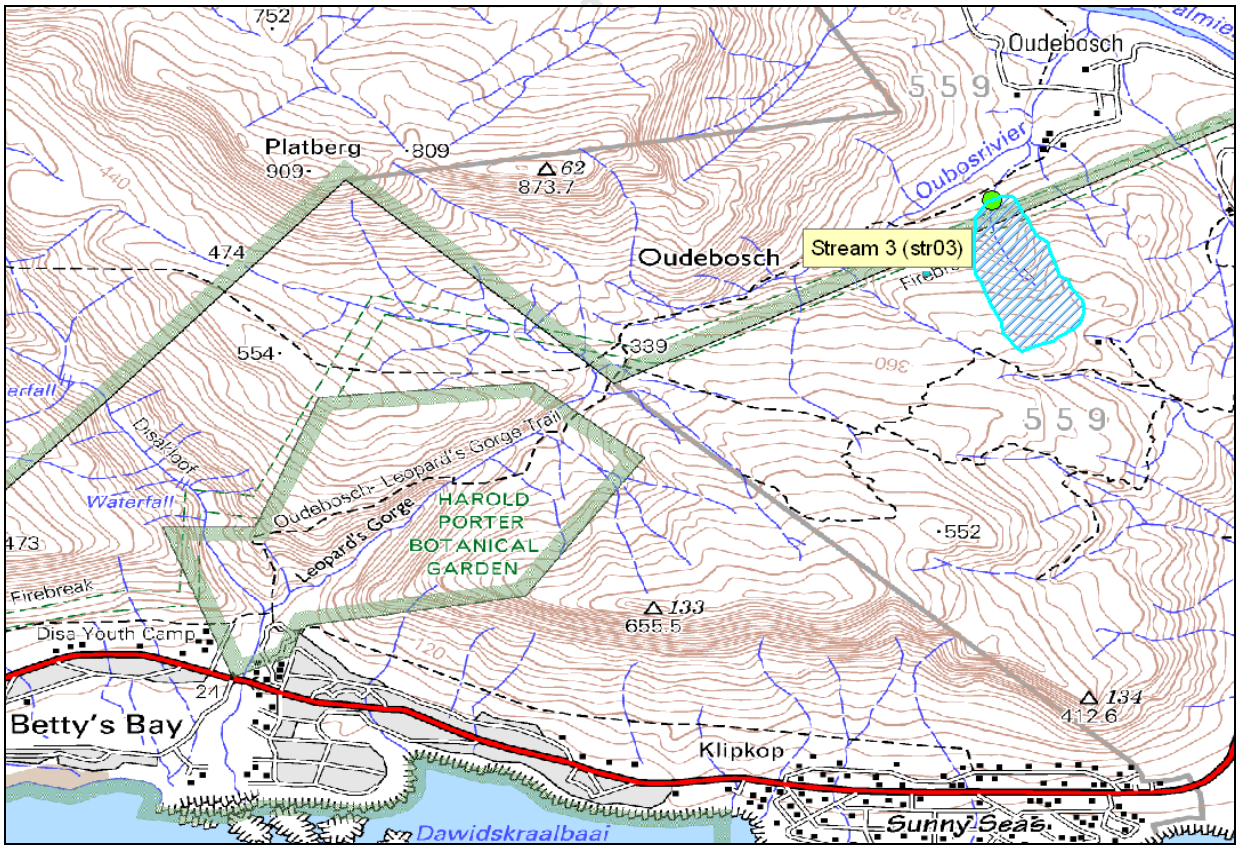

Figure C. 3. A topographic map of the study area overlain by the stream catchment area of stream 3. The green filled circle denotes the sampling point.

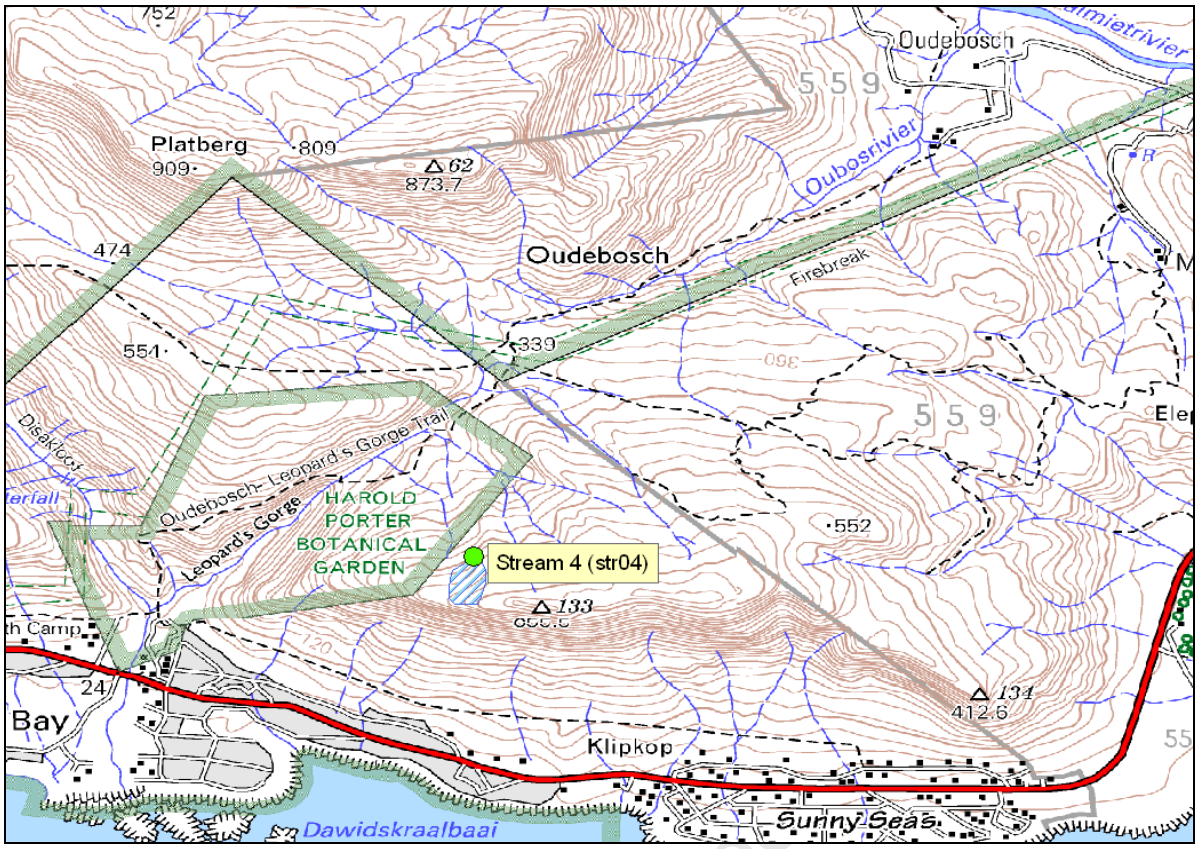

Figure C. 4. A topographic map of the study area overlain by the stream catchment area of stream 4 (mountain seep). The green filled circle denotes the sampling point.

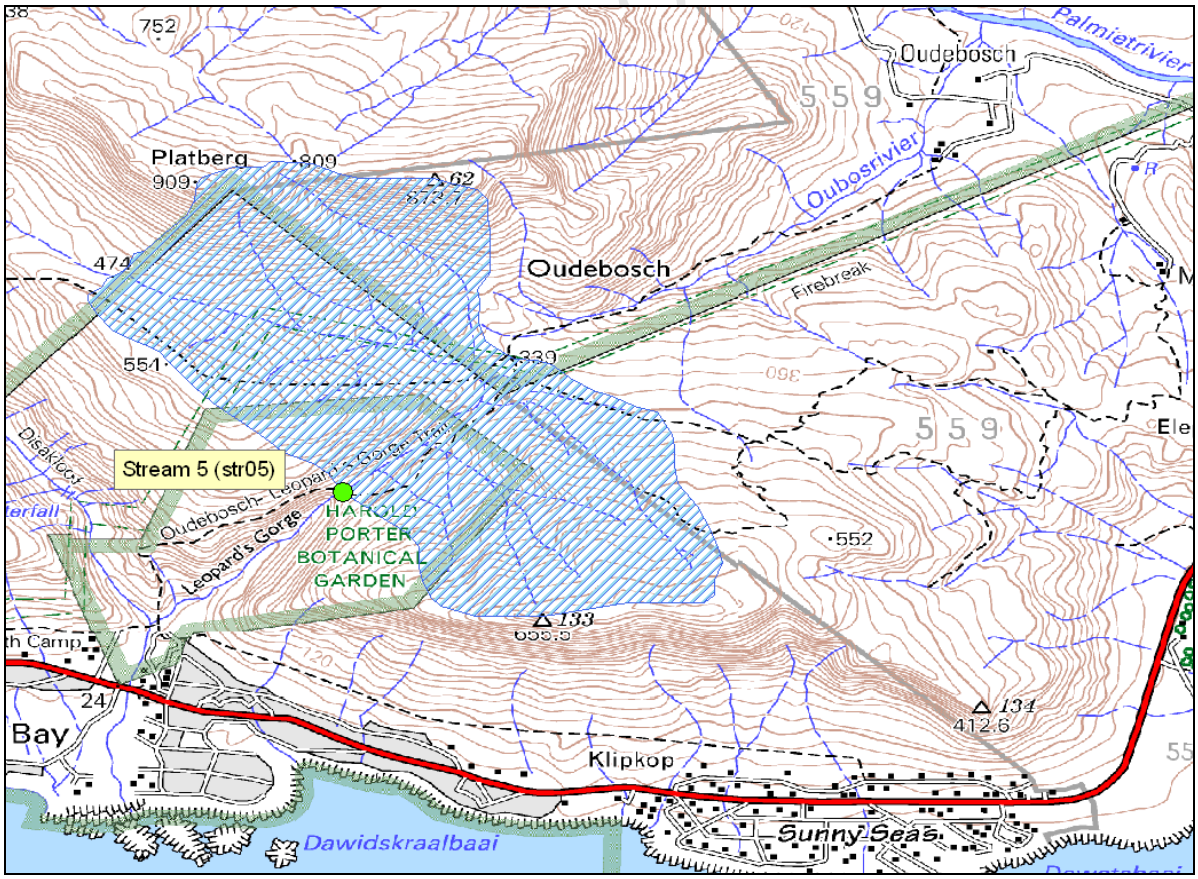

Figure C. 5. A topographic map of the study area overlain by the stream catchment area of stream 5. The green filled circle denotes the sampling point.

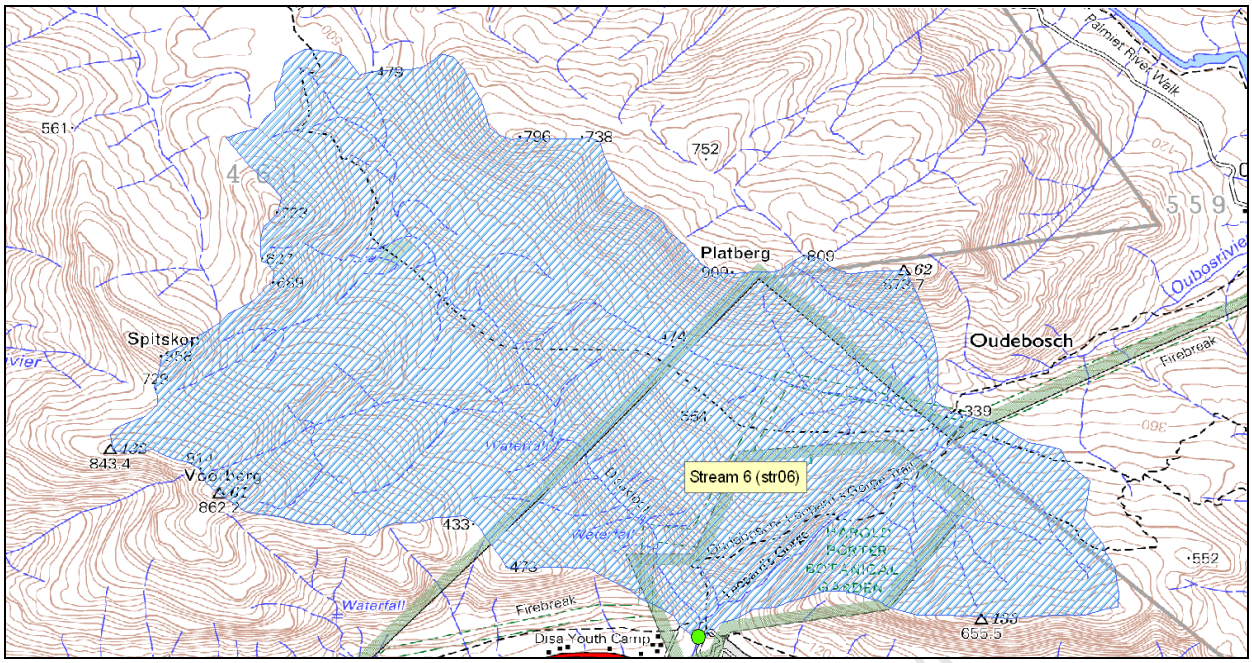

Figure C. 6. A topographic map of the study area overlain by the stream catchment area of stream 6. The green filled circle denotes the sampling point.

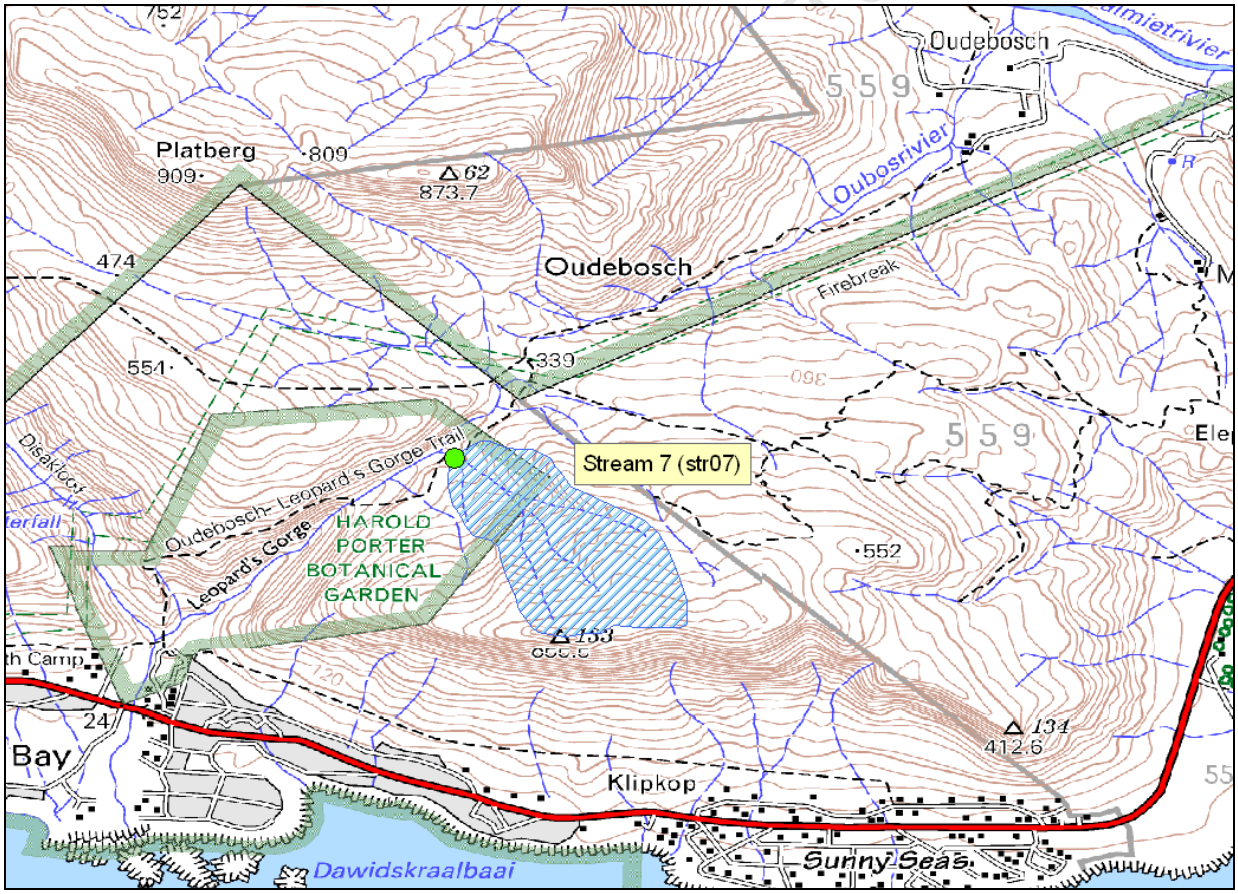

Figure C. 7. A topographic map of the study area overlain by the stream catchment area of stream 7. The green filled circle denotes the sampling point.

Appendix D: Pictures of the study area over a one year period

30 May 2010 | 17 June 2010 | 22 September 2010

23 November 2010 | 10 February 2011 | 1 June 2011

Figure D. 8. Vegetation regrowth over a one year period at site 1 in the HPNBG.

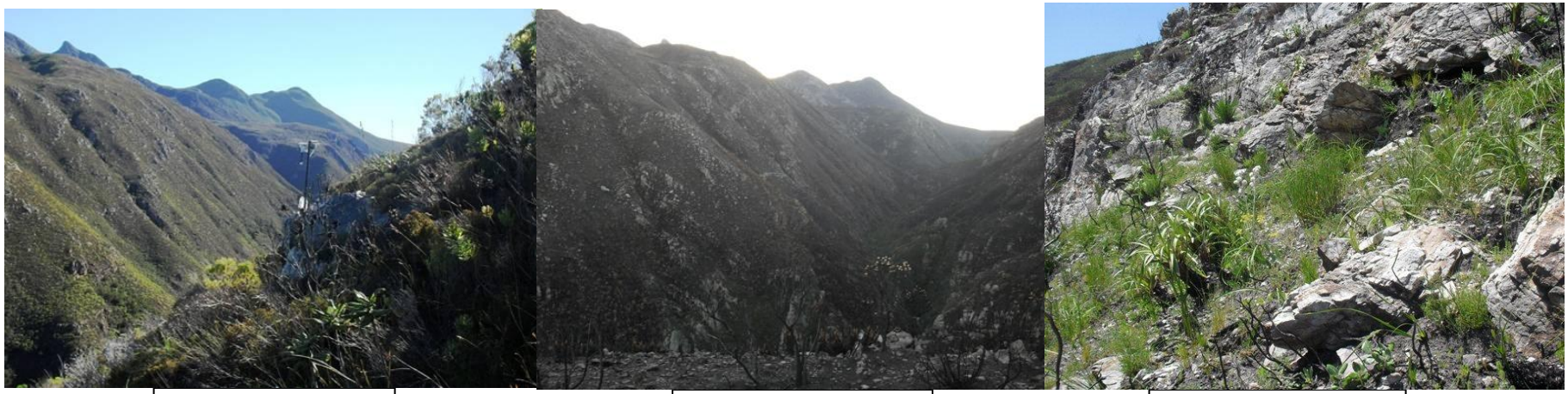

30 May 2010 | 17 June 2010 | 22 October 2010

23 November 2010 | 11 January 2011 | 29 April 2011

Figure D. 9. Vegetation regrowth over a one year period around site 2 in the HPNBG.

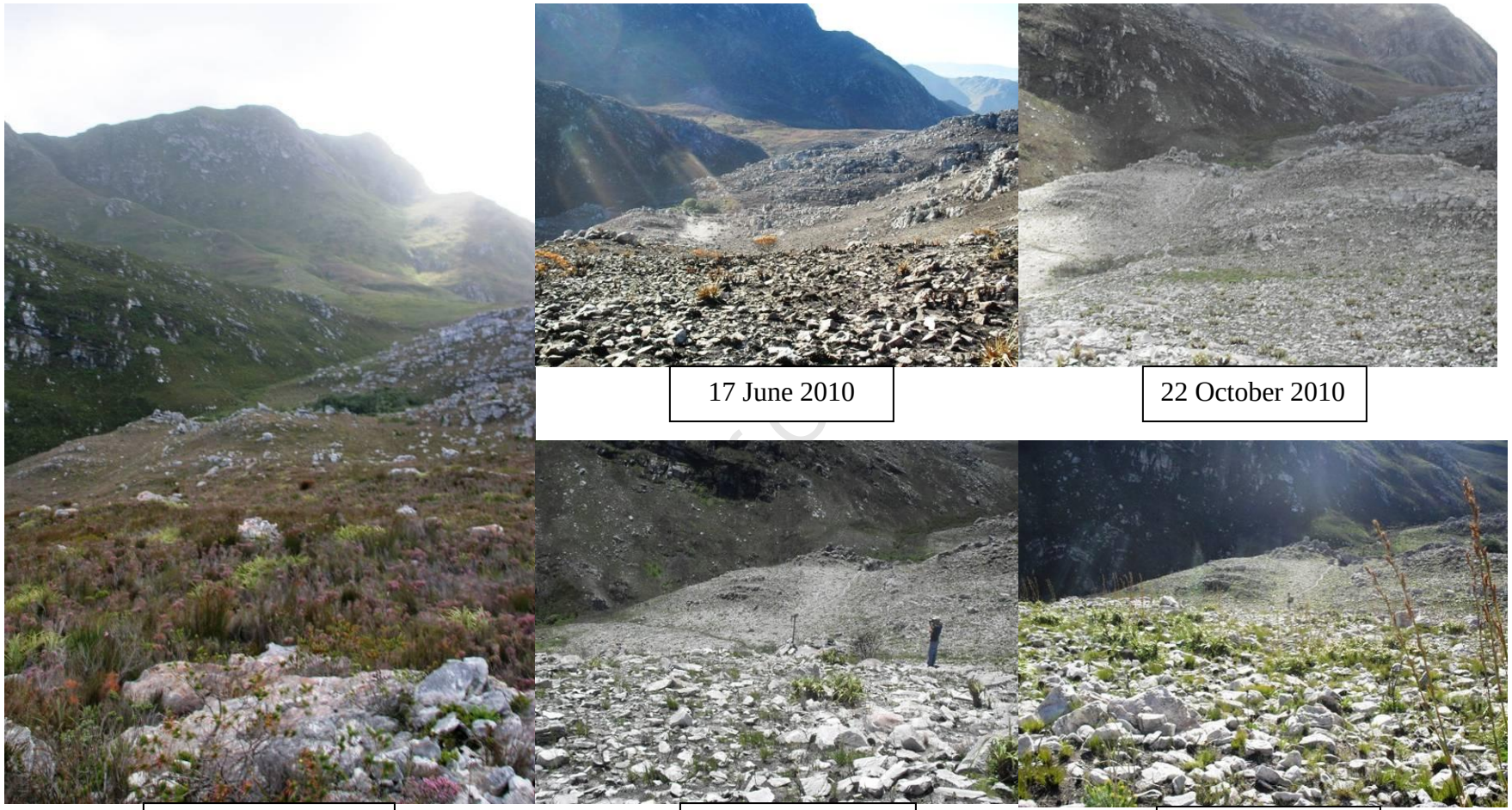

Figure D. 10. Vegetation regrowth over a one year period around site 3 in the HPNBG.

Figure D. 11. Vegetation regrowth over a one year period around site 4 in the HPNBG.

30 May 2010

22 September 2010

10 February 2011

1 June 2011

Figure D. 12. Vegetation regrowth over a one year period around site 5 in the KBR.

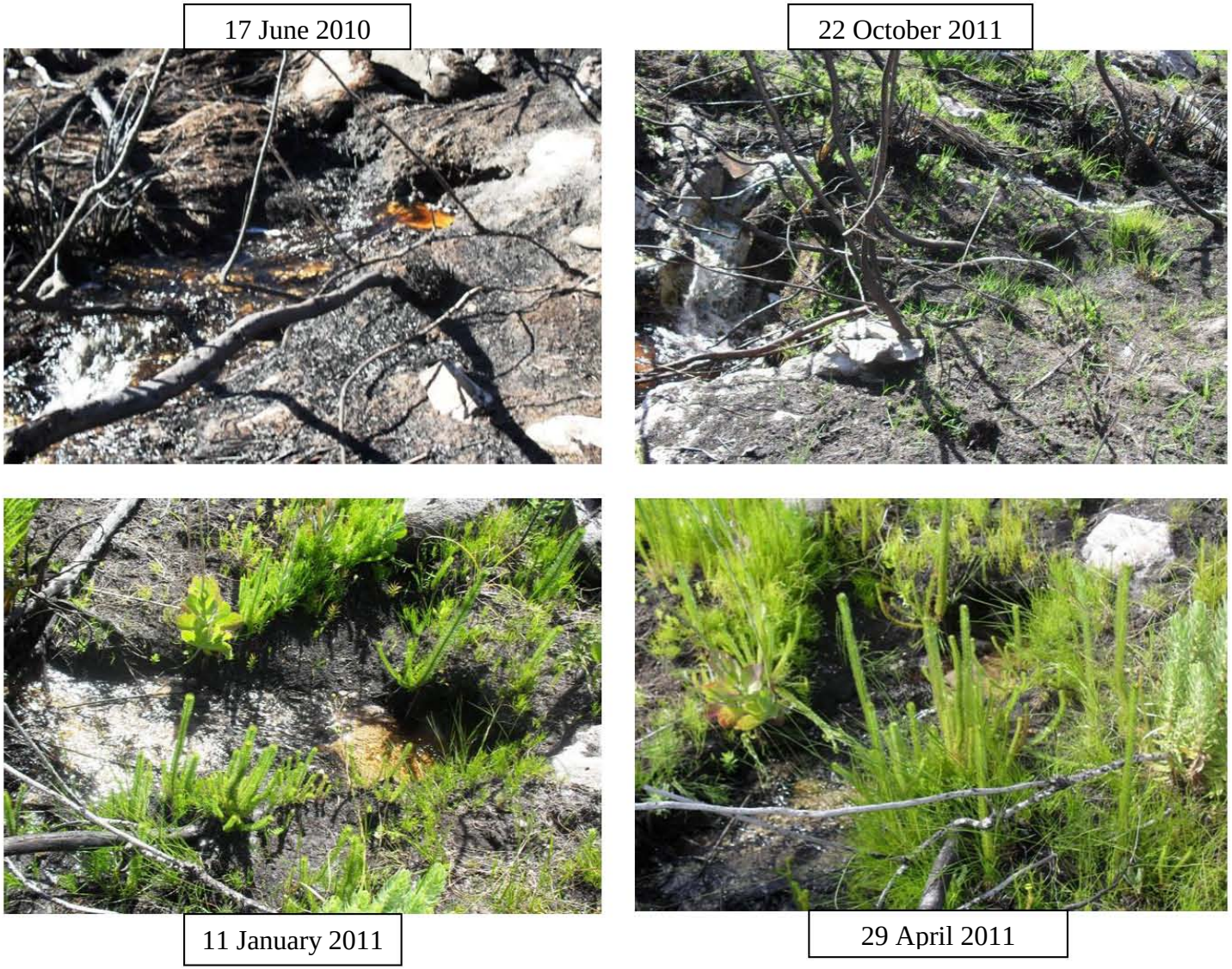

Figure D. 13. Vegetation regrowth over a one year period around stream 3 in the KBR.